

**ASPECTS OF MINERAL TRANSFORMATION
DURING WEATHERING OF VOLCANIC MATERIAL**

The microscopic and submicroscopic level

Ontvangen

01 SEP. 1994

UB-CARDEX



0000 0572 0525

Promotor:

Dr. N. van Breemen,
hoogleraar in de Bodemvorming en Ecopedologie.

Co-promotor:

Dr. P. Buurman,
universitair hoofddocent in de Bodemvorming.

PN08201, 1811

A.G. Jongmans

**ASPECTS OF MINERAL TRANSFORMATION
DURING WEATHERING OF VOLCANIC MATERIALS**

The microscopic and submicroscopic level

Proefschrift
ter verkrijging van de graad van doctor
in de landbouw- en milieuwetenschappen
op gezag van de rector magnificus,
Dr C.M. Karssen,
in het openbaar te verdedigen
op vrijdag 2 september 1994
des namiddags om half twee in de Aula
van de Landbouwuniversiteit te Wageningen.

15N296731

CIP-DATA KONINKLIJKE BIBLIOTHEEK, DEN HAAG

Jongmans, A.G.

Aspects of mineral transformation during weathering of volcanic materials : the microscopic and submicroscopic level / A.G. Jongmans. - [S.l. : s.n.]. - III.

Thesis Wageningen. - With ref. - With summary in Dutch.
ISBN 90-5485-279-8

Subject headings: volcanic soils ; weathering / micromorphology.

**BIBLIOTHEEK
LANDBOUWUNIVERSITEIT
WAGENINGEN**

Stellingen

1. De veronderstelling dat "neofomed clay coatings" schaarse verschijnselen zijn in bodems, blijkt voor vulkanische gronden onjuist te zijn.

Bullock et al., 1985. Handbook of soil thin section description. Waine research publications, Albrighton, UK.

2. De eis: aanwezigheid van 1% "clayfilms" om een argillic horizon te onderscheiden zal moeten worden herzien omdat geen rekening wordt gehouden met het kunnen voorkomen van kleinieuwvormings coatings .

Soil Survey Staff, 1992. Keys to soil taxonomy. Pocahontas press, Inc. Blacksburg, Virginia.

3. Verwerking van primaire mineralen en vorming van secundaire mineralen bepalen in sterke mate het verloop van de voortschrijdende bodemvorming in vulkanische gronden.

4. Optisch identieke, isotrope Al/Si coatings kunnen een verschillende chemische en mineralogische samenstelling hebben ten gevolge van verschillen in micro omgevingsfactoren.

dit proefschrift.

5. Micromorfologie en in-situ submicroscopie blijken onmisbaar te zijn in verwerings en nieuwvormingsstudies in vulkanische gronden.

dit proefschrift.

6. Het voorkomen van 2:1 phyllosilicates in vulkanische gronden ontwikkeld onder ferralitische omgevingsfactoren kan verklaard worden door overerving uit hydrothermaal beïnvloed moedergesteente.

dit proefschrift.

7. Imogolite zal meer aangetoond kunnen worden, als (schijnbaar) amorf materiaal in slijpplaten wordt geïsoleerd voor transmissie elektronen microscopie.

dit proefschrift.

8. Micro omgevingsfactoren kunnen tot op het nanometer schaalniveau de verwerking van primaire en de vorming van secundaire mineralen bepalen.

dit proefschrift.

9. Om verwerings- en nieuwvormingsverschijnselen in bodemhorizonten van vulkanische gronden juist te kunnen interpreteren is bestudering van het moedermateriaal en de saproliet essentieel.

dit proefschrift.

10. Cementatie van bodemhorizonten in vulkanische gronden kan het gevolg zijn van het voorkomen van amorfe Al/Si coatings.
11. De micromorfologie zal zich zo min mogelijk moeten bedienen van uitgebreide beschrijvingen en onbegrijpelijk jargon.
12. De wetenschappelijk onderzoeker moet leren leven met onzekerheid.
13. Creativiteit en nieuwsgierigheid vormen de basis voor het doen van onderzoek.
14. De uitspraak "De kalkoen en de poelier praten samen over het kerstdiner" geeft beeldend weer dat de huidige democratische bestuursstructuren van de LUW een personele reorganisatie dreigen te laten verzanden.
15. Meer beleid, minder faculteit.

Stellingen behorend bij het proefschrift "Aspects of mineral transformation during weathering of volcanic material. The microscopic and submicroscopic level". Toine Jongmans, 2 september 1994.

ABSTRACT

Mineral transformation at the earth surface is a complex process. In volcanic ejecta, such transformations tend to be fairly rapid. Many weathering studies on volcanic materials have been carried out at different scales of observations, mostly using bulk samples. However, to get a proper understanding of the mechanisms of weathering of primary minerals and formation secondary minerals it is necessary to obtain data of undisturbed material at the scale of observation that micromorphology and submicroscopy deal with. Weathering studies at the micrometre scale with help of micromorphology showed the heterogenous character of mineral weathering and the co-existence of different secondary minerals.

The main objective of papers in this thesis was to characterize and explain alteration of primary minerals and formation of secondary minerals at the particle level in volcanic soils in relation to (micro) environmental conditions.

Thin sections of volcanic soils were studied by micromorphology, and relevant features were characterized chemically and mineralogically by submicroscopical methods performed on (un)disturbed samples isolated from thin sections.

Mineral transformations were studied both on sites in the temperate humid zone and in the humid tropics.

In a chronosequence of Quaternary terraces of the Allier in France, micromorphological and sub microscopical analyses showed:

- Alteration of basaltic particles leads to clay formation whereas weathering of granite fragments contributes to the sand fractions.

- A relative increase in the contents of Ti, Al, and Fe and a decrease of K, Na, Ca, and Si occur in weathering rinds of basalt pebbles. Differences in weathering intensity are predominantly a function of chemical composition of the basalt rather than a function of time.

- A mass balance calculation carried out on an isovolumetric, altered basalt pebble with a fresh core, and on an enclosed, genetically related neoformed clay coating showed that all elements, except Fe were leached from all weathering rinds. Only Si, Al and some Ca were found in the clay coating, and part of the Al was derived from an external source.

- Isotropic and anisotropic coatings occur in a Paleosol in an older terrace. Micromorphological observations demonstrated that such coatings are genetically related. The isotropic coating consists of allophanic material with minor amounts of 2:1 phyllosilicates, whereas the anisotropic types consist of 2:1 phyllosilicates only. Both types result from recombination of trachytic weathering products under restricted leaching conditions during coating formation.

- Micromorphological observation demonstrated three types of coatings in two Planosols in two older terraces. Isotropic and anisotropic, translucent materials occur locally within one coating, suggesting a genetic similarity. These coatings are due to secondary mineral formation, The third type, anisotropic dusty clay coatings clearly resulted from clay illuviation. Cluster analyses reveal that the coatings of the same type were chemically more alike than different coatings in the same profile. About 83% of the grouped samples were classified correctly as either isotropic and anisotropic weathering coatings or anisotropic illuviation coatings.

A technique is described to isolate undisturbed microparts of pedofeatures from thin sections. Such microparts can subsequently be analysed by Transmission Electron Microscopy. This technique allows performance of micromorphological, mineralogical and chemical analyses on one undisturbed micro sample at micrometre to nanometre scales.

Isotropic coatings in the C horizon of a young Hapludand in Guadeloupe and in the C and R horizons of an old Hapludand in Costa Rica, both developed on andesitic volcanic materials were allophanic. Isotropic coatings present in the Bw horizons of both soils contain allophane and imogolite. The Al/Si molar ratios in the coatings in the Bw horizons are higher than those in the coatings of the C and R horizons. Anisotropic coatings are wholly gibbsitic and occur only in the Bw horizon of the older Costa Rican Hapludand. The gibbsitic coatings show a gradual transition to isotropic coatings and both types look alike in plane polarized light suggesting a genetic relationship. The allophane coatings resulted from initial weathering of the parent materials, whereas the gibbsite coatings represent the ultimate stage of secondary mineral formation. The differences in chemical and mineralogical composition of the coatings are thought to be the result of different leaching conditions at the macro and micro scale.

2:1 Phyllosilicates in Hapludands on Holocene andesitic beach ridges in Costa Rica occur as clay pseudomorphs after primary minerals. They are inherited from hydrothermally altered parent material from which the beach ridges were derived, and are not due to post depositional soil formation. Weathering and biological activity affect the clay pseudomorphs which leads to clay-sized particles consisting of 2:1 phyllosilicates. They are incorporated in the allophanic groundmass that results from actual soil formation in the Hapludands.

Isotropic coatings also found in a West Java (Indonesia) Oxisol on andesitic volcanic parent materials are probably due to weathering of airborne ash additions. The coatings recrystallize to anisotropic coatings suggesting a neofomed genesis. Both types of coatings appear to be common in three andesitic catenas in Indonesia. The amount of coatings and the crystallinity tend to increase as the dry season become more pronounced. The anisotropic coatings can easily be confused with illuviation coatings.

CONTENTS

CHAPTER 1. GENERAL INTRODUCTION	9
CHAPTER 2. WEATHERING OF PRIMARY MINERALS	17
2.1 Soil formation in a quaternary terrace sequence of the Allier, Limagne, France. Macro and micromorphology, particle size distribution, chemistry. <i>A.G. Jongmans, T.C.J. Feijtel, R. Miedema, N. van Breemen, and A. Veldkamp, 1991. Geoderma, 49:215-239</i>	
2.2 Alkalibasalt weathering in Quaternary Allier river terraces, limagne, France. <i>E. Veldkamp, A.G. Jongmans, T.C.J. Feijtel, A. Veldkamp, and N. van Breemen, 1990. Soil Sci. Soc. Am. J. 54:1043-1048.</i>	43
2.3 Micromorphological characterization and microchemical quantification of weathering in an alkali basalt pebble. <i>A.G. Jongmans, E. Veldkamp, N. van Breemen, and I. Staritsky. 1993. Soil Sci. Soc. Am. J. 57:128-134</i>	51
2.4 The progression from optical light microscopy to transmission electron microscopy. <i>F. van Oort, A.G. Jongmans, and A.M. Jaunet. 1994. Clay minerals (in press).</i>	59
CHAPTER 3. FORMATION OF SECONDARY MINERALS	
3.1 Morphology, chemistry, and mineralogy of isotropic aluminosilicate coatings in a Guadeloupe Andisol <i>A.G. Jongmans, F. van Oort, P. Buurman, A.M. Jaunet, and J.D.J. van Doesburg. 1994. Soil Sci. Soc Am. J. (in press)</i>	69
3.2 Allophane, imogolite, and gibbsite in coatings in an Costa Rican Andisol. <i>A.G. Jongmans, P. Verburg, A. Nieuwenhuyse, F. van Oort. 1994. Geoderma (in press).</i>	77
3.3 Micromorphology and submicroscopy of isotropic and anisotropic Al/Si coatings in a Quaternary Allier terrace. <i>A.G. Jongmans, F. van Oort, P. Buurman, and A.M. Jaunet. 1994. In: A. Ringrose-Vose (ed.) Proc. 9th Int. Work. Meet. on Soil Micromorph. Townsville, Australia, July 12-17, 1992. (in press)</i>	95
3.4 Inheritance of 2:1 phyllosilicates in Costa Rican Andisols. <i>A.G. Jongmans, F. van Oort, A. Nieuwenhuyse, A.M. Jaunet, and J.D.J. van Doesburg. 1994. Soil Sci Soc Am. J. (in press).</i>	105

CHAPTER 4. CLAY COATINGS FORMED BY ILLUVIATION OR BY IN-SITU PRECIPITATION		
4.1	Amorphous clay coatings in a lowland Oxisol and other Andesitic soils of West Java, Indonesia. <i>P.Buurman, and A.G. Jongmans, 1985. Pemberitaan Penelitian Tanah Dan Pupuk 7:31-40.</i>	113
4.2	Identification of clay coatings in an old Quaternary terrace of the Allier, Limagne, France. <i>T.C.J. Feijtel, A.G. Jongmans, and J.D.J van Doesburg, 1989. Soil Sci. Soc. Am J. 53: 876-882.</i>	125
CHAPTER 5. EPILOGUE		133
SAMENVATTING		137
NAWOORD		139
CURRICULUM VITAE		143

CHAPTER 1

GENERAL INTRODUCTION

GENERAL INTRODUCTION

Weathering can be defined as the ensemble of processes by which primary minerals are destroyed, and either disappear or are transformed into more stable secondary minerals (Delvigne, 1965; Delvigne and Stoops, 1990). Weathering transforms rocks to soil material which can be penetrated by plants and organisms and which can be used by men for agricultural purposes. Knowledge of mineral weathering and of formation of secondary minerals is essential for (i) a proper understanding of global bio-geochemical cycles, (ii) the rate of soil formation versus soil erosion, of plant nutrition, (iii) composition of ground- and surface waters, and (iv) the rate of buffering of acid substances from anthropogenic deposition.

Weathering of primary- and formation of secondary minerals is dominant soil forming process in materials which contain appreciable amounts of easily weatherable minerals. Most rocks and sediments contain weatherable primary minerals. Chemical, mineralogical and physical properties of soils formed on such parent materials are largely determined by the amount, nature, and distribution of the secondary minerals.

Differences in scales of observation.

In a review paper on quantitative modelling of pedogenesis, Hoosbeek and Bryant (1992) distinguished various levels of organisation relevant to pedology: molecular interactions, peds/aggregates, soil horizons, pedons, polypedons, catenae, and soil regions. Objects at each of these levels of organisation can be regarded as a system, each of which can be seen as combinations of subsystems at lower levels or as a subsystem at higher levels. Weathering processes of primary- and the formation of secondary minerals can be studied at different levels of observation, varying from the global to the submicroscopic level. Each level needs to be studied at a relevant scale of observation, which in turn determines the required analytic techniques and sampling strategies (Fig. 1).

Most research on weathering at the scale of a watershed, or a soil region, deals with quantitative determination of element transfer (mass balance studies) and weathering rates of rock-forming silicate minerals. Examples of such studies are e.g. Paces (1968, 1985). He measured elemental budgets in small, well defined watersheds in Central Europe and calculate rates of weathering and of erosion as influenced by acid emission and agricultural action. Velbel (1985) studied geochemical mass balances and weathering rates in forested watersheds in the USA to establish the rate at which the weathering front penetrates in fresh rock. He concluded that the observed values agree with the "average" denudation rate for the southern Appalachians. Such studies are carried out at a high scale of observation whereby even macroscopic spatial variability (m. to km.) is lumped or "averaged". Such studies cannot explain the mechanism of weathering and neoformation at the level of individual minerals. The same is true for studies of mineral weathering and formation of secondary minerals at the catena and pedon level, where the processes are related to the soil forming factors rock composition, topography, hydrology or climate (Chartres and Pain 1983; Mizota et al. 1988; Wada et al. 1989; Quantin et al. 1991). Such studies are based mainly on chemical and mineralogical data obtained from bulk samples of soil horizons and/or rocks, and yield general information about relationships between the soil forming factors and the gross rate of mineral weathering and the nature of secondary minerals formed. However, soils and rocks are heterogeneous in chemical and mineralogical composition, internal fabric, and porosity, and present a variety of micro-site conditions. Hence, there is no one-to-one relationship between soil forming factors and the nature of weathering and secondary mineral formed: different rates of weathering and different types of secondary minerals can be observed in different

micro environments in the same pedon (Meunier, 1983). As a result, soil profile studies based on bulk samples with respect to chemistry and mineralogy do not give direct information about the actual nature of weathering and secondary mineral formation at the mineral-grain level. Yet it is at this level that elements are liberated, start to migrate, and are regrouped into secondary materials. Pertinent information about those matters must be obtained at the level of observation that micromorphology and submicroscopy deal with. Numerous studies with respect to weathering and neoformation of minerals have been carried out at the microscopic/ submicroscopic level in rocks, saprolites and soils. (Asamada, 1988; Delvigne, 1965; 1983; Delvigne et al. 1979; Nahon and Colin 1982.; Berner and Scott, 1982; Nahon 1991). These studies are based on observations obtained by optical and submicroscopical techniques performed in-situ. The essential advantage of such methods is that data are obtained about the size, shape, arrangements and composition of the individual constituents i.e. the primary and secondary minerals (e.g. Chapter 2.4, 3.1 and 3.2). Such studies have demonstrated the heterogeneous character of mineral weathering and the coexistence of different secondary minerals at the micro scale. In addition, relicts of secondary minerals in soils deposited with the primary minerals, or formed under paleoclimates can more easily be recognized by microscopical and submicroscopical methods than by studying bulk samples. E.g. the occurrence of 2:1 phyllosilicates in volcanic soils has often attributed to in situ pedogenic processes or to rejuvenation as a result of aeolian addition (e.g. Mokma et al. 1972). However in chapter 3.4 we demonstrate that in Andisols on andesitic beach ridges in a perudic climate such phyllosilicates are derived from hydrothermal alteration of primary minerals in the volcanic parent rock from which the parent material of the Andisols was derived. So observations at a more detailed scale of observation are required for correct interpretation of data derived from bulk samples. The microscopic and sub-microscopic level of observation provides a better insight in the nature of weathering and neoformation mechanisms. The knowledge on mineral dissolution, element migration and regrouping of elements in secondary materials obtained at the microscale help to understand weathering mechanisms and can be incorporated in studies of weathering and neoformation at higher levels of observations. Chapter 3.1 and 3.2 reveal that neoformed coatings have different chemical and mineralogical composition if the micro-environmental conditions are different. Theories based on bulk data concerning formation and occurrence of allophane, imogolite and neoformed clay can be rejected, confirmed or adapted. Chapter 2.1 shows that weathering of basaltic fragments led to formation of clay, whereas weathering of granite fragments dominantly contributed to formation of sand in a Quaternary terrace sequence rich in volcanic fragments. Such data can be obtained only from micromorphology and submicroscopy. In addition, this study illustrates how these techniques provide different levels of detail about soil development in young and old terraces, making micromorphology an indispensable tool to unravel the complex story of pedogenesis of, particularly, the old soils.

Methods and objectives

Site conditions like climate, parent material, vegetation, drainage and age influence the rate of weathering of primary minerals and the mineralogy of the neoformed minerals. (Lowe, 1986; Parfitt and Kimble, 1989; Wada, 1989). Internal mineral factors and external environmental conditions may control weathering and neoformation on soil properties. To study these effects at the mineral level, micromorphology of undisturbed samples provides fundamental support (Meunier, 1983). Effects of alteration in relation to structural, chemical and physical discontinuities of the mineral itself and external micro- environments can be studied in-situ in thin sections of undisturbed soil samples. In addition, the amount, morphology and distribution of the secondary minerals can be examined.

Micromorphology itself has limited possibilities for chemical and mineralogical characterization of (partly) altered primary minerals and secondary minerals. For correct interpretation of the nature of the secondary minerals, the chemical and mineralogical composition of individual grains must be studied simultaneously. Scanning Electron Microscopy with Energy Dispersive X-Ray Analyzer (SEM-EDXRA, e.g. Bisdorn et al. 1990) is a widely used technique to characterize the chemical composition of features observed in uncovered thin sections.

Verschuren (1976) and Beaufort et al. (1983) introduced microdrilling in uncovered thin sections to sample micro quantities of material for mineralogical analysis with the help of Step scan X-ray diffraction (Meunier, 1983). We used the same technique to determine the mineralogical composition of secondary minerals.

Transmission electron microscopy can also be applied in determination of mineralogical and chemical composition and the size shape and arrangements of individual constituents at the nanometre level (Bisdorn et al. 1990). However, this technique requires ultra thin samples (50 nm) of uniform thickness to avoid artificial contrasts, and it is therefore not directly applicable to uncovered thin sections. Bresson (1981) used ion-milling to prepare such ultrathin sections for TEM, but the technique is not easily applicable and has disadvantages such as producing variable thickness. In the absence of a direct method to characterize the mineralogy of undisturbed features in thin section at the nanometre scale, we combined optical microscopy and TEM studies performed on ultra thin, undisturbed micro parts isolated by micro-drilling in uncovered thin sections (van Oort et al. 1994). This combination of techniques provided a possibility to determine, in-situ, size, shape, arrangements, and chemical and mineralogical composition of individual constituents.

All papers in this thesis are dominantly performed at the optical (μm) and submicroscopical ($\mu\text{-nm}$) scale of observation and deals with mineral transformation of individuals constituents in soils on volcanic materials. In some papers we extrapolate the results of these microstudies to soil formation at the pedon or catena level of organization (Hoosbeek and Bryant, 1992).

The major goals of the studies being reported in the following chapters are:

- i) To characterize the nature of weathering of primary minerals and their secondary products, and to unravel the impacts of these processes on soil development in chrono-sequences and polygenetic soils.
- ii) To set up quantitative weathering studies at the mineral level.
- iii) To test the hypothesis that coatings observed by microscopy consist of different secondary minerals, and to characterize their chemistry and mineralogy in relation to their morphology.
- iv) To establish the genesis of such coatings, in relation to micro-environmental conditions that may control their chemistry and mineralogy.
- v) To demonstrate the value of microscopical and submicroscopical studies of the parent material of volcanic soils for a good understanding and correct interpretation of the genesis of secondary minerals.

The outline of this thesis

This thesis consists of papers that have been published or will be published in international journals. Combination of such papers in one volume implies some duplication, especially in the method and reference sections. At the same time it reveals the development of the research. In the first stage research was focused on aspects of weathering of primary minerals and rock fragments; submicroscopical techniques except for SEM-EDXRA were not used. Later, we focused the research on formation of secondary minerals by using submicroscopy.

Chapter 2 deals primarily with weathering of primary minerals.

Paper 1 describes soil formation in a Quaternary Allier terrace sequence in France as a function of soil age. It is shown that alteration of basalt fragments led to clay formation, whereas alteration of granitic fragments contributed to the sand fraction. The occurrence of isotropic and anisotropic neoformed clay coatings is reported. Their chemical and mineralogical composition is further described in chapter 3 and 4.

In paper 2, alkali basalt weathering in a number of the Allier terraces of the chronosequence was studied by means of the isovolumetric method and the Ti-constant method in order to quantify compositional changes as a result of weathering.

In paper 3, a mass balance was set up to quantify the output of elements from an isovolumetric weathering rind of a basalt pebble from an older Allier terrace and the input of elements in a neoformed coating enclosing the pebble.

In paper 4, the use of transmission electron microscopy in studying clay micro fabrics isolated from thin sections is discussed. A technique is described to isolate undisturbed microbodies of neoformed clay from thin sections, which can further be used for TEM analyses. Examples are presented to illustrate the usefulness of the method.

Chapter 3 contains all papers focused on formation of secondary minerals

In paper 1, of this chapter, isotropic aluminosilicate coatings in an Andisol under perudic conditions are studied. In-situ submicroscopical analyses demonstrate different chemical and mineralogical composition of the coatings in relation to site conditions as a result from different leaching conditions.

In paper 2, the morphology, chemistry, mineralogy and genetic relationship of allophane, imogolite and gibbsite neoformed coatings in an Andisol developed in an andesitic lava in Costa Rica is discussed. Differences in coating composition are the result of different leaching conditions at the pedon and the micrometre level of organisation.

In paper 3, amorphous and crystalline coatings in a buried paleosol in an older Allier terrace in France are shown to be genetically related. In-situ submicroscopical analyses indicate that restricted leaching conditions and the composition of the primary minerals control the chemical and mineralogical composition of these coatings.

Paper 4 shows that the parent material rather than in situ soil formation, is the source of 2:1 phyllosilicates in Andisols developed on Holocene andesitic beach ridges in Costa Rica, under current perudic climatic conditions.

Chapter 4 discusses two possible ways of formation of clay coatings: illuviation or in-situ weathering.

Paper 1 deals with the presence of amorphous clay coatings and their recrystallization to 1:1 phyllosilicates in a lowland Oxisol and other Andesitic soils in Indonesia. The differences between microscopically similar but genetically different coatings, those consisting of secondary clay formed in situ and those formed by clay illuviation is discussed.

In paper 2, The occurrence of three types of coating was reported in an older endmember of the Allier terraces. The hypothesis

that these coatings differed chemically and mineralogically was tested. In addition, their genesis is discussed.

Justification of the authorships and co-authorships of the papers

Different techniques and soil data are used in the topics of the papers involved in this thesis. My expertise is mainly in the field of soil morphology and micromorphology. Others contributed to the thesis which appears from the multiple different co-authors in six papers, and my co-authorship in five other papers.

Paper 4.1 was mainly written by T. C. J. Feijtel. I was involved in defining the research problem, and in the micromorphological characterization and interpretation of the types of coatings that were distinguished. In addition T.C.J. Feijtel carried out the chemical and particle size class interpretation in chapter 1.1.

Paper 2.2 was mainly written by E. Veldkamp; my contribution was focused on the micromorphological and mineralogical aspects of the research topic. Furthermore, he prepared the mass-balance calculations and the sensitivity analyses in paper 2.3.

The technique discussed in chapter 2.4. was developed jointly by F. van Oort and myself. F. van Oort performed the interpretation of the TEM analyses in the other chapters.

I. Staritsky carried out the estimation of the areas of distinguished zones in paper 2.3.

Paper 4.1. was mainly written by P. Buurman. My contribution to this paper comprises the identification of the problem the study deals with, and the micromorphological and mineral aspects in terms of characterization and interpretation.

References

- Asumadu, K. R.J. Gilkes, T.M. Armitage, and H.M. Churchward, 1988. The effects of chemical weathering on the morphology and strength of quartz grains - an example from S.W. Australia. *Journal of Soil Science*, 1988:375-383.
- Beaufort, D.P., P. Dudoignon, D. Proust, J.C. Parneix, and A. Meunier, 1983. Microdrilling in thin section: a useful method for the identification of clay minerals in-situ. *Clay Miner.* 18:223-226.
- Berner, R.A. and J. Scott, 1982. Mechanism of pyroxene and amphibole weathering II. observations of soil grains. *Am. J. of Sci.* 282:1214-1231.
- Bisdorn, E., D. Tessier, and J.F.T. Schoute, 1990. Micromorphological techniques in research and teaching, In: L.A. Douglas (ed), *Soil micromorphology: a basic and applied science. Developments in Soil Science 19:581-603*, Elsevier, Amsterdam, New York.
- Bresson, L.M., 1981. Ion milling to the ultra-microtopic study of soils. *Soil Sci. Soc. Am. J.* 45:568-573.
- Delvigne, J., 1965. Pédogenèse en zone tropical; La formation des minéraux secondaires en milieu ferralitique. *Mém. ORSTOM Ed. Dunod Paris*, 13, 177p.
- Delvigne, J., 1973. Micromorphology of the alteration and weathering of pyroxenes in the Koua Bocca ultramafic intrusion, Ivory coast, Western Africa. *Sci. Géol. Mém.* 72: 57-68.
- Delvigne, J., E.B.A. Bisdorn, J. Sleeman, and G. Stoops, 1979. Olivines, their pseudomorphs and secondary products. *Pedologie XXIX,3:247-309*.
- Delvigne, J., and G. Stoops, 1990. Morphology of mineral weathering and neoformation. I. Weathering of most common silicates. In: L.A. Douglas (ed), *Soil Micromorphology: a basic and applied science. Developments in Soil Science 19: 471-481*, Elsevier, Amsterdam, New York.
- Hoosbeek, M.R. and R.B. Bryant, 1992. Towards the quantitative modelling of pedogenesis - a review, *Geoderma* 55:183-210.

- Lowe, D., 1986. Controls on the rates of weathering and clay mineral genesis in airfall tephros: a review and New Zealand case study. In: Colman, S.M. Dethier, D.P. Rates of mineral weathering of rocks and minerals. Academic Press, Orlando.
- Meunier, A. 1983. Micromorphological advances in rock weathering studies. pp 467-483. In: Soil Micromorphology Vol. 2, Proc. of the Intern. Work. Meet. on Soil Micromorph. August 1981.
- Mizota, C., I. Kawasaki, and T. Wakatsuki, 1988. Clay mineralogy and chemistry of seven pedons formed in volcanic ash, Tanzania. *Geoderma* 43: 131-141.
- Mokma, D.L., J.K. Syers, M.L. Jackson, R.N. Clayton, and R.W. Rex, 1972. Aeolian additions to soils and sediments in the south pacific area. *J. Soil Sci.* 23:147-162.
- Nahon, D.B. 1991. Introduction to the petrology of soils and chemical weathering. John Wiley and Sons, Inc. New York, Chichester. pp 313
- Nahon, D.B., and Colin, F. 1982. Chemical weathering of orthopyroxenes under lateritic conditions. *Am.J. of Sci* 282:1232-1243.
- Oort, van, F., A.G. Jongmans and A.M. Jaunet, 1993. The progression from optical light microscopy to transmission electron microscopy in the study of soils. *Clay Miner.* (submitted)
- Paces, T., 1985. Sources of acidification in Central Europe estimated from elemental budgets in small basins. *Nature*, Vol.315, No. 6014: 31-36.
- Paces, T., 1986. Weathering rates of gneiss and depletion of exchangeable cations in soils under environmental acidification. *Journal of the Geological Society, London*, Vol. 143: 1-5
- Parfitt, R., and J.M. Kimble, 1989. Condition for formation of allophane in soils. *Soil Sci. Soc. Am. J.* 53:971-977.
- Quantin, P., J. Balesdent, A. Bouleau, m. Delaune, and C. Feller, 1991. Premiers stades d'altération de ponces volcaniques en climat tropical humide (Montange Pelée, Martinique), *Geoderma* 50:125-148.
- Velbel, M.A., 1985. Geochemical mass balances and weathering rates in forested watersheds of the Southern Blue Ridge. *Am. J. of Sci.* 285:904-930.
- Verschuren, R.H., 1978. A microscope-mounted drill to isolate microgram quantities of minerals from polished thin sections. *Miner. Mag.* 42:499-503.
- Wada, K., 1989. Allophane and imogolite. p 1051-1087. In J.B. Dixon and S.B. Weed (ed), *Minerals in soil environment*. 2nd ed. SSSA Book Ser. 1. SSSA Madison WI, USA.
- Wada, K., O. Arnalds, Y Kakuto, L.P. Wilding, and C.T. Hallmark, 1992. Clay minerals of four soils in eolian and tephra materials in Iceland, *Geoderma*, 52: 351-365.

Figure 1. Organization levels in relation to observation scale, performed analysis techniques and sampling strategy.

Level	Scale (m)	Technique	Sampling strategy
Watershed, Landscape	km-m, 10^{+3}	Chemistry XRD Water analysis of drainage basin.	Bulksampling of soils/saprolites/rock
Catena, Pedon	m, 10^0	Morph.description XRD Chemistry	Naked eye Bulksampling of soil horizons
Soil micro aggregate, Individual constituents	$\mu\text{m } 10^{-6}$	Micromorphology SSXRD SEM-EDXRA	Undisturbed soil samples; Mineralogical micro sampling, disturbed, in situ Chemical micro sampling, undisturbed, in situ.
	nm 10^{-9}	TEM	chemical/ min. micro sampling undisturbed, in situ

SSXRD

Step Scan X-ray diffraction

SEM-EDXRA

Scanning electron microscopy + energy dispersive X ray analysis.

TEM

Transmission electron microscopy

XRD

X-ray diffraction

CHAPTER 2

WEATHERING OF PRIMARY MINERALS

- 2.1 Soil formation in a Quaternary terrace sequence of the Allier, Limagne, France. Macro- and micromorphology, particle size distribution, chemistry.

Geoderma, 49:215-239 (1991)

A.G. Jongmans, T.C.J. Feijtel, R. Miedema, N. van Breemen and A. Veldkamp.

Soil formation in a Quaternary terrace sequence of the Allier, Limagne, France. Macro- and micromorphology, particle size distribution, chemistry

A.G. Jongmans, T.C.J. Feijtel, R. Miedema, N. van Breemen and A. Veldkamp
*Department of Soil Science and Geology, Agricultural University Wageningen, P.O. Box 37,
6700 AA Wageningen, The Netherlands*

(Received April 10, 1990; accepted after revision January 31, 1991)

ABSTRACT

Jongmans, A.G., Feijtel, T.C.J., Miedema, R., van Breemen, N. and Veldkamp, A., 1991. Soil formation in a Quaternary terrace sequence of the Allier, Limagne, France. Macro- and micromorphology, particle size distribution, chemistry. *Geoderma*, 49: 215–239.

Soil formation in a terrace chronosequence of nine gravelly Quaternary terraces was studied, based on macro- and micromorphological, mineralogical, chemical, and physical characteristics.

Based on textural characteristics, the C horizon of the youngest soil appears to be representative for the parent material of lower B and C horizons in the youngest soils, and of all horizons in older soils. The parent materials contain a volcanic and a granitic component.

With increasing age of soils, the following stages of soil formation were observed: Holocene soils on lowest terraces show evidence for mixing of sedimentary layers by biological activity, resulting in texturally homogeneous A and B horizons. In the absence of periglacial processes, soil formation in Holocene and in Late Pleistocene terraces took place under continuously well-drained conditions.

Late Pleistocene soils on higher terraces show effects of clay illuviation, with prominent weathering features in A horizons.

Middle and Early Pleistocene soils on the highest terraces were influenced by periglacial conditions and display effects of various cycles of soil forming processes alternated with periglacial processes, increasing in complexity with age. Weathering of all minerals except quartz, neoformation of clay, and clay illuviation has resulted in distinct differentiation between sandy A and E horizons and a clayey B horizon. Periglacial processes during the Quaternary, weathering, clay formation and clay illuviation have caused a considerable compaction and decreased water permeability. This has resulted in imperfect drainage, now reflected by abundant, locally cemented, iron and manganese oxide segregations in the surface horizon, typical for surface water gley with evidence of ferrolysis. Ferrolysis, the increased weathering of clay under influence of alternating oxidation–reduction in the seasonally waterlogged surface soil, may have further contributed to the marked textural change between A and E versus B horizons. Easily weatherable minerals, observed in strongly leached surface layers of older end-members of the terrace sequence might be attributed to aeolian volcanic inputs.

The Holocene and Late Pleistocene soils are intensively used as arable land, as a result of the continuously well-drained conditions. On account of the poor drainage, the Middle and Early Pleistocene soils are used mainly for grassland and forest.

INTRODUCTION

Terrace sequences are particularly suitable for pedological studies because differences in soil development can be related to the factor time (Stevens and Walker, 1970). With increasing terrace age, the soils have been longer influenced by soil forming processes. Many terrace soil sequences, however, are not simple chronosequences (Chartres, 1980). Changes in environmental conditions like climate, vegetation and geomorphological processes over time influenced the nature and intensity of soil formation.

Before drawing definite conclusions about soil changes in chronosequences, the degree of uniformity of the parent materials needs to be established. Several sedimentological parameters describing the particle size distribution have been proposed to characterize the conditions under which soil materials were deposited (Barshad, 1967; Griffiths, 1967; Langohr et al., 1976). The particle size distributions and elemental chemical properties within and between soil profiles can provide valuable information about geogenetic and pedogenetic processes (Langohr et al., 1976; Torrent and Nettleton, 1979; Chittleborough et al., 1984).

Many pedogenetic studies of Quaternary soil sequences illustrate polycyclic

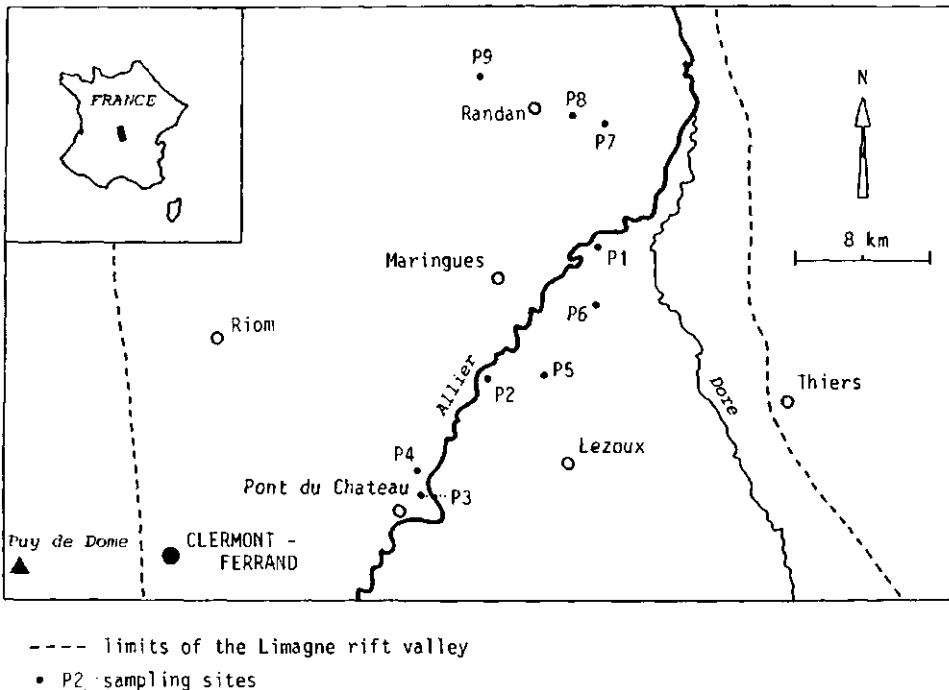


Fig. 1. Location of the sampling units in the Limagne Rift Valley.

soil development with increasing age of the soils (Bornand, 1978; Chartres, 1980; Macaire, 1986; Chittleborough et al., 1984). We investigated nine gravelly Quaternary Allier terraces in the Limagne Rift Valley, Massif Central, France (Fig. 1). Field observations revealed the following changes in soils of increasing age:

(1) increasing abundance of quartz and flint fragments and decreasing amounts of fresh granitic and volcanic fragments in A and E horizons; (2) vertical textural differentiation between sandy topsoils and clayey B horizons; (3) decreased biological activity and development of compacted B horizons; (4) the presence of many hard Fe-Mn concretions in albic E horizons, and vertical greyish tongues in underlying B horizons.

In a previous paper, Feijtel et al. (1988) described and discussed the genesis of Planosols in two older end-members of the Allier terrace sequence.

The goal of the present study is to assess the nature, intensity, mutual relationships, and the chronology of processes involved in the soils of the Allier terrace sequence by means of macro- and micromorphology, particle size distribution, and chemistry.

MATERIALS AND METHODS

Geology and soil site conditions

The terrace sequence comprises nine gravelly terrace levels (F1 through Fz) of the Allier in the Limagne Rift Valley formed from the Plio/Pleistocene to the Holocene period (Bouillet et al., 1972; Le Griel, 1983; Raynal, 1984; Pastre, 1986) (Fig. 1, Table 1).

Tertiary deposits consisting of sands, clays, marls and limestone underlie the 5 to 15 m thick terraces. Predominantly granite rocks of the Hercynic basement border the Limagne Rift Valley (Autran and Peterlongo, 1980). Tertiary and Quaternary volcanic deposits are present in and around the Limagne Rift Valley (Camus, 1975). All nine terraces contain various amounts of granite and volcanic fragments; limestone fragments are absent. Periglacial features like cryoturbation and frostwedges (French, 1976) were observed in excavations in several older terraces of the sequence.

All profiles are situated in a flat to almost flat position. Younger soils (P1 through P4) are well-drained and intensively used as arable land. The older soils (P6 through P9) are imperfectly drained and show seasonally wet A and E horizons and moist B horizons in late winter and spring, and are under grassland or forest. Soil P5 has intermediate characteristics, shows some evidence of imperfect drainage, and is used both as arable land and grassland.

Macro- and micromorphological methods

Based on field studies we selected from each terrace level (F1 through Fz)

TABLE I

Age, altitude, horizon development and classification of terraces and soils.

Profile	Terrace	Age	Altitude pr. riverbed ^a (m)	Horizon development	Classification (FAO, 1988)
P1	Fz	Holocene	0	A-Bw-C no-tc	Eutric Cambisol
P2	Fyz	Holocene	n.d.	A-Bw-C no-tc	Eutric Cambisol
P3	Fy	± 13.000 ^b	8	A-Bt(90 cm)-C mod-tc	Haplic Luvisol
P4	Fx	± 30.000 ^b	8-20	A-Bt(150 cm)-C mod-tc	Haplic Luvisol
P5	Fw	0.5 m.y. ^c	32-45	A-Eg-Btg (4 m) str-tc; a-tch	Eutric Planosol
P6	Fv	1.0 m.y. ^c	60-70	A-Eg-Btg (4 m) str-tc; a-tch	Eutric Planosol
P7	Fu	1.3 m.y. ^c	70-80	A-Eg-Btr (n.d.) str-tc; a-tch	Dystric Planosol
P8	Ft	1.7 m.y. ^c	90	A-Ems-Btg (4 m) str-tc; a-tch	Dystric Planosol
p9	Fl	± 2.4 m.y. ^d	100	A-Bh-Eg-Btg (n.d.) str-tc; a-tch	Dystric Planosol

^aAccording to Bouillet et al. (1972).^bAccording to Raynal (1984).^cAccording to Pastre (1986) (million years ± 0.1).^dAccording to Le Griel (1983).

no-tc=no textural contrast; mod-tc=moderate textural contrast; str-tc=strong textural contrast; a-tch=abrupt textural change; n.d.=not determined.

one representative soil profile. In addition to bulk samples for various analyses, a continuous sequence of undisturbed samples was taken for preparation of thin sections ($10 \times 10 \text{ cm}^2$) from each profile. Sampling and description of soils were done from pits and excavations. Soils were described and classified according to FAO (1977) and FAO (1988), respectively. Thin sections were prepared according to Fitzpatrick (1970) and described using the terminology of Bullock et al. (1985). Nature and amount of some important mineral grains and rock fragments were quantified by point counting of 500-700 points (ignoring both the $< 20 \mu\text{m}$ fraction and voids), giving a standard deviation of $< 4\%$ with 95% confidence limits (Van der Plas and Tobi, 1965). Similarly, quantification of illuviation clay coatings was carried out by point counting of 800 points, yielding a standard deviation of 2% at 95% confidence limits.

Particle size distribution analysis

Particle size distribution analysis was performed on duplicate samples of each horizon after sieving over a 2 mm sieve, removal of organic matter with 30% H₂O₂ and of carbonates with 0.2M HCL. Fractions > 2 mm were collected and weighed to determine the gravel content. The sand fractions > 50 μm (2000–1000, 1000–600, 600–420, 420–300, 300–210, 210–150, 150–105, 105–75, 75–50 μm) were collected by sieving on a Fritsch Analysette shaking apparatus. Fractions < 50 μm (50–32, 32–16, 16–8, 8–2, 2–0.2 μm) were determined with the pipette method after adding 4% sodium hexametaphosphate and 1% sodium hydroxide. The < 0.2 μm fraction was collected through centrifugation as follows: after shaking a suspension of the fraction < 50 μm and 1 hour of sedimentation, 200 ml of the supernatant suspension was pipetted into a centrifuge tube of 380 ml. Samples were centrifuged at 2500 rpm for the appropriate time to permit settling of fractions > 0.2 μm.

Chemical/mineralogical analysis

Clay fractions, (0.2–2 μm), fine clay (< 0.2 μm), and fine earth fractions (< 2 mm) were used for total analyses of major and minor elements by X-ray fluorescence on Li₂B₄O₇ glass disks. The fractions < 0.2 μm, < 16 μm, and < 50 μm of selected samples were analyzed similarly. The X-ray fluorescence system was calibrated using USGS geochemical standards as listed by Abbey (1980).

The clay fraction was dispersed by NaOH at pH 7–8. The elemental composition of the non-clay fraction was estimated from the clay content and the elemental compositions of fine earth and clay fraction, respectively (Barshad, 1967). Calculations of the mass fraction of elemental oxide components in % (EO) were performed according to:

$$\text{EO non-clay} = (\text{EO soil} \times 100 - \text{EO clay} \times \% \text{ clay}) / (\% \text{ non-clay})$$

Soil pH (1:2.5 in water and 0.01M CaCl₂) was determined by glass electrode; "free" Fe₂O₃ was extracted by Na-dithionite-EDTA at pH 4.5 (Begheyn, 1980). Exchangeable bases and CEC were determined by the modified Bascomb method according to Gillman (1979).

X-ray diffractograms were made of Mg-saturated clay samples before and after glycerol solvation, and of K-saturated clay after heating to different temperatures. Estimates of the relative amount of the different clay minerals present range from traces (±) to dominant (+++++).

RESULTS

Macromorphological data

Classification of soils, horizon development, age and terrace altitude with respect to the present-day riverbed are given in Table 1. Major macromorphological characteristics are shown in Table 2. With increasing age, soil colours in B horizons change from homogeneous brown to mottled grey, structures from subangular blocky to prismatic, consistence from friable to extremely firm, and worm activity decreases. P1 and P2 are texturally homogeneous soils down to 70 cm, with undisturbed sedimentary sand and gravel layers below 70 cm depth. All soil horizons contain fresh volcanic and granite fragments.

Soils P3 and P4 differ from P1 and P2 mainly by some textural differentiation between A and B horizons. Sedimentary stratification is absent in the upper 100 cm.

Soils P5 and P9 have a prominent textural contrast between sandy A and E versus clayey B horizons. Quartz, quartzite and flint occur in surface horizons increase in abundance with age, while contents of volcanic and granite fragments in A, E, and upper B horizons decrease with age (Table 2). Most of the granite fragments are friable, volcanic fragments are soft and show light grey coloured weathering rinds. Prominent iron and manganese mottling is present in albic E and greyish B horizons (10YR 5/2 to 5Y 7/2; Table 2). In P6 and P8 the Fe and Mn compounds are cemented. B horizons have vertical greyish-white tongues along weakly developed prismatic ped faces, that are lined with Fe oxides, and at some distance of the tongues, Mn oxides.

*Physical data**Comparative particle size distribution index*

The degree of uniformity of the parent materials was tested using a comparative particle size distribution index (CPSD; Fig. 2). The index is based on the method to superpose two particle size histograms, in order to measure the degree of similarity between them (Langohr et al., 1976). We used the CPSD index to compare all samples with the parent material of the youngest profile P1, indicated as profile 1 horizon No. 5 in Fig. 2. The degree of similarity between samples is expressed by the proportions of the matching parts. This allows for a so-called linkage grouping in which the indexes are ranked in descending order. The CPSD index was calculated for all 15 particle size classes, between 0.2 and 2000 μm (Fig. 2A) and for a limited data set involving the fractions between 50 and 600 μm only (Fig. 2B). Regardless of the data-set used, there appears to be a fairly good similarity between all samples from C and/or lower B horizons (horizon Nos. 4 and 5). Particle size distri-

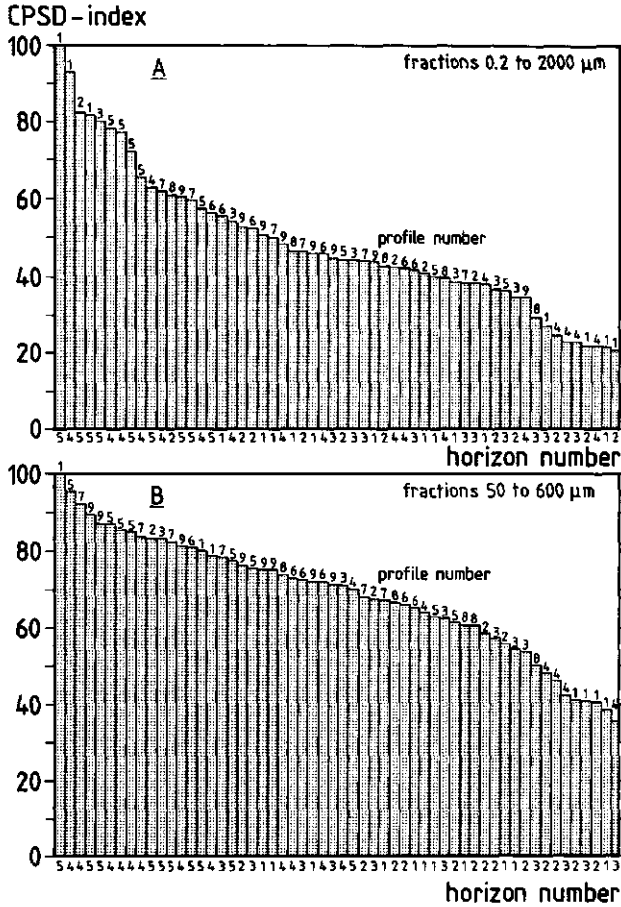


Fig. 2. Comparative particle size distribution index for the complete and a reduced data set.

bution of A, E, and upper B horizons in the older soils (profiles 6 to 9, horizon No. 1 to 3), differed considerably from that in the subsoil of profile 1 (horizon No. 5), as evidenced by CPSD indexes between 32 and 60 for the 0.2 to 2000 µm fraction. By using the 50 to 600 µm fraction, the CPSD index demonstrated values between 50 and 80. The greatest textural difference was found between the subsoil and surface horizons of profile 1 (CPSD index from 20 to 40).

Fine clay to total clay ratios, distribution and weathering of gravel

As soils get older, ratios of fine clay to total clay increase up to 0.8 and maxima shift to greater depth in the profile with increasing age (Fig. 3A, B).

Volcanic and granitic gravel (2 mm–7.5 cm) contents are high in the C horizon and lower B horizons of the youngest soils P1 through P4, and the

TABLE 2

Major macromorphological characteristics^a.

Profile	Horizon	Depth (cm)	Boundary	Colour (moist)	Texture	Coarse fragments	Structure	Consistence	Mottling	Worm casts	Cementation
P1	Ap	0	as	10YR 3/2	scl	sg ^b	QGB ^c	m fr	-	f ^d	-
	Bw	25	cw	10YR 4/2	l	sg	QGB	m fr	-	m	-
	Cl	70	as	10YR 7/2	ls	gr.	QGB	m v fr	-	f	-
	2C2	103/130		n.d.	ls	gr.	QGB	m l	-	-	-
P2	Ap	0	as	10YR 3/2	sl	sg	QGB	m fr	-	f	-
	Bw1	20	gs	10YR 4/2	sl	sg	QGB	m fr	-	m	-
	Bw2	60	gs	10YR 4/4	sl	sg	QGB	m fr	-	m	-
	BC	80	gs	10YR 4/4	ls	sg	QGB	m fr	-	f	-
	C1	120/150		10YR 5/4	ls	sg	QGB	m fr	-	-	-
P3	Ap	0	as	10YR 2/2	scl	sg	QGB	m fr	-	c	-
	Bt1	32	cs	10YR 3/2	l	sg	QGB	m fi	-	m	-
	Bt2	55	gs	10YR 3/2	l	sg	QGB	m fi	-	m	-
	Bt3	81	cs	10YR 4/4	sl	sg	QGB	m fr	-	m	-
	Bt4	103	gs	10YR 5/4	ls	sg	QGB	m v fr	-	c	-
	C1	120		n.d.	s	sg	QGB	m l	-	-	-
	Ap	0	as	10YR 3/2	sl	sg	QGB	d vh	-	m	-
P4	Bt1	20	gs	7.5YR 3/2	scl	sg	QGB	m v fi	-	f	-
	Bt2	35	cs	7.5YR 3/3	scl	sg	QGB	m v fi	-	f	-
	Bt3	60	gs	7.5YR 4/4	l	sg	QGB	m v fi	-	f	-
	Bt4	80	as	10YR 4/4	sl	sg	QGB	v.c.3pr	-	f	-
	Bt5	105	as	10YR 4/4	sl	vg	QGB	m fi	-	-	-
	C1	120		n.d.	-	vg	QGB	m l	-	-	-
P5	Ah	0	cs	10YR 3/2	scl	sg	QG	m v fr	-	-	-
	Eg	10	aw	10YR 4/2	scl	g	QGB	m v fr	-	c Fe Mn	-
	Btg1	30	cw	10YR 5/2	c	vg	QGB	m fi	-	m Fe Mn	-
	Btg2	50/120		10YR 5/4	scl/l/s	vg	QGB	m fi	-	c Fe	-

SOIL FORMATION IN A QUATERNARY TERRACE SEQUENCE

P6	Ap	0	as	10YR 4/2	sl	g	QG	cm	m fi	f Mn	-	-
	Eg	28	aw	10YR 5/2	sl	g	QG	cm	n d	m Mn Fe	-	cs
	Btg1	40	gs	5Y 5/1	c	sg	QGB	v.c.2pr	m fi	c Mn Fe	-	-
	Btg2	60	as	5Y 5/1	scl	sg	QGB	v.c.1pr	m fi	c Fe	-	-
P7	Btg3	80	as	5Y 5/1	scl	sg	QGB	cm	m fi	-	-	cw
	Btg4	84/120		10YR 3/3	sl	sg	QGB	cm	n d	-	-	-
	Ahg	0	cs	10YR 5/2	sl	g	QG	cm	m fr	c Fe Mn	-	-
	Eg	20	as	2.5YR 6/2	sl	sg	QG	cm	m fi	m Fe Mn	-	-
P8	Btr1	30	gs	5Y 6/2	c	g	QGB	v.c.2pr	m fi	c Fe	-	-
	Btg2	70	as	5Y 7/2	scl	sg	QGB	cm	m fi	m Fe	-	-
	Btg3	86/110		5Y 7/2	scl	vg	QGB	cm	n d	c Fe	-	-
	Ah	0	as	10YR 4/4	sl	g	Q	m.2sbk	m v fr	f Fe	-	-
P9	Eme	25	cs	10YR 6/2	ls	vg	Q	n.d.	n d	m Mn Fe	-	cs
	Eg	40	cs	5Y 5/1	scl	g	QG	c.1abk	m v fi	c Fe	-	-
	Btg1	60	n d	5Y 4/1	c	sg	QGB	v.c.2pr	m v fi	c Fe	-	-
	Btg2	80/110		5Y 4/1	c	g	QGB	v.c.2pr	m v fi	c Fe	-	-
P9	O	-7	as	7.5YR 3/4	-	-	-	cm	-	-	-	-
	Ah	0	aw	7.5YR 4/2	sl	g	Q	cm	n d	-	-	-
	Bh	1/3	cw	7.5YR 4/4	sl	g	Q	cm	m fr	-	-	-
	Eg1	6	gs	10YR 7/4	sl	g	Q	cm	m fr	-	-	-
P9	Btg1	25	aw	10YR 7/2	sl	g	Q	cm	m fr	c Fe	-	-
	Btg2	40	gs	5Y 6/3	c	g	Q	cm	m fi	m Fe	-	-
	Btg3	60/90		5Y 7/1	c	vg	QG	v.c.1pr	m fi	f Fe	-	-

^aAbbreviations according to Soil Survey Staff (1951, p. 139).

^bsg = slightly gravelly; g = gravelly; vg = very gravelly.

^cQ = Quartz; G = Granite; B = Basalt.

^df = few; c = common; m = many.

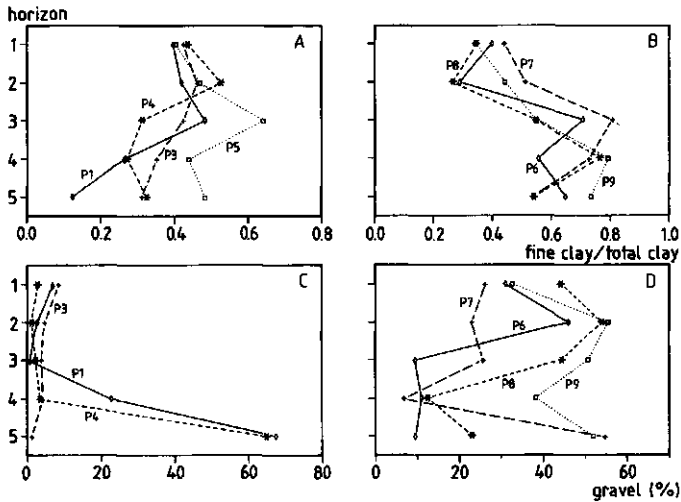


Fig. 3. Fine clay/total clay ratios with depth (A, B), and gravel content with depth (C, D).

older soils P6 through P9 (Fig. 3C, D). The older soils contain much gravel in the A and E horizons too, but this consists mainly of quartz, quartzite and flint.

Bulk densities

The average bulk densities in the B horizons of the nine profiles are for the P1 and P2 soils 1.3–1.5 g/cm³, for P3 and P4 1.2–1.5 g cm³, and for P5 to P9 1.7–1.9 g/cm³, respectively.

Chemical and mineralogical data

Geochemical variability of sediments

A principal component analysis was performed on the geochemical composition of the soils. In the *fine earth* fractions three factors accounted for more than 82% of the total geochemical variance (Table 3). The first factor, explaining 54% of the total variance, was strongly correlated with CaO, MgO, Na₂O, TiO₂ and to a lesser extent with Al₂O₃. The second principal component has a strong correlation with K₂O and SiO₂. Similar results were obtained when considering the *non-clay* fractions in order to account for possible interferences due to clay neoformation and clay illuviation (Table 3). The first factor then explains 62% of the total variance.

Selected chemical and mineralogical data

Selected chemical and mineralogical properties are given in Table 4. The

TABLE 3

Rotated factor patterns and regression for fine earth and non-clay geochemical fractions, respectively.

Variable	Fine-earth rotated pattern			Non-clay rotated pattern	
	F-1	F-2	F-3	F-1	F-2
SiO ₂	-0.42	0.77	-0.03	-0.67	-0.54
TiO ₂	0.83	-0.37	0.18	0.87	0.35
Al ₂ O ₃	0.68	-0.28	-0.18	0.93	-0.07
Fe ₂ O ₃	0.66	-0.46	0.45	0.64	0.66
MnO	0.10	-0.03	0.98	-0.04	0.72
MgO	0.87	-0.29	0.09	0.85	0.33
CuO	0.89	-0.12	0.14	0.90	0.28
Na ₂ O	0.82	0.30	0.20	0.86	-0.09
K ₂ O	-0.01	0.99	-0.06	-0.16	-0.84
<i>Variance (%) explained by each factor</i>					
	53.9	16.4	12.1	62.2	16.7
<i>Multiple regression analysis of principal components:</i>					
Factor-1 fine-earth	= 1.02 - 0.32 AGE + 0.18 HORIZON			$R^2 = 0.80^{**}$	
Factor-1 non-clay	= 0.98 - 0.33 AGE + 0.21 HORIZON			$R^2 = 0.82^{**}$	

surface horizons of the P1 through P4 soils are slightly acid, while in the lower horizons the pH_{H₂O} values increase to about 8. A and B horizons of the older profiles are moderately to strongly acid. An exception is P6 which has relatively high pH_{H₂O} values.

The average CEC of the B horizons in the P1 through P4 soils is 728 ± 166 (mmol_c/kg clay). The average CEC of the Eg + Btg1 and the Btg2 in the older soils P5 to P9 is 422 ± 67 and 557 ± 60 , respectively. The base saturation is high in the P1 to P6 soils, but decreases in the A, E, and upper B horizons of the older series.

The average of free iron content in the P1 through P4 soils is $2.7\% \pm 0.5$ without any depth trend. Higher free iron values, $5.2\% \pm 1.9$, occur in the Eg, Ems and/or Btg horizons of the soils older than P4.

In the fine earth, SiO₂ contents increase with age, while the inverse is true for MgO and CaO. In soils older than P3, Bt horizons show the lowest SiO₂ and the highest Al₂O₃ and Fe₂O₃ contents of all horizons, corresponding to higher clay contents.

The clay fraction of the youngest soils P1 and P2 contains mainly kaolinite and illite, with little smectite and vermiculite.

Smectite contents are low in the A and E horizons of the soils older than P4, and decrease with soil age in these horizons. Chlorites are present in small

TABLE 4

Selected chemical properties.

Profile	Horizon	Depth (cm)	Clay (%)	CEC (mmol ^c /kg soil)	Base sat. (%)	OM (%)	pH H ₂ O	pH CaCl ₂	m.fr. (%) of fine earth					MgO	Kaol. ^a	Ill.	Smect.	Chlorite
									SiO ₂	Al ₂ O ₃	Fe ₂ O ₃	CaO	CaO					
P1	Ap	0	19	117	100	1.2	6.8	6.6	63	15	6.1	2.3	2.0	++	++	±	-	
	Bw1	25	20	110	100	0.9	6.9	6.2	64	15	6.0	2.3	2.0	+++	+++	±	-	
	Bw2	50	15	77	100	0.5	7.0	6.2	67	14	5.3	2.1	1.9	+++	+++	±	-	
	C1	70	7	20	100	0.2	7.0	6.4	70	14	4.2	2.5	1.9	+++	+++	±	-	
	C2	60/103	1	19	100	0.2	7.0	6.4	73	12	4.0	1.5	1.8	nd	nd	nd	nd	
P2	Ah	0	19	136	100	1.6	6.8	6	64	14	5.7	2.2	1.9	+++	+++	+	-	
	Bw1	20	19	135	100	1.3	6.8	6.1	62	15	6.3	2.3	2.0	+++	+++	+	-	
	Bw2	60	16	126	100	0.8	7.0	6.5	64	15	5.8	2.4	2.0	+++	+++	+	-	
	BC	80	15	126	100	0.6	7.3	6.6	63	15	6.0	2.5	2.2	nd	nd	nd	nd	
	C	120/150	14	107	100	0.6	8.0	7.4	63	15	6.0	2.6	2.2	+++	+++	+	-	
P3	Ap	0	18	121	100	1.5	6.6	5.7	66	13	5.5	2.7	1.9	+++	+++	±	-	
	Bt1+2	32	28	169	100	0.7	7.4	6.5	63	15	6.4	2.8	2.0	+++	+++	±	-	
	Bt3	81	18	131	100	0.4	7.9	6.9	65	14	5.7	3.3	2.3	+++	+++	±	-	
	Bt4	103	7	80	100	0.2	8.0	6.9	68	13	5.2	3.4	2.4	+++	+++	±	-	
	C	120	2	38	100	0.2	8.0	7	72	11	4.1	3.3	2.3	nd	nd	nd	nd	
P4	Ap	0	15	57	100	0.8	6.4	5.6	69	13	5.1	1.6	1.3	+++	+++	±	-	
	Bt1+2	20	35	195	100	0.8	7.1	6.2	60	16	7.3	1.7	2.0	+++	+++	±	-	
	Bt3	60	28	188	100	0.7	7.4	6.6	62	16	7.4	2.5	2.4	+++	+++	+	-	
	Bt4	80	20	161	100	0.3	7.2	6.5	61	16	7.3	2.7	2.8	+++	+++	+	-	
	Bt5	105/120	11	91	100	0.3	7.6	6.6	62	13	8.1	3.6	3.5	nd	nd	nd	nd	
P5	Ap	0	21	122	91	3.0	5.1	4.7	68	12	3.9	0.7	0.7	+	+	+	±	
	Eg	10	20	91	100	1.6	5.7	5.0	70	12	4.5	0.7	0.7	+	+	+	±	
	Btg1	30	47	215	100	1.0	6.1	5.7	59	18	7.5	1.3	1.3	+	+	+	+	
	Btg2	50	24	160	100	0.3	6.7	5.9	62	14	9.2	1.6	1.6	+	+	+	+	
	Btg2	60/185	9	110	100	0.2	7.4	6.4	70	13	5.0	1.2	1.2	nd	nd	nd	nd	

SOIL FORMATION IN A QUATERNARY TERRACE SEQUENCE

P6	Ap	0	12	64	100	0.9	6.3	5.7	76	10	3.6	0.3	0.4	++	++	+	±
	Eg	28	16	71	100	0.1	6.4	6.0	70	12	6.5	0.3	0.4	+++	++	+	±
	Btg1	40	39	198	100	0.2	6.5	6.0	64	17	5.0	0.7	0.8	+++	++	+	-
	Btg2	60	29	155	100	0.2	6.2	5.8	64	18	4.6	0.8	0.7	+++	++	+	-
P7	Btg3	80	34	159	100	0.2	6.0	5.4	64	17	3.8	0.8	0.8	+++	++	+	-
	Btg4	84/120	21	107	100	0.1	6.0	5.1	57	17	3.8	0.9	0.7	nd	nd	+	nd
	Ahg	0	15	51	87	1.5	5.2	4.6	77	10	1.9	0.3	0.3	+++	++	+	±
	E	20	19	61	86	1.1	5.2	4.1	78	11	2.3	0.2	0.3	+++	++	+	-
P8	Btr1	30	49	236	69	0.4	4.6	3.9	67	16	5.2	0.3	0.9	+++	++	+	-
	Btg2	70	26	149	78	0.2	4.9	3.8	74	13	3.3	0.3	0.6	+++	++	+	-
	Btg3	86/110	24	190	85	0.1	4.9	3.5	71	13	5.3	0.3	0.7	+++	++	+	-
	Ah	0	19	52	48	2.9	4.9	4.0	73	10	3.1	0.1	0.3	+++	++	+	±
P9	Ems	25	10	26	69	0.4	5.3	4.5	70	9	9.9	0.0	0.4	+++	++	+	±
	Eg	40	28	79	57	0.4	5	4.0	72	13	4.5	0.1	0.6	+++	++	+	±
	Btg1	60	50	103	65	0.2	4.9	4.0	63	19	6.3	0.2	0.8	+++	++	+	±
	Btg2	80/110	33	167	76	0.2	5	4.0	66	16	5.2	0.4	0.7	+++	++	+	±
P9	O	-7	23	199	44	25.7	3.7	3.0	50	6	1.9	0.0	0.3	nd	nd	+	nd
	Ah	0	23	135	28	13.4	3.9	3.0	66	7	1.6	0.0	0.2	+++	++	+	-
	Bh+E	1/3	20	90	17	6.5	4.3	3.5	75	8	1.6	0.0	0.3	+++	++	+	-
	Btg1	25	31	128	26	0.8	4.6	3.7	75	11	2.9	0.0	0.4	+++	++	+	-
P9	Btg2	40	59	299	14	0.7	4.4	3.5	65	17	5.8	0.0	1.0	+++	++	+	-
	Btg3	60/100	36	210	19	0.3	4.5	3.5	73	14	3.1	0.0	0.7	+++	++	+	-

a-; not present; ± : traces to ++ : dominant; nd = not determined.

TABLE 5
Semi-quantitative analysis of major micromorphological observations.

Profiles	P1		P2		P3		P4		P5		P6		P7		P8		P9				
	Ap	Bw+C	Ap	Bw+C	Ap	Bt	Ap	Bt	C	A+E	Btg	C	A+E	Btg	C	A+E	Btg	C			
Horizons	0-23	-120	0-35	-80	0-32	-120	-140	0-28	-120	-200	0-30	-120	-400	0-30	-100	0-60	-110	-300	0-40	-130	-200
Depth (cm)																					
MICRO - STRUCTURE	<p>Subang-blocky: P1, P2, P3, P4, P5, P6, P7, P8, P9</p> <p>Sponge: P1, P2, P3, P4, P5, P6, P7, P8, P9</p> <p>Intergrain: P1, P2, P3, P4, P5, P6, P7, P8, P9</p> <p>Crack: P1, P2, P3, P4, P5, P6, P7, P8, P9</p>																				
VOIDS	<p>Biogenic: P1, P2, P3, P4, P5, P6, P7, P8, P9</p> <p>Fysicogenic: P1, P2, P3, P4, P5, P6, P7, P8, P9</p> <p>Clay + iron: P1, P2, P3, P4, P5, P6, P7, P8, P9</p>																				
FINE MATERIAL	<p>Clay + grainy aspects: P1, P2, P3, P4, P5, P6, P7, P8, P9</p> <p>Striated b - fabric: P1, P2, P3, P4, P5, P6, P7, P8, P9</p> <p>Type a: P1, P2, P3, P4, P5, P6, P7, P8, P9</p> <p>Type b: P1, P2, P3, P4, P5, P6, P7, P8, P9</p> <p>Type c: P1, P2, P3, P4, P5, P6, P7, P8, P9</p>																				
TEXTURAL PEDOFEATURES	<p>Type d: P1, P2, P3, P4, P5, P6, P7, P8, P9</p> <p>Type e: P1, P2, P3, P4, P5, P6, P7, P8, P9</p>																				
NEOFORMED PEDOFEATURES	<p>Fe + Mn nodules + hypo-coatings: P1, P2, P3, P4, P5, P6, P7, P8, P9</p>																				

----- few ——— common ——— many

amounts in the A horizons but are nearly absent in all underlying B horizons. Crystallinity of clay minerals was generally low, as indicated by XRD peak widths, especially in the upper horizons. Btg horizons of the soils older than P4 have lower contents of kaolinite and illite and higher contents of smectite.

Micromorphological data

In Table 5 major micromorphological properties are summarized. Three major groups of soils could be distinguished:

Group I, Profiles P1 and P2

Sponge microstructure dominates, with many channels and interconnected vughs in the B horizons.

All soil horizons contain unweathered volcanic and granitic fragments, alkali feldspars, plagioclase, pyroxene, and hornblende. Olivine grains demonstrate pellicular alteration, part of the biotite grains are exfoliated and iron-stained.

Group II, Profiles P3 and P4

Microstructure, voids, and mineralogical composition of the single and compound mineral grains are rather similar to those in group I. Partly weathered volcanic fragments with frayed surfaces occur, in particular the <200 μm fraction. Concentration of volcanic fragments increase with depth (Fig. 4). Isotropic, colourless, pendent coatings, with sizes up to 300 μm , identified by SEM-EDXRA as silica coatings were found at depths below 150 cm.

Microlaminated, orange yellow, limpid and dusty, strongly oriented coatings and infillings up to 500 μm thickness, and with silty impurities up to 20 μm in diameter (type *a* coatings) occur in B horizons (Fig. 5). The internal fabric of the coatings varies from parallel to convolute and cross-laminated. The profile clay illuviation index (Miedema and Slager, 1972) is 200% cm for the P3, and 1100% cm for the P4 soil, respectively. This index is defined as the sum of the percentages illuviated clay in each horizon and the horizon thickness, and expressed in per cent cm. Relatively few fragmented clay coatings occur.

Group III, Profiles P5 through P9

Crack microstructure with few skew and craze planes (Brewer, 1964) is dominant in B horizons. Excrement infillings are absent in these horizons (Table 5).

Fresh volcanic fragments predominantly consist of basalt with olivine and pyroxene phenocrysts and many small opaque iron minerals (<20 μm). Volcanic fragments are absent in the A horizons, their content in E and B horizons decreases with increasing soil age, while quartz contents in A and E horizons show an inverse relationship with depth and age. Granite fragments occur in the A horizon of P5, but are almost absent from A horizons of older soils, while the contents increase with depth in all older soils. Many volcanic

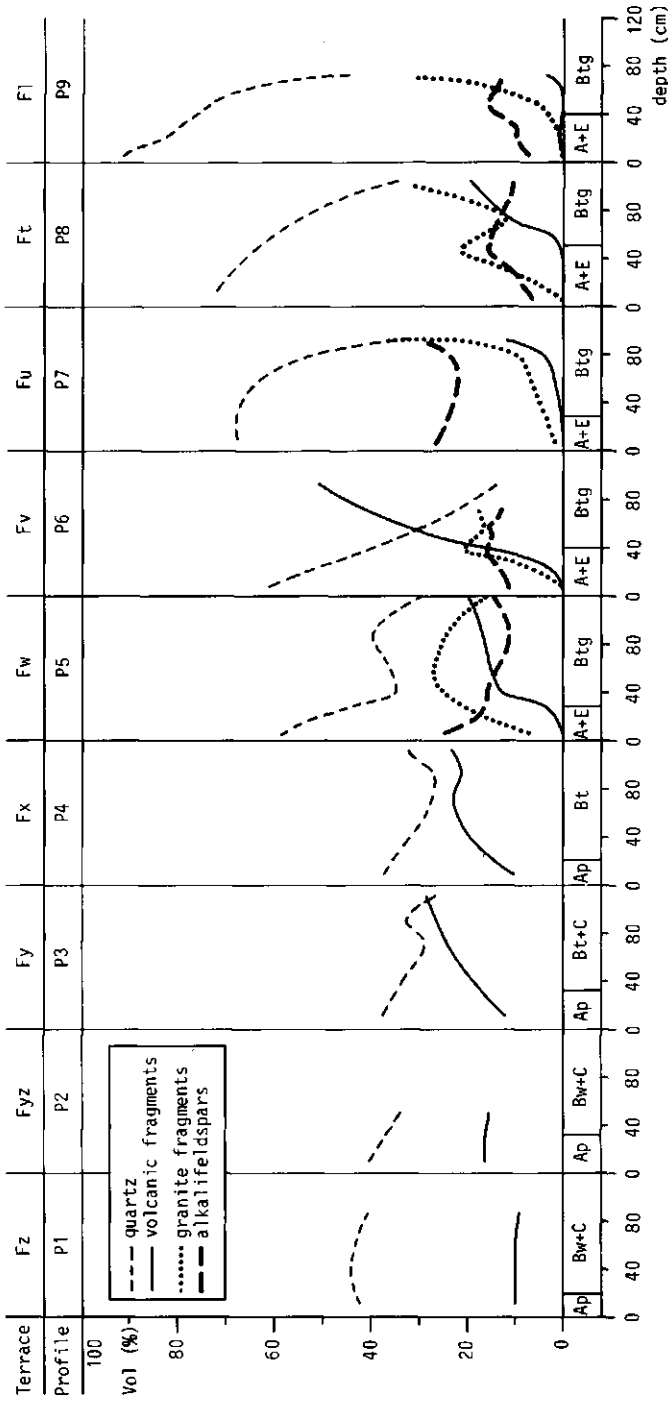


Fig. 4. Quantification (vol%) of quartz, volcanic fragments, granite and alkali feldspars on the solid mass (> 20 μm).

SOIL FORMATION IN A QUATERNARY TERRACE SEQUENCE

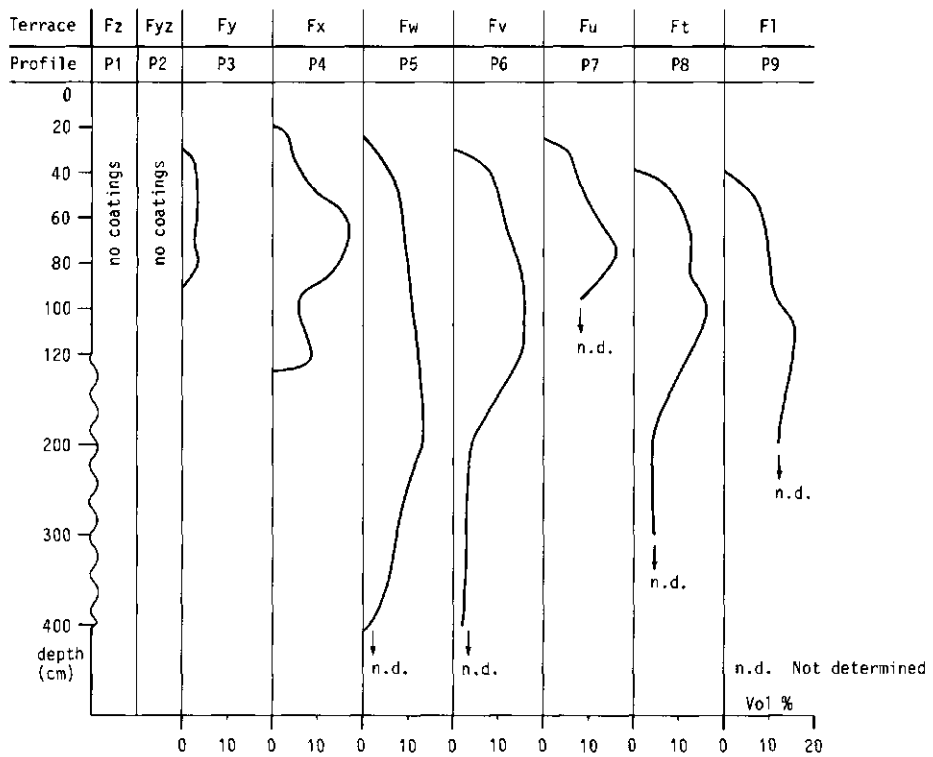


Fig. 5. Micromorphological quantification of clay illuviation type *a* coatings and limpid and dusty parts of type *b* clay coatings.

fragments have lost their original internal fabric and subrounded shape, and exhibit compressed structures and irregular shapes, suggesting fragmentation and deformation. The original nature of these fragments is still recognizable from the presence of clustered opaque iron minerals (Fig. 6, II). Totally altered fragments, with frequently well-developed b-fabrics, have become parts of the fine material (clay fraction), intensively mixed with coarse quartz, alkali feldspars and altered granite fragments. The granite fragments display irregular linear alteration and iron staining, predominantly along the micas. Altered granite breaks up into the elementary constituents quartz, alkali feldspar, biotite and muscovite as single mineral sand grains (Fig. 6, I). Single mineral grains of biotite, plagioclase, olivine, brownish hornblende and pyroxenes > 200 μm are absent in A and E horizons. Alkali feldspars exhibit pellicular irregular and crossbanded alteration patterns especially in A and E horizons. Many biotite and some muscovite grains show (thick) pellicular and parallel banded alteration patterns in B horizons. Their original interference colours shift to pale yellow and biotite grains appear to have partly

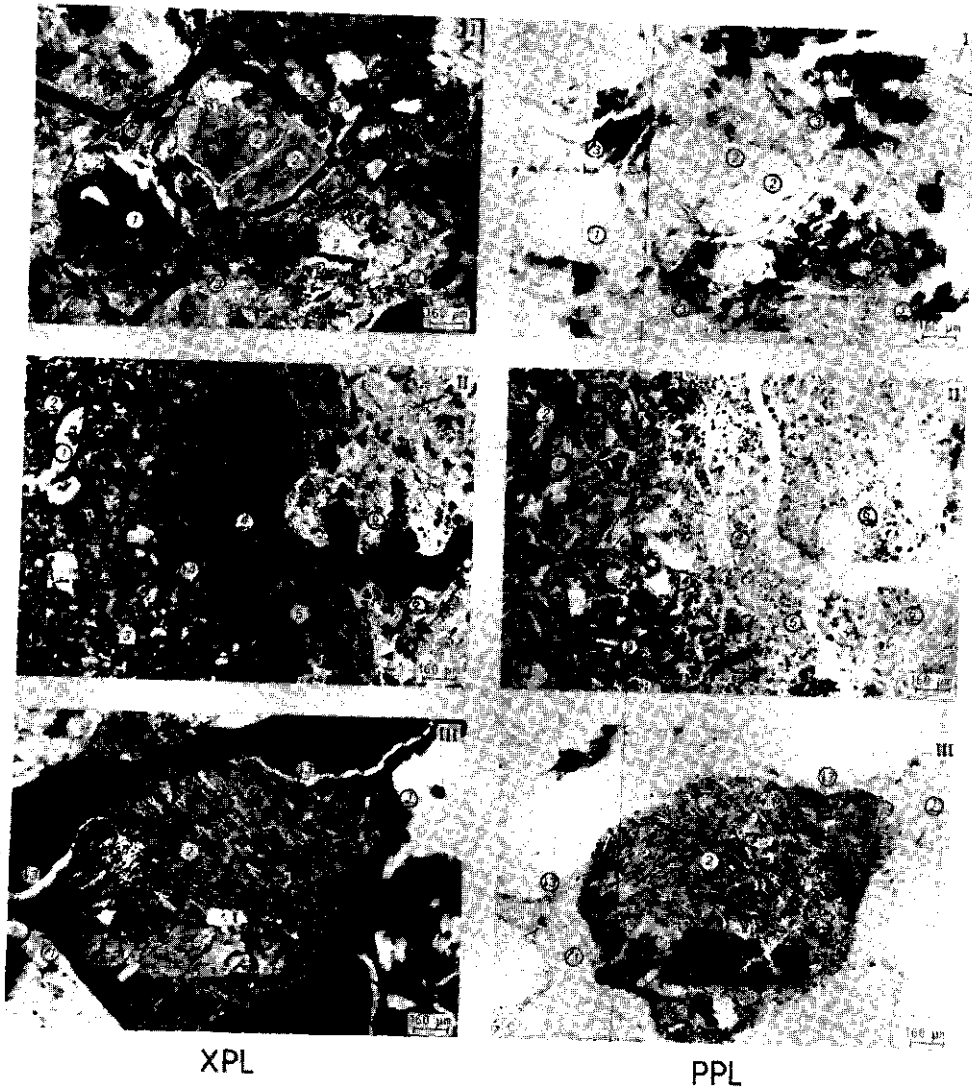


Fig. 6. Some important micromorphological features. (I) Partly alteration of granitic fragments into the elements constituents quartz (1), alkalifeldspar (2), iron-stained biotite (3), resulted into formation of sand-sized single mineral grains. (II) Partly altered volcanic fragments. The core still contains olivine phenocrysts (1) enveloped by iddingsite internal hypocoatings (2) in a fine groundmass consisting of volcanic glass, pyroxene and plagioclase (3); outer rind of the fragments demonstrates empty spaces of original olivines (4), absence of fine plagioclase, pyroxene and volcanic glass (5). Parts of the rind turn into fine material (clay fraction) (6). (III) Isotropic non-laminated neoformed type *d* coating (1), partly along fresh volcanic fragments (2), covered with an anisotropic iron-coating clay illuviation type *a* coating.

weathered to clayey material. The degree of alteration increases towards the soil surface and with increasing age of the soils (Table 2, Fig. 4).

The older soils also contain coatings of type *a* as described in the P3 and P4 soil. Colours are pale yellow to white in B horizons, but orange yellow in C horizons. In P5, P6, P8, and P9 coatings type *a* could be observed up to 4 m, 3 m, and 2 m, respectively, as a result of excavation depth. Based on the assumption that the occurrence of type *a* coatings ends in profiles P5 to P9 at 4 m, the calculated average profile clay illuviation index is $2500 \pm 400\%$ cm.

Compound layered, predominantly convolute and unsorted coatings, sometimes forming infillings, up to 1 mm thick, with variable amount of silt, clay and opaque iron minerals in clusters and streaks (type *b*), were found in soils P6 and P9, and to a lesser extent in P5.

Silty coatings and infillings up to 1 mm thick (type *c*), covering type *a* and *b* coatings occur in soils P6 through P9.

Limpid, non-laminated, unoriented, isotropic, coatings, up to 200 μm thick, pale yellow in plane polarized light (PPL) has been defined as type *d* (Fig. 6, III). In the C horizons of P6 and P8 at 4 m depth, these coatings are present in situ along all mineral grains, and in P6 they occupy 4% of the volume of the soil. In lower B horizons these coatings appear to be fragmented and deformed in between and partly along all mineral grains. Non-laminated, anisotropic, pale yellow, limpid clay coatings, up to 200 μm , moderately to strongly parallel oriented (type *e*) are present in upper B horizons. These coatings are fragmented and deformed and situated in between and partly along all mineral grains. Few, thin, in-situ coatings type *e* ($< 100 \mu\text{m}$) were observed in P5 and the younger P4 soil but exclusively around basaltic fragments. Coatings of types *d* and *e* may be present within one coating and are indistinguishable in PPL. In-situ coatings and fragmented parts of both types were covered by other textural pedofeatures.

Many manganiferous and ferruginous nodules and hypoc coatings are present in E and B horizons, covering clay coatings. The fine material in A and E in the greyish tongues in B horizons as well as many coatings of types *a*, *b* and *c* are distinctly isotropic and grainy in character ($< 5 \mu\text{m}$), with bright bluish reflections in incident light.

In the A and E horizons of P6 to P9, fine ($< 150 \mu\text{m}$) pellicular altered plagioclase, brownish hornblende and augite occurred frequently.

DISCUSSION

A comparative particle size distribution index higher than 70 suggests similarity, whereas values in excess of 85 indicate high similarity (Langohr and van Vliet, 1979; Chittleborough et al., 1984). Normalized CPSD indexes for the 50 and 600 μm fraction shows similarity values of 70% for all C and lower B horizons. Values calculated on the whole data-set will be affected by soil

forming processes (Langohr et al., 1976). Horizons affected by distinct clay eluviation and illuviation (horizons 1, 2 and 3) have values between 32 and 60 for the 0.2 to 2000 μm fraction. In conclusion, it appears that the C horizon of the youngest terrace P1 is texturally similar to highly similar to the parent material of the lower B and C horizons of the P1 to P4 soils and all horizons of the older soils. Greater similarity between samples least influenced by soil forming processes (horizon Nos. 4 and 5), illustrates effects of alteration and clay migration on particle size distributions, affecting clay, sand, and gravel fractions. The very low degree of similarity between the upper and deeper horizons of the youngest soils suggests fining-upward during sedimentation. The results of the principle component analyses of elemental oxides in the fine earth and non-clay fractions indicate that the parent material of all soils can be characterized by a volcanic (CaO , MgO , Na_2O , TiO_2 , Al_2O_3), and a granite (SiO_2 , K_2O) component.

Biological homogenization

The obliteration of sedimentary structures in the younger soils to depths of 70 cm (P1, P2) and 100 cm (P3, P4) respectively, the occurrence of sponge microstructures, many wormchannels and interconnected vughs indicate an intensive biological homogenization in the younger soils. Macro- and microstructures and void types indicate absence of earthworm activity in the older soils.

Weathering of primary- and formation of secondary minerals

In the P1 and P2 soils, macro- and micromorphology and chemical observations show little or no evidence of alteration of the single and compound mineral grains.

In the P3 and P4 soil, little biotite and olivine alteration occur. The relatively high quartz contents (Fig. 4), and partly weathered volcanic fragments in the surface horizons suggest selective weathering of small-sized volcanic fragments, and relative enrichment of quartz. Amorphous Si coatings below 150 cm depth points to secondary silica precipitation of dissolved silica, liberated by weathering at shallower depth.

The P5 to P8 soils contain strongly weathered volcanic and granite fragments and single mineral grains. Weathering intensity increases with soil age and extends over greater depths in the older endmembers (Fig. 4). Micro-morphological observations suggest that alteration of volcanic rock fragments and biotite are the main source of the clay fraction, while the alteration of granite fragments contribute to the sand fraction.

Single coatings containing both types *d* and *e*, indistinguishable in PPL, reveals that both coatings are genetically similar. The absence of crystalline

material in type *d*, and the presence of dominantly kaolinite in type *e* (Feijtel et al., 1989), the genetic similarity, and the non-laminated internal fabric suggest that both coating types resulted from weathering rather than from clay illuviation. Because they occur exclusively around basalt fragments in the P4 and P5 soils, basalt material is probably the source of the coatings.

Formation of textural contrasts

Increasing textural contrasts between A + E and B horizons as soils get older must be attributed in part to clay illuviation. Clay coatings of type *a* and the clayey parts of type *b* coatings are indeed characteristic for clay illuviation. With increasing soil age, the profile clay illuviation index increases strongly. The coarser parts of type *b* clay coatings are typical for sorting and accumulation processes due to micro-erosion of weakly stabilized aggregates. This process of internal colluviation may have been caused wholly or in part by saturated waterflow following snowmelt, (Van Vliet-Lanoë, 1975, 1988). The coatings and infillings of type *c* point to mass flow of soil material from A and E into B horizons, predominantly along cracks. Type *c* coatings cover coatings of types *a* and *b*, indicating that type *c* coatings are younger. Coatings of types *a*, *b* and *c* contribute to the marked textural differences between A and E versus B horizons. Large amounts of in-situ clay coatings in profile P4 revealed that biological homogenization took place before clay illuviation started.

Compaction

Physical data demonstrate distinctly higher bulk densities ($1.7\text{--}1.9\text{ g/cm}^3$) in B horizons in soils P5–P9, than in soils P1–P4 ($1.2\text{--}1.5\text{ g/cm}^3$). The dense material is characterized by deformed and fragmented volcanic and granite fragments, deformed and fragmented coatings of all types, mixed with single mineral grains and fine material having well-developed striated b-fabrics. The deformation and associated high bulk density are thought to be caused by periglacial processes during different periods of the Quaternary rather than swelling and shrinking processes (Feijtel et al., 1988; Miedema, 1987). Clay illuviation and internal colluviation may have further contributed to the high density of the B horizon. Clusters of fragmented coatings of types *a*, *b*, *d* and *e* in between coarse sand grains, which probably result from periglacial disturbance are covered by coatings of types *a* and *b*. These observations suggest that periglacial processes and clay illuviation alternated in time. Relatively low bulk densities ($1.2\text{ to }1.5\text{ g/cm}^3$ in B horizons) and predominantly intact type *a* clay coatings in P3 and P4 indicate that periglacial processes have not been active in these younger soils.

Surface water gleying

Uniformly brown matrix colours and absence of any segregation of Fe and Mn oxides in A and B horizons indicate that the soils P1 through P4 soils are well-drained, and lack temporary waterlogging. Macro- and micromorphological and chemical evidence of surface water-gley support that shallow groundwater perched on strongly compacted B horizons is a major aspect of soil formation in soils P5–P9. Because iron and manganese oxide mottling covers clay coatings, clay illuviation must have preceded surface water-gleying. Cementation by iron and manganese oxides of E horizons of the P6 and P8 profiles has further contributed to the already high bulk densities.

Ferrolysis

The grainy, isotropic character of many coating of types *a*, *b* and *c*, and occurrence of similar effects in the fine material of A, E, and in the greyish tongues of B horizons of soils P4–P9 must probably be ascribed to secondary silica formation during ferrolysis as described by Brinkman et al., 1973, and Brinkman, 1979. Chlorites in eluviated horizons (Table 4) were probably formed by interlayering of smectite during ferrolysis. Ferrolysis is absent in the younger P1 to P4 soils, is observed only in the lower E horizons of the P5 soil, and occurs more prominently and to greater depth in the B horizons of the successive older soils P6–P9.

Rejuvenation

The presence of easily weatherable minerals like plagioclase, augite, brownish hornblende in the old surface horizons of P6 to P9 indicates a rejuvenation by late Quaternary volcanic eruptions in and along the Rift Valley (Gewelt and Juvigné, 1988; Lenselink et al., 1990). The size of the mineral grains never exceeds 150 μm , which also points to an aeolian origin.

CONCLUSIONS

The soils in the chronosequence can be divided into three major groups on the basis of pedogenesis.

The Holocene P1 and P2 soils of group I show the formation of an A1 horizon with biological homogenization as the main process, and little (no) evidence of other soil forming processes.

The Late Pleistocene soils P3 and P4 group II show (1) biological homogenization to a greater depth, (2) pronounced mineral weathering in the A horizons and (3) distinct clay illuviation. Groups I and II showed soil for-

mation under continuously well-drained conditions as a result of absence of compaction by periglacial processes.

Group III comprises the Middle and Early Pleistocene soils P5–P9, which display distinct polycyclic soil formation, increasing in complexity with age. All mineral grains except quartz show signs of strong weathering, increasing in intensity with depth and age. The originally sandy and gravelly deposits have been transformed into a clayey substrate by neoformation of clay from volcanic fragments. Granite fragmentation contributes to the sand fraction.

Evidence of clay illuviation is more pronounced and present to greater depths in soils of group III than in soils of group II. Clay illuviation, weathering and clay neoformation contribute to the textural differentiation of soil horizons. Periglacial disturbance of the soil alternated with periods characterized by soil formation like weathering, clay neoformation and clay illuviation. Periglacial processes further increased strong soil compaction caused earlier by weathering, clay neoformation and clay illuviation. Decreased permeability following clay formation, clay illuviation and compaction gave rise to seasonal waterlogging, resulting in surface water-gley. Surface water-gley in turn favoured ferrollysis, which became more pronounced and extended to greater depth with increasing age of the soils and further contributed to the marked textural horizon differentiation of the soils of group III.

Finally, rejuvenation from wind-blown ejecta enriched the strongly leached top soils of group III.

ACKNOWLEDGEMENTS

The authors wish to thank Mr. O.D. Jeronimus for the preparation of thin sections. We are indebted to project coordinator Prof. Dr. S.B. Kroonenberg for his continuous support.

REFERENCES

- Abbey, S., 1980. Studies in "standard samples" for use in the general analysis of silicate rocks and minerals. Part 6: 1979 edition of usable values. *Geol. Surv. Can. Pap.*, 80-14: 30 pp.
- Autran, A. and Peterlongo, J.M., 1980. Le Massif Central. In: C. Lorenz (Editor), *Géologie des Pays Européens - France, Belgique, Luxembourg*. Dunot, Paris, pp. 3–123.
- Barshad, I., 1967. Chemistry of soil development. In: F.E. Bear (Editor), *Chemistry of the Soil*. Reinhold, New York, pp. 1–70.
- Begheyn, L., 1980. *Methods of Chemical Analysis for Soils and Waters*. Agricultural University Wageningen, Wageningen, 100 pp.
- Bornand, M., 1978. *Altération des Matériaux Fluvio-Glaciaires. Genèse et Evolution des Sols sur Terraces Quaternaires dans La Moyenne Vallée du Rhône*. Thèse Doctorat d'Etat-USTL, Languedoc; Publ. SES-INRA Montpellier, 329 pp.
- Bouillet, R., Giot, D. and Jeambrun, M., 1972. Carte Géologique Thiers XXVI-31, à l'échelle 1 : 50,000. Bureau de Recherches Géologiques et Minières, Orléans, 50 pp.

- Brewer, R., 1964. *Fabric and mineral Analysis in Soils*. Wiley, New York, 470 pp.
- Brinkman, R., 1979. Ferrollysis: A soil forming process in hydromorphic conditions. Doctoral thesis, Wageningen Agric. Res. Rept. 887, 106 pp.
- Brinkman, R., Jongmans, A.G., Miedema, R. and Maaskant, P., 1973. Clay decomposition in seasonally wet, acid soils: micromorphological, chemical and mineralogical evidence of individual argillans. *Geoderma*, 10: 259–270.
- Bullock, P., Fedoroff, N., Jongerius, A., Stoops, G. and Tursina, T., 1985. *Handbook for Soil Thin Section Description*. Waine Research Publications, England, 150 pp.
- Camus, G., 1975. *La Chaîne de Puys. Etude structurale et Volcanologique* Thèse Doctorat, Université de Clermont Ferrand, 321 pp.
- Chartres, C.J., 1980. A Quaternary soil sequence in the Kennet Valley, central southern England. *Geoderma*, 23: 125–146.
- Chittleborough, D.J., Walker, P.H. and Oades, J.M., 1984. Textural differentiation in chronosequences from eastern Australia I. Description, chemical properties and micromorphology of soils. *Geoderma*, 32: 181–202.
- FAO, 1977. *Guidelines for Soil Profile Description*. FAO, Rome, 2nd ed.
- FAO, 1988. *Revised Legend of the FAO–UNESCO Soil Map of the World* FAO, Rome, 109 pp.
- Feijtel, T.C., Jongmans, A.G., van Breemen, N. and Miedema, R., 1988. Genesis of two Planosols in the Massif Central, France. *Geoderma*, 43: 249–269.
- Feijtel, T.C., Jongmans, A.G. and van Doesburg, J., 1989. Identification of clay coatings in an older Quaternary terrace of the Allier, Limagne, France. *Soil Sci. Soc. Am. J.*, 53(3): 876–881.
- Fitzpatrick, E.A., 1970. A technique for the preparation of large thin sections of soils and consolidated material, In: D.A. Osmond and P. Bullock (Editors), *Micromorphological Techniques and Application*. Techn. Monogr. 2. Soil survey of England and Wales, Rothamsted Exp. Sta., Harpenden, pp. 3–13.
- French, H.M., 1976. *The Periglacial Environment*. Longman, London, 309 pp.
- Gewelt, M. and Juvigné, E., 1988. Tephrochronologie du tardiglaciaire et de l'holocène dans le Cantal, le Cézallière et le Mont Dore (Massif Central, France): Résultats nouveaux et synthèse, *Bull. Assoc. Fr. Etude Quat.*, 1: 25–34.
- Gillman, G.P., 1979. A proposed method for the measurement of exchange properties of highly weathered soils. *Aus. J. Soil Res.*, 17: 129–139.
- Griffiths, J.C., 1967. *Scientific Method in Analysis of Sediments*. McGraw-Hill, New York, N.Y., 508 pp.
- Langohr, R. and van Vliet, B., 1979. Clay migration in well to moderately well drained acid brown soils of the Belgian Ardennes: morphology and clay content determination. *Pédologie*, 29: 367–385.
- Langohr, R., Scoppa, C.O. and van Wambeke, A., 1976. The use of a comparative particle-size distribution index for the numerical classification of soil parent materials: application to Mollisols of the Argentinian pampa. *Geoderma*, 15: 305–312.
- Le Griel, A., 1983. Age et principales étapes du dépôt des sables et argiles du Bourbonnais. *Rev. Geol. Dyn. Geogr. Phys.*, 24: 425–433.
- Lenselink, G., Kroonenberg, S.B. and Loison, G., 1990. Late Weichselian and Holocene paleoenvironments in the Artière basin in the western Limagne rift Valley, Central Massif, France. *Quaternaire*, 2: 139–156.
- Macaire, J.J., 1986. Sequence of polygenetic soils formed in Plio–Quaternary alluvial deposits in the southwestern Paris Basin (France). Paleocological significance. *Catena*, 13: 29–46.
- Miedema, R. and Slager, S., 1972. Micromorphological quantification of clay illuviation. *J. Soil Sci.*, 23(3): 309–314.
- Miedema, R., 1987. *Soil Formation, Microstructure and Physical Behaviour of Late Weichse-*

SOIL FORMATION IN A QUATERNARY TERRACE SEQUENCE

- lian and Holocene Rhine Deposits in The Netherlands. Doct. Thesis, Agric. University Wageningen, Wageningen, 339 pp.
- Pastre, J.F., 1986. Altération et paleoaltération des minéraux lourds des alluvions Pliocènes et Pleistocènes du bassin de l'Allier (Massif Central, France). *Bull. Assoc. Fr. Etude Quat.*, 3/4: 257-269.
- Raynal, J.P., 1984. Chronologie des basses terraces de l'Allier en Grande Limagne (Puy de Dôme, France). *Bull. Assoc. Fr. Etude Quat.*, 1: 79-84.
- Soil Survey Staff, 1951. *Soil Survey Manual*. USDA. Handbook 18. US Government Printing Office, Washington, DC.
- Stevens, P.R. and Walker, P.H., 1970. The chronosequence concept and soil formation. *Q. Geol. Assoc.*, 72: 415-426.
- Torrent, J. and Nettleton, W.D., 1979. A simple textural index for assessing chemical weathering in soils. *Soil Sci. Soc. Am. J.*, 43: 373-377.
- Van der Plas, L. and Tobi, A.C., 1965. A chart for judging the reliability of point counting results. *Am. J. Sci.*, 263: 87-90.
- Van Vliet-Lanoë, B., 1975. Frost effects in Soils. In: J. Boardman (Editor), *Soils and Quaternary Landscape Evolution*: Wiley, Chichester, pp. 117-158.
- Van Vliet-Lanoë, B., 1988. *Le rôle de la glace de ségrégation dans les formations superficielles de l'Europe de Ouest*. Thèse de doctorat d'état. Université de Paris I-Sorbonne, 854 pp.

2.2 Alkalibasalt weathering in Quaternary Allier river terraces, Limagne, France.

Soil Sci. Soc. Am. J. 54:1043-1048 (1990)

E. Veldkamp, A.G. Jongmans, T.C.J. Feijtel, A. Veldkamp, and N. van Breemen.

Alkali Basalt Gravel Weathering in Quaternary Allier River Terraces, Limagne, France

E. Veldkamp, A. G. Jongmans,* T. C. Feijtel, A. Veldkamp, and N. van Breeman

ABSTRACT

Weathering of alkali basalt pebbles was studied in three Quaternary Allier terraces of different ages. The isovolumetric method and Ti-constant method were applied to quantify compositional changes due to weathering. Bulk density of fresh gravel in the younger terraces (Weichselian and Holocene) was adequately estimated from geochemical data by a multiple linear regression model ($R^2 = 0.81^{**}$, significant at $P = 0.01$). Since no chemical and micromorphological differences could be demonstrated between fresh gravel and the unweathered cores of partly weathered gravel, the regression model was also applied to calculate the bulk density of the cores of partly weathered pebbles in the older terraces. The decrease in bulk density of the rind, compared with that of the core, was used as a measure of weathering intensity. The chemical composition of the weathering rind revealed a relative increase in the contents of Ti, Al, Fe, and Mn and a decrease of K, Na, Ca, and Si. Changes were estimated considering Ti essentially immobile. Except for Fe and Mn, all elements tended to decrease in the rind. The relative elemental mobilities were as follows:



No relationship was found between weathering intensity and the age of the two oldest terraces or sampling depth. Differences in weathering intensity are predominantly a function of chemical (= mineralogical) composition of the alkali basalt pebbles.

ABSOLUTE CHEMICAL CHANGES are important to characterize the degree of weathering of rocks or sediments. Colman (1982) considered three methods to calculate absolute changes in elemental occurrences: the standard-cell-cations method, the isovolumetric method, and the Ti-constant method. The isovolumetric method has been used by many authors (e.g., Hendricks and Whittig, 1968; Trescases, 1975; Gardner et al., 1978; Eggleton et al., 1987). This method, introduced by Millot and Bonifas (1955), is based on the assumption that a unit volume of weathered rock has evolved from an equivalent volume of fresh rock. The method uses bulk density to convert mass percentage data to weight per unit volume. Until now, the isovolumetric method has been used only to quantify changes in weathering rock in situ. The method has not been applied to quantify elemental changes in sediments with heterogeneous parent material. The objective of this study was to quantify the elemental changes due to weathering of alkali basalt pebbles in three Quaternary Allier terraces of different ages. We

Dep. of Soil Science and Geology, Agric. Univ. Wageningen, P.O. Box 37, 6700 AA Wageningen, the Netherlands. Contribution of the Dep. of Soil Science and Geology, Agric. Univ. Wageningen. Received 5 July 1989. *Corresponding author.

Published in Soil Sci. Soc. Am. J. 54:1043-1048 (1990).

used the isovolumetric method, in combination with the Ti-constant method.

The youngest Holocene (Fz) terrace was used as a geochemical, physical, and mineralogical reference for the other samples on the assumption that weathering has not influenced the pebbles in this terrace yet. This seems justified, since Jongmans et al. (unpublished data) report only biological activity and alteration of single biotite grains in the ground mass in the Fz-terrace deposits.

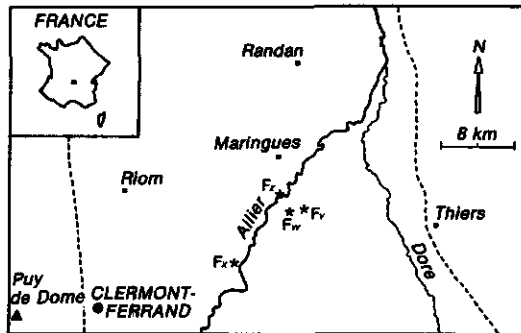
MATERIALS AND METHODS

Sites and Sampling

The Allier basin is comprised of the Limagne Rift valley (France) and surroundings, where extensive volcanic deposits occur. The Allier river terraces contain appreciable amounts of volcanic particles, including alkali basalt fragments. About nine main terrace levels (F1 through Fz) have been formed by the Allier (Bouillet et al., 1972). Terrace ages range from Holocene (Fz) to about 10^6 yr before present (Fv) (Pastre, 1986). Alkali basalt pebbles were collected from Fz, Fx, Fw, and Fv terraces of the Allier (Fig. 1). The soils developed in the terrace deposits are Distric Fluventic Eutrochrepts (Fz), Mollic Hapludalfs (Fx), and Typic Albaqualfs (Fw and Fv). Randomly distributed 60 by 10 cm rectangles were sampled at depths of 0 m (Fz = face of the present river bed) and 2 and 5 m (Fx, Fw, and Fv). To diminish the longitudinal sorting effect (Kroonenberg et al., 1988), the pebbles were sampled in a cross-valley transect.

Laboratory Analyses

After weighing, the pebbles from the weight class of 25 to 55 g were selected and bulk density measured using the clod method (Black et al., 1965). Total elemental analyses of the



--- limits of the Limagne rift valley
* sampling sites

Fig. 1. Location of sampling sites.

pebbles were performed by x-ray fluorescence (XRF) on $Li_2B_4O_7$ glass disks and presented as mass fractions of oxide components. Iron has been reported as Fe_2O_3 , although actually both Fe_2O_3 and FeO are present. The XRF system is calibrated using USGS geochemical standards as listed by Abbey (1980). If present on the pebbles of the older (Fw and Fv) terraces, the rind was mechanically removed and both rind and core were analyzed separately ($N = 21$). Final classification of all pebbles was based on the chemical composition of the core, by plotting SiO_2 against $Na_2O + K_2O$ (Cox et al., 1979). Only the pebbles classified as alkali basalts were used for further examination in the study. For the alkali basalts, twenty pebbles were randomly selected, and polished thin sections were prepared and left uncovered for analysis. Mineralogical composition of the pebbles was estimated by counting 800 points (van der Plas and Tobi, 1965).

A multiple-regression model was developed to estimate bulk density of unweathered pebbles based on their chemical

composition. The volume (V) occupied by the core (c) and rind (r) was estimated by counting about 800 points on a polished cross section of the pebble. The bulk density (D) of the weathered rind was calculated ($M = \text{mass}$, $t = \text{total}$):

$$D_t = M_t/V_t$$

$$D_r = M_r/V_r = (M_t - M_c)/V_r = (V_t D_t - V_c D_c)/V_r$$

The D_c in weathered pebbles (with rind) was estimated with the use of the multiple-regression model based on the relationship between D_c and chemical composition of the unweathered pebbles. The quantity of each element leached from the rind was calculated from the element/Ti ratios in both core and rind, assuming the amount of Ti to be constant. Statistical analyses were performed with SPSS/PC (Norusis, 1986).

RESULTS AND DISCUSSION

Morphological and Mineralogical Characteristics

Fresh alkali basalt pebbles were dark blue to black and weathered pebbles had grey to white patina rinds up to several millimeters thick. The boundary between rind and core was sharp but irregular (Fig. 2). This irregularity was apparently caused by microcracks resulting in differences in porosity.

Pebbles were holocrystalline or hypocrySTALLINE (volume of glass ranges from 3–28%). The texture was porphyritic with phenocrysts of olivine and clinopyroxene (<300 μm in diam.) embedded in a groundmass of microcrystalline plagioclase, pyroxene, and opaque minerals (mainly ilmenite and magnetite) as well as isotropic glass (Fig. 3). Nepheline minerals were found in some of the pebbles. Several pebbles had irregularly shaped (50–200 μm in diam.) calcite crystals.

In the Fz and Fx pebbles and in the pebble cores of Fv and Fw, alteration was restricted to thin (15- μm) translucent-yellow to reddish-brown coatings around olivine phenocrysts, similar to the so-called "iddingsite" coatings reported by Delvigne et al. (1979). Various authors (e.g., Wilshire, 1958; Eggleton et al., 1987) have reported that this mineral probably formed during final cooling of the basalt lava. In the pebbles, the thickness of these coatings increased closer to their

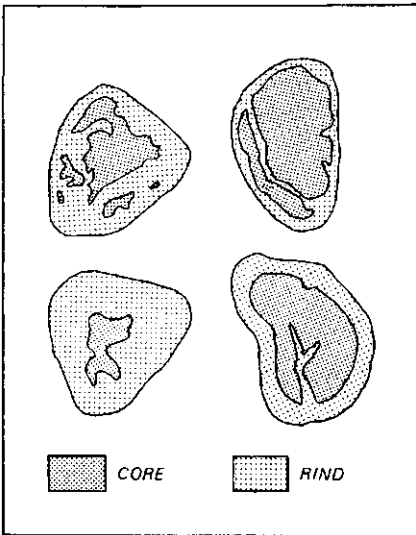


Fig. 2. Cross sections of some pebbles, showing irregular boundary between rind and core.

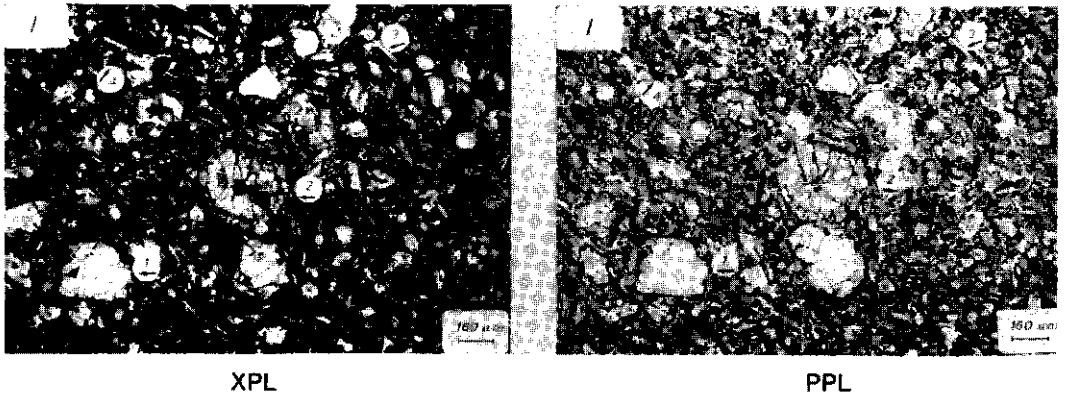


Fig. 3. Unweathered core of an alkali basalt in Fw terrace with olivine (1) and pyroxene (2) phenocrysts embedded in a fine-grained groundmass consisting of olivine, pyroxene, plagioclase (3), opaque Fe minerals (4) and glass. XPL = crossed polarized light, PPL = plane polarized light.

outer surface (Fig. 4 and 5), suggesting some alteration due to weathering. Three different alteration zones were recognized in the microcrystalline groundmass of the weathering rind. Each zone was characterized by the alteration of specific minerals. Micromorphologically, the boundary between core and rind showed an alteration of pinkish-brown isotropic glass to pale yellow (an)isotropic material (Fig. 4). In the weathering rind, olivine and pyroxene and, to a lesser extent, plagioclases had been partly or totally replaced or dissolved without changing the volume or shape of the pebble. The calcite in the rinds was coated or totally impregnated with Fe oxides and apparently protected from further weathering. Precipitates of Fe and Mn

oxides were also observed elsewhere in the rinds (Fig. 5).

Factors Affecting Bulk Density

To obtain insight into the factors that affect bulk density of the pebbles, a principal component analysis was performed on 20 randomly selected pebbles of the Fx and Fz terraces. The chemical data and bulk densities are summarized in Table 1. Principal-component analysis of the bulk density and elemental and mineral composition of the Fz and Fx pebbles ($n = 20$) shows that three components accounted for 68.6% of the variability (Table 2).

The first principal component explained 30.4% of

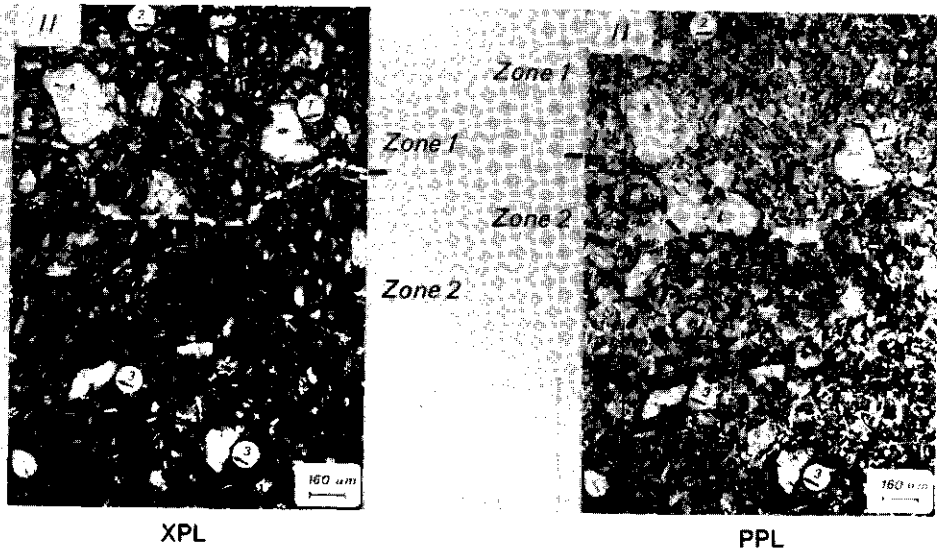


Fig. 4. Transition zone between unweathered core (Zone 1) and weathered rind (Zone 2). Zone 1 displays olivine phenocrysts with thin coatings of iddingsite (1), and unaltered glass (2). Zone 2 demonstrates distinct coatings of iddingsite (3) and altered glass, giving the groundmass a darker appearance (Fe impregnation). XPL = crossed polarized light, PPL = plane polarized light.

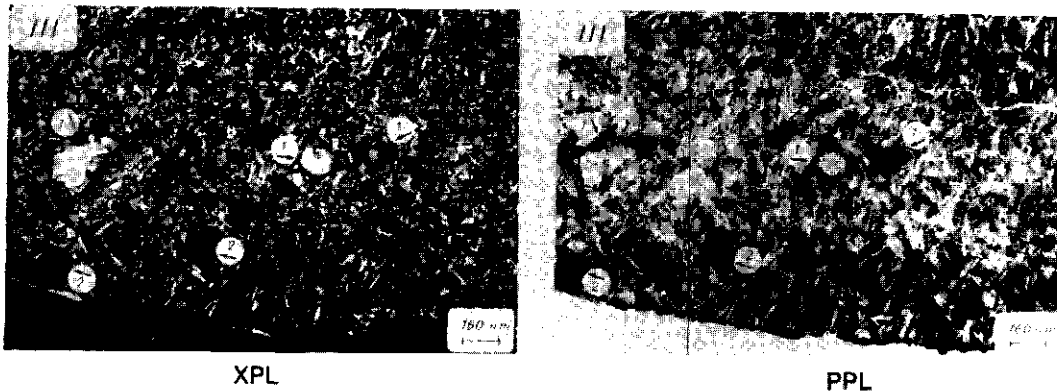


Fig. 5. Weathered rind of the alkali basalt, showing thick iddingsite coatings (1) and Fe-oxide pseudomorphs (2). Close to the pebbles' surface, an increase of Fe compound occurs, as well as a decrease in fine plagioclase microcrystals. XPL = crossed polarized light, PPL = plane polarized light.

Table 1. Chemical composition of alkali basalt gravel collected from four river terraces (Fz, Fx, Fw, and Fv).†

	Fz (n = 15)		Fx (n = 22)		Core Fw (n = 9)		Core Fv (n = 14)		Rind Fw (n = 9)		Rind Fv (n = 14)	
	Mean	SD	Mean	SD	Mean	SD	Mean	SD	Mean	SD	Mean	SD
	% (w/w)											
SiO ₂	45.8	1.6	45.1	2.2	44.5	2.1	44.7	1.1	42.2	2.2	42.5	1.5
TiO ₂	2.7	0.3	3.0	0.3	2.6	0.3	2.7	0.3	2.9	0.3	3.0	0.3
Al ₂ O ₃	14.1	0.8	15.0	1.8	15.4	1.2	14.6	0.9	16.0	1.9	15.1	1.1
Fe ₂ O ₃	12.0	0.5	11.6	0.9	12.1	1.4	12.5	0.7	13.3	1.7	14.0	1.1
MnO	0.2	0.0	0.2	0.0	0.2	0.0	0.2	0.0	0.2	0.0	0.2	0.0
MgO	8.4	2.6	7.0	2.7	8.0	2.2	9.0	1.6	8.0	2.4	8.8	1.7
CaO	10.4	0.9	10.7	1.3	10.6	0.9	10.6	0.7	10.7	0.7	10.7	0.7
Na ₂ O	2.4	0.3	2.6	0.5	2.0	0.8	2.1	0.4	1.0	0.4	1.1	0.4
K ₂ O	1.5	0.4	1.5	0.5	1.4	0.8	1.6	0.4	0.6	0.8	0.4	0.3
P ₂ O ₅	0.7	0.3	1.0	0.3	0.9	0.3	0.8	0.3	1.0	0.3	0.8	0.3
LOI‡	1.0	1.1	1.6	1.1	2.2	1.0	1.4	0.6	3.6	1.8	3.1	0.8
Bulk density	3.0	0.1	2.9	0.1	2.7	0.1	2.7	0.1	n.d.	n.d.	n.d.	n.d.

† Terrace ages range from holocene (Fz) to about 10⁶ yr (Fv).

‡ LOI = loss on ignition.

Table 2. Principle-component analysis of bulk density and elemental and mineralogical composition (n = 20). Principal-component extraction after varimax rotation.

	Component 1	Component 2	Component 3
Density	0.43	-0.03	-0.61
LOI†	0.28	0.12	0.88
SiO ₂	-0.89	-0.08	-0.09
TiO ₂	0.46	0.69	0.38
Al ₂ O ₃	-0.63	0.72	0.13
Fe ₂ O ₃	0.63	0.20	-0.21
MnO	-0.16	0.21	0.42
MgO	0.35	-0.66	-0.61
CaO	0.70	-0.15	0.43
Na ₂ O	-0.12	0.72	0.01
K ₂ O	-0.56	-0.21	-0.42
P ₂ O ₅	0.18	0.65	0.47
Pyroxene	0.86	-0.18	-0.06
Opaque minerals	0.06	0.70	-0.07
Plagioclase	-0.91	0.22	0.03
Olivine	0.12	-0.69	-0.57
Secondary minerals	0.21	0.02	0.77
Eigenvalue	5.168	4.766	1.732
Percent of variance‡	30.4	28.0	10.2

† LOI = loss on ignition.

‡ Total variance explained by these three components = 68.6%.

the variability of the data set. This component had high positive loadings of pyroxene, CaO, and Fe₂O₃ and high negative loadings of plagioclase, SiO₂, Al₂O₃, and K₂O. This suggests a strong relationship with the dominant primary minerals pyroxene and feldspar. The high positive loading of CaO is probably due to Ca-rich pyroxene. Also, the CaCO₃ crystals may have contributed to this loading.

The second principal component explained 28.0% of the total variance. It had large positive loadings of opaque materials, P₂O₅, Na₂O, Al₂O₃, and TiO₂ and negative loadings of olivine and MgO. These loadings may be a result of the chemical composition of the minor primary mineral groups of opaque minerals and olivine. The antithetic behavior of the opaque minerals and olivine is probably due to differences in time of crystallization of the minerals in the basalt.

The third principal component explained 10.2% of the total variance. It has positive loadings of LOI (loss on ignition) and secondary products (neoformed clay, iddingsite, etc.) and negative loadings of bulk density, MgO, and olivine. The third principal component sug-

gests that olivine alters to secondary products that contain H₂O, resulting in a decrease in bulk density. The contribution of this effect, however, is small (the third component explains only 10% of the variance).

A *t*-test to compare the bulk densities of Fz and Fx yielded no significant differences (*P* < 0.05). The chemical analyses also were too small to show differences in weathering between pebbles of the Fx and Fz terraces. Jongmans et al. (unpublished data) noticed that only volcanic fragments with diameters < 200 μm demonstrated distinct alteration in micromorphological studies. In view of these results, both Fx and Fz pebbles (*n* = 37) were used as reference material for studying the weathering of older sediments.

A Multiple-Linear-Regression Model Explaining the Bulk Density

Multiple linear regression was used to model the bulk density of the base-line pebbles, using their chemical composition. Chemical composition was used because it is easier to determine than the mineralogical composition. We randomly selected 25 Fz and Fx pebbles out of the total 37 in the model. The remaining 12 pebbles were used to test the model, using the stepwise-selection methods (Norusis, 1986). The resulting equation was

$$\text{bulk density} = 3.496 - 0.021(\text{SiO}_2) + 0.022(\text{MgO}) + 0.151(\text{K}_2\text{O}) \quad [1]$$

where (SiO₂), (MgO), and (K₂O) stand for mass fraction in percent.

The coefficient of determination (*R*²) of the regression (*n* = 25) is 0.81 (*P* < 0.01). The model successfully predicted the bulk density of Fz and Fx pebbles (Fig. 6). The coefficient of determination of the regression line is 0.67 (*P* < 0.01).

Quantification of Weathering in the Two Older Terraces

A *t*-test was performed on the chemical analyses of the reference (Fx and Fz) pebbles and the unweathered cores of the Fw and Fv pebbles. No significant difference could be demonstrated for the SiO₂, MgO, and

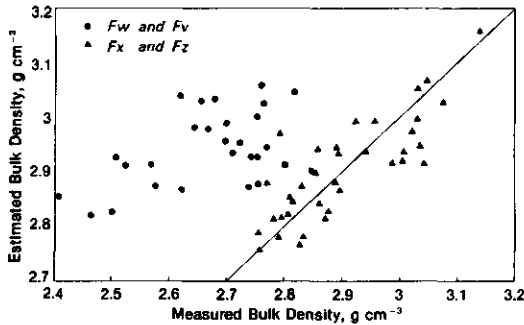


Fig. 6. Estimated bulk density related to measured bulk density for pebbles of two older (Fv and Fw) and two younger (Fx and Fz) river terraces.

K₂O concentrations. Furthermore, micromorphological observations indicated that cores of Fw and Fv weathered pebbles and the base-line pebbles were similar in terms of mineralogy, crystallinity, texture, and degree of alteration. We, therefore, estimated the bulk density of the fresh cores of weathered pebbles for the Fw and Fv terraces with the help of Eq. [1]. The bulk densities of whole pebbles (rind and core) were measured. Figure 6 illustrates that measured bulk densities of the pebbles in the Fw and Fv terraces were significantly lower than those estimated for the cores. However, no difference existed between bulk densities of Fw and Fv ($P > 0.5$).

A *t*-test was performed to test whether the differences in chemical composition between core and rind were significant (Table 3). Rind samples had significantly higher values of LOI and of mass fraction of TiO₂, Al₂O₃, Fe₂O₃, and MnO and lower contents of SiO₂, Na₂O, and K₂O. This could have been caused by either a relative depletion of Si, Na, and K, by enrichment of Fe and Mn, or by a combination of both. No significant differences (at the $P = 0.01$ level) could be demonstrated for MgO, CaO, and P₂O₅. To evaluate relative mobilities, TiO₂ was selected as a reference component because it is essentially immobile in view of its very low solubility above pH 2.5 (Colman, 1982) and because it is relatively abundant in the opaque minerals in the pebbles examined in this study. Jongmans et al. (unpublished data) reported that, in the case of complete weathering of volcanic fragments, optically unaltered opaque minerals were still present in a clustered distribution pattern in the groundmass. A paired *t*-test was performed to test whether the differences between element/TiO₂ ratios in core and rind were significant (Table 4). Except for Fe₂O₃ and MnO, all elements decrease relative to TiO₂ in the rind. In some of the pebbles, Fe₂O₃ and MnO increased relative to TiO₂. Micromorphological observations demonstrated Fe oxide pseudomorphs after olivine and pyroxene, and hypocrotings of Fe and Mn along microcracks. Feijtel et al. (1988) noted immobilization and translocation of Fe and Mn compounds due to weathering and pseudogley processes.

Assuming that Ti remains immobile, the loss of

Table 3. Differences in chemical composition between rind and core of 20 pebbles from the two older terraces.

	Rind	Core	Difference	SD	<i>t</i> value
	%(w/w)				
SiO ₂	42.4	44.6	-2.3***	1.3	-7.54
TiO ₂	3.0	2.7	0.3**	0.2	7.11
Al ₂ O ₃	15.5	14.9	0.6**	0.7	3.00
Fe ₂ O ₃	13.7	12.3	1.4**	0.7	8.35
MnO	0.2	0.2	0.2**	0.0	3.25
MgO	8.5	8.6	-0.1ns	0.5	-1.52
CaO	10.7	10.6	0.1ns	0.4	1.08
Na ₂ O	1.1	2.1	-1.0**	0.5	-8.10
K ₂ O	0.5	1.5	-1.0**	0.6	-6.87
P ₂ O ₅	0.9	0.9	-0.03**	0.1	1.83

** Significant at $P < 0.01$; ns = not significant.

Table 4. Element-oxide/TiO₂ ratios and differences between core and rind of 20 pebbles from the two older terraces.

	Rind	Core	Difference	SD	<i>t</i> value
SiO ₂	14.37	16.76	-2.40**	1.38	-7.15
Al ₂ O ₃	5.28	5.60	-0.32**	0.19	-6.98
Fe ₂ O ₃	4.69	4.62	0.07*	0.11	2.41
MnO	0.07	0.07	-0.00ns	0.01	-0.94
MgO	2.91	3.26	-0.35**	0.28	-5.09
CaO	3.61	3.92	-0.31**	0.14	-9.30
Na ₂ O	0.36	0.77	-0.42**	0.18	-9.78
K ₂ O	0.13	0.55	-0.43**	0.21	-8.33
P ₂ O ₅	0.30	0.32	-0.02**	0.02	-4.12

*,** Significant at $P < 0.05$ and 0.01 , respectively; ns = not significant.

other elements from the rind in percent can be calculated as follows (Rel = element/TiO₂ ratio):

$$(\text{Rel}_c - \text{Rel}_r)/\text{Rel}_c 100$$

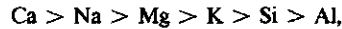
The sequence of mobility, based on the relative loss of each element in the weathering rind, compared with the unweathered core, is



This sequence differs from that described by Colman (1982) for basalt weathering:



and with the general mobility sequence for igneous rocks:



derived from stream-water composition (Colman, 1982). The most striking exceptions are the higher mobility of K and the lower mobility of Ca in our study, compared with Colman's sequences. Colman, however, studied alteration of alkali basalt rocks in situ. He stated that K is adsorbed within the weathered rock during formation of halloysite. In his mobility sequence, therefore, K has not been leached. We studied individual alkali basalt pebbles in alluvial deposits. In these deposits, Feijtel et al. (1989) reported inclusion of K in clay coatings on the surface of basaltic pebbles. Immobilization of K on the surface of the basalt pebbles resolves the apparent disagreement between our and Colman's results. Our low Ca mobility may be related to the fact that some calcite in the rinds is coated or impregnated with Fe compounds, which prevent leaching of CaCO₃.

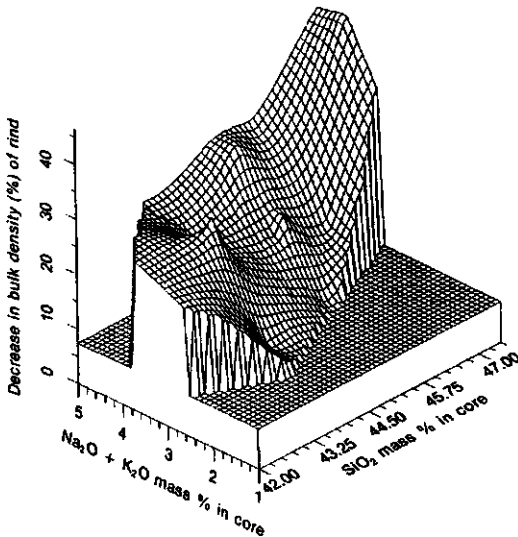


Fig. 7. Three-dimensional plot of core SiO_2 , core Na_2O and K_2O , and the density decrease of the rind in pebbles of the two older terraces.

A more or less linear relationship was found between element loss and decrease in bulk density for the most mobile elements ($R^2 = 0.57$ for Na_2O). These relations suggest that individual pebbles differ in their degree of weathering. The degree of weathering showed no significant relationship with either terrace age or sampling depth. Since weathering rinds that may have been present before sedimentation would have been removed during the transport of the pebbles, source-area weathering can be neglected. The observed differences in degree of weathering are probably caused by specific properties of the stones rather than terrace age or sampling depth. To test this hypothesis, the relation between the original chemical composition (of core) and degree of weathering was investigated by plotting a three-dimensional graphic of the SiO_2 of the core, the Na_2O and K_2O of the core (the classification criteria), and the density decrease (%) of the rind (Fig. 7). The results indeed suggest a relationship between original chemical composition of the alkali basalt pebbles and the degree of weathering. Comparable graph-

ics can be made by substituting the density decrease by Na_2O or K_2O decrease. Alkali basalts with a high content of Na_2O and K_2O appear to be most susceptible to weathering. These differences in degree of weathering may be related to the occurrence of easily weatherable undersaturated minerals like nepheline in the fine groundmass of the alkali basalt involved.

ACKNOWLEDGMENTS

The authors are grateful to Dr. S.B. Kroonenberg for suggestions and encouragements.

REFERENCES

- Abbey, S. 1980. Studies in 'standard samples' for use in the general analysis of silicate rocks and minerals. Part 6: 1979 ed. of useable values. Pap. 80-14. Geol. Surv. Can., Ottawa.
- Black, C.A., D.D. Evans, J.L. White, L.E. Ensminger, and F.E. Clark. 1965. Methods of soil analysis. Part 1. Physical and mineralogical properties. ASA, Madison, WI.
- Bouillet, R., D. Giot, and M. Jeambu. 1972. Carte géologique thiers XXVI-31, à l'échelle 1:50 000. Bur. Rech. Geol. Min., Orléans.
- Colman, S.M. 1982. Chemical weathering of basalts and andesites: Evidence from weathering rinds. U.S. Geol. Surv. Prof. Pap. 1246.
- Cox, K.G., J.D. Bell, and R.J. Pankhurst. 1979. The interpretation of igneous rocks. Allen and Unwin, London.
- Delvigne, J., E.B.A. Bisdorn, J. Sleeman, and G. Stoops. 1979. Olivines, their pseudomorphs and secondary products. *Pedologie* 26(3):247-309.
- Eggleton, R.A., C. Foudoulis, and D. Varkevissier. 1987. Weathering of basalt: Changes in rock chemistry and mineralogy. *Clays Clay Miner.* 35:161-169.
- Fejtel, T.C., A.G. Jongmans, N. van Breemen, and R. Miedema. 1988. Genesis of two Planosols in the Massif Central, France. *Geoderma* 43:249-269.
- Fejtel, T.C., A.G. Jongmans, and J. van Doesburg. 1989. Identification of clay coatings in an older quaternary terrace of the Allier, Limagne, France. *Soil Sci. Soc. Am. J.* 53:876-882.
- Gardner, L.R., I. Kheuerromne, and H.S. Chen. 1978. Isovolumetric geochemical investigation of a buried granite saprolite near Columbia, SC, U.S.A. *Geochim. Cosmochim. Acta* 42:417-424.
- Hendricks, D.M., and L.D. Whittig. 1968. Andesite weathering. II. Geochemical changes from andesite to saprolite. *J. Soil Sci.* 19:147-153.
- Kroonenberg, S.B., M.L. Moura, and A.T.J. Jonker. 1988. Geochemistry of the sands of the Allier river terraces, France. *Geol. Mijnbouw* 67:75-89.
- Millot, G., and M. Bonifas. 1955. Transformations isovolumétriques dans les phénomènes de latéritisation et de bauxitisation. *Bull. Serv. Carte Géol. Alsace Lorraine* 8:3-20.
- Norusis, M.J. 1986. Advanced statistics SPSS/PC+ for the IBM/XT/AT. SPSS, Inc., Chicago.
- Pastre, J.F. 1986. Altération et paléoaltération des minéraux lourds des alluvions Pliocènes et Pleistocènes du bassin de l'Allier Massif Central, France. *Bull. Assoc. Fr. Etude Quaternaire* 3/4:257-269.
- Trescases, J.J. 1975. L'évolution géochimique supergène des roches ultrabasiqes en zone tropicale. *Mém. ORSTOM* 78:250.
- van der Plas, L., and A.C. Tobi. 1965. A chart for judging the reliability of point-counting results. *Am. J. Sci.* 263:87-90.
- Wilshire, H.G. 1958. Alteration of olivine and orthopyroxene in basic lavas and shallow intrusions. *Am. Mineral.* 43:120-146.

2.3 Micromorphological characterization and microchemical quantification of weathering in an alkalibasalt pebble.

Soil Sci. Soc. Am. J. 57:128-134 (1993)

A.G. Jongmans, E. Veldkamp, N. van Breemen, and I. Staritsky.

Micromorphological Characterization and Microchemical Quantification of Weathering in an Alkali Basalt Pebble

A. G. Jongmans,* E. Veldkamp, N. van Breemen, and I. Staritsky

ABSTRACT

Optical and submicroscopic techniques enable in situ chemical and mineralogical quantification of weathering and neof ormation of minerals. A mass balance can be set up if the neoformed minerals can be related to their source. In this section, a partially weathered basalt pebble enclosed by a weakly anisotropic, partially isotropic nonlaminated clay coating was examined. Such coatings were absent around any other adjacent grain surface and voids. Both observations indicated that the clay coating formed from precipitation of constituents weathered from the pebble. Weathering was considered isovolumetric because original shapes and volumes of the dissolved phenocrysts and groundmass of the pebble are maintained. The weathering rind closest to the unaltered core was characterized by weathering of glass. The strongly altered outer weathering rind was characterized by intensive pyroxene alteration. Chemical trends of various zones were in good agreement with micromorphological observations and mineralogical calculations. Mass balance calculations indicated that all elements except Fe were leached from the entire weathering rind. Essentially all Na and K, a considerable part of the Mg (44%), Ca (58%), and Si (29%), and a small amount of the Ti (15%) were leached from the rind. Only Si, Al, and a small amount of Ca were found in the neoformed coating. More Al was found in the coating than may have been leached from the rind, suggesting an external Al source when isovolumetric weathering is assumed. Sensitivity analysis of the calculation method concerning the consequences of changes in bulk density of core, rind, and coating showed similar trends in the elemental chemical amounts, except for Al. The isovolumetric method was successfully applied in this microscale weathering study.

SOIL GENESIS involves, in part, the weathering of primary minerals and rock fragments and the formation of secondary minerals. To relate rock weathering to soil formation, it is important to understand the chemical and mineralogical changes attending mineral weathering reactions (Eggleton et al., 1987).

Micromorphological and submicroscopic analyses can substantially support studies on weathering phenomena (Meunier, 1983; Bisdom, 1981). Alteration of rock fragments and individual minerals is a complex process that is determined by conditions on a microscale (Delvigne et al., 1979; Glassman and Si-

monson, 1985; McCaire et al., 1988). Determination of the degree of alteration of the parent material is supported by quantification of chemical changes. The isovolumetric method and the Ti-constant method are commonly used for this purpose (Gardner et al., 1978; Colman, 1982; Cramer and Nesbitt, 1983; Veldkamp et al., 1990). The isovolumetric method is based on the assumption that a unit volume of weathered rock has evolved from an equivalent volume of fresh rock. The Ti-constant method is based on the assumption that Ti is immobile (or less mobile than other elements) during weathering. Element/TiO₂ ratios can be used to calculate relative elemental mobility sequences.

Several authors (Chartres et al., 1985; Buurman and Jongmans, 1987; Feijtel et al., 1989) have found neoformed clay coatings and have characterized these chemically and mineralogically. Generally, it is not possible to relate neoformed coatings to their source and to set up a mass balance for weathered grains and neoformed coatings, because these coatings generally occur around both weathered and fresh single and compound mineral grains.

We studied a single, partially weathered basalt pebble in the weathering zone of a Pleistocene terrace (Fw) of the Allier River, France. In this section, a weakly anisotropic to partially isotropic, nonlaminated, limpid coating was noted surrounding the pebble. Similar coatings were absent around any other adjacent grain surfaces and voids. Feijtel et al. (1989) interpreted similar coatings as neoformed rather than illuviation coatings in soils situated in an older Pleistocene terrace (Fv) of the Allier terrace sequence. Optical characteristics and internal fabric suggested that the coating was neoformed, and derived entirely from the partially altered basalt pebble. Micromorphological, mineralogical, and chemical characteristics of optically different weathering zones of the altered basalt pebble were compared, and an attempt was made to set up a quantitative chemical mass balance of the fresh core, the weathering rind, and the neoformed coating.

MATERIALS AND METHODS

Undisturbed soil samples were taken from the 60-cm depth in the Btg horizon of a Typic Albaqualf (Planosol), developed in a gravelly Quaternary Allier terrace in France (Fw terrace):

Dep. of Soil Science and Geology, Agricultural Univ., P.O. Box 37, 6700 AA, Wageningen, the Netherlands. Contribution from the Dep. of Soil Science and Geology, Agricultural Univ., Wageningen. Received 17 May 1991. *Corresponding author.

Published in Soil Sci. Soc. Am. J. 57:128-134 (1993).

Bouillet et al., 1972). The parent material is characterized by large amounts of basaltic and granitic pebbles and sand. Jongmans et al. (1991) extensively discussed pedogenesis in the soils of the Allier terraces.

Thin sections were prepared, following FitzPatrick's (1970) method, and described following the terminology of Bullock et al. (1985). Mineral point counts, based on 150 to 450 points, were performed according to Van der Plas and Tobi (1965).

In situ microchemical analyses of uncovered polished thin sections were performed using a Phillips scanning electron microscope (Phillips, Eindhoven, the Netherlands) equipped with an energy-dispersive x-ray analyzer (SEM-EDXRA). Multiple block analyses (5 by 3 to 20 by 15 μm) were made on various micromorphological weathering zones. Peak-to-background heights of the EDXRA signal were linearly transformed to elemental percentages by measuring standard mineral probes at the same beam intensity and size. Elemental mass fractions were recalculated to oxide mass fractions. No distinction was made between Fe^{2+} and Fe^{3+} , and all Fe was assigned to Fe_2O_3 . This, as well as structural H_2O , cause deviations from 100% for total oxides. Therefore, the reported data are scaled to total 100% (without H_2O , which was not determined).

Bulk density of the unweathered core was calculated using the relation introduced by Veldkamp et al. (1990):

$$\text{Bulk density} = 3.496 - (0.021 \text{ SiO}_2) + (0.022 \text{ MgO}) + (0.151 \text{ K}_2\text{O})$$

(with SiO_2 , MgO , and K_2O in mass percentages). Density of the rind was estimated by interpolating the relationship between decrease in density and chemical composition (Fig. 1, taken from Veldkamp et al., 1990). A complete section of the pebble and enveloped coating was photographed in a thin section with a Leitz-Wild macroscope (Leica bv, Rijswijk, the Netherlands). Areas of various zones were estimated from digitized photographic data using Arc-Info (Environmental Systems Research Institute, 1989).

RESULTS AND DISCUSSION

Micromorphological Characterization

The weathered basalt pebble and its neoformed coating were situated in a gravelly sandy loam Btg horizon

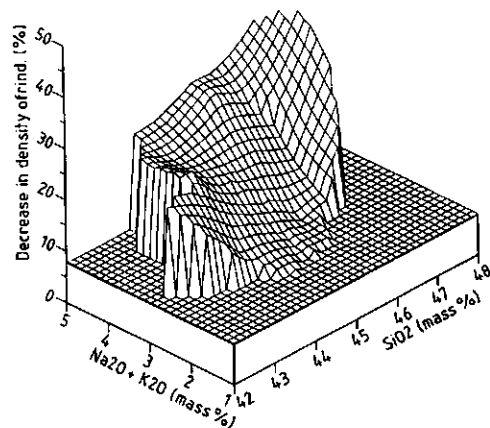


Fig. 1. Three-dimensional plot of SiO_2 content of the core, $\text{Na}_2\text{O} + \text{K}_2\text{O}$ content of the core, and the density decrease in alkali basalt pebbles of two older terraces of the Allier (from Veldkamp et al., 1990).

of the Fw terrace at a depth of 60 cm. The studied deposits contain appreciable amounts of similar basaltic fragments, but basalt pebbles with similar weathering rinds enveloped by undisturbed coatings are absent. Groundmass and pedofeatures surrounding the selected pebble have different mineralogical compositions (Jongmans et al., 1991). Four zones, indicated as I, IIa, IIb, and III, could be distinguished micromorphologically in the pebble and coating (Fig. 2 and 3):

Zone I: The Core

The core (Fig. 4) has a fine-grained, microcrystalline, seriate texture. Sizes and volumetric percentages of the constituent minerals of the core are given in Table 1. The completely isotropic, glassy groundmass has a light yellowish brown color (2.5YR 6/4) in plane-polarized light. Relatively large olivine phenocrysts intersect all zones. Neither the glass groundmass nor the other minerals exhibit alteration features in optical examination, so the core is interpreted as the unaltered part of the pebble.

Zone IIa: The Initial Alteration Zone

This zone (Fig. 5) enclosed the fresh core. Content, mineralogy, texture, size, and optical properties of constituent minerals are identical to Zone I, except for the glassy groundmass and few olivine phenocrysts. Near the fresh core, isotropic glass is stained yellow (2.5YR 8/6), but changes to reddish yellow (10YR 6/8–7.5YR 6/8) at 150- to 400- μm distance from the core, indicating liberation of Fe as a result of initial alteration of volcanic glass. Olivine crystals occasionally show translucent, yellow to reddish yellow coatings (10YR 7/8–5YR 6/8, thickness of 10 μm) on surfaces and along fractures, which may consist of the initial weathering product "id-

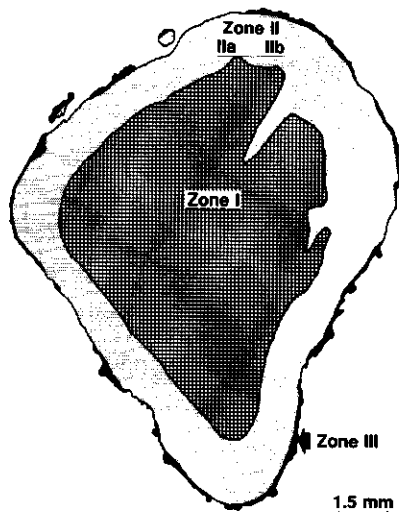


Fig. 2. Distinguished zones in a digitized cross section of the alkali basalt pebble studied.

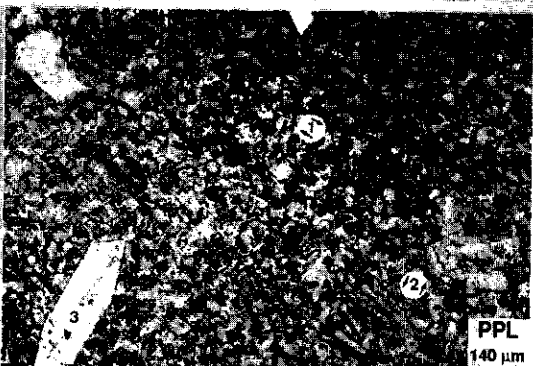
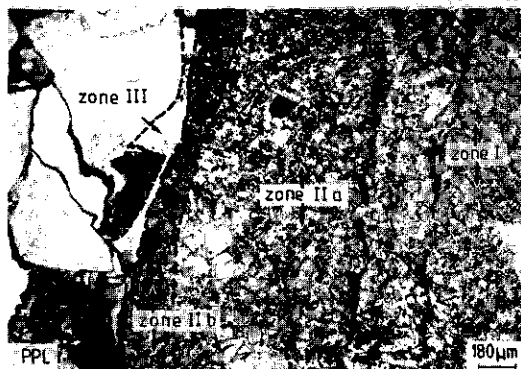
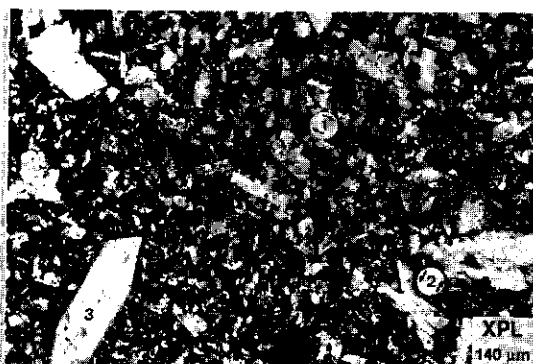


Fig. 3. The core (Zone I), the initial weathering zone (Zone IIa), the strong alteration zone (Zone IIb), and the neoformed coating (Zone III) under crossed-polarized light (XPL) and plane-polarized light (PPL).

Fig. 4. Detail of the fresh core of the pebble: isotropic volcanic glass showing groundmass (1), pyroxene phenocryst (2), and olivine phenocryst (3) under crossed-polarized light (XPL), and plane-polarized light (PPL).

dingsite" (Delvigne et al., 1979). Zone IIa is considered to be characteristic of the first stage in weathering of the basalt pebble.

Zone IIb: The Strong Alteration Zone

This zone (Fig. 5) forms the outer rind of the pebble. Its groundmass is a mixture of weakly anisotropic, stipple-speckled, translucent yellow (2.5Y 8/6) fine material, and isotropic to anisotropic, nonoriented, red (2.5YR 4/8) fine material. These observations suggest complete alteration of glass, resulting in continuing oxidation of Fe and formation of speckled, oriented, neoformed clay. Most pyroxene crystals < 100 μm in diameter show pellicular and linear alteration, sometimes leading to nearly complete dissolution of the crystals. Some pyroxenes change into red (2.5YR 4/8) fine material or into stipple-speckled, yellow (2.5Y 8/6) fine material, difficult to distinguish from the groundmass. The pyroxene content is 23 ± 7% (v/v). Intense weathering of pyroxene was noticed, resulting in both complete loss of pyroxene crystals and occurrence of products similar to those described for the alteration of glass. Olivine crystals display the same sizes, content, nature, and degree of

weathering as those in Zone IIa. Effects of weathering are relatively less important in the large olivine phenocrysts than in the smaller pyroxene crystals. Similar effects were noticed by Hendricks and Whittig (1968). Colman (1982) reported similar volcanic glass, olivine, and pyroxene alteration phenomena. In our study, neither optical differences nor differences in the content of opaque minerals were observed. The original shapes and volumes of the totally dissolved minerals seem to be maintained. Groundmass volume decrease was not observed, so the alteration of glass, pyroxene, and olivine is considered isovolumetric. Dark red (2.5YR 3/6) diffuse Fe oxide nodules and streaks, as well as microcracks up to 50 μm wide locally lined by Fe oxide, occur,

Table 1. Sizes and contents of the minerals in the core.

Mineral	Size	Content
	μm	% (v/v)
Pyroxene	10-100	49 ± 5
Glass	groundmass	32 ± 4.5
Opaque minerals	10-50	10 ± 3
Olivine	100-1000	9 ± 3
Plagioclase	5-30	< 1

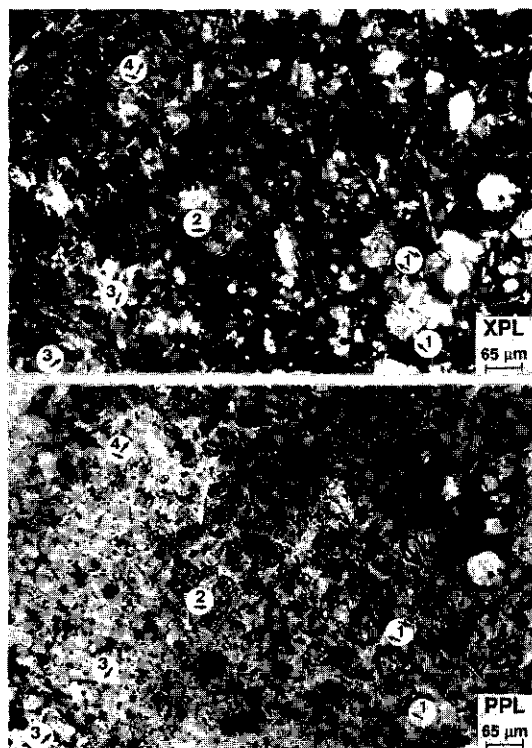


Fig. 5. The initial alteration zone with fresh pyroxene phenocrysts (1), and the strong alteration zone with weathered and almost dissolved pyroxene phenocrysts, pellicular alteration of pyroxene (2), minute residues of pyroxene and dissolution void (3), and stipple-speckled fine material after pyroxene crystals (4) under crossed-polarized light (XPL), and plane-polarized light (PPL).

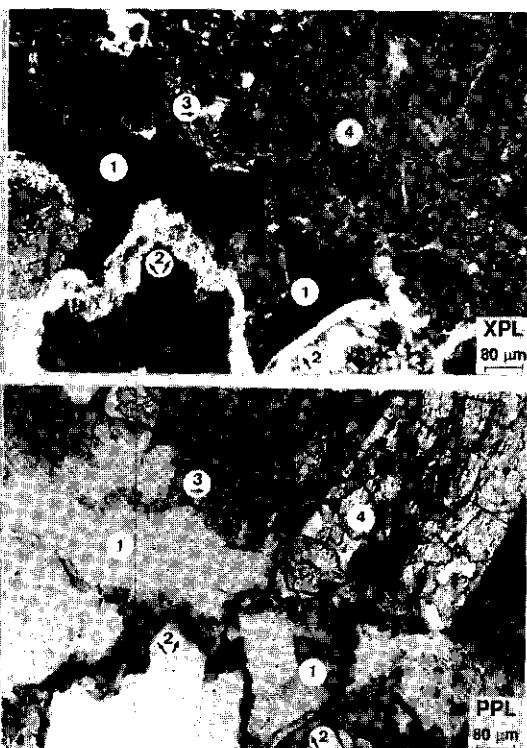


Fig. 6. The nonlaminated, isotropic to stipple-speckled neoformed coating (1), covered by an anisotropic, microlaminated, dusty, strong continuous oriented clay illuviation coating (2), partially impregnated with Fe compounds, irregular linear alteration of a pyroxene (3), olivine phenocryst (4) under crossed-polarized light (XPL) and plane-polarized light (PPL).

suggesting Fe impregnation of Zone IIb as a result of pseudogley processes in the Planosol.

Zone III: The Neoformed Coating

A pale yellow, nonlaminated, partially isotropic and partially anisotropic, stippled-speckled coating (20–150 µm) encloses the basalt pebble (Fig. 6). In plane-polarized light, isotropic and anisotropic parts are indistinguishable, indicating a similar genetic origin. Feijtel et al. (1989) and Jongmans et al. (1991) interpreted these coatings as neoformed clay coatings rather than clay illuviation coatings, because the latter never exhibit isotropic parts as a result of total crystallinity of the clay constituents within illuviation coatings. In addition, absence of any lamination in the studied coating suggests a neoformed origin as well. On the basis of the birefringence fabric and lack of lamination, Bullock et al. (1985) interpreted such coatings as neoformed. In older terraces (Fv and Ft) of the sequence, larger amounts of such coatings were observed around and adjacent to all types of mineral grains and in voids, but they were partially or totally fragmented and deformed. Therefore no other

basaltic pebble with different weathering rinds and a fresh core totally enclosed by an in situ neoformed coating was available in the studied thin sections to repeat the experiment. The pebble and coating studied were not fragmented or deformed. A few isolated coatings, like the one studied but fragmented and deformed, were observed exclusively around or near to other basaltic pebbles (Jongmans et al., 1991). This observation, and the absence of similar coatings on adjacent mineral grain surfaces or in voids in the immediate neighborhood of the studied pebble, as well as the micromorphological characteristics (mentioned above) suggest that the coating results from precipitation of dissolved constituents liberated from the weathering zones of the pebble.

Limpid to dusty, anisotropic, strongly continuous oriented, microlaminated, yellow (10YR 7/8) clay coatings were observed in the surrounding groundmass, characteristic for the process of clay illuviation (Bullock et al., 1985; FitzPatrick, 1984), and a diagnostic criterion for the presence of an argillic horizon in Alfisols. Clay-illuviation coatings partially cover the studied neoformed coating, but based on its different micromorphological characteristics they are clearly separable (Fig. 6).

Table 2. Average chemical compositions of the three major zones in the alkali basalt pebble.

	Zone I (n = 5)	Zones IIa and IIb (n = 6)	Zone III (n = 10)
	% (w/w)		
SiO ₂	43.9 (0.6)†	42.4 (2.5)	51.2 (1.6)
Al ₂ O ₃	11.5 (0.3)	14.8 (1.2)	27.4 (2.5)
Fe ₂ O ₃	8.4 (0.7)	14.4 (3.3)	8.8 (1.5)
Na ₂ O	2.5 (0.1)	0.0 —	0.0 —
K ₂ O	2.3 (0.1)	0.0 —	0.0 —
CaO	11.9 (1.3)	6.8 (0.9)	0.7 (0.5)
MgO	4.7 (0.5)	3.6 (0.9)	0.0 —
TiO ₂	4.3 (0.3)	5.0 (0.8)	0.0 —

† Standard deviations given in parentheses.

Microchemical Characterization

The average chemical composition of the distinguished pebble zones is given in Table 2. Zone I, the core, represents the original average chemical composition of the fresh basalt pebble. Zones IIa and IIb include the two weathering stages of the rind. In these zones, Na and K are completely removed, CaO content decreases by 40%, and MgO by 24%. There is also a relative increase of Al₂O₃ and Fe₂O₃. Zone III, the neoformed clay coating, contains SiO₂, Al₂O₃, and Fe₂O₃, with little CaO. The components Na₂O, K₂O, MgO, and TiO₂ are absent in the coating. Table 3 shows the average chemical compositions of the groundmass, pyroxenes, and opaque Fe minerals in the major zones of the pebble. In Zone IIa, Na₂O, K₂O, and MgO were completely removed from the glassy groundmass, whereas CaO content decreases by 80%. Aluminum oxides, and to a minor extent Fe₂O₃, are concentrated in the altered groundmass. Pyroxenes in Zone IIa do not show compositional changes relative to those in Zone I. In the opaque min-

erals, SiO₂ content decreases slightly, whereas Fe₂O₃ increases slightly in Zones IIa and IIb. Observed chemical variation of pyroxenes and opaque minerals may result from mineralogical differences. Glass weathers most readily, as is indicated by leaching of nearly all basic cations. These observations coincide with those reported by Hendricks and Whittig (1968), Colman (1982), and Eggleton et al. (1987). Pyroxenes in Zone IIb, particularly those adjacent to the pebble surface, show a strong loss of MgO and CaO, and a relative enrichment of Al₂O₃ and Fe₂O₃. Titanium oxides in the opaque minerals decrease across Zone II. Zone IIb is characterized by intensive weathering of pyroxene. Chemical trends in the weathering of Zones I, IIa, and IIb agree with those derived from micromorphological observations.

Mass-Balance Calculations

Micromorphological observations indicated isovolumetric weathering of the basalt pebble. As a consequence, bulk density decreases during weathering. The bulk density of the core was calculated as: bulk density = 3.496 - 0.021(43.9) + 0.022(4.702) + 0.151(2.306) = 3.026 Mg m⁻³, using the transfer function of Veldkamp et al. (1990). The decrease in density of the rind was obtained by interpolation of Fig. 1 with the help of kriging techniques. The interpolated value was 26% (prediction error: 7%, Fig. 7), corresponding with a density of 3.02 - 0.79 = 2.13 Mg m⁻³. For the bulk density of the coating, we used a value of 2.3 Mg m⁻³ (Deer et al., 1962).

The volumes of the core (Zone I), the complete weathering rind (Zones IIa and IIb) and coating (Zone III) were estimated as follows: Three concentric spheres were described with radii that enclosed volumes for core, rind, and coating, corresponding with the areas measured in the thin section (Fig. 2). The volumes of core, rind, and coating were calculated as 0.24 × 10⁻⁶, 0.39 × 10⁻⁶, and 0.022 × 10⁻⁶ m³, with corresponding masses of 0.72, 0.87, and 0.05 g, respectively. For an example of the mass balance calculations, see the appendix.

Table 3. Average chemical composition of three mineral types in three zones, the core (Zone I), the initial weathering zone (Zone IIa), and the strong alteration zone (Zone IIb), of the alkali basalt pebble.

	Groundmass			Pyroxene				Opaque minerals		
	I glass (n = 10)	IIa stained glass (n = 12)	IIb neoformed material (n = 10)	I (n = 10)	IIa (n = 12)	IIb inner (n = 7)	IIb outer (n = 5)	I (n = 7)	IIa (n = 6)	IIb (n = 8)
	% (w/w)									
SiO ₂	44.7 (2.3)†	46.1 (1.8)	44.2 (2.6)†	43.5 (2.2)	45.2 (2.0)	44.2 (1.8)	38.6 (3.6)	21.8 (0.6)	17.7 (0.7)	18.5 (0.9)
Al ₂ O ₃	13.0 (1.9)	21.9 (5.7)	18.9 (4.0)	6.9 (1.1)	7.8 (0.9)	6.1 (0.6)	13.1 (4.2)	3.7 (1.7)	3.7 (0.8)	4.0 (0.5)
Fe ₂ O ₃	8.7 (2.8)	11.9 (4.0)	15.8 (3.8)	7.9 (2.1)	7.3 (1.0)	8.2 (1.5)	21.3 (5.9)	37.9 (1.8)	44.7 (1.8)	42.9 (3.2)
Na ₂ O	3.1 (1.0)	0.0 —	0.0 —	0.0 —	0.0 —	0.0 —	0.0 —	0.0 —	0.0 —	0.0 —
K ₂ O	3.3 (0.6)	0.0 —	0.0 —	0.0 —	0.0 —	0.0 —	0.0 —	0.0 —	0.0 —	0.0 —
CaO	7.2 (1.1)	1.49 (0.4)	1.6 (0.4)	21.4 (2.2)	20.2 (1.6)	21.7 (1.4)	1.2 (0.2)	0.0 —	0.0 —	0.0 —
MgO	3.0 (0.5)	0.0 —	0.0 —	9.1 (2.2)	10.4 (0.8)	10.5 (1.0)	1.1 (0.2)	2.7 (1.6)	3.4 (0.4)	4.3 (0.3)
TiO ₂	3.5 (1.6)	4.29 (1.3)	4.4 (2.1)	4.7 (1.2)	4.3 (0.7)	4.1 (0.9)	5.6 (2.4)	18.3 (2.2)	16.4 (1.5)	13.1 (1.5)

† Standard deviation.

Table 4. Mass balance of weathered alkali basalt pebble, assuming isovolumetric weathering and spherical shape for the pebble.

	Na ₂ O	MgO	Al ₂ O ₃	SiO ₂	K ₂ O	CaO	TiO ₂	Fe ₂ O ₃
	% (w/w)†							
Loss from rind	100	44	5	29	100	58	15	-27‡
Recovered in coating	0	0	10	5	0	0	0	5
Removed by leaching	100	44	-5	24	100	58	15	-31

† All numbers expressed as a percentage by mass of material originally present in the weathering rind.
‡ Negative numbers indicate enrichment.

Table 5. Influence of a change in the method used to calculate volume of the pebble on the amount recovered in the coating.

Method	Na ₂ O	MgO	Al ₂ O ₃	SiO ₂	K ₂ O	CaO	TiO ₂	Fe ₂ O ₃
	% (w/w)							
Sphere	0	0	10	5	0	0	0	5
Area	0	0	9	4	0	0	0	4
Ellipsoid	0	0	12	6	0	0	0	5

All elements are leached from the rind except for Fe, as indicated by mass balance calculations (Table 4). The observed absolute enrichment in Fe corresponds with micromorphological observations of microcrack fillings and must be attributed to Fe supplied from the surrounding soil, presumably as Fe²⁺ during periods of waterlogging. Sodium and K are totally leached from the rind and are not recovered in the coating. A considerable part of Ca, Mg, and Si is leached from the rind. No Mg and only relatively small amounts of Ca and Si are recovered in the coating. Also a relatively small amount of Ti is leached from the rind and not recovered in the coating. This suggests that the use of Ti as an immobile constituent to calculate changes in elemental abundances on an absolute scale is precarious. Kaub and Carter (1987) also noticed Ti mobility within, and a net loss of Ti from, a Paleustalf as a result of weathering, translocation, and leaching.

Interestingly, Al recovery in the coating exceeds its removal from the rind. Thus, part of the Al in the coating may come from an external source.

Sensitivity Analysis of the Applied Calculation Method

Certain assumptions were made when calculating volumes and bulk densities of the distinguished zones. Sensitivity of the results to variability of parameters was tested to estimate the accuracy of the calculation method. This was done by calculating the effects of changes in volume and bulk density estimates for the coating, core, or rind on the amounts calculated to have leached from pebble and coating.

Variations in volume estimates did not result in large differences in estimates of elemental contents in the coating (Table 5).

Variation in bulk density of the coating does not have a noticeable effect on the mass balance (Table 6). The error in predicted decrease of density in the rind is about 7% (Fig. 7), so the bulk density of the rind is probably between 2.01 and 2.44 g cm⁻³, with 2.22 g cm⁻³ as the central estimate. The effect of variation of bulk density (D) on the calculation of the mass balance is demon-

Table 6. Sensitivity analysis of calculation method; the consequences of a change in calculated bulk density on the amount totally leached.

Bulk density	MgO	Al ₂ O ₃	SiO ₂	CaO	TiO ₂	Fe ₂ O ₃
	% (w/w)					
	Coat					
2.1	43.8	-4.7	24.2	58.1	14.5	-30.8
2.2	43.8	-5.1	24.0	58.1	14.5	-31.0
2.3	43.8	-5.6	23.7	58.1	14.5	-31.2
2.4	43.8	-6.0	23.5	58.1	14.5	-31.3
2.5	43.8	-6.5	23.3	58.1	14.5	-31.5
	Rind					
2.0	49.6	4.3	31.1	62.4	23.3	-18.1
2.1	47.1	-0.0	27.9	60.5	19.5	-23.8
2.2	44.5	-4.3	24.7	58.6	15.7	-29.5
2.3	42.0	-8.6	21.5	56.7	11.8	-35.1
2.4	39.5	-12.9	18.3	54.9	8.0	-40.8
	Core					
2.8	39.4	-13.9	17.7	54.8	7.8	-41.5
2.9	41.5	-10.0	20.6	56.3	11.0	-36.6
3.0	43.4	-6.3	23.2	57.8	13.9	-32.0
3.1	45.3	-2.9	25.7	59.1	16.7	-27.8
3.2	47.2	0.4	28.0	60.4	19.3	-23.8

strated in Table 6. Even in a worst-case situation (i.e., D_{coat} = 2.5, D_{rind} = 2.4, and D_{core} = 2.8, or D_{coat} = 2.1, D_{rind} = 2.0, and D_{core} = 3.2) the trends for MgO, SiO₂, CaO, TiO₂, and Fe₂O₃ remain the same.

In the worst-case situations, the calculated amount of Al leached from the rind varies from a loss of 11% to an enrichment of 23%. Thus, given the accuracy of our data, no definite answer can be given concerning enrichment or loss of Al from the rind.

CONCLUSIONS

In this study, micromorphological observations and microchemical analyses were in good agreement, indicating the applicability of the isovolumetric method on a microscale. Observations indicate that neof ormation of the coating is a result of weathering of the corresponding basalt pebble.

ACKNOWLEDGMENTS

The authors wish to thank E. Meijer and C. Anbeek for their valuable comments on the manuscript.

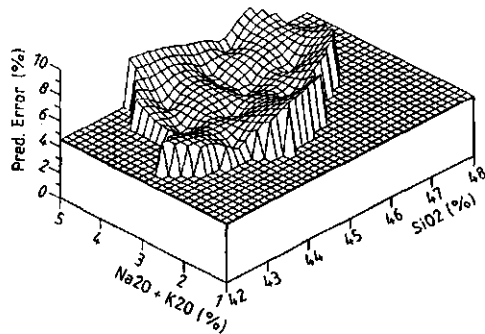


Fig. 7. Predicted error for decrease in density in Fig. 1.

APPENDIX

Mass-Balance Calculations Using Silicon Dioxide

We applied the isovolumetric method. This implies that the original bulk density of the rind (before weathering) is equal to the present bulk density of the core, and that the original composition of the rind is the same as the present composition of the core. Original mass of rind = bulk density (core) \times volume (rind) = $3.02 \times 10^6 \times 0.3916 \times 10^{-6} = 1.183$ g. Originally, 43.9% of the rind consisted of SiO_2 . So 43.9% of 1.183 g = 0.519 g SiO_2 originally present in the rind. Presently, 42.4% of the rind consists of SiO_2 . The mass of the rind = bulk density (rind) \times volume (rind) = $2.23 \times 10^6 \times 0.3916 \times 10^{-6} = 0.8733$ g. So, $0.424 \times 0.8733 = 0.370$ g SiO_2 is present.

Loss from the rind can be calculated as $0.519 - 0.371 = 0.149$ g. As a percentage of that originally present, this is $0.149/0.519 \times 100 = 28.7\%$ (proportion of SiO_2 in the core that was leached to form the rind.)

In the coating, we find 51.2% SiO_2 . This corresponds with $0.512 \times 0.05 = 0.026$ g SiO_2 and $0.026/0.519 \times 100 = 5.0\%$ of SiO_2 originally present. Finally, the amount removed by leaching can be calculated as $28.7 - 5.0 = 23.7\%$.

REFERENCES

- Bisdom, E.B.A. (ed.). 1981. Submicroscopy of soils and weathered rocks. *Worksh. Int. Working group on submicroscopy of undisturbed soil materials 1st*, Wageningen. June 1980. PU-DOC, Wageningen, the Netherlands.
- Bouillet, R., D. Giot, and M. Feambrun. 1972. Carte Géologique Thiers XXVI-31 / à l'échelle 1:50 000. Bureau de Recherches Géologiques et Minières, Orléans.
- Bullock, P., N. Fedoroff, A. Jongerius, G. Stoops, and T. Turina. 1985. Handbook for soil thin section description. *Wayne Res. Publ.*, Albrighton, England.
- Buurman, P., and A.G. Jongmans. 1987. Amorphous clay coatings in a lowland Acrisol and other andesitic soils of West Java, Indonesia. *Pemberitaan Penelitian Tanah dan Pupuk* 7:31-40.
- Chartres, J.F., A. Wood, and P.C. Pain. 1985. The development of micromorphological and chemical properties of volcanic ash soils in highland Papua New Guinea. *Aust. J. Soil Res.* 23:339-354.
- Colman, S.M. 1982. Chemical weathering of basalts and andesites: Evidence from weathering rinds. *U.S. Geol. Surv. Prof. Pap.* 1246.
- Cramer, J.J., and H.W. Nesbitt. 1983. Mass-balance relation and trace-element mobility during continental weathering of igneous rocks. *Colloq. Int. CNRS* 73:63-74.
- Deer, W.A., R.A. Howie, and J. Zussman. 1962. *Rock-forming minerals*. Vol. 3. Sheet silicates. Longmans, London.
- Delvigne, J., E.B.A. Bisdom, J. Sleeman, and G. Stoops. 1979. Olivines, their pseudomorphs and secondary products. *Pedologie* 24(3):161-169.
- Eggleton, R.A., C. Foudoulis, and D. Varkevisser. 1987. Weathering of basalt: Changes in rock chemistry and mineralogy. *Clays Clay Miner.* 35:161-169.
- Environmental Systems Research Institute. 1989. *Users guide: ARCEDIT*. ESRI, Redlands, CA.
- Feijtel, T.C., A.G. Jongmans, and J.D.J. van Doesburg. 1989. Identification of clay coatings in an older Quaternary terrace of the Allier, Limagne, France. *Soil Sci. Soc. Am. J.* 53:876-882.
- FitzPatrick, E.A. 1970. A technique for the preparations of large thin sections of soils and consolidated material. p. 3-13. *In* D.A. Osmond and P. Bullock (ed.) *Micromorphological techniques and applications*. *Tech. Monogr. 2*. Rothamsted Exp. Sta., Harpenden, England.
- FitzPatrick, E.A. 1984. *Micromorphology of soils*. Chapman and Hall, London.
- Gardner, L.R., J. Kheornromne, and H.S. Chen. 1978. Iso-volumetric geochemical investigation of a buried granite saprolite near Columbia, S.C., USA. *Geochim. Cosmochim. Acta* 42:417-424.
- Glassman, J.R., and G.H. Simonson. 1985. Alteration of basalt in soils of western Oregon. *Soil Sci. Soc. Am. J.* 49:262-273.
- Hendricks, D.M., and L.D. Whittig. 1968. Andesite weathering: 1. Mineralogical transformation from andesite to saprolite. *J. Soil Sci.* 19:147-153.
- Jongmans, A.G., T.C. Feijtel, R. Miedema, N. van Breemen, and A. Veldkamp. 1991. Soil formation in a Quaternary terrace sequence of the Allier, France. Macro- and micromorphology, particle size distribution, chemistry. *Geoderma* 49:215-239.
- Kaub, B.S., and B.J. Carter. 1987. Determining Ti source and distribution within a Paleustalf by micromorphology, submicroscopy, and elemental analysis. *Geoderma* 40:141-156.
- McCaire, J.J., A. Perruchot, and J. Dejou. 1988. Transformations Géochimiques au Cours de l'altération Météorique d'une Basalte Pliocène du Massif Central Français. *Geoderma* 41:287-314.
- Meunier, A. 1983. Micromorphological advances in rock weathering studies. p 467-483. *In*: P. Bullock and C.P. Murphy (ed.) *Soil micromorphology*. Vol. 2: Soil genesis. *Proc. Int. Work. Meet. Soil Micromorph.*, London. August 1981. Academic Publ., Berkhamstead, England.
- Van der Plas, L., and A.C. Tobi. 1965. A chart for judging the reliability of point counting results. *Am. J. Sci.* 263:87-90.
- Veldkamp, E., A.G. Jongmans, T.C. Feijtel, A. Veldkamp, and N. van Breemen. 1990. Alkali basalt gravel weathering in quaternary Allier river terraces, Limagne, France. *Soil Sci. Soc. Am. J.* 54:1043-1048.

2.4 The progression from optical light microscopy to transmission electron microscopy in the study of soils.

Clay Minerals, 1994 (in press)

F. van Oort, A.G. Jongmans, and A.M. Jaunet.

THE PROGRESSION FROM OPTICAL LIGHT MICROSCOPY TO TRANSMISSION ELECTRON MICROSCOPY IN THE STUDY OF SOILS

F. VAN OORT, A. G. JONGMANS AND A. M. JAUNET*

Station de Science du Sol, INRA, Route de Saint-Cyr, 78026 CEDEX, Versailles, France and * Dept. of Soil Science and Geology, Agricultural University, P.O. Box 37, 6700 AA Wageningen, The Netherlands

(Received 27 January 1993; revised 27 September 1993)

ABSTRACT: The use of electron microscopy to study clay microfibrils in thin-sections is discussed. A technique is described to isolate undisturbed microparts of pedofeatures from thin-sections, which are subsequently used for TEM analysis. Re-embedding with a polyester resin of undisturbed, *in situ*, neoformed clay microfibrils, obtained by microdrilling and preparation of ultrathin sections by microtoming with a diamond knife are emphasized; these steps enable micromorphology, clay mineralogy, microchemical and HRTEM analysis to be performed on one unique microsample of clay fabrics, with conserved micro-organization. Two examples on clay neoformation are presented to demonstrate that this technique can successfully be applied to unravel the impact of mineral alteration and clay neoformation in undisturbed soil samples on a micro- and a nanometer scale.

Clay neoformation studies in thin-sections still encounter difficulties regarding the analysis of chemical and mineralogical composition, and of the size, shape and arrangement of individual particles. The later parameters particularly influence the optical behaviour of clay fabrics. These difficulties are mainly due to the low resolving power of the optical microscope. Sub-microscopical techniques, such as transmission electron microscopy (TEM), combined with energy dispersive spectroscopy (EDS), scanning electron microscopy-energy dispersive X-ray analysis (SEM-EDXRA) and step scan X-ray diffraction (SSXRD) subsequent to microdrilling have been developed in order to counter this problem (Bisdorf, 1981; Meunier & Velde, 1982; Beauford *et al.*, 1983; Feijtel *et al.*, 1989). However not all of such techniques allow *in situ* studies in thin-sections. Transmission electron microscopy studies on clay microfibrils are often carried out on dispersed clay fractions (Tessier, 1984; Bisom *et al.*, 1990) where the original spatial arrangement cannot be studied. In studies on mineral weathering and clay neoformation, TEM is usually performed on separated grains, collected by hand using a binocular microscope (Velbel, 1989; Banfield & Eggleton, 1990). Consequently, problems of non-representative sampling may arise, because of mineral micro-

impurities. Moreover, isolation of mineral grains becomes very difficult as their size decreases.

In mineral weathering and clay neoformation studies, as well as study on microstructure and microfibrils, it is important to know the morphology of individual constituents and their arrangement. Transmission electron microscopy can be used, but undisturbed, ultrathin (60 nm) samples of uniform thickness are required in order to avoid artefacts such as undesirable contrast. Bresson (1981) proposed that ion micro-milling be adapted for soil micromorphological studies on mineral weathering, microstructures and fabrics. For heterogeneous soil samples, this thinning technique presents major disadvantages such as thickness variations due to the amorphous state of some phases. Therefore, an important hiatus still exists between microscopic observations of a unique sample on a micrometric and a nanometric scale.

In order to rectify this hiatus we combined optical microscopy of clay fabrics in thin-sections with TEM. The latter technique was performed on undisturbed, micromorphologically characterized clay features, obtained by isolating selected areas in uncovered thin-sections. Thus, a combination of analytical methods can be performed on one unique microsample of clay fabrics, showing its original micro-organization. The goal of this

paper is to describe the technical procedure, to emphasize the specific steps (re-embedding of the microsamples and ultramicrotomy using a diamond knife) and to present two examples illustrating its utility in pedogenic studies, especially in weathering and in the neoformation of minerals.

METHODS

Thin-section preparation and analysis

Uncovered thin-sections (5 × 3 cm) were prepared according to FitzPatrick (1970) and Miedema *et al.* (1974) using a polyester resin (Synolith 544); the micromorphological interpretation is based on the terminology of Bullock *et al.*, (1985). *In situ* chemical analysis of clay fabrics on thin-sections can be carried out using SEM-EDXRA (Bisdorn *et al.*, 1990).

Selection, isolation and re-embedding of micro-samples

Micro-areas of features are selected with a petrographic microscope by studying an uncovered thin-section which is placed in a microscope stage-mounted micromanipulator to enable horizontal sample movement. Isolating an undisturbed micro-sample was carried out with a microscope-mounted drill (Verschure, 1978) which can be moved in a vertical direction, and has a hardened stainless steel needlepoint, sharpened to a 20 µm tip. Isolating a micro-sample of about 30 × 30 µm starts with removal of all surrounding soil material over a distance of 100 µm by microdrilling (Fig. 1). The powdery soil material produced, is removed and the cleaned micro-sample, only connected now with the underlying glass slide, is covered with a small drop of distilled water. The top of the non-rotating drill is then placed between the micro-sample and the glass slide. The micro-sample is carefully loosened from the glass slide by moving the microscope stage, and finally floats in the water drop.

Small gelatine capsules filled with hardened polyester resin (Synolith 544) are used for re-embedding the micro-sample. After inverting the thin-section, the droplet containing the micro-

drilled sample is placed in contact with the surface of the resin-filled gelatine capsule and, due to surface tension forces, is transferred to the resin surface (Beauford *et al.*, 1983). The effectiveness of the sample transfer and eventual disturbance are controlled using a binocular microscope. After evaporation of the excess water, the micro-sample is covered with a droplet of Synolith resin. In order to avoid air inclusions in the resin droplet and around the micro-sample, it is recommended that re-embedding under vacuum is performed.

Microtomy and TEM

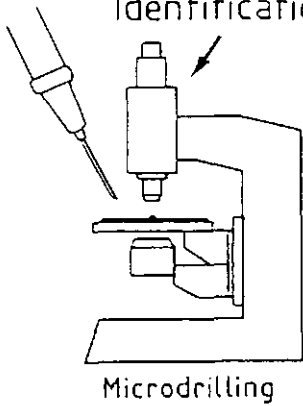
The upper side of the gelatine capsule is cut with a glass knife to a pyramidal shape so that the microsample is centred at the top of the pyramid. Then ultrathin sections ~60 nm thickness are obtained with a Reichert Ultracut E, using a diamond knife. Possible micro-disturbance of these sections depends on size, texture and mineral heterogeneity of the sample, as well as the effectiveness of re-embedding. The ultrathin sections are finally observed with a Philips 420 TEM. Low magnifications enable observation of micro-disturbance and selection of undisturbed areas. A Link AN 1000 EDS analyser allows qualitative and quantitative microchemical analysis.

MATERIALS

Two examples of studies on microdrilled *in situ* clay features from thin-sections are presented. Samples of the first example were taken at 10m depth in a grey coloured, fine, andesitic ash deposit, underlying a ferrallitic soil cover in Guadeloupe (French Antilles). The ash layer is poorly drained, because its contact with the underlying pyroclastic deposit is cemented. The resulting accumulation of leached silica and basic cations from the overlying ferrallitic soil cover gives rise to a dominant neoformation of high swelling smectitic clay minerals (van Oort & Jaunet, 1990).

Samples for the second example were collected in an older Quaternary Allier river terrace in France. Weathering of large amounts of volcanic fragments resulted in neoformation of different types of clay coatings (Jongmans *et al.*, 1991).

Identification of Micromorphological Features on thin sections

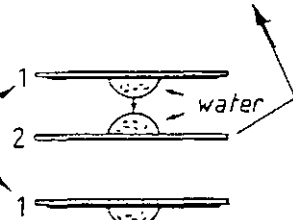


Microdrilling

SEM EDXRA
Scanning Electron Microscope
Energy Dispersive
X Ray Analysis

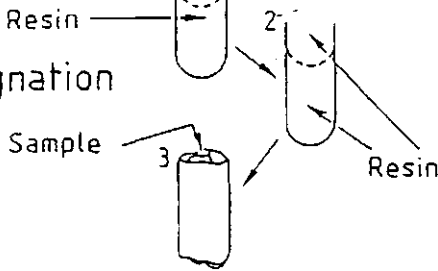
Step Scan
X Ray Diffraction

Sample
Transfer

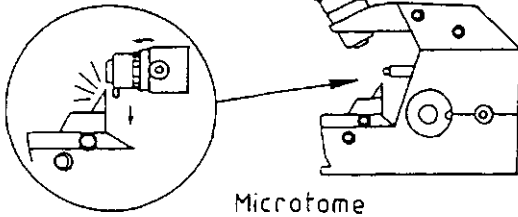


in situ study of:
- optical behaviour
- mineralogical nature
- chemical composition
- size, morphology and
arrangements of soil
constituents and
microfabrics

Re-impregnation



High Resolution
Transmission Electron
Microscopy



Microtome

FIG. 1. Schematic presentation of the main steps of the technical procedure.

RESULTS AND DISCUSSION

Example 1, Ash deposits, Guadeloupe

Isovolumetric pyroxene weathering, resulting in complete dissolution of the fresh pyroxene minerals, has led to the formation of open clay boxwork pseudomorphs (Delvigne, 1983). Micro-morphological study reveals that the pseudomorphs consist of anisotropic, limpid, non-laminated, pale greenish-yellow, neoformed clay infillings in which clay domains are mainly parallel to former walls of intramineral cracks (Fig. 2, I, II, B). Neoformed, parallel clay domains with similar properties, as described above, are often perpendicular to facies B (Fig. 2, I, II, A), demonstrating a denticulated (Velbel, 1989) outer boundary. These neoformed clay domains show straight extinction parallel to the *c*-axis indicating that the original mineral consisted of an orthopyroxene (Delvigne & Stoops, 1990). Very fine (<10 µm) cracks, filled with anisotropic clay, connected with larger clay-filled intra-mineral fissures run across these neoformed clay facies (A) in all directions. Absence of an oxyhydroxide stage with well crystallized goethite in the boxwork indicates that local weathering conditions do not reach a ferrallitic level (Delvigne, 1983; Nahon & Colin, 1983). Opacally, no differences in clay mineralogy could be observed in the neoformed clay pseudomorph. Step scan X-ray diffraction (not shown) performed on small fragments obtained by microdrilling in the boxwork pseudomorph revealed broad reflections around 1.4 and 0.73 nm, suggesting the presence of 2:1 and possibly some 1:1 type clay minerals.

Transmission electron microscopy observations, performed on the isolated, undisturbed subsamples of the boxwork pseudomorphs, reveal two distinctive clay microfabrics (Fig. 2, III): relatively large, highly oriented clay domains (facies A) occur perpendicular to small bands composed of circular bodies (facies B). At low magnifications (Fig. 2, III), the related distribution pattern of facies A and B is fairly similar to the related distribution patterns of the neoformed clay infillings (facies B) and the denticulate shaped facies A observed in thin-sections. High-resolution lattice-fringe imaging reveals elementary spacings of 1.4 nm for facies A and 0.73 nm for facies B (Fig. 2, IV). Both facies are generally separated by a very thin zone of amorphous

compounds. The occurrence of voids, occasionally observed between clay facies A and B (Fig. 2, IV), is interpreted as an artificial separation due to the high vacuum conditions of TEM. Microchemical analysis show low Al/Si and Al/Fe ratios for facies A, whereas the Al/Si ratio is close to 1 for facies B (Fig. 2, IV).

Results of SSXRD, TEM and microchemical analysis suggest an initial transformation of the orthopyroxene to close packed, smectitic (non-tronitic) clay domains along former cleavage planes. Increased drainage conditions in intramineral cracks result in the formation of well crystallized halloysite particles, homogeneous with respect to size and morphology. In this example, TEM performed on a fragment of a clay pseudomorph after pyroxene, enables us to visualize and to characterize the presence and the related distribution pattern of two different clay types within 5 µm, suggesting two totally different geochemical neoformation conditions over this distance.

Example 2, Allier terrace, France

Micromorphological studies of soils developed on volcanic substrates have indicated that both crystalline and non-crystalline neoformed materials are important constituents (Wada, 1980; Chartres *et al.*, 1985; Buurman & Jongmans, 1987; Eggleton, 1987). Weathering of volcanic rock fragments in an older end-member of a Quaternary Allier terrace sequence has resulted in the formation of neoformed clay coatings at depths of 1 m (facies C) and 5 m (facies D) respectively (Jongmans *et al.*, 1991).

Optical light microscopy on thin-sections shows that both facies are isotropic to partially weak anisotropic, limpid, non-laminated, pale yellow clay coatings and, consequently, similar from a micromorphological point of view (Fig. 3 I, II). According to Bullock *et al.* (1985), isotropism of the coatings is generally attributed to the occurrence of short-range ordered material or randomly oriented halloysite particles.

In the step scan X-ray diffractogram of facies D, no peaks occur, demonstrating that this facies is X-ray amorphous. Multiple SSXRD analyses of facies C show broad bands between 1.0 and 0.7 nm, but suggest also the occurrence of some 2:1 minerals. The Al/Si ratio is close to 1 for facies C

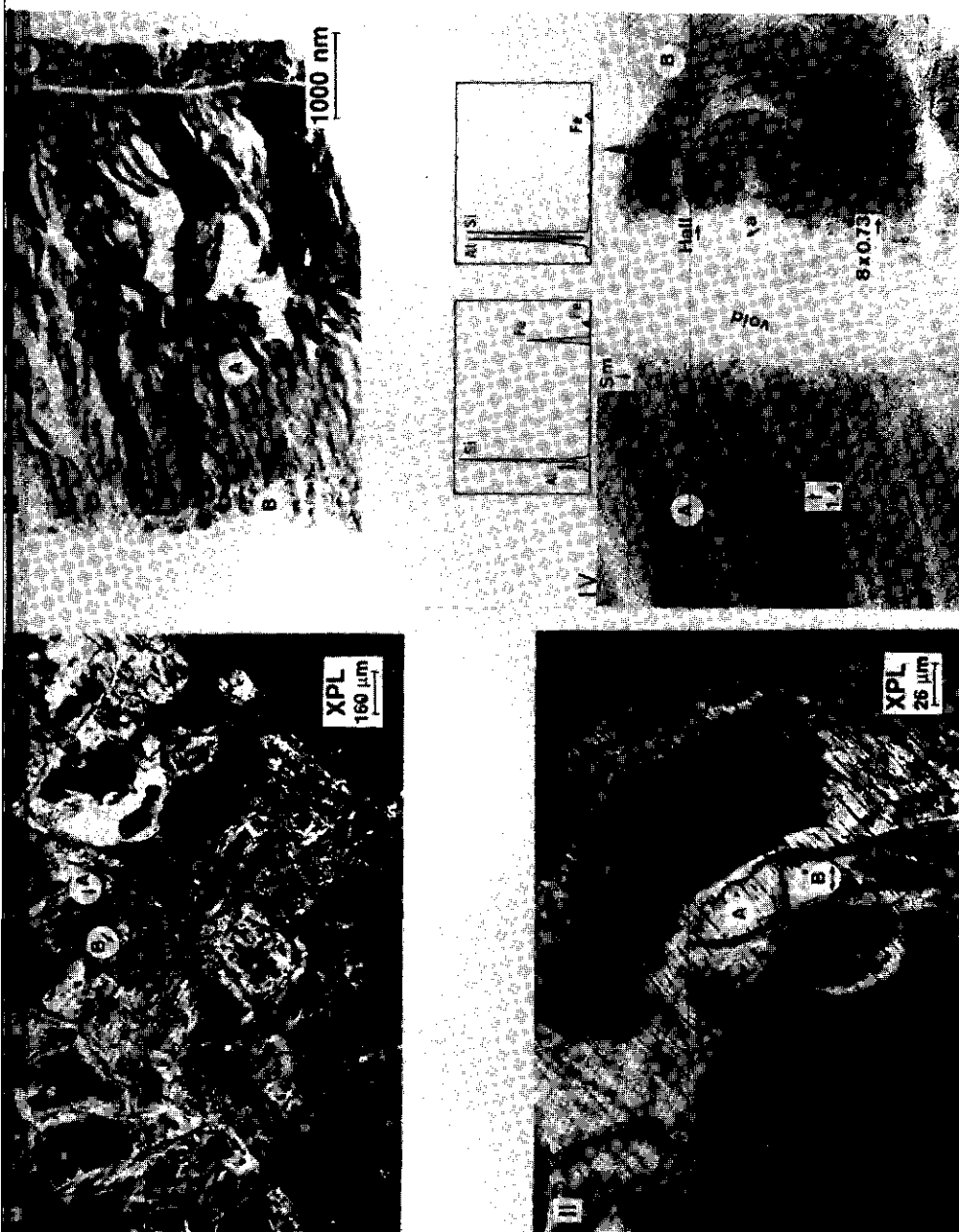


FIG. 2. Optical light microscopy and TEM of example 1. I: micromorphological overview of an open boxwork pseudomorph with facies A and B; II: micromorphology of facies A and B; III: TEM images of facies A and B; IV: detail of Fig. 2, III with corresponding EDS microchemical analysis of facies A and B (Al = amietite; Hall = halloysite; a = amorphous material; individual clay layer thickness in nm).

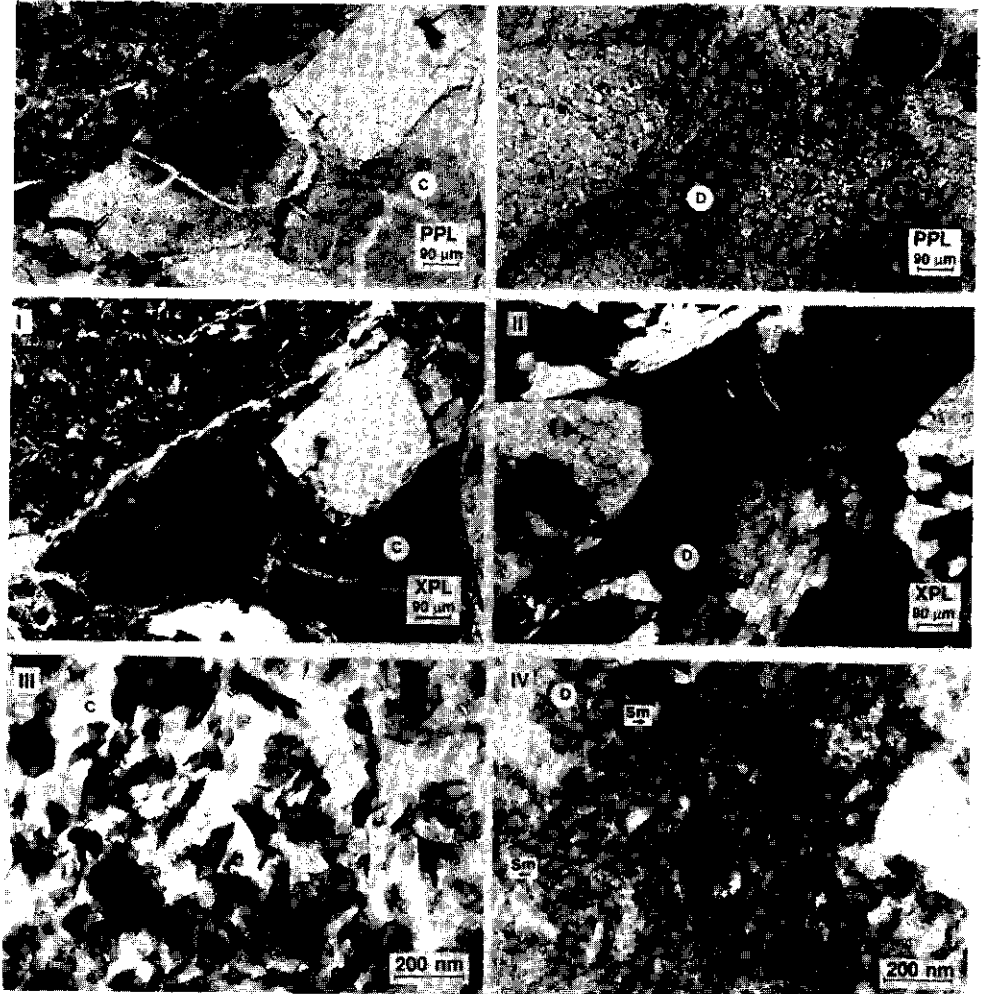


FIG. 3. Optical light microscopy and TEM of example 2. I micromorphology of facies C; II micromorphology of facies D; III TEM image of facies C; IV TEM image of facies D. (XPL = crossed polarized light; PPL = plain polarized light; Sm = smectite; a = amorphous material).

and 0.5 for facies D, as measured by SEM-EDXRA (Feijtel *et al.*, 1989), indicating 1:1 phases and amorphous compounds, respectively.

The TEM study performed on the *in situ* micro-organization of microdrilled subsamples shows that facies C consists exclusively of halloysitic clay minerals in a random distribution pattern (Fig. 3, III). Facies D, however, consists predominantly of amorphous material (Fig. 3, IV); well crystallized phyllosilicates occur locally and both parti-

cle morphology and lattice-fringe imaging point to smectitic clay domains.

In this example, TEM analyses on the *in situ* micro-organization of undisturbed microparts of two optically identical clay coatings, demonstrate differences in their mineralogical composition. Such findings evidently influence pedogenetic interpretations. Facies C is frequently covered by clay illuviation coatings (Jongmans *et al.*, 1991). Hence, disagreements between SSXRD and

TEM data for facies C (traces of 2:1 minerals) may be explained by the occurrence of impurities in the microdrilled samples used for SSXRD analysis. Facies C coatings are yet to be subjected to further examination.

In addition, preliminary work on perfecting this technique was carried out on the neoformation of halloysite on weathered andesite fragments (van Oort *et al.*, 1990). The combination of SSXRD and SEM-EDXRA revealed identical mineralogical and chemical compositions for optically distinct different clay features (1:1 clay); TEM allowed observations of the variability in optical behaviour that resulted from differences in size, shape and arrangement of individual halloysitic clay particles.

CONCLUSIONS

Until now, application of TEM on *in situ* clay microfabrics in thin-sections encountered difficulties because of the lack of a suitable technique to reduce the impregnated fragments of thin-sections to a required thickness of 60 nm. The specific steps of our technical procedure consist of: (1) re-embedding of very small (<50 µm) undisturbed microparts of micromorphologically characterized features, obtained by microdrilling in uncovered thin-sections and: (2) subsequent careful microtomy of these microquantities using a diamond knife, producing ultrathin sections (60 nm). As a result, our technique yields suitable samples for TEM analysis on the undisturbed organization of *in situ* neoformed clay microfabrics.

The two examples presented clearly demonstrate that pedogenic studies cannot be limited to observations of optical properties of clay fabrics in thin-sections. The TEM study on ultrathin sections of undisturbed microfabrics, obtained by microdrilling in thin-sections showed that different optical properties can be linked to differences in mineralogical and chemical compositions, and to the size, shape or arrangement of individual clay particles. In example 1, the occurrence of neoformed smectite next to halloysite, within a few nm, is evident in an open boxwork pseudomorph after an orthopyroxene. The existence of different clay species in microsites of mineral weathering is well known. Our technique, however, enables the user to visualize and to analyse

these minerals in their natural organization, resulting from local geochemical conditions according to inherited primary mineral crystal structures (e.g. cleavage planes, intra- and inter-mineral cracks). Hence, in the study of soil formation, the technique described appears to be well adapted for unravelling the impact of *in situ* mineral weathering and clay neoformation on micro- and nanometer scales.

ACKNOWLEDGMENTS

The authors thank Mrs R. Dupont, Mrs M. Lemain, Mr J.D.J. van Doesburg and Mr A. van Dijk for skilled technical assistance, Mrs F. Elsass and Mr M. Robert for their continuous support, and Mrs S. Staunton for critical reading of the English version.

REFERENCES

- BANFIELD J.F. & EGGLESTON R.A. (1990) Analytical transmission electron microscope studies of plagioclase, muscovite and K-feldspar weathering. *Clays Clay Miner.* 38, 77-89.
- BEAUFORD D., DUDIGNON P., PROUST D., PARNEX J.C., & MEUNIER A. (1983) Microdrilling in thin sections: A useful method for identification of clay minerals *in situ*. *Clay Miner.* 18, 219-222.
- BISDOM E.B.A. (editor) (1981) Sub microscopy of soils and weathered rocks. 1st workshop of the international working-group on submicroscopy of undisturbed soil materials 1980, Wageningen, The Netherlands. 320pp.
- BISDOM E.B.A., TESSIER D. & SCHOUTE J.F.Th. (1990) Micromorphological techniques in research and teaching (submicroscopy). Pp. 581-603 in: *Soil Micromorphology: a Basic and Applied Science*. (L.A. Douglas, editor). Developments in Soil Science 19, Elsevier, Amsterdam.
- BRESSON L.M. (1981) Ion micromilling to the ultramicroscopic study of soils *Soil Sci. Soc. Am. J.* 45, 568-573.
- BULLING P., FEDOROFF N., JONGERUS A., STOOFS G. & TUKSMA T. (1985) *Handbook for Soil Thin Section Description*. Waine Res. Pub., Albrighton, England.
- BUURMAN P. & JONGMANS A.G. (1987) Amorphous clay coatings in a lowland oxisol and other andesitic soils of East Java, Indonesia. *Pembertanian Penelitian Tanah dan Pupuk* 7, 31-40.
- CHARTLES C.J., WOOD A. & PAIN C.F. (1985) The development of micromorphological features in relation to some mineralogical and chemical properties of volcanic ash soils in highland Papua New Guinea. *Aust. J. Soil Res.* 23, 339-354.

- DELVIGNE J. (1983) Micromorphology of the alteration and weathering of pyroxenes in the Koua Bocca ultramafic intrusion, Ivory Coast, West Africa. *Sci Géol. Mém.* 72, 57-68.
- DELVIGNE J. & STROOPS G. (1990) Morphology of mineral weathering and neoformation. I. Weathering of most common silicates. Pp. 471-481 in: *Soil Micromorphology: a Basic and Applied Science* (L.A. Douglas, editor). Developments in Soil Science 19, Elsevier, Amsterdam.
- EGGLETON R.A. (1987) Noncrystalline Fe-Si-Al oxyhydroxide. *Clays Clay Miner.* 35, 29-37.
- FÉJTEL T.C., JONGMANS A.G. & VAN DOESBURG J.D.J. (1989) Identification of clay coatings in an older Quaternary Terrace of the Allier, Limagne, France. *Soils Sci. Soc. Am. J.* 53, 876-882.
- FITZPATRICK E.A. (1970) A technique for the preparation of large thin sections of soil and consolidated material. Pp. 3-13 in: *Micromorphological Techniques and Applications*. (D.A. Osmond & P. Bullock, editors). Soil Survey Technical Monograph 2, Harpenden, UK.
- JONGMANS A.G., FÉJTEL T.C., MIEDEMA R., VAN BREEKON, N. & VELDKAMP A. (1991) Soil formation in a Quaternary terrace sequence of the Allier, Limagne, France. Macro- and micromorphology, particle size distribution, chemistry. *Geoderma* 49, 215-239.
- MEUNIER A. & VELDE B. (1982) X-ray diffraction of oriented clays in small quantities (0.1 mg). *Clay Miner.* 17, 259-262.
- MIEDEMA R., PAPE T. & VAN DER WAAL G.J. (1974) A method to impregnate wet soil samples, producing high-quality thin sections. *Neth. J. Agric. Sci.* 22, 37-39.
- MAHON D.B. & COLIN F. (1983) Chemical weathering of orthopyroxenes under lateritic conditions. *Amer. J. Sci.* 282, 1232-1243.
- VAN OORT F. & JAUNET A.-M. (1990) Origin, mineralogical behaviour and spatial distribution of 2:1 clay minerals in a ferrallitic soil cover on volcanic parent rock of Guadeloupe. *Sci Géol. Mém.* 85, 205-213.
- VAN OORT F., JONGMANS A.G., JAUNET A.-M., VAN DOESBURG J.D.J., ELSASS F., FEJTEL T.C. (1990) Characterization of clay formation in thin sections. A case study on halloysite neoformation in weathered pyroclastic parent rock in Guadeloupe. *Trans. 14th Int. Congr. Soil Sci. Kyoto, Japan*, 7, 100-105.
- TESSIER D. (1984) *Etude expérimentale de l'organisation des matériaux argileux. Hydratation, gonflement et structuration au cours de la dessiccation et la réhumectation*. Thèse, Univ. Paris VII, France.
- VELSEL M.A. (1989) Weathering of hornblende to ferruginous products by a dissolution-precipitation mechanism: petrography and stoichiometry. *Clays Clay Miner.* 37, 515-524.
- VERSCHURE R.H. (1978) A microscope-mounted drill to isolate microgram quantities of mineral material from polished thin sections. *Mineral. Mag.* 42, 499-503.
- WADA K. (1980) Mineralogical characteristics of Andisols. Pp. 87-107 in: *Soils with Variable Charge* (B.K.G. Theng, editor) N.Z. Soc. Soil Sci., Soil Bureau, DSIR, Lower Hutt, New Zealand.

CHAPTER 3

FORMATION OF SECONDARY MINERALS

3.1 Morphology, chemistry, and mineralogy of isotropic aluminosilicate coatings in an Andisol of Guadeloupe

Soil Sci. Soc. Am. J., 58: 501-507 (1994)

A.G. Jongmans, F. van Oort, P. Buurman, A.M. Jaunet, and J.D.J. van Doesburg.

Morphology, Chemistry, and Mineralogy of Isotropic Aluminosilicate Coatings in a Guadeloupe Andisol

A. G. Jongmans,* F. van Oort, P. Buurman, A. M. Jaunet, and J. D. J. van Doesburg

ABSTRACT

Few micromorphological and *in situ* submicroscopical studies exist of neoformed amorphous and crystalline clay coatings, and little is known about the genesis and distribution patterns of these coatings and their dependence on site conditions. Our study describes the distribution and composition of isotropic coatings, infillings, and pseudomorphs after roots in a Hapludand on Holocene andesitic pyroclastics in humid tropical Guadeloupe. Field observations show the occurrence of fine-textured, very pale brown to yellow (10YR 8/3-8/6) coatings, infillings, and pseudomorphs after roots in large pores in the Bw2 and 2C horizons of the soil. Thin-section analyses demonstrated that these features are isotropic, translucent, nonlaminated, and appear pale yellow in plane polarized light, indicating that they consist of amorphous material. *In situ* submicroscopical analyses revealed that the coatings in the Bw2 horizon consist of allophane and imogolite with an Al/Si ratio of 2, whereas those in the 2C horizon consist exclusively of allophane with an Al/Si ratio of 1.4. The fine groundmass adjacent to the coatings in the Bw2 horizon has an Al/Si ratio of 1.4. The coatings resulted from precipitation of weathering products of mainly volcanic glass and plagioclase. The observed differences in composition of the coatings in the Bw2 and 2C horizons are thought to be the result of different leaching conditions.

ALLOPHANE is a group of short-range order clays that contain silica, aluminum, and water (Parfitt, 1990). Imogolite is a paracrystalline thread-like aluminosilicate with longer range order (Wada, 1989). Allophane and imogolite are common in Andisols (Brown et al., 1978), but also occur in Inceptisols and Spodosols (Tait et al., 1978; Parfitt and Webb, 1984; Parfitt and Saigusa, 1985; Farmer et al., 1985; Shoji and Yamada, 1991; Wang et al., 1986). In parent materials rich in easily weatherable minerals, Al will precipitate with Si from the soil solution to form Al/Si gels like allophane and imogolite as long as the weathering environment is not dominated by organic acids. Shoji et al. (1982), Shoji and Fujiwara (1984), and Mizota and van Reeuwijk (1989) reported an inverse relationship between the formation of Al-humus complexes and allophane or imogolite.

Although chemical and mineralogical studies of allophane and imogolite in Andisols are common (Aomine and Mizota, 1973; Farmer and Fraser, 1977; Shoji and Saigusa, 1977; Lowe, 1986; Wada, 1989; Parfitt, 1990), studies of allophane and imogolite by micromorphological and submicroscopical techniques in undisturbed soil samples by means of thin sections are scarce. Wada and Matsubara (1968) described the spatial relationship between allophane and imogolite in weathered pumice, but they did not use micromorphological techniques. Aomine and Wada (1962) reported occurrence of hydrated halloysite along channels that were situated in a Si-rich allophanic groundmass in ash deposits in Japan. Occurrence of isotropic coatings in volcanic soils was described by Dalrymple (1964, 1967) and Chartres et al. (1985), but these authors did not attribute the coatings to allophane. Farmer et al. (1985) reported the occurrence of allophane and imogolite gel deposits in a B horizon of a Spodosol. Buurman and Jongmans (1987) and Jongmans et al. (1993) described the occurrence of allophane as isotropic coatings and infillings in the voids of volcanic soils in Indonesia and France, respectively, and concluded that the different chemical compositions of the coatings resulted from variations in parent material and drainage conditions.

Amorphous materials appear to be widespread in soils that formed from parent materials rich in easily weatherable minerals. The amorphous materials apparently formed by precipitating from the soil solution. Because larger pores play a major role in the transport of the soil solution, coatings of allophane and imogolite on pore walls should be a common feature. Because allophane and imogolite may transform into long-range order clay minerals, depending on leaching conditions and the soil's temperature and moisture regime, such transformations could also be found in allophane and imogolite coatings. Buurman and Jongmans (1987) and Jongmans et al. (1993) demonstrated that allophane in coatings can transform to either 1:1 or 2:1 anisotropic phyllosilicate coatings, which are easily confused with clay illuviation coatings.

A. G. Jongmans, P. Buurman, and J. D. J. van Doesburg, Dep. of Soil Science and Geology, Agricultural Univ., P. O. Box 37, 6700 AA, Wageningen, the Netherlands; F. van Oort, INRA, Station Agropedoclimatique, B.P. 1232, F-97185 Pointe à Pitre Cédex, Guadeloupe, France; and A. M. Jaunet, INRA, Station Science du Sol, Route de St-Cyr, 78026 Cédex, Versailles, France. Joint contribution of the Agricultural Univ., Wageningen, and the INRA, Versailles and Guadeloupe. Received 15 Oct. 1992. *Corresponding author.

Abbreviations: Al_o, acid ammonium oxalate extractable Al; Fe_o, acid ammonium oxalate extractable Fe; Si_o, acid ammonium oxalate extractable Si; Fe_p, pyrophosphate-extractable Fe; Al_p, pyrophosphate-extractable Al; Fe_d, dithionite-extractable Fe; Al_d, dithionite-extractable Al. SEM-ED-XRA, scanning electron microscopy-energy-dispersive x-ray analysis; SSXRD, step scan x-ray diffraction; TEM, transmission electron microscopy; CEC, cation-exchange capacity.

In the Bw2 and 2C horizons of an Andisol in Guadeloupe (French Antilles), we observed fine-textured, very pale brown to yellow coatings, infillings, and pseudomorphs after roots (replacement of the root by inorganic compounds with preservation of the original external shape and volume of the root). The soil was formed under humid tropical conditions, where soil weathering normally leads to formation of amorphous materials. The goal of our study was to establish the morphology, chemistry, and mineralogy of the coatings, infillings, and pseudomorphs at different depths in this Andisol using micromorphological and submicroscopical techniques. In addition, the mineralogical and chemical differences of the features were studied in relation to environmental conditions.

MATERIAL AND METHODS

The study site is situated on a toeslope (2–5%, altitude 1000 m) of the Souffrière, the active volcano on the island of Basse Terre in Guadeloupe (de Reynal de Saint-Michel, 1966). The soil has an isothermic temperature regime and a perudic moisture regime. Annual rainfall exceeds 4500 mm. The vegetation is grassland and the site is presently used for extensive grazing. The parent material consists of andesitic ash deposits of 1.50 m in thickness and ≈ 500 yr old. Andesitic ash (with particles <3 mm in diam.) from the 1967 eruption was observed in the upper 25 cm. Andesitic tuff that is ≈ 3000 yr old occurs below a depth of 150 cm (Dagain, 1981). The consistence varies between extremely firm and firm. Plagioclase, augite, hypersthene, and opaque minerals dominate the single mineral grains; andesitic rock fragments, frequently with a glassy groundmass, are the major compound mineral grains in the deposits. The soil is well drained.

The soil was described following the guidelines of the Food and Agriculture Organization of the United Nations (1990), and was classified as a hydrous, isothermic Acrudoxic Hapludand (Soil Survey Staff, 1992). Thixotropy of the soil horizons was determined in the field as proposed by Soil Survey Staff (1975). Bulk samples of each horizon were taken for chemical and physical analyses. Clay contents of the soil horizons were determined by sedimentation after destruction of the organic matter with H_2O_2 , and dispersion in sodium hexametaphosphate. Maximum dispersion was obtained by sonication and adjustment of the suspension pH to 4 with 1 M HCl.

Soil pH was measured potentiometrically in a 1:5 ratio of soil to water and 1 M KCl solution ratio. Organic C was determined following the Walkley-Black method (Walkley, 1947).

Exchangeable basic cations were determined in a 1 M NH_4OAc extract (van Reeuwijk, 1992). Cation-exchange capacity was determined by percolating the soil with $NaOAc$, replacement of the Na with NH_4 , and Na determination (van Reeuwijk, 1992).

Content of Fe_o , Al_o , Si_o , Fe_p , Al_p , Al_k and Fe_k were determined following the methods described in van Reeuwijk (1992). Concentrations of Al, Fe, and Si in the extracts were measured with atomic adsorption spectrometry. Allophane content was calculated according to the method of Mizota and van Reeuwijk (1989). Phosphate retention was determined by the method of Blackmore et al. (1987). Bulk density at field moisture content was measured on 10 samples that had volumes of ≈ 5 to 10 cm^3 per horizon. Moisture retention at 1.5 MPa was estimated by equilibrating a slurry from field-moist soil on a pressure plate for 72 h.

Undisturbed samples (8 by 8 cm) of the selected soil horizons were taken in tins. Before impregnation with polyester resin, the water in these samples was replaced by acetone according to the method of Miedema et al. (1974). Thin sections (8 by 8 cm) were made following the method of FitzPatrick (1970), and examined with a petrographic light microscope in plane polarized, and crossed polarized light. The micromorphological description used the terminology of Bullock et al. (1985). Volcanic glass content was quantified by counting 600 to 800 points in each thin section (ignoring the fraction $<15 \mu m$), to achieve standard deviations of $<3\%$ by volume for 95% confidence limits (Van der Plas and Tobi, 1965).

Multiple, in situ microchemical analyses of isotropic coatings, infillings, and pseudomorphs after roots that were present in the Bw2 and 2C horizons, as well as analyses of the adjacent groundmass in the Bw2 horizons, were performed on uncovered thin sections using SEM-EDXRA (Philips, Eindhoven, the Netherlands). The peak to background heights of the EDXRA signals were linearly transformed to element-mass percentages by comparison with standard minerals.

In situ isolation of microquantities of coatings and infillings from uncovered thin sections was performed with a microscope-mounted drill (Verschuren, 1978). X-ray diffraction patterns of this material were obtained with SSXRD, using $Co-K\alpha$ radiation with steps of $0.05^\circ 2\theta$ and counting times of 75 s per step.

Undisturbed sections of 50-nm thickness were cut from reimpregnated undisturbed fragments (size $\pm 50 \mu m$) of optically selected coatings in thin sections and were then prepared for TEM examination according to the method described in van Oort et al. (1989). Specimens were examined using TEM (Philips 420, Eindhoven, the Netherlands), which was also fitted with a Link AN 10000 EDS (Link System Ltd., Bucks, UK) for microchemical analysis.

RESULTS AND DISCUSSION

Macromorphological Data

Macromorphological properties are summarized in Table 1. All soil horizons are thixotropic, suggesting the presence of amorphous materials. Many biopores are present, and some contain root remnants. Many coarse fragments are soft and display weathering rinds, indicat-

Table 1. Selected macromorphological properties of the Hapludand studied.

Horizon	Depth cm	Munsell color (moist)	Textural class	Coarse fragments		Structure‡	Consistence§	Mottling¶	Pores	Coatings
				Abundance	Alteration†					
				% (v/v)						
A	0–25	10YR 3/2	loam	2–5	fr-sw	om	mfr,wss	–	m	–
Bw1	25–50	10YR 5/8	loam	2–5	sw-stw	f1sbk	mfr,wss	–	a	–
Bw2	50–150	7.5YR 4/6	loam	5–15	sw-stw	c1pr	mfr,wss	m	c	c
2C	>150	10YR 6/3	loam	15–40	fr-stw	om	mfi,mefi	–	c	m

† fr = fresh, sw = slightly weathered, stw = strongly weathered.

‡ om = structureless, massive; f1sbk = fine, weak subangular blocky; c1pr = coarse weak prismatic.

§ mfr = moist, friable; wss = wet, slightly sticky; mfi = moist, firm; mefi = extremely firm.

¶ – = not present; c = common; m = many; a = abundant.

ing that they were affected by weathering. The structure in the Bw horizon changes with depth from weak subangular blocky to weak prismatic. The wet consistence in the Bw is slightly sticky, slightly plastic, and the moist condition consistence is friable. In the 2C horizon the consistence varies from firm to extremely firm (moist). In the Bw2 and 2C horizons, many pores are lined or filled with fine-textured, very pale brown to yellow (10YR 8/3-8/6), coatings or infillings and pseudomorphs after roots, demonstrating precipitation of translocated material. From about 80 cm downward, common Fe (hypo) coatings (yellowish red, 5YR 5/8) are present on pore walls and ped surfaces, decreasing in amount with depth. At 3 m in depth these features are absent.

Physical and Chemical Data

As shown in Table 2, the clay content decreases with increasing depth. The higher sand content in the A horizon than in the Bw horizon reflects the addition of fresh particles as a result of the 1976 eruption of the Souffrière volcano. The 1500-kPa water retention of the B horizon is 650 g kg⁻¹. Bulk density values range from 0.41 Mg m⁻³ in the A horizon to 0.8 Mg m⁻³ in the 2C horizon, and meet the bulk density requirements for andic soil properties (Soil Survey Staff, 1992).

Comparison of pH values measured in water and KCl (Table 2) indicates that negative charges from organic matter exceed positive charges from allophane in the A1 horizon (pH[H₂O] > pH[KCl]). In the Bw2 horizon, the adsorption complex is dominated by positive charges (acidic properties, pH[H₂O] < pH[KCl]), while the Bw1 and C horizons have an intermediate position. The CEC decrease from 17.6 cmol_e kg⁻¹ in the A1 horizon to 12.1 cmol_e kg⁻¹ in the 2C horizon is probably due to the decrease of organic matter. Exchangeable cations are <0.4 cmol_e kg⁻¹ in all horizons. These low values in a soil with appreciable amounts of weatherable minerals apparently resulted from extensive leaching due to high rainfall (<4500 mm) and the high permeability of the soil as indicated by the porosity.

Both Al_o and (Al - Al_o) increase with depth, indicating a decreasing proportion of organically complexed Al and an increasing proportion of inorganically bound Al in the lower horizons. The latter is corroborated by Si_o contents and the calculated allophane content (Table 2), which also increase with depth. The phosphate retention throughout the pedon is >93%. The Fe_o values range from 19 in the A horizon to 27 g kg⁻¹ in the Bw1 horizon, and decrease in the 2C horizon to 2 g kg⁻¹. The Fe_p values are 13 g kg⁻¹ in the A and Bw1 horizon, whereas in the Bw2 horizon they are negligible. The

Fe_a values range from 30 to 43 g kg⁻¹ in the A and Bw horizon, and decrease in the 2C horizon to 7 g kg⁻¹. The (Al_o + 1/2Fe_o) value of >2, bulk density values of <0.9 g cm⁻³, and P retention values of >85% indicate andic soil properties in all sampled horizons.

Micromorphology of the Groundmass

Fresh andesitic rock fragments in the 2C horizon at a depth of 3 m have a porphyritic to seriate texture with many empty vesicles up to 100 μm in width. The andesite rock fragments consist of light brown, isotropic volcanic glass (19 ± 2.8% [v/v]), mixed with fine (<10 μm), lath-shaped plagioclases, pyroxenes, and opaque minerals. The large phenocrysts (up to 2 mm) are subhedral and euhedral plagioclase (locally with <30-μm isotropic glass and pyroxene impurities), augite, hypersthene, and opaque minerals.

In the groundmass of the 2C horizon at the 3-m depth, one-half of the volcanic glass and much of the small, lath-shaped plagioclase have been dissolved. The color of the remaining glassy groundmass shifts to yellowish brown, remains isotropic, and contains opaque minerals (<10 μm in diam.). Cross-banded and complex alteration patterns characterize plagioclase phenocrysts. The dissolution voids that have apparently formed in these plagioclases are filled with translucent, nonlaminated, pale yellow, isotropic fine-textured material (Fig. 1A and 1B) which is distinguishable from the altered isotropic glass in the groundmass by the absence of fine opaque Fe minerals. This observation indicates pseudomorphosis of the plagioclase minerals. In addition, many small and large open boxwork pseudomorphs after plagioclase with minute residues of plagioclase also occur (Fig. 1C-1F). These pseudomorphs consist of material similar to that in the partly weathered plagioclase phenocrysts. Cristobalite grains are common in this horizon. It appears that glass and plagioclase are dominantly affected by weathering, whereas pyroxenes remain relatively unaltered, which is in agreement with the findings of Aomine and Wada (1962) for volcanic ash and pumice deposits in Japan.

In the Bw horizons (25-150 cm), and in the A horizon (0-25 cm), the mineral components are: (i) plagioclase with cross-banded, complex, and pellicular alteration patterns and empty dissolution voids, suggesting high leaching activity in these horizons; (ii) hypersthene and augite with weak, pellicular alteration, indicating the inception of weathering of these minerals in these horizons; (iii) andesite fragments displaying pellicular alteration, which contain cross-banded and complexly altered plagioclase with empty dissolution voids; (iv) fresh volca-

Table 2. Selected physical and chemical data for the Hapludand studied.

Horizon	Depth cm	Texture			Bulk density Mg m ⁻³	Moisture content kg kg ⁻¹	pH		Organic C g kg ⁻¹	CEC†	Al _o ‡				Si _o	P retention %	Allophane %
		Clay	Silt	Sand			H ₂ O	KCl			Al _{o1} ‡	Al _{o2} ‡	Al _{o3} ‡	Al _{o4} ‡			
A1	0-25	23	40	37	0.41	1.3	5.7	4.8	85	17.6	21	13	16	4	96	3.2	
Bw1	25-50	19	56	25	0.49	1.5	5.0	5.0	48	11.5	37	10	20	13	99	10.0	
Bw2	50-150	13	63	24	0.59	1.2	4.8	5.3	27	10.2	72	6	16	32	99	25.0	
2C	150-300	10	45	45	0.80	0.8	5.2	5.0	5	12.1	74	4	4	38	93	28.0	

† Cation-exchange capacity.

‡ Subscripts o for ammonium oxalate extractable, p for pyrophosphate extractable, and d for dithionite extractable.

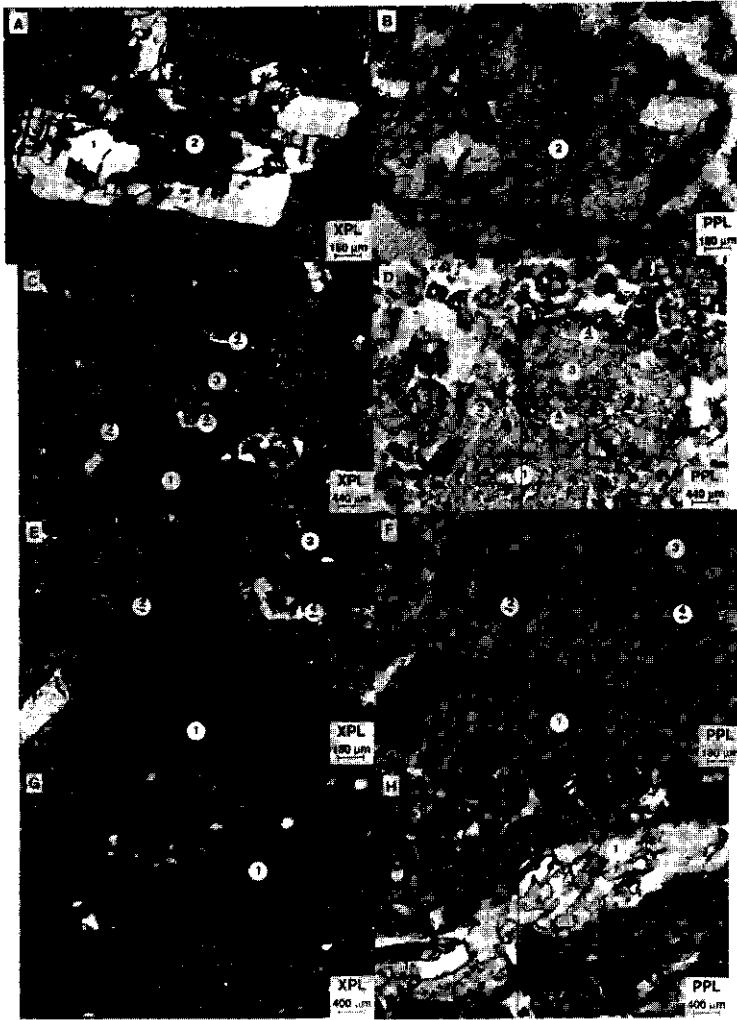


Fig. 1. Micromorphological images of coatings and infillings found in the 2C and Bw2 horizons. A and B: Cross-banded and complex alteration of plagioclase (1) in the 2C horizon (3 m depth). The dissolution voids are filled with an isotropic, translucent, pale-yellow isotropic fine-textured pseudomorph after plagioclase (2). XPL = crossed polarized light, PPL = plane polarized light. C and D: Shown for the 2C horizon are: an isotropic, translucent, pale-yellow infilling (1), a pseudomorph after a root (2), and an isotropic, translucent pseudomorph after plagioclase (3) with minute plagioclase residues (4). E and F: Details of C and D. G and H: Shown for the Bw2 horizon are an isotropic, translucent, pale-yellow coating-infilling (1); the part exposed to the void is impregnated with Fe compounds (hypocoating).

nic glass—the glass content in the Bw horizon is $4.7 \pm 1.7\%$ (v/v), and in the A horizon $5.6 \pm 1.9\%$ (v/v), indicating a stronger weathering of the glass in both horizons than in the C horizon; (v) opaque minerals up to $50 \mu\text{m}$ in diameter; and (vi) mineral components present only in the A horizon: fresh andesite fragments, plagioclase grains, and partly altered pumice fragments, indicating recent addition of mineral grains, probably during the 1976 eruption of the Souffrière.

The A and Bw horizons have a spongy microstructure resulting from biological activity. Both horizons are highly permeable.

Isotropic Coatings, Infillings, and Pseudomorphs after Roots

In the Bw2 and 2C horizons it is common to see pale yellow coatings, dense complete and incomplete

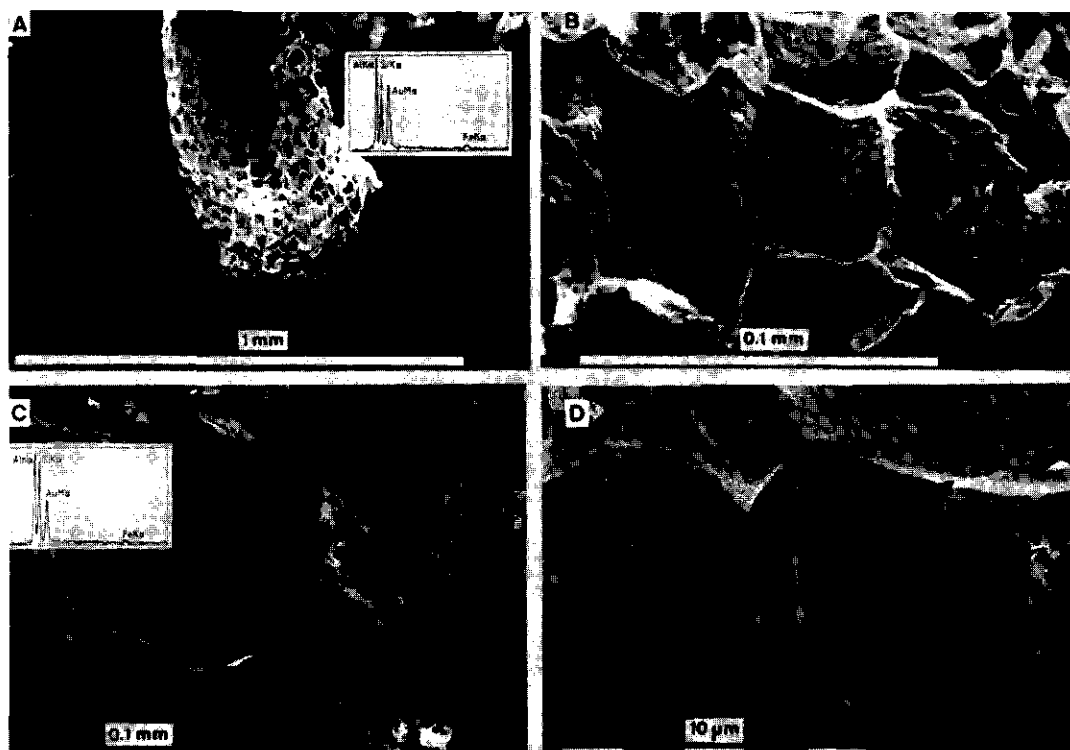


Fig. 2. Scanning electron micrographs and SEM-EDXRA analyses that show: (A) an overview and (B) detailed micrograph of a pale-yellow pseudomorph after a root consisting of Al and Si in the Bw2 horizon; and (C) an overview and (D) detailed micrograph of pale-yellow, nonlaminated coatings consisting of Al and Si in the 2C horizon.

infillings, and pseudomorphs after roots that are isotropic, translucent, and nonlaminated. These features occur predominantly in voids that are $>200 \mu\text{m}$ in diameter (Fig. 1C-1H). In the Bw2 horizon, the parts of the coatings that lie within the void are locally impregnated with Fe compounds, which form hypocoatings. The presence of isotropic material indicates precipitation of amorphous gels in these horizons. They are probably the result of co-precipitation of dissolved Al and silica liberated through weathering of volcanic glass and plagioclase. Presence of halloysite in the coatings cannot be determined by microscopic observation, because randomly oriented halloysite may also give an isotropic appearance under crossed polarized light. However, in the SSXRD analysis (not shown) of the isotropic coatings in the Bw2 and 2C horizons, crystalline clay minerals were not encountered. Scanning electron micrographs of a pale yellow pseudomorph after a root in the Bw2 at 60 to 90 cm, and of pale yellow, nonlaminated coatings in the 2C horizon at 3 m are illustrated in Fig. 2. Qualitative microchemical analyses (Fig. 2) reveal that both materials consist of Si and Al, but the Si content of the coating in the 2C horizon appears to be higher. The occurrence of isotropic Al-Si pseudomorphs after roots in both horizons indicates

that these features represent neoformations of amorphous Al-Si material.

Transmission electron micrographs show that the coatings in the Bw2 horizon are associated with amorphous, structureless material, and threads that have diameters between 10 and 20 nm (Fig. 3A). These are interpreted to be allophane and imogolite, respectively. Wada et al. (1979) reported the formation of synthetic imogolite at $\text{pH} < 5$. The pH of the Bw2 horizon is 4.8, so imogolite may have formed under such conditions. However, care has to be taken because bulk soil analyses do not necessarily reflect the environmental conditions at the scales of observation shown in the micrographs.

The SEM-EDXRA analyses (Table 3) of coatings, infillings, and pseudomorphs after roots in the Bw2 horizon show that they consist of Al and Si. A number of coatings and infillings displayed low-intensity EDXRA signals, which may be artifacts caused by the impregnation resin in the coatings, or of variable thicknesses of the carbon coating fitted on the surface of the uncovered thin section. Mass percentages of both Al and Si are low in such cases, but Al/Si ratios are not significantly affected by the signal intensity. Therefore only the molar Al/Si ratios are considered in the following discussion. The mean Al/Si molar ratio of the coatings, infillings,

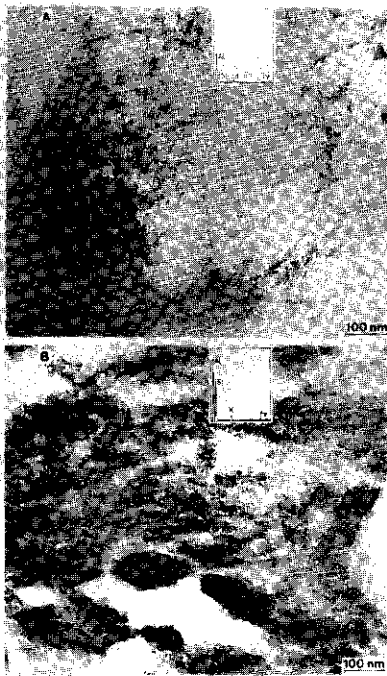


Fig. 3. Transmission electron micrographs that show coatings and infillings of: (A) allophanic material and imogolite threads in the Bw2 horizon; and (B) allophanic material in the 2C horizon.

and pseudomorphs after roots is 2 in the Bw2 horizon, and thus is similar to that of imogolite (Wada, 1989) or imogolite-like allophane (Parfitt and Kimble, 1989). The groundmass of the Bw2 horizon that is adjacent to the pores in which the isotropic features occur has an Al/Si molar ratio of 1.4. The higher ratio in the coatings is probably due to the fact that leaching of silica along the voids is stronger than in the adjacent groundmass. The formation of imogolite coatings under such leaching conditions is in agreement with observations of Wada and Masubara (1968), and Henmi and Wada (1976). Also Shoji and Saigusa (1977) reported dominant formation of imogolite as a result of strong desilication from intense weathering in a shallow-buried Andisol of Japan. Aomine and Mizota (1973) reported that macropores are required in combination with an ample supply of Al ions, water, and a suitable Si concentration to form imogolite. Such

conditions are provided in the Bw2 horizon of the studied Hapludand. Aomine and Wada (1962) reported that differential weathering of volcanic ash and pumice resulted in formation of hydrated halloysite along (root) channels, whereas the adjacent groundmass still consisted of allophane with Si/Al ratio of 2. They concluded that the chemical weathering is a process of desilication, and suggested that local variations in leaching activity contribute to the differential formation of halloysite.

The TEM morphological data in our study demonstrate the coexistence of allophane and imogolite in one coating, but we could not establish whether their formation is simultaneous or sequential, or whether allophane transforms to imogolite.

The TEM images of coatings in the 2C horizon (Fig. 3B) show amorphous structureless material, which is interpreted to be allophane. The SEM-EDXRA analyses (Table 3) of coatings, infillings, and pseudomorphs in the 2C horizon show that these coatings consist of Al and Si with a mean Al/Si molar ratio of 1.4. Thus these isotropic features have higher Si contents than those in the Bw2 horizon. The pH in the 2C horizon is 5.2, and within the range that Wada et al. (1979) reported for formation of synthetic allophane. In such environments, imogolite is apparently absent (Farmer and Frazer, 1977; Brown et al., 1978; Wada et al., 1979) but, as stated above, care has to be taken in using bulk analyses for the interpretation of features observed at micrometer and nanometer scales in the TEM micrographs.

Depth of burial and thickness of the overlying deposits have influences on pedogenesis (Shoji and Saigusa, 1977; Lowe, 1986). Burial of the 2C horizon may have resulted in decreased leaching and formation of allophane coatings, infillings, pseudomorphs with higher Si content than those in the overlying horizon. Resilication as a result of illuviation from overlying younger horizons may be possible as well, but this could not be substantiated.

CONCLUSIONS

Weathering of volcanic glass and plagioclase has resulted in the formation of isotropic aluminosilicate coatings, infillings, and pseudomorphs after roots. These neoformed features are macro- and micromorphologically similar, but their chemical and mineralogical composition changes with depth. Coatings, infillings, and pseudomorphs after roots consisting of allophane and imogolite are present in the large pores of the Bw2 horizons. Allophane coatings, infillings, and pseudomorphs are present in large pores of the 2C horizon. The occurrence of allophane and imogolite within one

Table 3. Analyses of Al and Si in selected features of the Bw2 and 2C horizons.

Feature	Horizon	Depth	Measurements	Al	Si	Al/Si
				% (w/w)		
		cm	no.			
Coatings	Bw2	60-90	29	14.9 ± 5.7†	7.9 ± 2.8	2.0 ± 0.1
	2C	300	12	22.0 ± 0.8	16.7 ± 0.7	1.4 ± 0.0
Difference				**	**	**
Groundmass	Bw2	60-90	4	13.9 ± 1.4	9.9 ± 1.1	1.4 ± 0.2
	2C	300	4	20.8 ± 0.4	16.8 ± 0.4	1.3 ± 0.1

** Difference in the two means within a column is significant at the $P = 0.01$ level.

† Mean ± standard deviation.

coating demonstrate heterogeneity at a nanometer scale, but their specific relationship could not be established. The differences in mineralogy and Al/Si molar ratios of the coatings at different depths is attributed primarily to differences in the amounts of water that have flowed through the horizons, but silica supply and pH may also influence these differences.

REFERENCES

- Aomine, S., and C. Mizota. 1973. Distribution and genesis of imogolite in volcanic ash soils of northern Kanto, Japan. p. 207-213. *In* Proc. Int. Clay Conf. 5th, Madrid. 23-30 June 1972. Div. Ciencia CSIC, Madrid.
- Aomine, S., and K. Wada. 1962. Differential weathering of volcanic ash and pumice, resulting in formation of hydrated halloysite. *Am. Mineral.* 47:1024-1048.
- Blackmore, L.C., P.L. Searle, and B.K. Daly. 1987. Methods for chemical analyses of soils. N.Z. Bur. Sci. Rep. 80. N.Z. Soil Bureau, Lower Hutt, New Zealand.
- Brown, G., A.C.D. Newman, J.H. Rayner, and A.H. Weir. 1978. The structures and chemistry of soil clay minerals. p. 29-178. *In* D.J. Greenland and M.H.B. Hayes (ed.) *The chemistry of soil constituents*. John Wiley & Sons, New York.
- Bullock, P., N. Fedoroff, A. Jongerius, G. Stoops, and T. Tursina. 1985. *Handbook for soil thin section description*. Waine Res. Pub. Wolverhampton, England.
- Buurman, P., and A.G. Jongmans. 1987. Amorphous clay coatings in a lowland Oxisol and other andesitic soils of West Java, Indonesia. *Pemberitaan Penelitian Tanah dan Pupuk* 7:31-40.
- Chartres, C.J., A. Wood, and C.F. Pain. 1985. The development of micromorphological features in relation to some mineralogical and chemical properties of volcanic ash soils in highland Papua, New Guinea. *Aust. J. Soil Res.* 23:339-354.
- Dagain, J. 1981. *La mise en place du massif volcanique Madeleine-Souffrière, Basse Terre de Guadeloupe, Antilles*. Thèse troisième cycle. Université de Paris Sud, Orsay.
- Dalrymple, J.B. 1964. The application of soil micromorphology to the recognition and interpretation of fossil soils in volcanic ash deposits from the North Island, New Zealand. p. 339-349. *In* A. Jongerius (ed.) *Soil micromorphology*. Elsevier, Amsterdam.
- Dalrymple, J.B. 1967. A study of paleosols in volcanic ash-fall deposits from the North Island, New Zealand, and the evaluation of soil micromorphology for establishing their stratigraphic correlation. p. 104-122. *In* R.B. Morrison and H.E. Wright (ed.) *Quaternary soils*. Univ. of Nevada, Reno.
- de Reynal de Saint-Michel, A. 1966. *Carte géologique détaillée de la France, Département de la Guadeloupe: 1:50 000. Feuille de Basse Terre et notices explicatives*. Paris.
- Farmer, V.C., and A.R. Fraser. 1977. Synthetic imogolite, a tubular hydroxy aluminum silicate. *Dev. Sedimentol.* 27:547-553.
- Farmer, V.C., J. McHardy, L. Robertson, A. Walker, and M.J. Wilson. 1985. Micromorphology and sub-microscopy of allophane and imogolite in a podzol Bs horizon: Evidence for translocation and origin. *J. Soil Sci.* 36:87-95.
- Food and Agriculture Organization of the United Nations. 1990. *Guidelines for soil profile description*. 3rd ed. (revised). FAO, Rome.
- FitzPatrick, E.A. 1970. A technique for the preparation of large thin sections of soils and consolidated material. p. 3-13. *In* D.A. Osmond and P. Bullock (ed.) *Micromorphological techniques and applications*. Tech. Monogr. 2. Soil Surv. of England and Wales, Rothamsted Exp. Sta., Harpenden.
- Hennü, T., and K. Wada. 1976. Morphology and composition of allophane. *Am. Mineral.* 61:379-390.
- Jongmans, A.G., F. van Oort, P. Buurman, and A.M. Jaunet. 1993. Micromorphology and submicroscopy of isotropic and anisotropic Al/Si coatings in a Quaternary Allier terrace (France). *Proc. Int. Work. Meet. Soil Micromorphol.* 9th, Townsville, Australia. 12-17 July 1992. Elsevier, Amsterdam (in press).
- Lowe, D.J. 1986. Controls on the rates of weathering and clay mineral genesis in airfall tephra: A review and New Zealand case study. p. 265-330. *In* S.M. Colman and D.P. Dethier (ed.) *Rates of chemical weathering of rocks and minerals*. Academic Press, New York.
- Miedema, R., T. Pape, and G.J. van der Waal. 1974. A method to impregnate wet soil samples, producing high-quality thin sections. *Neth. J. Agric. Sci.* 22:37-39.
- Mizota, C., and L.P. van Reeuwijk. 1989. Clay mineralogy and chemistry of soils formed in volcanic material in diverse climatic regions. *Soil Monogr.* 2. ISRIC, Wageningen, the Netherlands.
- Parfitt, R. 1990. Allophane in New Zealand—A review. *Aust. J. Soil Res.* 28:343-360.
- Parfitt, R., and J.M. Kimble. 1989. Conditions for formation of allophane in soils. *Soil Sci. Soc. Am. J.* 53:971-977.
- Parfitt, R., and M. Saigusa. 1985. Allophane and humus-aluminum in Spodosols and Andepts formed on the same volcanic ashbeds in New Zealand. *Soil Sci.* 139:149-155.
- Parfitt, R.L., and T.W. Webb. 1984. Allophane in some South Island yellow-brown shallow and stony soils and high country and upland yellow-brown earths. *N.Z. J. Sci.* 27:37-40.
- Shoji, S., and Y. Fujiwara. 1984. Active aluminum and iron in humus horizons of Andosols from north eastern Japan: Their forms, properties and significance in clay weathering. *Soil Sci.* 137:216-226.
- Shoji, S., Y. Fujiwara, I. Yamada, and M. Saigusa. 1982. Chemistry and clay mineralogy of Andosols, Brown Forest soils, and Podzolic soils from recent Towada ashes, north eastern Japan. *Soil Sci.* 133:69-86.
- Shoji, S., and M. Saigusa. 1977. Amorphous clay minerals of Towada Andosols. *Soil Sci. Plant Nutr.* 23:437-455.
- Shoji, S., and I. Yamada. 1991. Comparison of mineral properties between tephra-derived Spodosols from Alaska and nontephra-derived Spodosols from New England. *Soil Sci.* 152:162-183.
- Soil Survey Staff. 1975. *Soil taxonomy: A basic system of soil classification for making and interpreting soil surveys*. USDA-SCS Agric. Hand. 436. U.S. Gov. Print. Office, Washington, DC.
- Soil Survey Staff. 1992. *Keys to soil taxonomy*. Soil Manage. Support Serv. Tech. Monogr. 19. 5th ed. Pocahontas Press, Blacksburg, VA.
- Tait, J.M., N. Yoshinaga, and B.D. Mitchell. 1978. The occurrence of imogolite in some Scottish soils. *Soil Sci. Plant Nutr.* 24:145-151.
- van der Plas, L., and A.C. Tobi. 1965. A chart for judging the reliability of point-counting results. *Am. J. Sci.* 263:87-90.
- van Oort, F., A.G. Jongmans, A.M. Jaunet, J.D.J. van Doesburg, and T. Feijtel. 1989. Andesite weathering and halloysite neoformation in a ferrallitic soil environment in Guadeloupe. *In-situ study of different halloysite faces on thin sections by SEM-EDXRA, microdrilling, step scan XRD and TEM*. *C.R. Acad. Sci. Ser.* 2 310:425-431.
- van Reeuwijk, L.P. 1992. *Procedures for soil analysis*. Tech. Pap. no. 9. 3rd ed. ISRIC, Wageningen, the Netherlands.
- Verschuren, R.H. 1978. A microscope-mounted drill to isolate microgram quantities of mineral material from polished thin sections. *Mineral. Mag.* 42:449-503.
- Wada, K. 1989. Allophane and imogolite. p. 1051-1087. *In* J.B. Dixon and S.B. Weed (ed.) *Minerals in soil environment*. 2nd ed. SSSA Book Ser. no. 1. SSSA, Madison, WI.
- Wada, K., and I. Matsubara. 1968. Differential formation of allophane, "imogolite" and gibbsite in the Kitakami pumice bed. p. 123-133. *In* J.W. Holmes (ed.) *Trans. Int. Congr. Soil Sci.* 9th, Adelaide. 1968. Vol. 3. Elsevier, New York.
- Wada, S.I., A. Eto, and K. Wada. 1979. Synthetic allophane and imogolite. *J. Soil Sci.* 30:347-355.
- Walkley, A. 1947. A critical examination of a rapid method for determining organic carbon in soils: Effects of variations in digestion conditions and of inorganic soil constituents. *Soil Sci.* 63: 251-363.
- Wang, C., J.A.M. McKeague, and H. Kodama. 1986. Pedogenic imogolite and soil environment: Case study of Spodosols in Quebec, Canada. *Soil Sci. Soc. Am. J.* 50:711-715.

3.2 Allophane, imogolite, and gibbsite in coatings in a Costa Rican Andisol

Geoderma, 1994 (in press)

A.G. Jongmans, P. Verburg, A. Nieuwenhuyse, F. van Oort.



ELSEVIER

Geoderma 00 (1994) 000-000

GEODERMA

Allophane, imogolite, and gibbsite in coatings in a Costa Rican Andisol

A.G. Jongmans^a, P. Verburg^a, A. Nieuwenhuys^b, F. van Oort^c

^a*Department of Soil Science and Geology, Agricultural University, P.O. Box 37, 6700 AA, Wageningen, Netherlands*

^b*Estacion Experimental "Los Diamantos", Guapiles, Costa Rica*

^c*INRA, Station Agropédologique, Pointe-à-Pitre, Guadeloupe*

(Received October 14, 1993; accepted after revision February 24, 1994)

Abstract

Neoformation of allophane, imogolite, and gibbsite has been studied extensively in soils in humid climates, but little is known about their micro distribution patterns. Such information may provide insight about the conditions at the micro-site scale, responsible for their formation and disappearance.

Our study describes amorphous and crystalline coatings in a Melanudand on a 13,000 yr old andesitic lava in Costa Rica. Fine-textured, white to yellow coatings could be observed in the B, C, and R horizon in the field. In thin sections the coatings are translucent and isotropic in plane polarized light (PPL), indicating that they consist of amorphous material. In the B horizon, under crossed polarized light, isotropic coatings show a gradual transition towards crystalline outer margins and spots, while in PPL such transition cannot be observed, suggesting a genetic relationship. Submicroscopical analyses reveal that the amorphous coatings in the R and C horizon consist of allophanic material with a molar Al/Si ratio of 0.9, those in the B horizon consist of allophanic material and imogolite with a molar Al/Si ratio of 1.4. The amorphous coatings resulted from precipitation of Al and Si liberated upon weathering of primary minerals in an initial stage of lava weathering. The crystalline coating parts in the B horizon consist of gibbsite and represent the ultimate stage of mineral neoformation. The different coating composition in the soil horizons is the result of different leaching conditions at a macro and micro scale.

Care should be taken to compare results obtained at different sampling scales with different analytical methods.

1. Introduction

Short-range order material, 1:1 phyllosilicates and gibbsite are the most common secondary minerals formed by weathering of volcanic parent rocks in humid climate (Mizota and Van Reeuwijk, 1989; Wada, 1989; Nahon, 1991; Quantin et al., 1991). These secondary

minerals may occur as coatings and infillings, both in the saprolite and overlying soils horizons (Dalrymple, 1964; Buurman and Jongmans, 1985; Jongmans et al., 1994a). Such coatings are formed in situ and solely consist of secondary, fine-textured material. Therefore, in situ analysis on coatings may better reflect the effect of external conditions on the composition of weathering products than analysis on bulk samples. Our study focuses on the characterization of isotropic and anisotropic coatings at different depths in an Andisol in humid tropical Costa Rica. The objective of this paper is: (1) to establish the morphology, chemistry, and mineralogy of the coatings; (2) to examine whether differences in optical behaviour within one coating or between coatings at different depths reflect changes in chemical and mineralogical composition; (3) to establish their genesis and to relate differences within or between coatings to (micro) environmental factors.

2. Site conditions

The study site is situated in a relatively flat position on the summit of a blocky, andesitic lava, at 200 m above mean sea level. Wood found at the base of this lava has an age of $18,190 \pm 130$ yr according to ^{14}C data, meaning that the lava is younger (Nieuwenhuysen et al., 1994). Deforestation has taken place between 20 and 50 years ago, and the current vegetation consists of grass, shrubs and trees.

The climate is isohyperthermic (mean annual air temperature 24.5°C), and perudic (mean annual rainfall 4500 mm) (Soil Survey Staff, 1992). The soil is well drained.

Fresh rock fragments, < 1 m in diameter, are present up to the soil surface. The fresh andesitic rock is phanero-microcrystalline with seriate and porphyritic textures (MacKenzie et al., 1984). The fine rock groundmass consists of glass, pyroxenes, plagioclase, and opaque iron minerals (diameter < $40\ \mu\text{m}$). The large phenocrysts (length < 4 mm) have a similar mineralogical composition, but glass is absent.

3. Analytical methods

Based on macromorphological descriptions, undisturbed samples (8 cm \times 8 cm) at 6 m, 2.5 m and 0.9 m depth were taken for micromorphological research. Undisturbed field-moist samples were impregnated after removing the water by acetone according to the method of Miedema et al. (1974), to preserve mineralogical composition and field structure. Thin sections were prepared according to Fitz Patrick (1970) and described using the terminology of Bullock et al. (1985).

Isolation of micro-quantities of coatings and infillings from uncovered thin sections was done with a microscope-mounted drill (Verschure, 1978). The material was transferred to Al slides following the method of Beaufort et al. (1983). The X-ray diffractograms were obtained by step scanning (SSXRD; Meunier and Velde, 1982) with steps of $0.05^\circ/2\theta$ and scan times of 70 s. Undisturbed sections of 50 nm thickness, cut from undisturbed reimpregnated coating fragments, were prepared according to Van Oort et al. (1994). The sections were analyzed with a Philips 420 transmission electron microscope (TEM), whereas a Link 10000 EDS analyzer allowed chemical analyses at the nanometre scale. In

situ, semi-quantitative chemical analyses of the coatings were performed with a scanning electron microscope energy dispersion X-ray analyzer (SEM-EDXRA) at the micron scale. The peak to background heights of the EDXRA signal were linearly transformed to element percentages by comparison with standard minerals. In addition, studies of rough coating surfaces at 2.5 m and 6 m depth provided micrographs, and qualitative chemical spectra.

4. Results and discussion

4.1. Soil characteristics, andic soil properties, and classification

The morphological, chemical and mineralogical characterization of the Andisol is extensively reported by Nieuwenhuys et al. (1994). The major macromorphological characteristics are shown in table 1.

The C horizon from 1.50 to 3.00/4.00 m contains many fresh boulders, stones and gravel. Clayey groundmass material is scarce, but fine-textured yellow coatings are dominantly present. The number of rock fragments with an alteration rind is lower than in the B horizon, indicating that weathering processes are not intensive at this depth. Below the C horizon, the unaltered blocky lava with randomly distributed cracks occurs. No alteration rinds are visible, indicating absence of weathering.

From 0.80 to 1.50 cm a lighter coloured (10YR 4/6) Bw horizon occurs. Coarse rock fragments in the A and B horizon have light-coloured alteration rinds, indicating that weathering affected these fragments. Between the coarse fragments in the A and B horizons, fine material with a loamy texture and a crumb structure is present, the latter indicating a high faunal activity between the coarse fragments. The content of fine material decreases with depth.

From 0 to 0.80 m a dark coloured Ah horizon is present (10YR 2/1–3/3), indicating the presence of appreciable amounts of organic matter. Such a dark topsoil high in organic matter is characteristic for young volcanic soils (Mizota and Van Reeuwijk, 1989). The organic matter content decreases with depth.

Table 1
Major macromorphological characteristics^a

Horizon	Depth (m)	Colour	Texture	Structure	Thixotropy	Coatings	Coarse Fragments
Ah1	0	10YR 2/1	loam	m3 granular	–	–	many
Ah2	0.05	10YR 2/2	loam	fml ang.bl	–	–	many
Ah3	0.3	10YR 2/2	loam	f2 crumb	moderate	–	many
AB	0.8	10YR 3/3	loam	f3 crumb	strong	–	many
Bw	0.9	10YR 4/6	clay loam	f3 crumb	strong	–	many
C	1.5	nd	nd	nd	strong	many	abundant
R	3/4	nd	nd	–	–	common	–

^aAccording to FAO (1990). Structure: f = fine; m = medium; l = weak; 2 = moderate; 3 = strong; ang bl = angular blocky; nd = not determined.

P-retention values are >95%, the bulk density values are <600 kg m⁻³, and ammonium-oxalate extractable (Al + 1/2 Fe) data are >4.9% in the A and B horizons, indicating that the soil meets the requirements for andic soil properties (Soil Survey Staff, 1992). In addition the base saturation values are <50% in the A and B horizon. As a result, the profile was classified as a Pachic Melanudand (Soil Survey Staff, 1992) or an Umbric Andosol (FAO, 1988).

4.2. Coatings in the unaltered rock

Field observations at 6 m below the soil surface show common <0.1 mm thick, white (10YR 8/2), fine-textured coatings, discontinuously distributed below rock boulder surfaces.

Micromorphological observations (Fig. 1) revealed that the coatings are <20 μm thick, colourless, and isotropic with a non-laminated translucent (limpid, Bullock et al., 1985) internal fabric, indicating that they consist of neoformed, amorphous material.

SEM micrographs (not shown) and qualitative chemical spectra performed on rough coating surfaces show that the coatings are non-laminated, and consist of Al and Si without other metal oxide components.

Semi-quantitative SEM-EDXRA analyses (Table 2) on coatings in thin sections show that the coatings dominantly consist of Al and Si with a mean Al/Si molar ratio of 0.8.

Because the primary minerals appear to be completely unaltered, the amorphous coatings cannot be derived from weathering of the blocky lava at this depth, and must have resulted from co-precipitation of dissolved aluminum and silica liberated by weathering at shallower depth.

4.3. Coatings in the C horizon

Many, <1 mm thick, discontinuous, yellow (10YR 8/6), fine-textured coatings along and below rock boulders are observed in the field. X-ray diffractograms from such coatings, isolated by hand with the help of a binocular, did not encounter crystalline clay minerals.

Micromorphology (Fig. 2) reveal clay-sized coatings (50 to 500 μm) on surfaces and in voids of rock fragments. The coatings have a micro-laminated, isotropic, translucent internal fabric. The inner part is dominantly colourless, whereas the outer part displays pale yellow colours, suggesting impregnation with Fe³⁺ oxides compounds. Lenticular micro-voids (diameter 5 to 20 μm) are frequently observed (Fig. 2).

A SEM micrograph (Fig. 3) made from rough coating surfaces shows that the coatings are fine-textured, micro-laminated, and have a botryoidal outer surface, suggesting that they are neoformed, since clay illuviation normally produces coatings with smooth surfaces. Lenticular shaped micro-voids (1–20 μm) are frequently present. Qualitative chemical spectra demonstrate that the coatings dominantly consist of aluminum and silica. The Al content tends to exceed the Si content. The Al content is highest in the outer part of the coatings whereas some Fe is locally present here as well.

TEM micrographs (Fig. 4) of undisturbed parts of the coatings show exclusively amorphous, structureless material. The qualitative chemical spectra (Fig. 4a) reveal that the Al content tends to exceed the Si content. Lenticular micro-voids (20 to 100 nm), probably

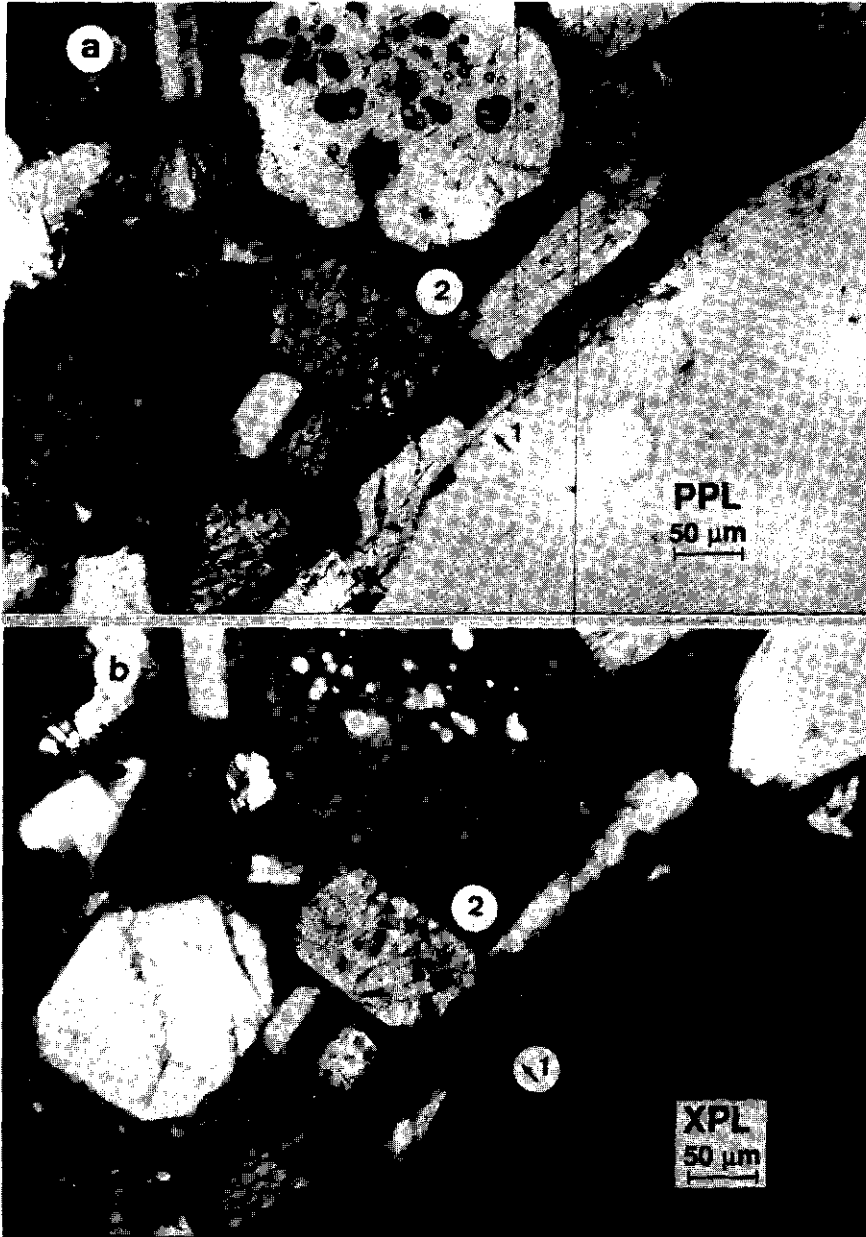


Fig. 1. Micrograph in plane polarized light (a), and crossed polarized light (b) of a colourless, isotropic, translucent coating (1) on a rock surface (2) in the R horizon (6 m).

Table 2
SEM-EDXRA data of isotropic coating type A and anisotropic type G in the RPA profile

Horizon	Depth (cm)	Feature	Al Si Fe			Al/Si	n	t
			(%)					
B	90	type A	11.3 ± 2.2	8.7 ± 1.4	2.4 ± 1.6	1.4 ± 0.1	12	-8.6
C	250	type A	10.9 ± 1.3	11.4 ± 1.3	5.5 ± 3.2	0.9 ± 0.06	10	
R	600	type A	11.6 ± 1.8	14.4 ± 3.3	3.1 ± 2.1	0.8 ± 0.09	13	-2.6
B	90	type G	20.1 ± 4.4	4.4 ± 1.7	3.5 ± 0.5	5.3 ± 2	9	
B	90	groundmass	8.9 ± 2.3	7.4 ± 1.5	4.6 ± 3.3	1.3 ± 0.1	8	

Type A = isotropic (fragmented) coatings; Type G = fine crystalline anisotropic coatings/spots in fragmented coatings; n: number of observations; t: t-value on Al/Si ratio.

reflect a loss of water upon desiccation of the coatings in the field, because such a void type has been observed at all scales of observation.

Semi-quantitative SEM-EDXRA analyses (Table 2) in thin sections also demonstrate that coatings consist of Al and Si and minor amounts of Fe. The Al/Si molar ratio of 0.9 is similar to values at 6 m depth.

All the above mentioned observations indicate that the coatings consist of amorphous structureless material, probably allophanic material similar to those in the unweathered parent rock at 6 m depth. Their number is higher in the C horizon than in the R horizon.

In the weathering rinds around rock fragments volcanic glass is absent, and the plagioclase and pyroxene phenocrysts demonstrate pellicular, linear and complex alteration patterns. This indicates dissolution of primary minerals and liberation of basic cations, Al and Si. However, the weathering rinds are scarce in the C horizon compared to the A and B horizon, suggesting that more Al and Si is liberated in the latter horizons. These observations suggest that the coatings in the C horizon result from co-precipitation of Al and Si, that is liberated mainly by weathering in the overlying horizons. The same is valid for Fe which impregnated the outer parts of the coatings. However, part of the Al, Si and Fe may be supplied by weathering of C horizon material.

4.4. Coatings in the B horizon

In the field no coatings could be detected in this horizon, so SEM micrographs of rough surfaces could not be obtained.

Micromorphological observations show few, 20 to 400 μm thick, isotropic, translucent, pale yellow coatings in the weathering rinds, or totally surrounding rock fragments of 1–2 mm in diameter (Fig. 5). These features are interpreted as neofomed coatings consisting of amorphous materials.

The fine groundmass material in the B horizon is dominantly present as impure or unsorted spherical bodies of 100 to 600 μm in diameter (Figs. 5, 6). The spheres consist of isotropic, fine, mineral material mixed with small organic matter fragments and < 30 μm cubic opaque iron minerals. Between the spheres many intergranular voids occur. In situ coatings are

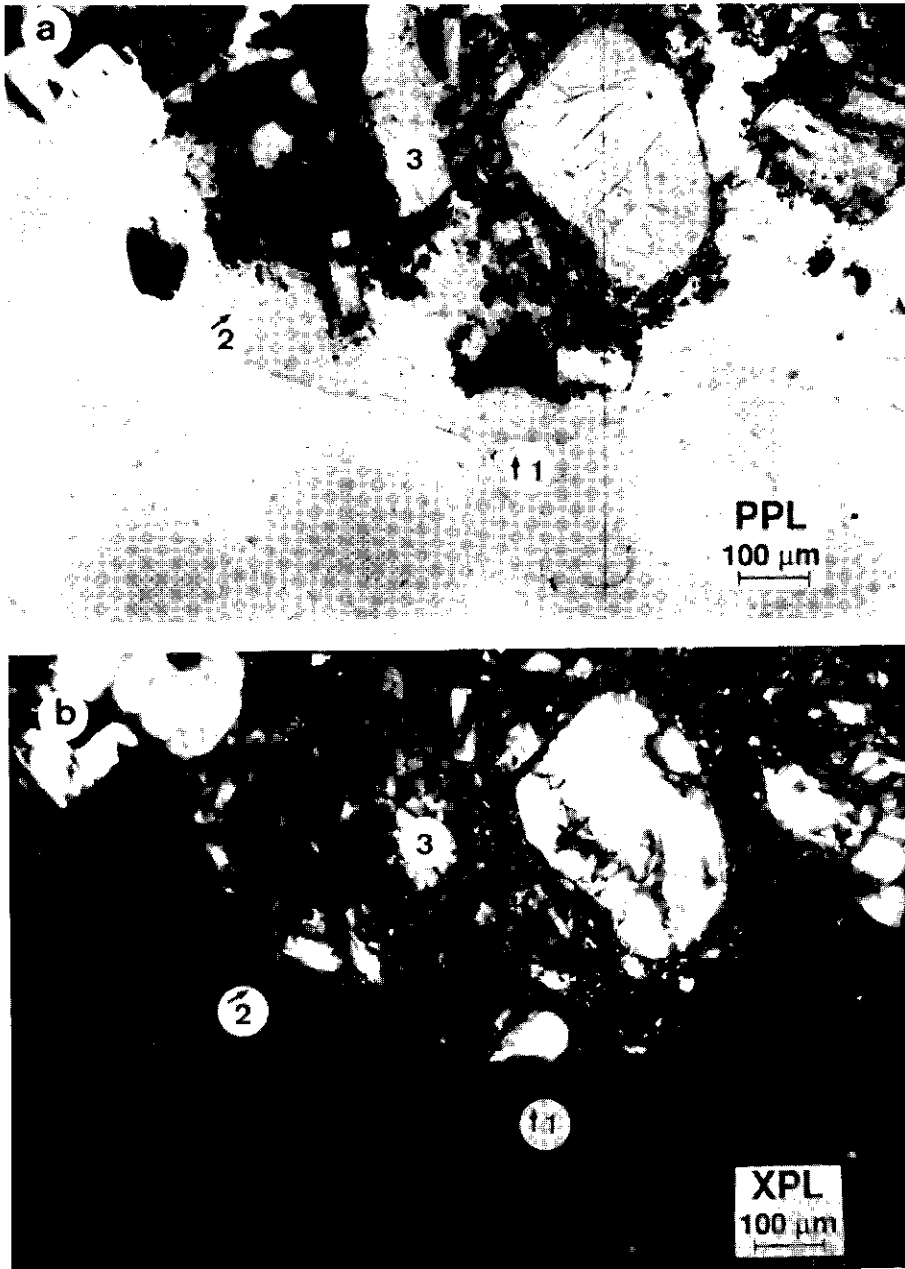


Fig. 2. Micrograph in plane polarized light (a), and crossed polarized light (b) of a pale-yellow, isotropic, translucent coating (1) with lenticular micro-voids (2) on a rock surface (3) in the C horizon.

absent in the intergranular voids between those groundmass spheres. However, many isotropic, translucent (limpid), spherical bodies (Fig. 6) occur. They have similar sizes as the impure and unsorted spherical groundmass bodies. Considering their internal fabric, the

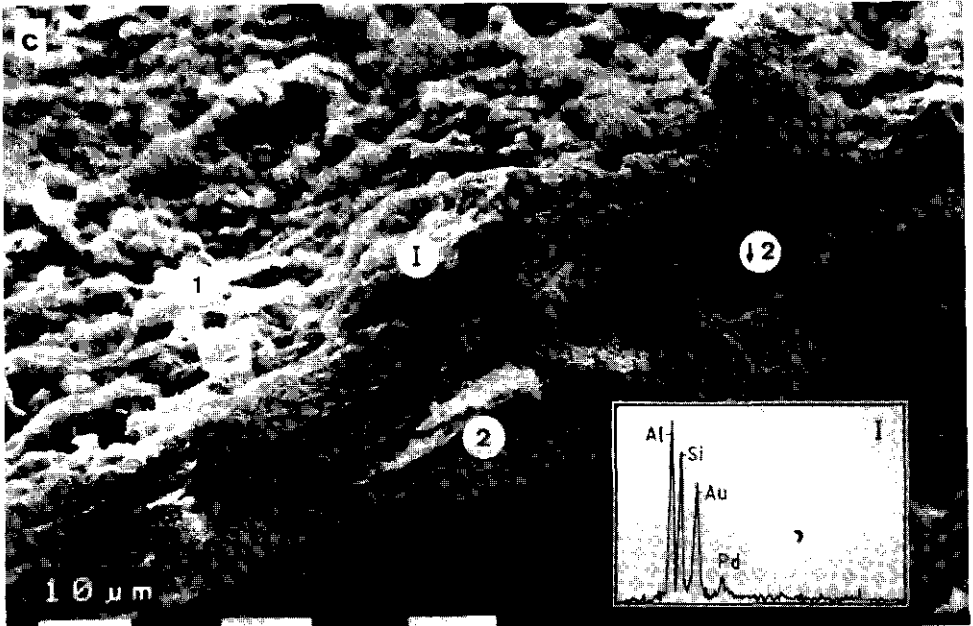


Fig. 3. SEM micrograph and qualitative chemical spectra of a coating with a botryoidal coating surface (1) and lenticular microvoids (2) in the C horizon (2.5 m). I: location of the chemical spectrum.

translucent spheres are interpreted as fragmented neoformed coatings. The exclusive occurrence of non-fragmented coatings in and around rock fragments (Fig. 5), and their absence as non-fragmented coatings in the soil groundmass indicate that the coatings are precipitated in voids already present in the blocky lava before a fine textured groundmass was formed. It appears that the coatings represent an initial stage of mineral neoformation in the lava. Upon ongoing weathering of the lava the coatings become fragmented and incorporated in the groundmass of the Bw horizon. Faunal biological activity is thought to be the cause of their spherical shapes, but considering the internal fabric and the different sizes of both groundmass spheres and fragmented coating spheres, it is not likely that they are excrements. We speculate that the spherical shape and the different sizes resulted from transportation of soil "aggregates" by animals like, e.g., ants.

Towards the outer margins of the isotropic coatings, a gradual transition to anisotropic fine crystalline coatings is visible under crossed polarized light. In plain polarized light, no transition can be seen (Fig. 5). In addition, anisotropic, fine crystalline spots, occur in the fragmented coatings, showing a gradual transition towards their isotropic coating parts. Both observations suggest a genetic relationship between the amorphous (fragmented) coatings and the fine crystalline coatings and spots. To establish the mineralogical composition of the crystalline material, micro-quantities were isolated by micro-drilling in thin sections and analyzed by SSXRD. The diffractogram (not shown) reveals a prominent peak at 4.84 Å indicating gibbsite.

TEM micrographs of undisturbed parts of fragmented coatings show a dominant occurrence of imogolite threads (10–20 nm in diameter, Fig. 7), and a co-existence with amorphous, structureless material (< 5 nm, Fig. 7) and probably crystalline material (Fig. 8). Qualitative chemical spectra demonstrate that the Al content exceeds the Si content in the

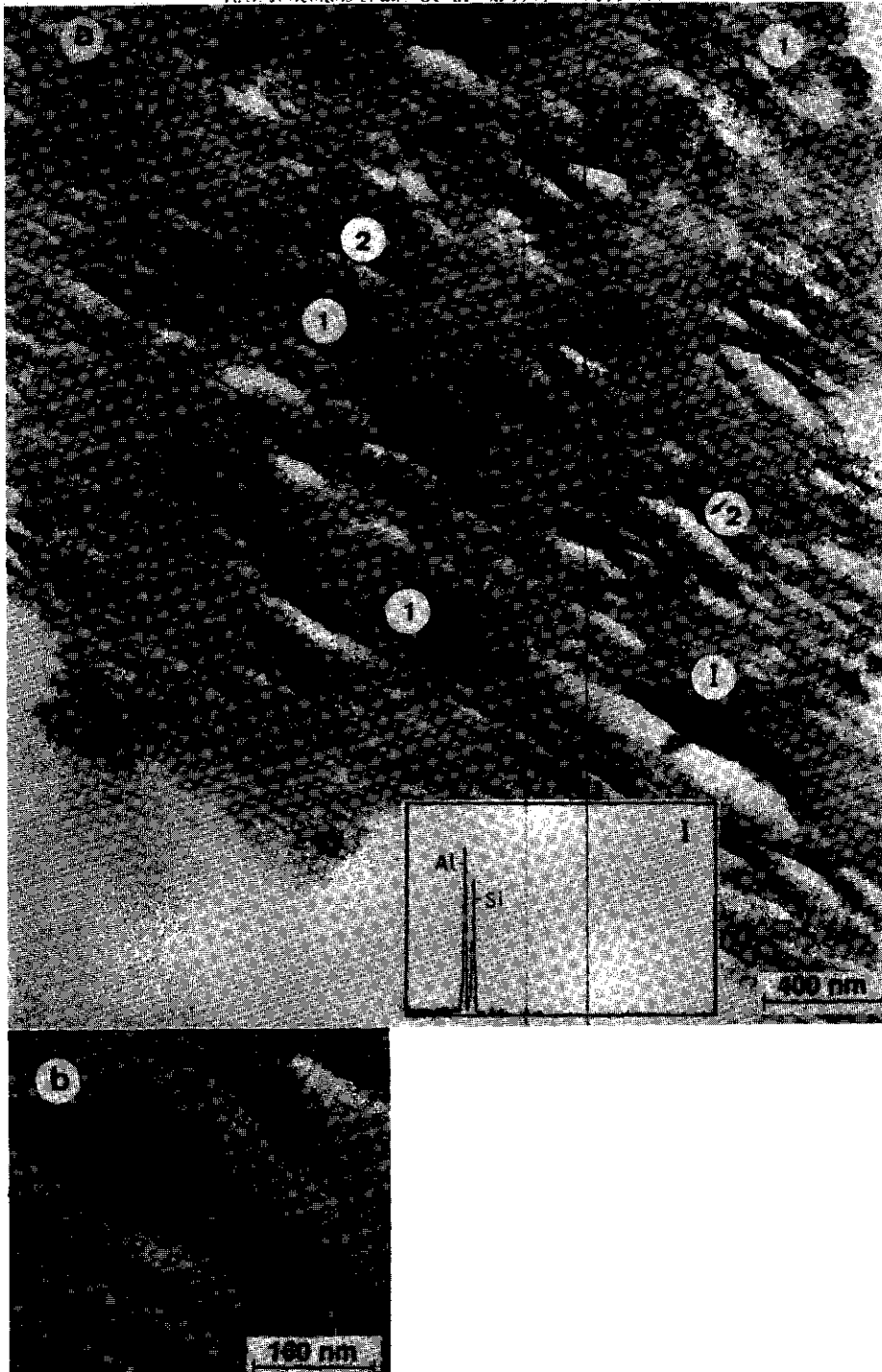


Fig. 4. TEM micrograph (a: general overview, b: detailed view) and a qualitative chemical spectrum of an undisturbed part of a coating in the C horizon showing allophanic material (1), and lenticular micro-voids (2).

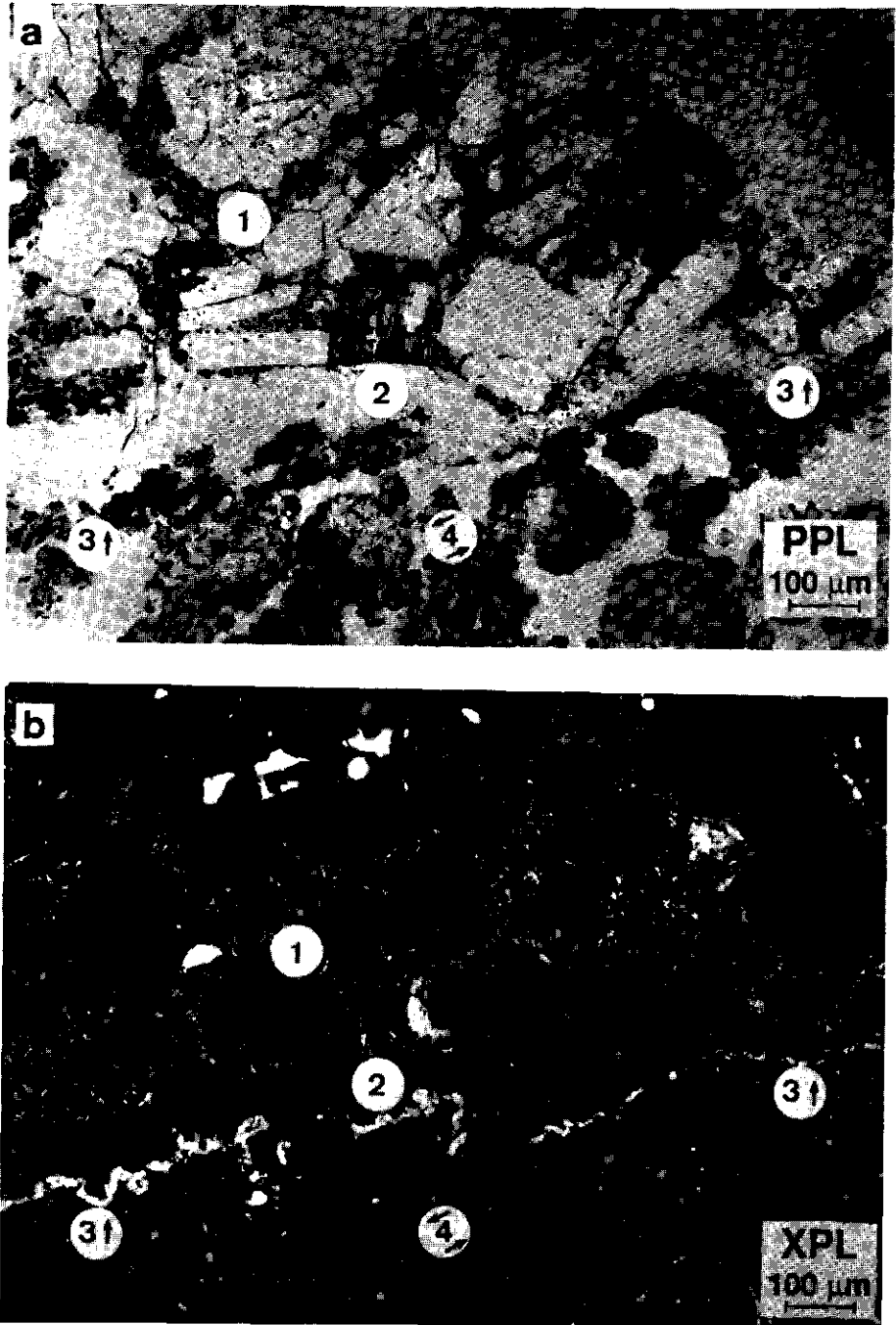


Fig. 5. Micrograph in plane polarized light (a) and crossed polarized light (b) showing an andesitic rock fragment (1) in the B horizon, surrounded by an isotropic, translucent coating (2); the outer margins of the coating consist of fine crystalline gibbsite (3); (4) impure and unsorted spherical groundmass bodies.

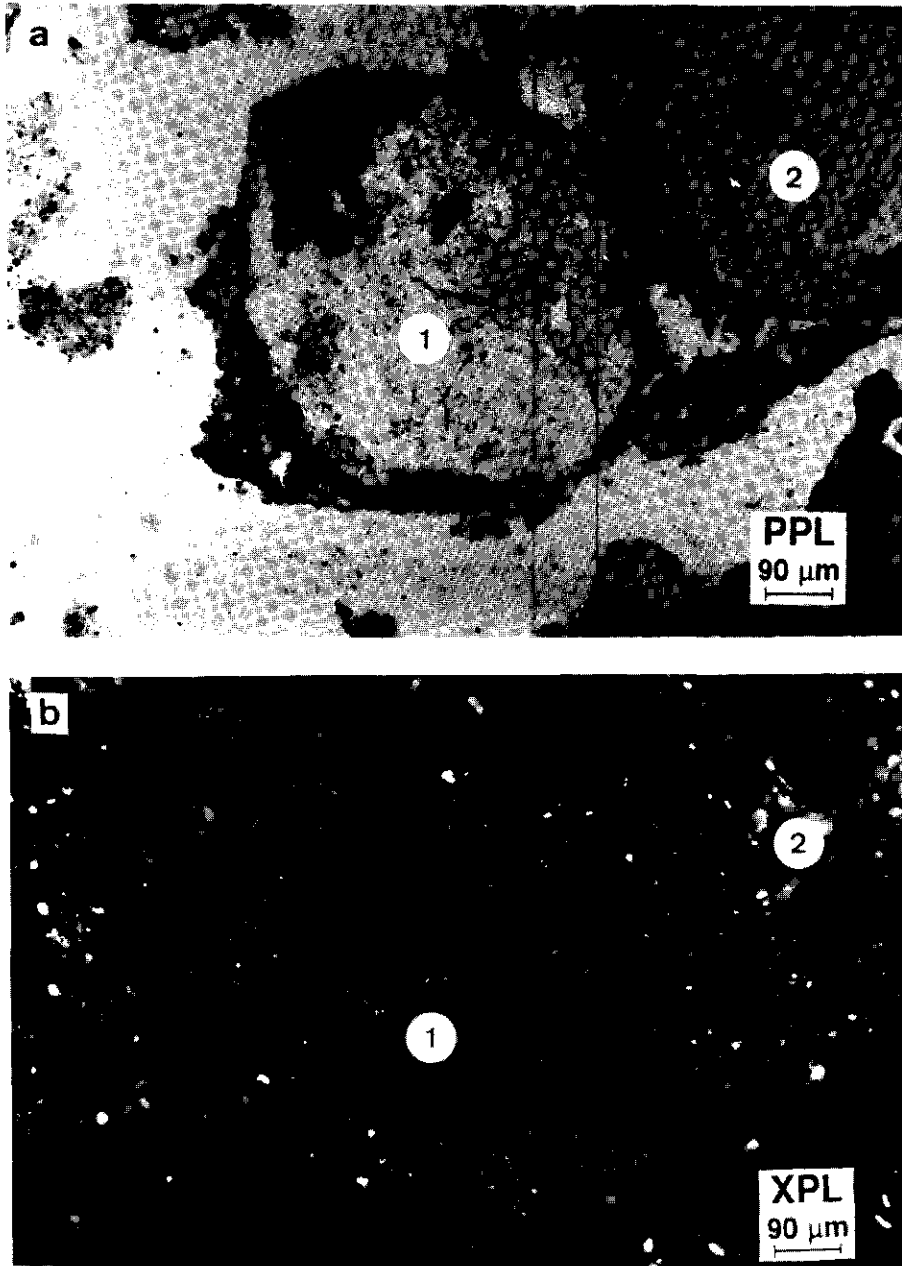


Fig. 6. Micrograph in plane polarized light (a) and crossed polarized light (b) of an isotropic, translucent spherical body (1, fragmented neoformed coating) in the B horizon, and an unsorted spherical groundmass body (2).

imogolite threads and the amorphous features (Fig. 7-I), whereas the crystalline phenomena exclusively consist of Al (Fig. 8-I). As a result, we speculate that the amorphous features are allophanic materials and we interpret the crystalline phenomena as gibbsite.

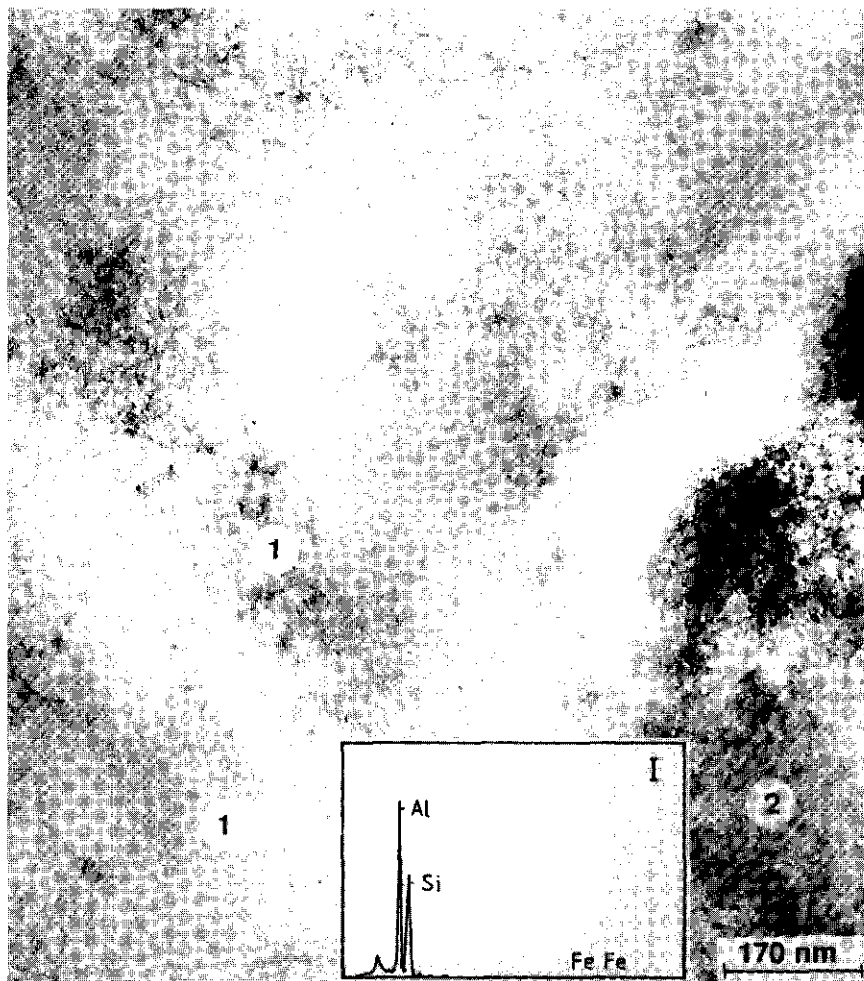


Fig. 7. TEM micrograph in an undisturbed section of an isotropic, translucent, spherical body in the B horizon, showing occurrence of imogolite threads (1), and allophanic material (2). The qualitative chemical spectrum (I) shows the amounts of Al and Si in the imogolite.

Semi-quantitative SEM-EDXRA analyses (Table 2) show that the isotropic part of coatings and fragmented coatings dominantly consist of Al and Si with minor amounts of Fe. The Al/Si molar ratio is 1.4. The fine crystalline, anisotropic material mainly consists of Al and has an Al/Si molar ratio of 5.4, confirming the gibbsite composition.

The coarse material in the B horizon consists of single mineral grains and andesitic rock fragments. The single mineral grains are pyroxene and plagioclase, both showing pellicular, linear and complex alteration patterns. Open iron boxwork pseudomorphs after pyroxene occur (Nahon, 1991). The andesitic rock fragments display alteration rinds with pellicular, linear and complex altered plagioclase and pyroxene. The observations indicate that the mineral particles are partially dissolved. Considering the degree of alteration, it is obvious that weathering is most advanced in the B horizon indicating that leaching in this horizon is more intense than in the C horizon and the cracked fresh rock at 6 m. The Al/Si ratio of 90

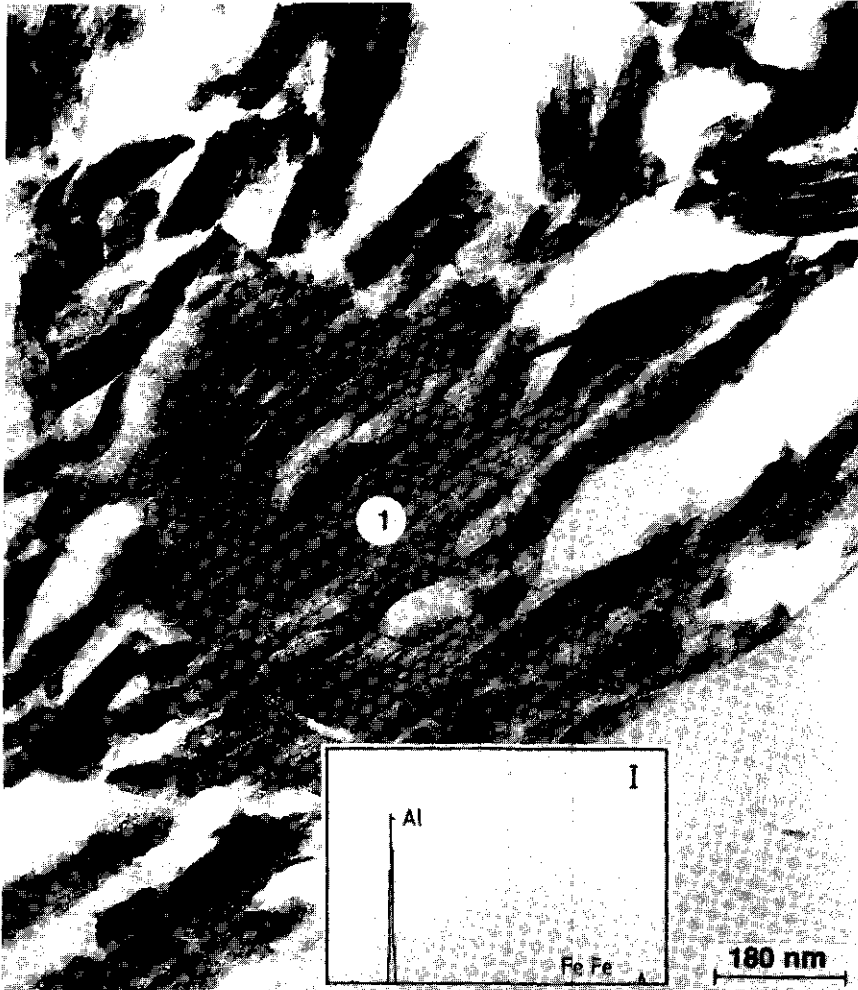


Fig. 3. TEM micrograph in an undisturbed section of an isotropic spherical body with anisotropic spots in the B horizon, showing the presence of gibbsite as indicated in the qualitative chemical spectrum (I).

the isotropic coatings increases towards the soil surface, and is thought to be the result of stronger desilication in the porous B horizons as compared to the lower horizons of the lava.

4.5. Chemical and mineralogical changes within and between coatings

All isotropic coatings consist of amorphous materials. The coating thickness at 6 m depth restricted isolation of undisturbed micro-parts for TEM analyses, so the mineralogical composition could not be established. However, the Al/Si molar ratio of the coatings is 0.8. Different workers (Parfitt and Kimble, 1989; Wada, 1989) reported that Al/Si molar ratios around 2 are common for imogolite. In addition, isotropic coatings in the C horizon exclusively consist of amorphous structureless material, probably allophanic material (Fig. 4),

and they display a (micro) morphological and chemical similarity with the coatings at 6 m depth. Therefore we speculate that the latter also consist of allophanic material.

In the B horizon, allophanic material, imogolite, and gibbsite co-exist within one coating. Jongmans et al. (1994b) found both allophane and imogolite within neoformed coatings in the Bw horizon of a 500 yr old Andisol in Guadeloupe; gibbsite was absent. Other workers (Wada and Matsubara, 1968; Brown et al., 1978; Lowe, 1986) also reported the co-existence of these materials in soils. Imogolite formation is often associated with desilication processes in the soil (Wada and Matsubara, 1968; Henmi and Wada, 1976; Shoji and Saigusa, 1977).

In situ coatings are always formed in voids. Water percolates preferentially through these voids and is therefore in close contact with the coating surfaces. The outer margins of the fragmented coatings are in close contact with the percolating water, in particularly when intergranular voids are present adjacent to the fragmented coatings (Figs. 5, 6). This implies that in the B horizon the leaching conditions at a micro scale favours desilication of the (fragmented) coatings and the formation of imogolite and even gibbsite. Wada and Harward (1974) stated that transformation of allophane and imogolite to gibbsite takes place in (micro-)environments where strong desilication is favoured. Aomine and Mizota (1973) reported that a high porosity and ample supply of Al ions, water and a suitable Si concentration is required in order to form imogolite, and that lower Si concentrations in the soil solution are required for gibbsite formation. Aomine and Wada (1962) suggested that local variation in leaching conditions contribute to the differential formation of neoformed materials.

The presence of gibbsite coatings, overlying the (fragmented) coatings containing imogolite represents an ongoing desilication process at their outer surfaces. The presence of gibbsite spots within the fragmented coatings is thought to be facilitated by the presence of the lenticular micro-voids, which create differences in leaching conditions at a micro scale within the coatings.

4.6. Chemical variation between different methods and at different sampling scales

All chemical data, performed with different analytical methods display the same trends with respect to the Al and Si contents and molar ratios in the coatings. However, the semi-quantitative SEM-EDXRA analyses (Table 2, micron scale) carried out in thin sections, give higher Si contents than the qualitative chemical spectra (not shown) measured on rough coating surfaces (micron scale), and in TEM samples (Figs. 4, 7, nanometre scale). The different analytical methods may be the source of these differences. However, it should be realized that the differences in scale between the different analyses may also play an important role in creating differences in chemical composition. For example, SEM-EDXRA analyses in thin sections of the B horizon were carried out in the coatings which contain both allophanic materials and imogolite with Al/Si ratios of 1.4. TEM analyses in the same coatings were exclusively focused on imogolite threads with Al/Si ratios of approximately 2 (estimated from chemical spectra in Fig. 7-I), so this difference in sampling scale may be the source of the different Al/Si molar ratio values.

5. Conclusions

The study reveals that all isotropic coatings and fragmented coatings observed at different depths resulted from co-precipitation of Al and Si, liberated upon weathering of primary minerals and are neoformed in an initial stage of weathering of the blocky lava.

Micromorphology suggests that the isotropic coatings at different depths are similar and homogeneous, but in situ submicroscopical analyses demonstrate changes in chemical and mineralogical composition towards the soil surface as a result of desilication.

The transmission electron microscope data in our study reveal the co-existence of allophane, imogolite and gibbsite within one coating. We could not establish whether the allophanic materials and imogolite are formed simultaneously or sequentially, or whether allophane transforms to imogolite through dissolution. Gibbsite represents the ultimate result of an ongoing desilication process at a micro scale.

The results of this study show that care should be taken when comparing results obtained with different analytical methods and/or obtained at different sampling scales.

References

- Aomine, S. and Mizota, C., 1973. Distribution and genesis of imogolite in volcanic soils of northern Japan. *Proc. 5th Int. Clay Conf.*, 1972, pp. 207–213.
- Aomine, S. and Wada, K., 1962. Differential weathering of volcanic ash and pumice resulting in formation of halloysite. *Am. Mineral.*, 47: 1024–1048.
- Beaufort, D., Dudoignon, P., Proust, D., Parneix, J.C. and Meunier, A., 1983. Microdrilling in thin sections: A useful method for the identification of clay minerals in situ. *Clay Mineral.*, 18: 223–226.
- Brown, G., Newman, A.C.D., Rayner J.H. and Weir A.H., 1978. The structure and chemistry of soil clay minerals. In: D.J. Greenland and M.H.B. Hayes (Editors). *The Chemistry of Soil Constituents*. Wiley, Chichester, pp. 29–178.
- Bullock, P., Fedoroff N., Jongerius A., Stoops, G. and Tursina, T., 1985. *Handbook for Soil Thin Section Description*. Waine Res. Publ., Albrighton, England, 152 pp.
- Buurman, P. and Jongmans, A.G., 1985. Amorphous clay coatings in a lowland Oxisol and other andesitic soils of West Java, Indonesia. *Pemberitaan Penelitian Tanah Dan Pupuk*, 7: 31–40.
- Dalrymple, J.B., 1964. The application of soil micromorphology to the recognition and interpretations of fossil soils in volcanic ash deposits from the North Island, New Zealand. In: A. Jongerius (Editor), *Soil Micromorphology*. Elsevier, Amsterdam, pp. 339–349.
- FAO, 1988. *FAO/Unesco Soil Map of the World, Revised Legend*. World Resources Report 60, FAO, Rome. Reprinted as Technical Paper 20. ISRIC, Wageningen, 138 pp.
- FAO, 1990. *Guidelines for Soil Profile Description*. 3rd (revised) ed. FAO, Rome / ISRIC, Wageningen, 70 pp.
- Fitz Patrick, E.A., 1970. A technique for the preparation of large thin sections of soils and unconsolidated material. In: D.A. Osmond and P. Bullock (Editors), *Micromorphological Techniques and Application*. Techn. Monogr. 2. Soil Survey of England and Wales, Rothamsted Exp. Sta., Harpenden, pp. 3–13.
- Henmi, T. and Wada, K., 1976. Morphology and composition of allophane. *Am. Mineral.*, 61: 379–390.
- Jongmans, A.G., Van Oort, F., Buurman, P. and Jaunet, A.M., 1994a. Formation and recrystallization of amorphous aluminium-silicate coatings. Micromorphology and submicroscopy of isotropic and anisotropic coatings in a Quaternary Allier terrace sequence (France). In: *Proc. IXth Int. Working Meeting of Soil Micromorphology*, Townsville, Australia, July 1992, in press.
- Jongmans, A.G., Van Oort, F., Buurman, P., Jaunet, A.M. and Van Doesburg, J.D.J., 1994b. Morphology, chemistry, and mineralogy of isotropic aluminosilicate coatings in an Andisol of Guadeloupe. *Soil Sci. Soc. Am. J.*, in press.

- Lowe, D.J., 1986. Controls on the rate of weathering and clay-mineral genesis in airfall tephra: A review and New Zealand case study. In: S.M. Colman and D.P. Dethier (Editors), *Rates of Chemical Weathering of Rocks and Minerals*. Academic Press, New York, pp. 265–330.
- MacKenzie, W.S., Donaldson, C.H. and Guilford, C., 1984. *Atlas of Igneous Rocks and Their Textures*. Longman, Essex, England, 148 pp.
- Meunier, A. and Velde, B., 1982. X-ray diffraction of oriented clays in small quantities (0.1 mg). *Clay Miner.*, 17: 259–262.
- Miedema, R., Pape, T. and Van der Waal, G.J., 1974. A method to impregnate wet soil samples, producing high-quality thin sections. *Neth. J. Agric. Sci.*, 22: 37–39.
- Mizota, C. and Van Reeuwijk, L.P., 1989. Clay mineralogy and chemistry of soils formed in volcanic material in diverse climatic regions. *Soil Monograph 2*. ISRIC, Wageningen, 185 pp.
- Nahon, D.B., 1991. *Introduction to the Petrology of Soils and Chemical Weathering*. Wiley, New York, 313 pp.
- Nieuwenhuysse, A., Verburg, P. and Jongmans, A.G., 1994. Short range order materials, kaolin, and gibbsite in a tropical andesitic chronosequence. *Soil Sci. Soc. Am. J.*, submitted.
- Parfitt, R.L. and Kimble, J.M., 1989. Conditions for formation of allophane in soils. *Soil Sci. Soc. Am. J.*, 53: 971–977.
- Quandin, P., Balesdent, J., Bouleau, A., Delaune, M. and Feller, C., 1991. Premier stades d'alteration de ponces volcaniques en climat tropical humide. (Montagne Pelée, Martinique). *Geoderma*, 50: 125–148.
- Shoji, S. and Saigusa, M., 1977. Amorphous clay minerals of Towada Andosols. *Soil Sci. Plant Nutr.*, 23: 437–455.
- Soil Survey Staff, 1992. *Keys to Soil Taxonomy*. SMSS Tech. Monograph No. 19, fifth ed. Pocahontas Press, Blacksburg, VA, 422 pp.
- Van Oort, F., Jongmans, A.G. and Jauner, A.M., 1994. The progression from optical light to transmission electron microscopy in the study of soils. *Clay Miner.*, in press.
- Verschure, R.H., 1978. A microscope-mounted drill to isolate microgram quantities of mineral material from polished thin sections. *Miner. Mag.*, 42: 449–503.
- Wada, K., 1989. Allophane and imogolite. In: J.B. Dixon and S.B. Weed (Editors), *Minerals in Soil Environment*. 2nd ed. SSSA Book Series, 1. Madison, WI, pp. 1051–1087.
- Wada, K. and Harward, M.E., 1974. Amorphous clay constituents of soils. *Adv. Agron.*, 26: 211–260.
- Wada, K. and Matsubara, I., 1968. Differential formation of allophane, "imogolite" and gibbsite in the Kitakami pumice bed. In: *Trans. 9th Int. Congr. of Soil Science, Adelaide, Australia, 1968*. Vol. III. Halstead Press, Sydney.

3.3 Micromorphology and submicroscopy of isotropic and anisotropic Al/Si coatings in a Quaternary Allier terrace, (France)

Proc. 9th Int. Work. Meet. on Soil Micromorph.. Townsville, Australia, July 12-17, A. Ringrose-Vose (Ed), 1994 (in press).

A.G. Jongmans, F. van Oort, P. Buurman, and A.M. Jaunet.

Micromorphology and submicroscopy of isotropic and anisotropic Al/Si coatings in a Quaternary Allier terrace, (France).

A.G.Jongmans¹, F. van Oort², P. Buurman¹, and A.M. Jaunet³.

¹ Dep. of Soil Science and Geology, Agricultural University, P.O.Box 37, 6700 AA Wageningen, The Netherlands. ² INRA, Station Agropedoclimatique, B.P.1232, F-97185, Pointe à Pitre Cédex, Guadeloupe, France. ³ INRA, Station Science du Sol, Route de St-Cyr, 78026 Cédex, Versailles, France.

ABSTRACT

Optical studies of a middle Pleistocene Allier river terrace in France reveal the occurrence of isotropic non-laminated coatings and anisotropic non-laminated coatings with a stipple-speckled b-fabric in a buried paleosol, rich in trachytic pumice fragments. Optical and SEM-EDXRA analyses, in-situ microdrilling for step scan X-ray diffraction, and TEM analyses of undisturbed parts of the coatings were used to establish their chemistry, mineralogy and internal microfabric. Micromorphological observations indicate that both coatings are genetically identical. Both kinds were formed by clay neoformation rather than by clay illuviation. The isotropic type consists of amorphous material with a low molar Al/Si ratio, and is the first step in clay neoformation. These coatings contain minor amounts of 2:1 clay. The anisotropic type is formed by recrystallization of isotropic coatings, and consists of unoriented domains of 2:1 clay. The formation of the coatings and their typical chemical and mineralogical characteristics are due to: (1) weathering of trachytic pumice fragments, and (2) occurrence of restricted leaching conditions during coating formation.

INTRODUCTION

Non-crystalline material, appearing as neoformed coatings and infillings, is produced upon weathering of volcanic components in the middle and early Pleistocene Allier river terraces (Jongmans et al, 1991). The occurrence of isotropic non-crystalline coatings under different climatic conditions in soils developed in parent material containing pyroclastic components has been reported earlier (e.g. Dalrymple, (1964); Chartres et al,

(1985). Recrystallization of such coatings was reported by Buurman and Jongmans (1987) in soils with pyroclastic components from Indonesia. Veldkamp and Jongmans (1991) studied the occurrence and weathering of pumice clasts in a paleosol found at 5 m. in middle Pleistocene Allier terrace deposits, and observed partially altered trachytic pumice fragments, together with isotropic and anisotropic coatings. In the present paper the morphology, chemistry, and mineralogy of these coatings are studied, to determine their genesis and relationship. Micro fabrics of the coatings were examined by TEM to assess the distribution pattern of the individual clay domains. Together, these analyses should give insight in coating genesis in relation to the environmental conditions of the paleosol.

SOIL SITE CHARACTERISTICS

The paleosol is approximately 1m thick and consists of cryoturbated sand and clay bodies (Veldkamp and Jongmans, 1991). The colour of the soil is grey (10YR 5/1). The clayey parts show a distinct angular blocky structure, whereas the sandy parts are structureless massive. Soft, white (10 YR 8/2), rounded, trachytic pumice fragments (up to several mm, Al/Si ratio = 0.36) and fresh and partially weathered volcanic and granitic fragments are present. Many biogenic channels occur, surrounded by a clear porostriated birefringent fabric. Cryoturbation features, pedal structures, and channels are absent in the 4-5m thick gravel sediment that overlies the paleosol. A stratified gravel deposit with a firm consistence, as a result of close packing of different grain sizes, underlies the paleosol

ANALYTICAL METHODS

Undisturbed samples (8x8 cm) from the sandy and clayey parts of the paleosol, and the directly adjacent underlying and overlying sediments were taken, and thin sections were made according the method of FitzPatrick (1970). For thin section description the terminology of Bullock et al (1985) was used. *In-situ* microchemical analyses on isotropic and anisotropic coatings were performed in uncovered thin sections with a Philips scanning electron energy dispersive X-ray analyser (SEM-EDXRA). Four coatings of both kinds were analysed, and five block ($12 \mu\text{m}^2$) analyses were made of every coating (n=20). The peak to background heights of the EDXRA signal were linearly transformed to element percentages by comparison with standard minerals of a known chemical composition, analysed in the same measurement. Isolation of microquantities of

coatings from uncovered thin sections was performed with a microscope-mounted drill (Verschuren, 1978), and X-ray diffraction patterns of this material were obtained by step scan X-ray diffraction (SSXRD) (Meunier and Velde, 1982). Undisturbed sections of 50 nm thickness, cut from undisturbed fragments ($\pm 100 \mu\text{m}^2$) of both coating types were prepared according the method of Van Oort et al. (1990), and analysed with a Philips 420 transmission electron microscope (TEM). A Link AN 10000 EDS analyser permitted microchemical analysis.

RESULTS

Micromorphological observations show that isotropic (A) and anisotropic (B) coatings (Fig.1) are found in the paleosol, and in the upper part of the underlying sediment. They are absent in the overlying deposit. Coatings are common around partially altered pumice fragments. The pale yellow, isotropic coatings, are unoriented and non-laminated. Locally, anisotropic spots occur with a weak stipple-speckled b-fabric. Anisotropic coatings are unoriented, non-laminated, pale yellow, and display a stipple-speckled b-fabric. Both variations frequently occur within one coating and cannot be distinguished in plane polarized light. They may be weakly impregnated by ferruginous hypocoatings. Muscovite grains ($10 \times 3 \mu\text{m}$) are sometimes enclosed in both types. Fig. 2 shows the results of SSXRD of both coating types. Anisotropic coatings show a clear broad peak at 1.9 nm (expanded smectite) and small peaks at 1 nm (mica) and 0.7 nm (kaolinite/halloysite). No peaks occur in the diffractogram of the isotropic coatings.

Table 1 shows SEM-EDXRA analyses of the isotropic coating (A) and anisotropic (B) coatings. Mg, Ca, and K contents are very low in the isotropic type. Ca and K tend to be higher in the anisotropic type but concentrations are still low. Some coatings contain minor amounts of Ti. Al is slightly lower in the anisotropic type B, while Si and Fe demonstrate the opposite. The molar Al/Si ratios in both coating types are lower than normal allophane values; type B has the lowest value.

Fig. 3 shows the transmission Electron Microscope (TEM) images of the studied coatings. In Fig 3.I the isotropic coating (A) consists of amorphous material with some randomly distributed 2:1 clay-domains. The anisotropic coating (B) consists of randomly distributed domains of 2:1 clay. High resolution lattice-fringe imaging (Fig. 3-III) reveals basal spacings of 1.4 nm. Microchemical analyses of individual clay-domains in the anisotropic type B show high Si and low Al contents and an inverse relationship between Al and Fe (Fig.3.III).

DISCUSSION

The presence of isotropic (A) and anisotropic parts (B) within one coating and their similarity in plane polarized light indicate that they are genetically related. The limpid texture and non-laminated internal fabric of the coatings, and the occurrence of types A and B within one coating suggest that A and B are due to clay neoformation rather than clay illuviation. Moreover, clay illuviation coatings should be anisotropic because they always consist of crystalline clay minerals, while an isotropic character points to amorphous material (Bullock et al., 1985). SSXRD shows that the isotropic type A is X-ray amorphous, while TEM observations demonstrate occurrence of small amounts of 2:1 clay domains in an amorphous groundmass. Anisotropic coatings B predominantly consists of crystalline 2:1 phyllosilicates. TEM analyses show absence of preferred orientation patterns between the clay domains, which is in agreement with the micromorphologically observed stipple-speckled b-fabric. This suggests that the precipitation of the amorphous, isotropic coatings is the first step, and recrystallization of these coatings to anisotropic coatings is the second step in clay neoformation. The isotropic coatings may be allophane-like, although they are relatively rich in silica. Parfitt and Kimble, (1989) reported Al/Si ratios of allophane are usually around 2, but variations may occur between 0.5 and 4. These values are strongly influenced by the chemical composition of the parent material and its resistance against weathering, and the prevalent leaching/drainage conditions (Parfitt, 1989; Singleton et al; 1989). As a result, the weathering of trachytic pumice fragments (Al/Si ratio 0.36) in the paleosol, and restricted leaching conditions during coating formation are thought to be the main sources of large amounts of liberated Si, resulting in formation of Si-rich allophanes and subsequent formation of 2:1 clay minerals rich in Si. After burying of the paleosol, the coatings were preserved.

Both coating types have a relatively high Fe content, probably due to iron impregnation, but partial incorporation of variable amounts of iron in the smectite lattice cannot be excluded. The observed muscovite in type B may explain the 1.0 nm. diffraction peak, and are parts of the adjacent parent material mixed in the gels during transport. The difference between the SSXRD diagram and TEM images concerning the measured basal spacings of the smectite might be a result of the use of acetone during sample preparation (swelling), and/or high vacuum used during TEM analysis (partial collapsing).

CONCLUSIONS

Weathering of trachitic pumice under restricted leaching conditions in a quaternary river terrace in France resulted in the formation of optically isotropic allophanic coatings with a Al/Si ratio up to 0.5. With time, these coatings may partially crystallize to anisotropic coatings consisting predominantly of randomly distributed smectitic clay domains. Although such coatings may still form in similar environments they are believed to be preserved by burial in the case reported here.

REFERENCES

- Bullock, P., Fedoroff, N., Jongerius, A., Sloops, G. and Tursina, T., 1985. Handbook for soil thin section description. Waine Research Publications, England, 150 pp.
- Buurman, P. and Jongmans, A.G., 1987. Amorphous clay coatings in a lowland Oxisol and other andesitic soils of West-Java, Indonesia. *Pemberitaan Penelitian Tanah Dan Pupuk* 7:31-41.
- Chartres, C.J., Wood, A. and Pain, C.F., 1985. The development of micromorphological features in relation to some mineralogical and chemical properties of volcanic ash soils in highland Papua New Guinea. *Australian Journal of Soil Research* 23: 339-345.
- Dalrymple, J.B. 1964. The application of soil micromorphology to the recognition and interpretation of fossil soils in volcanic ash deposits from the north Island, New Zealand. In: A. Jongerius (ed.) *Soil micromorphology* Elsevier, Amsterdam, pp. 339-349.
- FitzPatrick, E.A., 1970. A technique for the preparation of large thin sections of soils and consolidated material. In: D.A. Osmond and P. Bullock (Editors), *Micromorphological techniques and application*. Techn.monogr. 2, Soil Survey of England and Wales, Rothamsted Exp. Sta., Harpenden, pp. 3-13.
- Jongmans, A.G., Fijtel, T.C., Miedema, R., van Breemen, N. and Veldkamp, A., 1991. Soil formation in a Quaternary terrace sequence of the Allier, Limagne, France. Macro- and micromorphology, particle size distribution, chemistry. *Geoderma* 49: 216-239.
- Meunier, A. and Velde, B., 1982. X-ray diffraction of oriented clays in small quantities (0.1 mg). *Clay Miner.* 17: 259-262.
- Oort, van F., Jongmans, A.G., Jaunet, A.M., van Doesburg, J., and Feijtel, T., 1990. Andesite weathering and

halloysite newformation in a ferralitic soil environment in Guadeloupe. In situ study of different halloysite facies on thin sections by SEM-EDXRA, microdrilling, step scan XRD and TEM. C.R. Acad. Sci. Paris, t. 310, Serie II, p. 425-431.

Parfitt, R.L. and Kimble, J.M., 1989. Conditions for formation of allophane in soils. Soil Sci. Soc. Am. J. 53: 971-977.

Singleton, P.L., Mcloed, M., and Percival, H.J., 1989. Allophane and halloysite content and soil solution silicon in soils from Rhyolitic volcanic material, New Zealand. Aust. J. Soil Res.,27: 67-77.

Veldkamp, A. and Jongmans, A.G., 1991. Trachitic pumice clasts in Middle Pleistocene Allier terrace deposits, Limagne, France: A chronostratigraphic marker. In: A. Veldkamp, Quaternary river terrace formations in the Allier basin, France. Thesis, Wageningen, Agric. University: pp 27-35.

Verschuren, R.H. 1978. A microscope-mounted drill to isolate microgram quantities of mineral material from polished thin sections. Mineral. Mag. 42: 499-503.

Table 1

SEM-EDXRA analyses of isotropic coatings (A) and anisotropic coatings (B) (WT%; N=20)

	coating A	coating B	t value	significance
Mg	0.09 ± 0.09	0.06 ± 0.06	1.857	*
Al	5.3 ± 0.8	4.1 ± 0.9	4.56	**
Si	12.4 ± 1.4	14.3 ± 2.2	-3.23	**
K	0.004 ± 0.1	0.2 ± 0.3	-1.81	*
Ca	0.6 ± 0.4	1.1 ± 0.2	-3.39	**
Fe	7.2 ± 1.2	9.6 ± 1.8	-5.84	**
Al/Si molar	0.5	0.3		

*, **, Significant at P <0.05 and 0.01, respectively

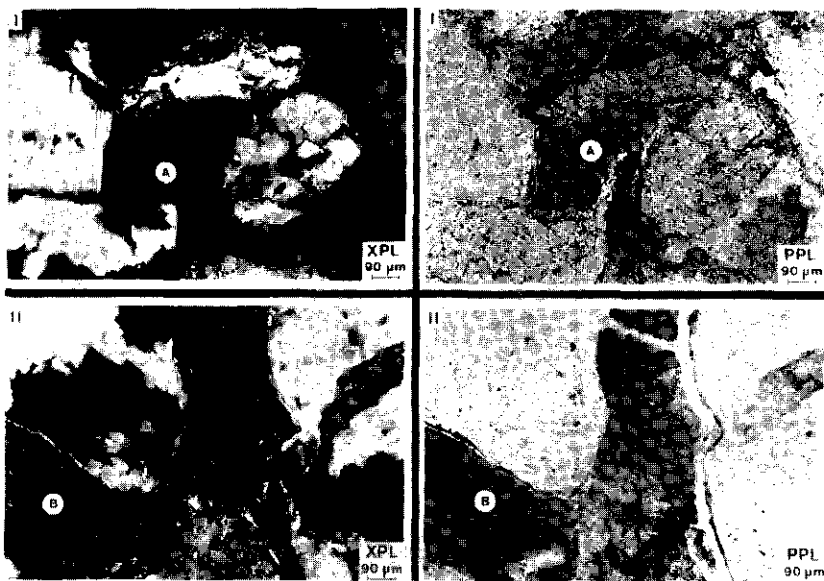


Fig.1 Micromorphological characterization of the isotropic and anisotropic coatings.

I: isotropic coating (A)

II anisotropic coating (B)

XPL = crossed polarized light; PPL = plane polarized light.

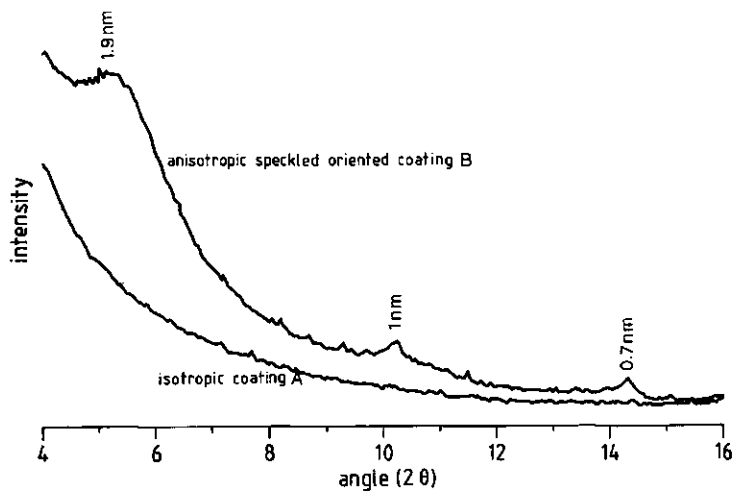


Fig.2 Step scan X-ray diffractograms (Co-K α radiation) of microquantities of the isotropic (A), and anisotropic (B) coatings obtained by microdrilling.

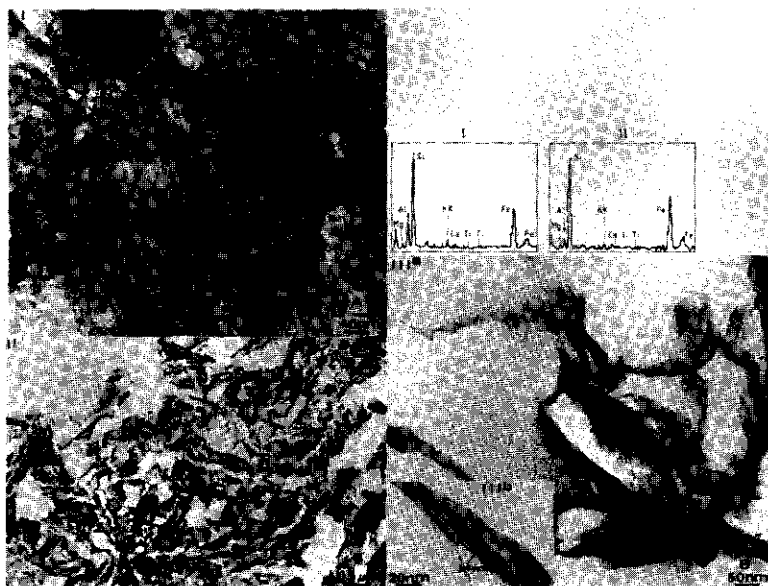


Fig. 3 TEM observations of undisturbed parts of the isotropic (A) and anisotropic (B) coatings, and microchemical analyses of clay domains.
 a = allophane; Sm = swectite

3.4 Inheritance of 2:1 phyllosilicates in Costa Rican Andisols

Soil Sci. Soc. Am. J. 58: 494-501 (1994).

A.G. Jongmans, F. van Oort, A. Nieuwenhuysse, A.M. Jaunet, and J.D. van Doesburg.

ABSTRACT

The occurrence of 2:1 phyllosilicates in Andisols is variously ascribed to in situ pedogenic origin, aeolian addition, or the presence of hydrothermally altered rock fragments. We studied the origin of 2:1 phyllosilicates that occur in Holocene Hapludands on andesitic, sandy beach ridges in Costa Rica by micromorphological, mineralogical, and submicroscopical techniques. The 2:1 phyllosilicates also occur as pseudomorphs after primary minerals in fresh rock of the inland volcanoes, from which the parent material of the beach ridges was mainly derived. Hydrothermal processes are most likely responsible for the formation of such pseudomorphs. Rock weathering produces sand-sized rock fragments with clay pseudomorphs and also liberates individual pseudomorphs. Subsequent erosion and alluvial transport affect their shape, but not their internal fabric. In the beach ridges, clay pseudomorphs appear as individual, sand-sized clay bodies, and inside sand-sized andesitic rock fragments. Submicroscopical analyses

A. G. Jongmans, A. Nieuwenhuysse, P. Buurman, and J. D. J. van Doesburg, Dep. of Soil Science and Geology, Agricultural Univ. P.O. Box 37, 6700 AA Wageningen, the Netherlands; F. van Oort, INRA, Station Agropédologique, Guadeloupe, France; A. M. Jaunet, INRA, Station de Science du Sol, Versailles, France. Received 31 Aug. 1992. *Corresponding author.

Published in *Soil Sci. Soc. Am. J.* 58:494-501 (1994).

of these individual clay bodies and andesitic rock fragments with clay pseudomorphs indicate a predominance of 2:1 phyllosilicates. This implies that they are inherited from the parent material and are not due to postdepositional soil formation in the beach ridges. Weathering and biological activity affect the clay bodies and rock fragments with clay pseudomorphs, leading to the formation of clay-sized particles consisting of 2:1 phyllosilicates. Toward the soil surface, these particles are incorporated into the allophanic groundmass resulting from actual soil formation. The geographically extensive occurrence of 2:1 phyllosilicates in Andisols suggests that the genetic processes described here may have more than regional validity.

ALLOPHANE and 1:1 phyllosilicates are the most common secondary minerals in soils formed in pyroclastic deposits in humid tropical areas without a distinct dry season (Mizota and van Reewijk, 1989; Parfitt and Kimble, 1989; Quantin et al., 1990). The occurrence of 2:1 phyllosilicates has often been reported in such soils

Abbreviations: EDS, electron diffraction spectrometer; EG, ethylene glycol; SSXRD, step-scan x-ray diffraction; TEM, transmission electron microscope; XRD, x-ray diffraction.

(Wada, 1980; Pevear et al., 1982; Shoji et al., 1985, 1987; van Oort, 1988), but there are different concepts concerning their genesis (Lowe, 1986). Shoji and Yamada (1981) and Shoji et al. (1982) favored an in situ pedogenic origin, and suggested that 2:1 phyllosilicates are formed by weathering of volcanic glass. Other workers such as Mokma et al. (1972) and Mizota and Takahashi (1982) attributed the presence of 2:1 phyllosilicates in soils on tephra deposits to later aeolian additions. Dudas and Harward (1975), Pevear et al. (1982), and Ping et al. (1988) ascribed the occurrence of 2:1-type phyllosilicates in airfall tephra deposits to hydrothermally altered rock fragments that were ejected during eruptions. Hydrothermal alteration in volcanic rocks transforms primary minerals such as olivine, pyroxenes, and plagioclase into clay pseudomorphs (Kristmannsdottir, 1979; Fan, 1979). Dudas and Harward (1975) demonstrated that 2:1 phyllosilicates in some volcanic ash horizons could be relicts of an underlying montmorillonite-containing paleosol.

Micromorphology and related in situ submicroscopy were not carried out in the cited studies, except for Pevear et al. (1982). Consequently, the properties of the individual soil constituents in terms of size, shape, arrangement, and composition were not studied. Among other factors, these properties influence the occurrence of clay minerals in soils formed on volcanic deposits (Nahon, 1991; Jongmans et al., 1994), so they need to be examined in studies concerning mineral weathering and neoformation.

In a chronosequence of Andisols and younger Tropopsamments on Holocene andesitic beach ridges of Costa Rica, Nieuwenhuysse et al. (1994) reported the occurrence of 2:1 phyllosilicates. These soils were formed under humid tropical conditions where soil weathering (super-gene alteration, Delvigne, 1990) has led to formation of short-range order material. The goal of our study was to determine the origin and genesis of the observed 2:1 phyllosilicates in the Andisols of the Costa Rican beach ridge sequence by means of micromorphological, mineralogical, and in situ submicroscopical techniques of undisturbed samples.

MATERIALS AND METHODS

Five Andisols (2000–5000 yr old) and three Tropopsamments (<100–500 yr old) are developed in a chronosequence of eight separate andesitic beach ridges of Holocene age parallel to the northeastern Caribbean coastline of Costa Rica (10°35'N,

83°35'W). The study was focused on the Andisols. The pedons were described according to the Food and Agriculture Organization of the United Nations (1990) and classified according to the Soil Survey Staff (1992). Their geological and geomorphological setting, as well as soil formation, were reported by Nieuwenhuysse and Kroonenberg (1993, unpublished data) and Nieuwenhuysse et al. (1993, 1994). The parent material of the sandy ridges is mainly derived from volcanic rocks of the Cordillera Central. Soil-forming processes are strongly determined by the prevailing isohyperthermic soil temperature regime (mean annual air temperature of 25–26°C) and the perudic moisture regime (mean annual rainfall of 5400 mm) (Soil Survey Staff, 1992). With increasing age, texture changes from sand to loam, while the drainage class shifts from excessively drained to imperfectly drained (Food and Agriculture Organization of the United Nations, 1990).

Thin sections (10 by 10 or 3 by 5 cm) were made of undisturbed samples from the eight pedons and of fresh rock of the Irazu volcano (Cordillera Central). These were prepared following the method of FitzPatrick (1970) and described using the terminology of Bullock et al. (1985).

Grain size fractions of <2, 2 to 20, 20 to 50, 50 to 200, and 200 to 2000 µm of the A (0–14 cm), Bw (40–60 cm) and the C horizon (>150 cm) of Hapludand AT7 were studied by XRD. The fractions were prepared after removal of organic matter by buffered (pH 5.5) H₂O₂ treatment, repeated washing with distilled water (5–10 times) and addition of 0.005 M NaCl solution. The XRD was performed after grinding of the separated particle size fractions. In order to improve the quality of the XRD diagrams, part of the ground material was ultrasonically dispersed and sequentially extracted in darkness with ammonium oxalate at pH 3.3 (Tamm, 1922; Robert and Tessier, 1974), then with sodium citrate at pH 7.3 (Tamura, 1957). The XRD patterns were obtained from Mg-saturated, oriented pastes before and after EG solvation and from K-saturated, oriented pastes after heating. Finally, fresh rock collected on the Irazu volcano was ground and ultrasonically dispersed. The XRD was performed on the clay fraction after Mg and K saturation. The allophane content was calculated by the method proposed by Parfitt and Wilson (1985).

From four Hapludands, microquantities of sand-sized, anisotropic, clay bodies from uncovered thin sections were isolated with a microscope-mounted drill (Verschure, 1978). The material was transferred to glass or Al slides according to the method of Beauford et al. (1983). The XRD analyses of the microquantities were obtained by SSSRD, (Meunier and Velde, 1982) with steps of 0.05° 2θ and counting times of 80 s per step.

Two sand-sized, anisotropic clay bodies from Hapludand AT7 were selected optically and removed from uncovered thin sections without disturbing them according to the method proposed in van Oort et al. (1990). After reimpregnation of these clay bodies, undisturbed sections of 50-nm thickness

Table 1. Selected properties and classification of five Andisols from Costa Rica.

Profile	Classification	Particle-size distribution						Chemical and physical properties			
		A horizon		B horizon		C horizon		A horizon		B horizon	
		Clay	Sand	Clay	Sand	Clay	Sand	Organic matter	pH (H ₂ O)	Bulk density	Allophanet
		g kg ⁻¹									
AT4	Typic Hapludand	170	690	110	800	0	1000	128	6.0	0.8	56
AT5	Acrodoxic Hapludand	205	570	100†	810	0	1000	148	5.4	0.9	60
AT6	Acrodoxic Hapludand	205	620	80†	800	0	1000	120	5.5	0.7	79
AT7	Aquic Hapludand	270	500	110†	700	0	980	321	4.6	0.6	91
AT8	Hydric Hapludand	210†	480	100†	650	0	990	413	4.5	nd	94

† Calculated according to the method of Mizota and van Reewijk (1989), values taken from Nieuwenhuysse et al. (1994).

‡ These values should be considered minimum values, since flocculation was observed in the sedimentation cylinders.



Fig. 1. Micromorphological characterization of some important features: (A) subhedral clay pseudomorphs (1) showing mosaic speckled b-fabric, continuous birefringent flakes and opaque Fe veins in a hypogenically altered rock fragment of the Irazu volcano; (B) ellipsoidal clay body, having a stipple speckled b-fabric and strongly oriented, continuous birefringent flakes (1) in the C horizon of Hapludand AT7; (C) ellipsoidal clay body with a stipple speckled b-fabric (1), and a strongly oriented, continuously birefringent band with denticulated outer boundaries in the C horizon of Hapludand AT6; and (D) andesitic rock fragment with subhedral neoformed clay pseudomorphs (1), and a sand-sized clay body with mosaic speckled b-fabric (2) in the C horizon of Hapludand AT4.

were prepared according to the method of van Oort et al. (1990), and analyzed with a Philips 420 TEM (Philips, Eindhoven, the Netherlands). A Link AN 10000 EDS analyzer (Link System Ltd., Bucks, UK) allowed microchemical analysis.

RESULTS AND DISCUSSION

Soil Properties

Typic Tropopsamments (Soil Survey Staff, 1992) are the characteristic soils on the three youngest beach ridges; Acrudoxic and Aquic Hapludands occur on the five older ones. Selected soil properties of the Hapludands are shown in Table 1. The A horizons display dark colors (10YR 2/2 and 2/3), and their organic matter content increases with soil age ($128\text{--}413\text{ g kg}^{-1}$). The soils show abundant faunal activity, and sedimentary structures are fully obliterated. All C horizons consist of sand ($53\text{--}425\text{ }\mu\text{m}$), whereas in the upper soil horizons sand contents decrease with soil age. The pH increases with depth, but decreases with soil age in the A horizons. Bulk densities of the A and B horizons are $<0.9\text{ Mg m}^{-3}$. The allophane content ranges from 0% in the youngest Tropopsamment to 10% in the oldest Hapludand. Small amounts of 2:1 and 1:1 phyllosilicates were observed (XRD) in the clay fraction of the Hapludands and the Tropopsamments. Addition to the soils of volcanic ash particles with diameters $>5\text{ }\mu\text{m}$ is unlikely, because optical studies revealed that such particles are absent in a 4450-yr-old peat deposit located between the volcanoes (Central Cordillera) and the studied location. Moreover, the prevailing wind directions are inland (Nieuwenhuysen et al., 1993).

2:1 Phyllosilicates in Hypogene-Altered Rock from the Inland Mountains

The parent material of the beach ridges is derived from the mainly volcanic Cordillera Central, to which the Irazu volcano belongs. Optical observations in thin sections of fresh rock, collected from the slopes of the Irazu, demonstrate the absence of pellicular or linear alteration in the dominant constituents (plagioclase and pyroxene). This indicates the absence of supergene weathering (Delvigne, 1990). Furthermore, these thin sections reveal the presence of anisotropic, euhedral and subhedral, clay pseudomorphs, probably after hypersthene and olivine ($20\text{--}400\text{ }\mu\text{m}$, Fig. 1A). They contain some opaque Fe veins and display similar colors and b-fabrics as sand-sized clay bodies, and clay pseudomorphs in sand-sized andesite rock fragments observed in the Hapludands, which will be described in detail below.

The XRD pattern of the clay fraction of the rock after Mg saturation demonstrates clear 1.4- (Fig. 2A) and 0.93-nm peaks. After EG solvation, the 1.4-nm peak shifted to 1.7 nm (Fig. 2B). The diffractogram of a heated, K-saturated sample (500°C) obtained under vacuum shows a collapse to 0.97 nm (Fig. 2C and 2D). These observations indicate the presence of swelling 2:1 phyllosilicates and probably some talc (0.93 nm). Since the hard, fresh rock was not affected by supergene weathering and expansible 2:1 phyllosilicates are not part of

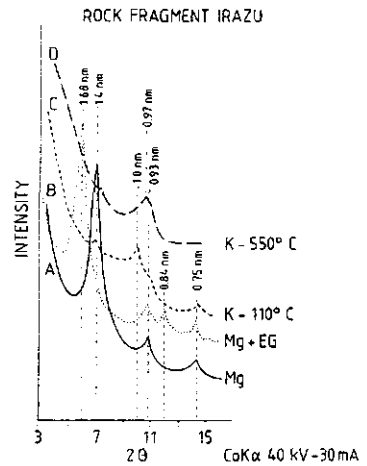


Fig. 2. X-ray diffractograms of a fresh rock fragment from the Irazu volcano.

the primary rock composition, these rocks must have been influenced by hydrothermal processes.

Hydrothermal alteration in volcanic rocks transforms primary minerals (phenocrysts) into clay pseudomorphs (hypogene weathering, Delvigne, 1990). The opaque Fe veins in the clay pseudomorphs may be inherited from hydrothermal alteration (Nahon, 1991). Kristmannsdottir (1979) studied hydrothermal alteration of basaltic rocks in Iceland and reported formation of smectite below 200°C , and transformation of the smectite into mixed layer clay minerals (smectite and chlorite) and swelling chlorites at $200\text{--}240^\circ\text{C}$. Kawano and Tomita (1992) demonstrated the formation of allophane and smectite during experimental hydrothermal alteration of volcanic glass below 200°C . Hydrothermal processes in the andesitic rocks of the Cordillera Central are probably responsible for the transformation of part of the primary minerals (probably pyroxene and some olivine) into hypogene clay pseudomorphs, which consist dominantly of 2:1 phyllosilicates.

2:1 Phyllosilicates in the Fine-Earth Fraction of the Hapludands

Micromorphological observations show that anisotropic, smooth rounded to ellipsoidal clay bodies, (up to $400\text{ }\mu\text{m}$, Fig. 1B and 1C) make up 3 to 11% (v/v) of the mineral grains in the sand fraction of the Hapludands. Their color varies from greenish blue and yellowish green to yellowish brown, and they mostly have a stipple-speckled to mosaic-speckled b-fabric. Between these b-fabrics, sharply bounded, strongly oriented, continuously birefringent flakes ($20\text{--}100\text{ }\mu\text{m}$) and bands ($20\text{--}50\text{ }\mu\text{m}$) are observed (Fig. 1B and 1C), sometimes with a denticulate outer boundary. Locally, the strongly oriented flakes have a radial structure. Except for their shapes, the clay bodies are similar to the clay pseudomorphs in the Irazu rock. Toward the soil surface, some clay bodies, which

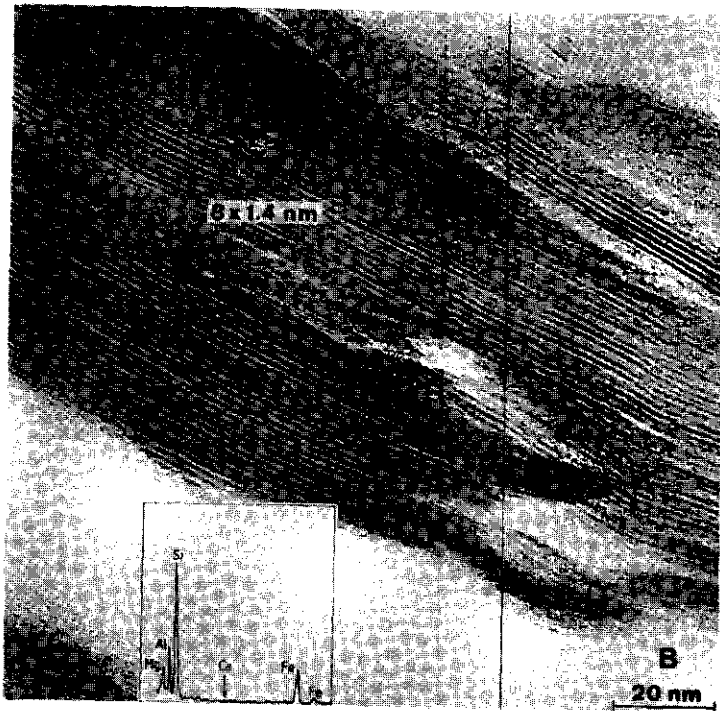


Fig. 3. Transmission electron microscope images of the anisotropic clay body shown in Fig. 1C: (A) overview and electron diffraction spectrometer (EDS) elemental analysis of an in situ isolated clay body fragment at low magnification. The dense homogeneous primary mineral residue is bordered by curled mineral domains; (B) high-resolution lattice fringe image and EDS elemental analysis showing occurrence of 2:1 phyllosilicates in the mineral domains.

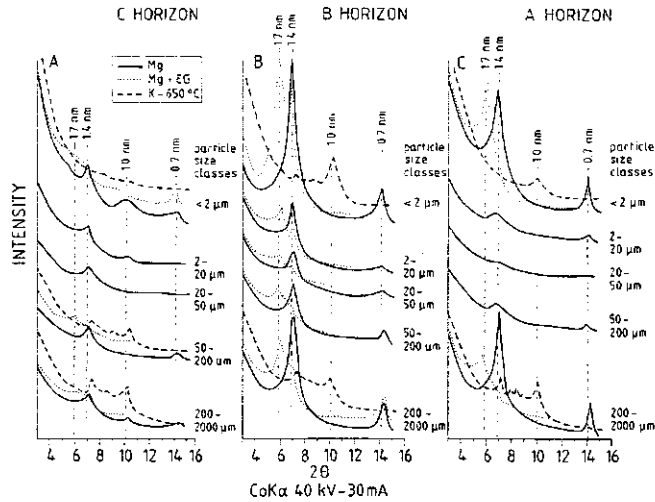


Fig. 4. X-ray diffractograms of different particle-size classes from different depths in Hapludand AT7.

can be crushed with a needle, break up into smaller fragments (2–200 μm).

Andesitic rock fragments (up to 400 μm) in the Hapludands frequently contain yellowish green to yellowish brown, rectangular, euhedral to subhedral clay pseudomorphs (10–100 μm), with colors and b-fabrics similar to those of the rounded and ellipsoidal clay bodies (Fig. 1D). Toward the soil surface, these fragments show pellicular alteration, and diminish in size or break up into the individual constituents. Similar clay bodies and andesitic rock fragments with clay pseudomorphs occur in the younger Tropopsammings.

Step-scan XRD on clay bodies isolated from thin sections by microdrilling demonstrates clear peaks at 1.4 nm, indicating the presence of 2:1 phyllosilicates (diffractograms now shown). Small, broad peaks at 0.72 nm may either be a second-order reflection, or indicate the presence of 1:1 phyllosilicates. Step-scan XRD of the andesitic rock fragments with clay pseudomorphs shows, in addition to reflections of major primary minerals, a weak shoulder at 1.4 nm and a weak peak at 0.72 nm.

Figure 3 shows TEM micrographs of undisturbed sections of the anisotropic clay body shown in Fig. 1C. At low magnification (Fig. 3A), areas of dense, homogeneous primary mineral residues are visible. Microprobe analysis of these areas shows high Si content and appreciable amounts of Mg, Ca, and Fe; the Al content is low. At the border of these areas, the material starts to curl, and high-resolution lattice fringe imaging (Fig. 3B) reveals elementary spacings of 1.4 nm, supporting the conclusion that this material consists of 2:1 phyllosilicates. Microprobe analysis demonstrates high amounts of Si and appreciable quantities of Al, Mg, and Fe.

The sand fraction of the C horizon (Fig. 4A) of Hapludand AT7 shows a dominant presence of 2:1 clay phyllo-

silicates. Before chemical treatment, only weak 1.4-nm peaks could be observed (not shown). After ammonium oxalate and sodium citrate treatment, an asymmetric peak occurred at 1.4 nm that partially shifted to higher spacings after EG solvation. Heating of a K-saturated sample to 650 $^{\circ}\text{C}$ caused an incomplete collapse of the peak to 1.4 and 1.0 nm. This behavior is characteristic for smectitic and chloritic clay minerals. The 2:1 phyllosilicates are also observed in the silt and clay fractions, which represent <2% of the total particle-size distribution. These fractions probably result from sample pretreatments. In the B horizon, peaks indicating 2:1 phyllosilicates are observed in all particle size classes. The XRD patterns are similar to those of the sand fraction of the C horizon (Fig. 4B). The persistence of the 0.7-nm peak with EG indicates some 1:1 clay minerals. In the A horizon (Fig. 4C), 2:1 phyllosilicates only occur in the coarse sand fraction and the clay fraction. The XRD patterns of the coarse sand fraction are identical to those of the C horizon. The XRD patterns of the clay fraction suggest the presence of a smectitic clay mineral.

Physical breakdown, as a result of weathering and high faunal activity, reduced the sand-size clay pseudomorphs and rock fragments with clay pseudomorphs into silt- and clay-size particles in the B horizon. The absence of 2:1 phyllosilicates in the fine sand and silt fractions of the A horizons suggests further breakdown of the clay pseudomorphs to finer grain sizes. Consequently, 2:1 phyllosilicates are progressively incorporated in the allophanic groundmass of the Hapludands.

In summary, the sandy parent material of the beach ridges in Costa Rica was derived from hydrothermally altered andesitic rock in the Cordillera Central. Weathering liberated individual mineral grains, as well as individual clay pseudomorphs that were present in the hydrothermally influenced andesitic rock (Fig. 1A). In addition,

physical weathering produced sand-sized andesitic rock fragments with clay pseudomorphs (Fig. 1D). During subsequent erosion and fluvial and marine transport, the clay pseudomorphs, which have a cohesive, massive microfabric, act as soft mineral grains and lose their angular shapes. As rounded and oval bodies, these clay grains (Fig. 1B and 1C), constitute part of the sand fraction and are deposited in the beach ridges together with andesite rock fragments, which contain clay pseudomorphs and primary mineral grains.

Current pedogenesis in these Andisols is dominated by chemical dissolution of primary minerals and allophane formation. The 2:1 phyllosilicates progressively appear in the allophanic groundmass as a result of physical breakdown of inherited, sand-sized clay grains in the parent material.

CONCLUSIONS

Hydrothermal alteration of primary minerals to 2:1 phyllosilicates is a common process that accompanies the formation of volcanic rocks. Hence, the products of hydrothermal alteration should be common in soils formed from volcanic materials. Our data indicate the 2:1 phyllosilicates in the five Costa Rican Andisols studied are from the parent material and are not pedogenic. We speculate that the widespread occurrence of 2:1 phyllosilicates reported in Andisols reflects, at least in part, the inheritance of these hydrothermal alteration products. Our study demonstrates that micromorphological and related *in situ* submicroscopical techniques are useful in studies concerning mineral weathering and neoformation in soils developed in volcanic deposits.

REFERENCES

- Beauford, D., P. Dudoignon, D. Proust, J.C. Parneix, and A. Meunier. 1983. Microdrilling in thin sections: A useful method for the identification of clay minerals *in situ*. *Clay Miner.* 18:223-226.
- Bullock, P.N., N. Fedoroff, A. Jongerus, G. Stoops, and T. Tursina. 1985. Handbook for soil thin section description. *Wayne Res. Publ.*, Albrighton, England.
- Delvigne, J. 1990. Hypogene and supergene alteration of orthopyroxene in the Koua Bocca ultra mafic intrusion, Ivory Coast. *Chem. Geol.* 84:49-53.
- Dudas, M.J., and M.E. Harward. 1975. Inherited and detrital 2:1 type phyllosilicates in soils developed from Mazama ash. *Soil Sci. Soc. Am. Proc.* 39:571-576.
- Fan, P.F. 1979. Clays and clay minerals of hydrothermal origin in Hawaii. p. 369-374. *In* M.M. Mortland and V.C. Farmer (ed.) *Developments in sedimentology*. Proc. Int. Clay Conf. 6th, Oxford, 10-14 July 1978. Elsevier, Amsterdam.
- Food and Agriculture Organization of the United Nations. 1990. Guidelines for soil profile description. 2nd ed. FAO, Rome.
- FitzPatrick, E.A. 1970. A technique for the preparation of large thin sections of soils and consolidated material. p. 3-13. *In* D.A. Osmond and P. Bullock (ed.) *Micromorphological techniques and application*. Tech. Monogr. 2. Soil Surv. of England and Wales, Rothamsted Exp. Stn., Harpenden.
- Jongmans, A.G., F. van Oort, P. Buurman, A.M. Jaunet, and J. van Doesburg. 1994. Morphology, chemistry, and mineralogy of isotropic aluminosilicate coatings in a Guadeloupe Andisol. *Soil Sci. Soc. Am. J.* 58:501-507 (this issue).
- Kawano, M., and K. Tomita. 1992. Formation of allophane and beidellite during hydrothermal alteration of volcanic glass below 200°C. *Clays Clay Miner.* 40:666-674.
- Kristmannsdottir, H. 1979. Alteration of basaltic rocks by hydrothermal activity at 100-300°C. p. 359-367. *In* M.M. Mortland and V.C. Farmer (ed.) *Developments in sedimentology*. Proc. Int. Clay Conf. 6th, Oxford, 10-14 July 1978. Elsevier, Amsterdam.
- Lowe, D.J. 1986. Control on the rates of weathering and clay mineral genesis in airfall tephra; a review and New Zealand case study. p. 265-330. *In* S.M. Colman and D.P. Dethier (ed.) *Rates of chemical weathering of rocks and minerals*. Academic Press, New York.
- Meunier, A., and B. Velde. 1982. X-ray diffraction of oriented clays in small quantities (0.1 mg.). *Clay Miner.* 17:259-262.
- Mizota, C., and Y. Takahashi. 1982. Eolian origin of quartz and mica in soils developed on basalts in northwestern Kyushu and San-in, Japan. *Soil Sci. Plant Nutr.* (Tokyo) 28:369-378.
- Mizota, C., and L.P. van Reewijk. 1989. Clay mineralogy and chemistry of soils formed in volcanic material in diverse climatic regions. [SRIC, Wageningen, the Netherlands].
- Mokma, D.L., J.K. Syers, M.L. Jackson, R.N. Clayton, and R.W. Rex. 1972. Eolian additions to soils and sediments in the South Pacific area. *J. Soil Sci.* 23:147-162.
- Nahon, D.B. 1991. Introduction to the petrology of soils and chemical weathering. John Wiley & Sons, New York.
- Nieuwenhuysse, A., A.G. Jongmans, and N. van Breemen. 1993. Andisol formation in a Holocene beach ridge plain under a humid tropical climate; an example of the Atlantic coast of Costa Rica. *Geoderma* 57:423-442.
- Nieuwenhuysse, A., A.G. Jongmans, and N. van Breemen. 1994. Mineralogy of a Holocene chronosequence on andesitic beach sediments in Costa Rica. *Soil Sci. Soc. Am. J.* 58:485-494 (this issue).
- Parfitt, R.L., and J.M. Kimble. 1989. Conditions for the formation of allophane in soils. *Soil Sci. Soc. Am. J.* 53:971-977.
- Parfitt, R.L., and A.D. Wilson. 1985. Estimation of allophane and halloysite in three sequences of volcanic soils, New Zealand. p. 1-8. *In* E. Fernandez Caldas and D.H. Yaalon (ed.) *Volcanic soils*. Catena Suppl. 7. Catena Verlag, Braunschweig, Germany.
- Pevear, R.R., D.P. Dethier, and D. Frank. 1982. Clay minerals in the 1980 deposits from Mount St. Helens. *Clays Clay Miner.* 30:241-252.
- Ping, C.L., S. Shoji, and T. Ito. 1988. Properties and classification of three volcanic ash-derived pedons from Aleutian Islands and Alaska peninsula, Alaska. *Soil Sci. Soc. Am. J.* 52:455-462.
- Quantin, P., J. Balesdent, A. Bouleir, M. Delaune, and C. Feller. 1990. Premiers stades d'altération de ponces volcaniques en climat tropicale humide (Montagne Pelée, Martinique). *Geoderma* 50:125-148.
- Robert, M., and D. Tessier. 1974. Méthodes de préparation des argiles des sols pour études minéralogiques. *Ann. Agron.* 25:859-882.
- Shoji, S., T. Ito, M. Saigusa, and I. Yamada. 1985. Properties of nonallophanic Andosols from Japan. *Soil Sci.* 140:264-277.
- Shoji, S., Y. Suzuki, and M. Saigusa. 1987. Clay mineralogy and chemical properties of nonallophanic Andepts (Andisols) from Oregon, USA. *Soil Sci. Soc. Am. J.* 51:986-990.
- Shoji, S., and I. Yamada. 1981. Mobilities and related factors of chemical elements in the topsoils of Andosols in Tohoku, Japan: 2. Chemical and mineralogical compositions of size fractions and factors influencing the mobilities of major chemical elements. *Soil Sci.* 132:330-346.
- Shoji, S., I. Yamada, and M. Saigusa. 1982. Chemistry and clay mineralogy of Andosols, Brown Forest soils, and Podzolic soils formed from recent Towada ashes, northeastern Japan. *Soil Sci.* 133:69-86.
- Soil Survey Staff. 1992. Keys to soil taxonomy. *Soil Manage. Support Serv. Tech. Monogr.* no. 19. 5th ed. Pocahontas Press, Blacksburg, VA.
- Tamm, O. 1922. Eine methode zur bestimmung der anorganischen komponenten der gelkcomplexen in boden. *Medd. für statens Skogsf.* 19:385-404.
- Tamura, T. 1957. Identification of the 14 Å clay mineral component. *Am. Mineral.* 42:107-110.
- Verschure, R.H. 1978. A microscope-mounted drill to isolate microgram quantities of mineral material from polished thin sections. *Mineral. Mag.* 42:499-503.
- van Oort, F. 1988. Présence et évolution des minéraux accessoires de type 2:1 dans les sols ferrallitiques d'origine volcanique de la Guadeloupe. *Conséquences physicochimiques*. C.R. Acad. Sci.

- Ser. 2 307: 297-1302.
- van Oort, F., A.G. Jongmans, A.M. Jaunet, J.D. van Doesburg, and T.C.J. Feijtel. 1990. Andesite weathering and halloysite neoformation in a ferrallitic soil environment in Guadeloupe (F.W.I.): An in-situ study on thin sections using SEM-EDXRA, microdrilling, step scan x-ray diffraction and TEM. C.R. Acad. Sci Ser. 2. 310: 425-431.
- Wada, K. 1980. Mineralogical characteristics of Andisols. p. 87-107. In B.K.G. Theng (ed.) Soils with variable charge. N.Z. Soc. Soil Sci., Lower Hutt, New Zealand.

CHAPTER 4

CLAY COATINGS FORMED BY ILLUVIATION OR BY IN SITU PRECIPITATION

- 4.1 Amorphous clay coatings in a lowland Oxisol and other Andesitic soils of West Java, Indonesia.

Pemberitaan Penelitian Tanah dan Pupuk, 7:31-40, 1985

P. Buurman and A.G. Jongmans.

Amorphous Clay Coatings in A Lowland Oxisol and Other Andesitic Soils of West Java, Indonesia

Selaput Liat Amorf pada Oxisol Dataran Rendah dan Tanah-tanah Andesitik Lainnya di Jawa Barat, Indonesia

P. BURMAN, and A.G. JONGMANS¹

ABSTRACT

Isotropic allophanic coatings were found in a West Java Oxisol on andesitic volcanic products. These coatings recrystallize toward birefringent, probably halloysitic coatings that are easily confused with illuviation argillans. The allophane is probably due to weathering of airborne ash additions. Both amorphous and (partly) crystalline coatings appear to be common in the three andesitic catenas investigated except for the perhumid part of the catenas. Crystallization and abundance of the coatings tend to increase in soils which suffer a distinct dry season, but in some soils it is not possible to unequivocally distinguish recrystallized coatings from illuviation argillans. Amorphous and recrystallized coatings are thought to occur in many ash-influenced soils throughout Indonesia.

Index words: *allophane, argillans, allophanans, oxisol, clay illuviation, volcanic ash, andesite, andosols.*

ABSTRAK

Selaput alofan isotropik ditemukan pada Oxisol dan tanah andesitik lainnya di Jawa Barat. Selaput-selaput ini mengkristal ke arah birefringent, kemungkinan besar selaput berhalloisit yang mirip dengan illuviasi argillans. Alofan ini kemungkinan hasil pelapukan abu vulkanik yang terbawa angin. Kedua selaput yang amorf dan terkristal sebagian tampaknya lumayan pada tiga catena berandesit yang diteliti, kecuali pada bagian dengan curah hujan paling tinggi. Pengkristalan dan jumlah selaput cenderung bertambah pada tanah-tanah yang mengalami musim kering yang jelas. Tetapi pada beberapa tanah terlalu sulit untuk membedakan antara selaput mengkristal dan illuviasi argillan. Selaput amorf dan terkristal diperkirakan terjadi pada tanah-tanah yang berbahan abu vulkanik di seluruh Indonesia.

INTRODUCTION

A major part of the soils of Java is formed in volcanic products of mainly andesitic character. Depending on rainfall, temperature, and age of the deposit, these soils develop into Ultisols, Alfisols, Oxisols, Inceptisols or Vertisols. In East Java, with a monsoon climate that features a distinct dry season, soils are classified as Oxisols, Ultisols, Alfisols, Vertisols, and Inceptisols. In West Java, without a clearly defined dry season, Vertisols and Alfisols are not found.

Because micromorphological analyses of Indonesian soils are still scarce, recognition of the argillic

horizon is mainly based on textural discontinuities and, consequently, the classification of many soils, especially those on stratified volcanic deposits, is still open to discussion.

The exploratory soil map of West Java (Lembaga Penelitian Tanah, 1974) indicates, in the area between Bogor and Jakarta, an association of Red Latosols and Reddish Brown Latosols. Subardja and Burman (1980) classified these soils as Eutrothox and Dystropepts, and this classification was corroborated by investigations of Nanere *et al.* (1982).

In 1980, several profiles of the catena described by Subardja and Burman (1980) were collected for display in the International Soil Museum (now International Soil Reference and Information Centre = ISRIC) at Wageningen, the Netherlands. These soils were resampled and thin sections of various horizons were prepared. Micromorphological analysis was first carried out by Astiana (1982), who described argillans in the lowland member of the catena. This would have required a reconsideration of the classification of this profile. Upon reexamination, these coatings were completely different from the classic illuviation argillans of layer lattice clays that are prerequisite to the argillic horizon. Part of the clay coatings was isotropic, and this is very unusual for tropical lowland soils.

These findings merited further elaboration. The profile was restudied completely, and its micromorphology is reported here. Amorphous coatings and related features that occur in this profile were also encountered in other Indonesian catenas on andesitic rocks. To put the findings of the West Java profile in its proper context, the relevant information on these catenas is presented as well.

¹ Both are Soil Scientists of the Department of Soil Science and Geology, Agricultural University, Wageningen, the Netherlands. Present address of the first author is at Center for Soil Research, Bogor, Indonesia.

MATERIAL**The profile**

The profile investigated is Profile P2 of Subardja and Buurman (1980), and is registered as INS 1 at the ISRIC. The abbreviated profile description is as follows:

- Profile number : P2 (Subardja and Buurman, 1980); INS 1 (ISRIC, Wageningen monolith)
- Location : Parung, West Java, Indonesia; 6°23'10" S and 106°32'15" E
- Morphology : Dissected alluvial fan
- Parent material : Andesitic volcanic tuff
- Elevation : 140 m
- Mean annual temperature : 26°C
- Mean annual precipitation : 2600 mm
- Landuse : Former irrigated rice field, now cultivated with bananas
- Drainage class : Well drained
- Short description :

- Apl 0-23 cm : Brown to dark brown (7.5 YR 4/4, moist) clay; strong very fine granular structure; many pores, friable to firm when moist; slightly sticky and slightly plastic when wet; common fine roots; abrupt and smooth to:
- Apg 23-51 cm : Brown to dark brown (7.5 YR 4/4, moist) clay; weak angular blocky structure; common to many fine and very fine pores; firm when moist, slightly sticky and slightly plastic when wet; many distinct fine iron mottles (7.5 YR 5/8) and common fine black manganese mottles. At contact with Ap1 manganese and iron segregations along root channels; clear and smooth to:
- Bwg 51-78 cm : Yellowish red (5 YR 4/6, moist), clay; weak subangular blocky structure; many fine and very fine pores; friable when moist;

many prominent medium irregular black manganese mottles along pores and peds; gradual and smooth to:

- Bw 78-150 cm : Yellowish red and yellowish brown (5 YR 4/6 and 10 YR 5/6, moist) clay; weak subangular blocky structure; many fine and very fine pores; very friable when moist; few faint fine manganese mottles, decreasing with depth (sampled 78-100 and 100-150 cm).
- Classification : (USDA; Soil Survey Staff, 1975): Typic Eutrorthox, very fine clayey, halloysitic, isohyperthermic (FAO, 1974): Orthic Ferralsol (Indonesia; Suhardjo and Soepraptohardjo, 1981): Oksisol Eutrik.

RESULTS**Chemical and mineralogical properties**

Chemical and mineralogical data of Profile INS 1 are provided in Tables 1 and 2. Because the soil was formerly used for irrigated rice cultivation, it has a distinct iron manganese pan at the bottom of the puddled zone. Organic matter content in the topsoil is low, while clay content is extremely high. On the other hand water dispersible clay which is characteristic for Oxisols, is very low. Cation exchange capacity (CEC)-clay in the subsoil is low enough to qualify for an oxic horizon, and so are other exchange properties of the Bw horizon. The sand fraction of these horizons amounts to only 1% and therefore its considerable content of weatherable minerals should not interfere with the denomination *oxic*. Soil reaction (pH) in NaF indicates an increasing reactivity with depth, but oxalate-extractable Al and Si indicate that the total amount of amorphous matter is fairly low. (In Andosols of the same catena, the sum of oxalate-extractable matter may amount to more than 9%). The plowpan is clearly indicated by a high amount of extractable Mn.

Table 1. Chemical characteristics of profile INS 1

Soil characteristics	Ap	Apg	Bwg	Bw1	Bw2
pH					
H ₂ O	5.1	5.0	5.3	5.3	5.4
KCl	4.0	4.2	4.4	4.4	4.5
NaF 1	8.5	9.1	9.4	9.5	9.6
NaF 60	9.6	9.8	10.1	10.1	10.2
Texture					
sand (%)	1.0	1.2	1.2	1.1	1.0
clay (%)	85.7	91.2	88.4	89.8	89.3
WDC (%)	10	2	2	2	0
Exchangeable					
bases (me/100 g soil)	6.0	6.2	6.2	6.2	6.8
Al (me/100 g soil)	0.8	0.2	0.1	0.1	0.0
H (me/100 g soil)	1.4	0.6	0.1	0.1	0.3
CEC soil					
PC (me/100 g soil)	6.8	6.4	6.3	6.5	6.8
NH ₄ Cl (me/100 g soil)	9.3	8.8	10.3	8.2	9.0
CEC7 (me/100 g soil)	18.1	15.6	16.0	13.6	14.0
CECS (me/100 g soil)	22.8	20.6	20.6	19.8	19.0
CEC clay					
PC (me/100 g clay)	8	7	7	7	8
pH7 (me/100 g clay)	21	17	18	15	16
Base saturation					
CEC7 (%)	33	40	39	47	49
PC (%)	88	97	99	99	99
Dithionite and oxalate extractable matter					
Fe _d (%)	6.06	5.76	6.29	6.31	6.69
Al _d (%)	0.80	0.77	0.86	0.80	0.75
Si _d (%)	0.18	0.21	0.21	0.19	0.24
Mn _d (%)	0.33	1.14	0.23	0.21	0.21
Fe _o (%)	0.54	0.46	0.38	0.39	0.39
Al _o (%)	0.33	0.31	0.31	0.32	0.28
Si _o (%)	0.02	0.11	0.21	0.13	0.15
Bulk density					
dry (g/cm ³)	0.95	0.93	—	0.86	—
1/3 bar (g/cm ³)	1.23	1.27	—	1.17	—
Organic C (kg/m ³)	8.3				

WDC = water dispersible clay; PC = permanent charge (bases + Al); CEC7 = CEC in NH₄OAc at pH7; CECS = CEC by sum of cations (BaCl₂, pH 8.2); Al and H in 1M KCl.

d = dithionite; o = oxalate.

The mineralogical analysis of the sand fraction (Table 2) indicates that the parent material is almost purely andesitic, but consists of several strata. The clay fraction is dominated by halloysite, but the diffractograms show a distinct reflection at 1.2 nm, which can be attributed to stacking in allophane (Van der Gaast, *et al.*, 1985).

Micromorphology

Micromorphological features have been summarized in Table 3.

Skeleton grains: are mainly quartz and volcanic glass. Quartz is angular, 50-100 microns; volcanic glass is spherical or irregular, sometimes vesicular, 20-200 microns, and most abundant in upper horizons. Other primary minerals are augite, hypersthene, and plagioclase, all strongly weathered and angular, 50-200 microns. Some basaltic fragments, consisting of glass with small plagioclase phenocrysts are encountered. Of secondary origin are subrounded sharply bounded gibbsite nodules (20-200 microns). **Plasma:** mainly consists of clay, with fair amounts of organic matter in the topsoil and high contents of iron in the lower parts of the profile. The plasmic fabric is undulic, but sepic fabrics are regularly encountered throughout the profile (lattiseptic, glaesepic, omni-sepic).

Voids: are mainly biogenic and of sizes between 50 microns and several millimeters: compound packing voids, interconnected vughs and channels. In the plowpan, craze and skew planes are a common feature.

Special features:

A. Oriented clay:

Type a. Yellow, birefringent clay coatings with a continuous orientation pattern, but without stratification (Figure 1 c-f), are common in sections 1808 and 1807. They occur in recent biogenic voids and have a thickness of 20-50 microns. Papules derived from these cutans are extremely rare but occur in section 1806.

Type b. Yellow, partially birefringent, partially isotropic clay coatings without stratification (Figure 1 a, b), are common in section 1808. Birefringent parts of these coatings have a continuous orientation pattern and are fully comparable to type a cutans. Type b cutans, 20-50 microns thick also occur in recent biogenic voids; derived papules were not encountered.

Type c. Clay papules up to 200 microns in diameter, shaped like the volcanic glass fragments. Such papules are birefringent, yellow, and have a strong continuous orientation pattern. They are

Table 2. Mineralogical composition of the sand and clay fractions of profile INS 1

Horizon	Sand fraction													Clay fraction							
	Total fraction										Heavy fraction								Light fraction		
	opaque quartz	iron concr	min. fragm.	rockfragm.	volcanic glass	plagioclase	augite	hypersthene	others	opaque	augite	hypersthene	zircon	quartz	volcanic glass	lebradorite	halloysite	allophane 1.2 nm	goethite	quartz	
Ap	20	15	18	7	3	15	4	1	16	1	12	16	72	-	57	17	26	+++	++	+	(+)
Apg	16	15	29	7	5	10	6	-	12	-	29	6	65	-	63	18	19	+++	++	+	(+)
Bwg	33	11	27	8	3	7	1	1	8	1	45	15	40	-	65	18	17	+++	++	+	(+)
Bw1	58	12	21	4	2	-	-	-	1	2	80	2	17	1	76	14	10	+++	++	+	(+)
Bw2	36	11	39	9	3	-	-	-	1	1	78	1	15	6	90	6	4	+++	++	+	(+)

- +++ abundant
- ++ common
- + present
- (+) traces

Table 3. Some micromorphological observations of profile P2 (INS 1)

Depth (cm)	0	10	20	30	40	50	60	70	80	90
Horizon	Apl		Ap2			Bwg			Bw	
Sample	1806		1808			1807			1809	
Skeleton grains										
- volcanic glass	-----									
- hypersthene/augite	-----									
- plagioclase	-----									
- quartz	-----									
Plasma										
- undulic plasmic fabric	-----									
- in- latti- glae- omni sepic plasmic fabric	-----									
- clay minerals, iron and org. matter	-----									
- clay minerals and much iron	-----									
Voids										
- biogenic: (compound packing voids interconnected vughs)	-----									
- physiogenic: (craze/skew planes, vughs)	-----									
Special features										
- yellow strongly birefringent clay coatings	-----									
- yellow, partially birefringent partly isotropic clay coatings	-----									
- normal void neo mangans	-----									
- manganiferous nodules, irregular	-----									
- normal void neo ferrans	-----									
- ferric nodules, irregular	-----									
- matric faecal pellets	-----									

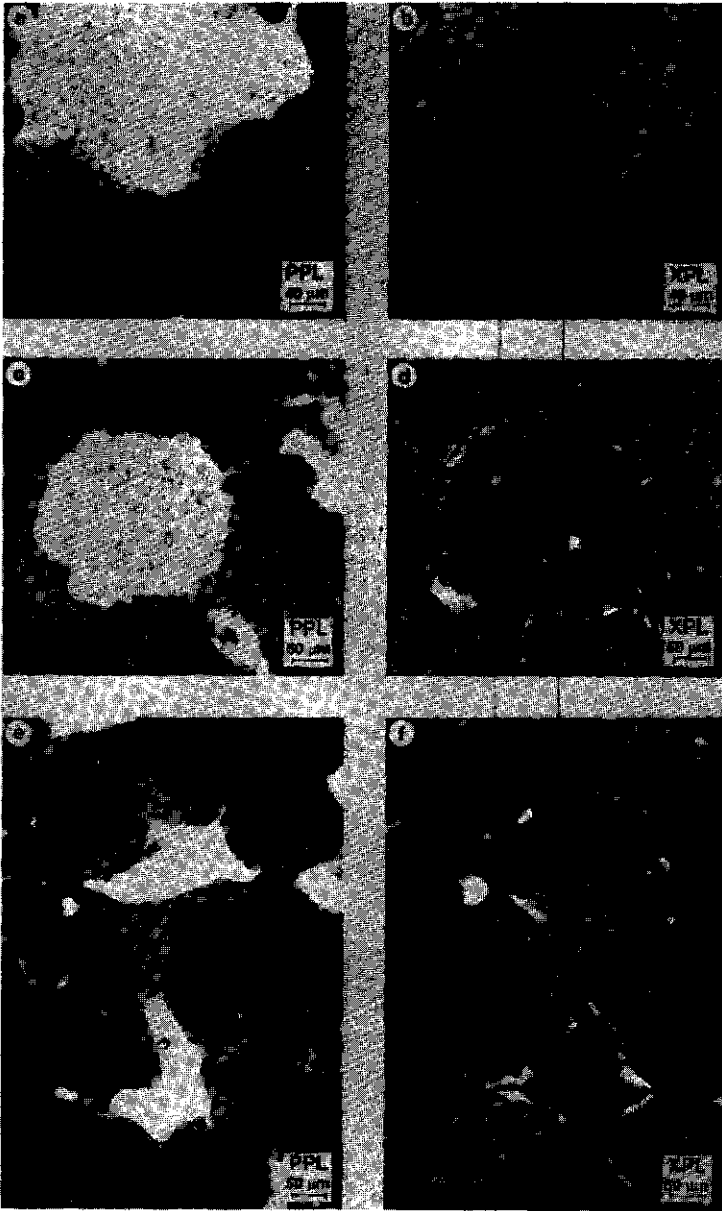


Figure 1. Thin sections of isotropic and birefringent coatings.
a/b : nearly amorphous coating. Section 1807, plain light/crossed polarizers.
c/d : yellow birefringent type a coating with discontinuous orientation pattern. Section 1808, plain light/crossed polarizers.
e/f : yellow birefringent type a coating with continuous orientation pattern. Section 1807, plain light/crossed polarizers.

derived from colourless, isotropic volcanic glass through intermediary pale yellow forms with weak, local birefringence. Type c papules are not stratified. They are not common in the present profile, but abundant in profiles in higher parts of the catena. The papules are very similar to type a cutans but are not at all related.

B. Iron and manganese segregations:

Type d. Normal void neomangans are abundant in the lower part of section 1808, common in the upper part of 1807, and scarce in the upper part of 1809.

Type e. Manganiferous nodules are common in the lower part of section 1808, scarce in the upper part, and sporadic in 1809.

Type f. Normal void neoferrans are abundant in the upper part 1808, scarce in the lower part and in 1807.

Type g. Ferric nodules (sharp, irregular) are common in sections 1807 and 1808, scarce in 1809.

C. Structures related to biological activity:

Type h. Matric faecal pellets (20-200 microns) are abundant throughout the profile except the plowpan.

Interpretation of micromorphological features

Distribution of skeleton grains and their degree of weathering indicate rejuvenation of the profile, probably with airborne volcanic material which was incorporated in the profile by strong biological mixing. This is corroborated by the trend with depth of weatherable minerals and volcanic glass. Part of the volcanic glass fraction and the basaltic fragments shows a pseudomorphosis to birefringent clay papules.

The amount of clay plasma is very large and the occurrence of sepic fabrics points to a dominance of crystalline clay minerals. The overall presence of undulic fabrics is probably due to masking of clay birefringence by the fairly large amount of iron compounds (Brewer, 1964). Shape of voids and abundance of matric faecal pellets point to a high biological

activity, which is somewhat suppressed in the former plowpan.

Cutans of types a and b are genetically similar, because in type b isotropic parts and strongly and continuously birefringent parts occur within one cutan. In one-way polarized light, the two types of cutans are completely similar. Isotropism points to amorphous material, while birefringence points to crystallinity and orientation. Obviously, crystallization occurs after formation of the cutans. As crystallinity is better in the Ap2 than in the lower horizons, it is probably related to periodic desiccation and slightly more elevated temperatures. Electron microscopic (EDAX) analyses of the cutans (Table 4) corroborate the chemical similarity of type a and b coatings and indicate that their composition is within the normal range for allophane. Similar coatings are common in higher members of the catena (Buurman *et al.*, in preparation). Because the allophane tends to crystallize into halloysite in these soils on andesitic material, the crystalline, birefringent coatings are probably halloysitic. Halloysite coatings found by Cady (1965) were not birefringent, but this is not necessarily applicable to halloysite formed through crystallization of allophane. The formation of allophanic coatings and their recrystallization are clearly recent processes: the coatings occur in recent voids, and the absence of papules indicates that very little reworking has taken place.

The iron and manganese segregations are typically related to former use of the land for irrigated rice cultivation. The typical distribution of iron with respect to manganese points to pseudogley (artificial ponding), and manganese segregations are found deeper in the oxidized subsoil than are iron segregations.

Table 4. EDAX analyses of isotropic and birefringent coatings (7-10 analyses per sample)

Sample	Al ₂ O ₃	SiO ₂	Fe ₂ O ₃	Al/Si (atomic)
A	33.0 ± 1.7	52.7 ± 2.7	14.2 ± 1.9	0.91
B	36.8 ± 1.4	50.6 ± 1.1	12.4 ± 2.4	0.86
C	38.1 ± 1.2	52.7 ± 0.7	9.0 ± 0.8	0.85

A = isotropic coating similar to Fig. 1. a/b.

B = birefringent coating similar to Fig. 1. c/d.

C = birefringent coating similar to Fig. 1. e/f.

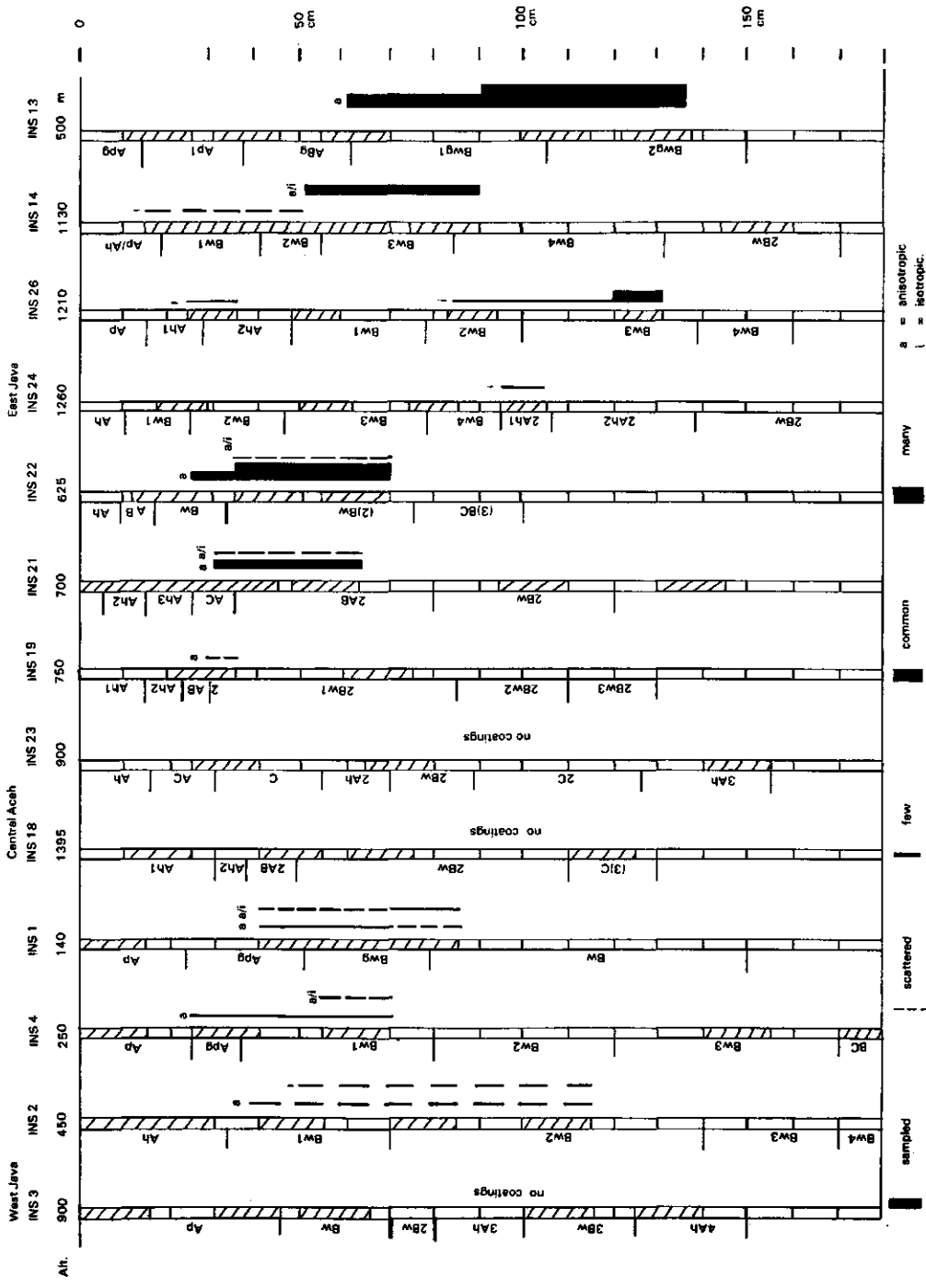


Figure 2. Distribution of isotropic and anisotropic coatings in profiles of three catenas

Data from other catenas

The profiles investigated are given in Table 5. The Central Aceh profiles are from the Geureudong volcanic complex; the West Java profiles from the Gede/Pangrango system; and the East Java profiles from the surroundings of Malang. Details on stratification and horizon sequence can be deduced from Figure 2. The profiles INS 1 through 3 are equivalent to the numbers P2, P5, and P8 of Subardja and Buurman (1980). Complete descriptions and analyses of all these profiles will appear in a complete publication on the three catenas, (Buurman *et al.* in preparation). They are not necessary for the present purpose.

Table 5. Profiles of the West Java, Central Aceh and East Java catenas

Profile	Altitude	Annual rainfall	Classification	Area
	m	mm		
INS 1	140	2600	Typic Eutrochox	West Java
INS 2	450	4400	Typic Humitropept	West Java
INS 3	900	3350	Andic Humitropept	West Java
INS 4	250	3800	Oxic Dystrypept	West Java
INS 18	1395	1800	Typic Hydrandept	Central Aceh
INS 19	750	2200	(Andic) Oxic Humitropept	Central Aceh
INS 21	700	2600	Typic Hydrandept	Central Aceh
INS 22	625	2200	Oxic Dystrypept or Orthoxic Tropudult	Central Aceh
INS 23	900	2600	Typic Hydrandept	Central Aceh
INS 13	500	1700	Anthraquic Hapludoll or Typic Argiudoll	East Java
INS 14	1130	2350	(Cumulic) Andic Eutropept	East Java
INS 24	1260	2300	Hydic Dystrandep	East Java
INS 25	50	1125	Vertisol	East Java
INS 26	1210	2200	Andic Humitropept	East Java

In these soils, the amorphous coatings and (partly) birefringent coatings occur in varying amounts, depths and altitudes. A compilation is given in Figure 2.

Due to partial sampling for micromorphology, information on all these soils is incomplete. However, some trends are obvious:

1. Cutans are more common in the Aceh and East Java catenas than in the West Java catena;
2. Isotropic cutans are more common in the deeper part of the profiles;
3. In the Aceh catena, the coatings are nearly restricted to buried soil horizons, but are also found in overlying nearly fresh ash (Bw of INS 22);
4. Anisotropic coatings are most abundant in the East Java catena; the isotropic coatings here are found above the anisotropic ones;
5. In all catenas, there is a tendency for coatings to become more abundant at lower altitudes, although there are strong differences between catenas. Coatings are lacking altogether in some of the higher members of the West Java and Aceh catenas.

An additional observation is that amorphous coatings are frequent in pores (vesicles) in fragments of weathered volcanic glass, both in the saprolite and in other parts of profiles.

In profiles INS 13 and INS 14 of the East Java catena, organomatri-ferriargillans are common to abundant. These coatings, are due to instability of surface structure (slaking). Slaking may occur when strongly dried-out soils are suddenly wetted, e.g. by rain or irrigation water.

DISCUSSION

The crystallized parts of the clay coatings found in these soils (type a) are easily confused with argillans that are due to layer lattice clay illuviation, and are distinguished mainly by their lack of stratification. As far as they are associated with (partly) isotropic coatings, they are certainly not due to illuviation of crystalline clay and should therefore not be regarded as argillans.

The coatings have probably formed by precipitation of allophanic material from the soil solution and the precipitation of allophane in these soils is probably comparable to that of allophanic coatings in andosols and that of (proto) imogolite and allophane in brown soils and podzols (e.g. Farmer *et al.*, 1985). Similar isotropic coatings were described by Dalrymple (1964, 1967) in fossil andosols of New Zealand; birefringent coatings were described by Pain (1971) and by Chartres *et al.*, 1985) from volcanic soils in Papua New Guinea. None of these authors, however, attributed the coatings to allophane and its crystallization products.

Formation of isotropic coatings is clearly an actual process, as these coatings may be found close to the surface as well as in deeper parts of the profile. The extent of crystallization will depend on a number of external factors which cannot be properly asserted as yet. Desiccation may play an important role.

Climates are rather different for the three catenas and for profiles within one catena and, therefore, part of the differences should probably be attributed to this factor. In the lower part of the East Java catena, evaporation exceeds precipitation even on a yearly basis, which implies a very distinct dry season. On the contrary, the higher soils of the West Java catena are under a perhumid moisture regime and the soil does not dry out in normal years. The Central Aceh catena is in an intermediate position, with its upper members probably perhumid. Thixotropy in this catena clearly illustrates that the soils, except at lesser altitudes, do not normally dry out completely.

Coatings are not found in the highest members of the West Java and Central Aceh catenas, which might be due to the strong leaching and perhumid moisture regime of these profiles.

Figure 2 suggests that coatings become more abundant in soils which suffer a more pronounced dry season and that crystallinity increases with the severity of this season.

In INS 1 and other strongly weathered profiles, weathering of volcanic glass and other airborne volcanic material is the probable source for sufficiently high concentrations of silica and aluminum. The total amount of oxalate-extractable material in these soils is low and almost constant with depth, but its crystallization towards the top of the profile is accompanied by a decrease of pH in NaF.

In the soils that have high amounts of volcanic glass and feldspars, the source of allophanic matter is obviously this primary material.

Because isotropic coatings are very scarce in profiles of the East Java catena, attribution of the birefringent coatings in INS 13 and 14 of this catena to crystallization of amorphous material cannot be proven. Nevertheless, this possibility deserves serious consideration.

It is remarkable that in INS 1, the horizon with oxyc properties has the highest pH in NaF and the lowest bulk density. Nevertheless, the amount of

amorphous material is not sufficient to seriously influence soil properties or change its classification.

CONCLUSION

The formation of amorphous coatings is apparently an active process. It can be expected, therefore, that many lowland soils, in and outside Java, that have recent additions of volcanic ash, will show amorphous and recrystallized coatings as described above. This once more emphasizes the problem of identifying the argillic horizon in soils influenced by volcanic material.

ACKNOWLEDGEMENTS

The authors thank the International Soil Information and Reference Centre (ISRIC), Wageningen, for permission to use thin sections and analytical data. EDAX analyses were carried out by Dr. A. Boekestein of the Technical and Physical Research Service (TFDL), Wageningen. Ir. Hidayat Wiranegara of the Bogor Agricultural University (IPB) assisted in collecting the West Java profiles.

REFERENCES

- Astana. 1982. Micromorphological and Mineralogical Study of a Toposequence of Latosols on Volcanic Rocks in the Bogor-Jakarta Area (Indonesia). M.Sc thesis, Ghent.
- Buurman, P., A.G. Jongmans, L.P. Van Reeuwijk, and J. Tersteeg (in preparation). Three catenas on andesitic rocks from Indonesia. ISRIC, Wageningen, the Netherlands.
- Brewer, R. 1964. Fabric and Mineral Analysis of Soils. Wiley, New York.
- Cady, J.G. 1965. Petrographic microscope techniques. In C.A. Black (ed). Methods of Soils Analysis, 1: 604-631. American Society of Agronomy, Madison.
- Chartres, C.J., A. Wood, and C.F. Pain. 1985. The development of micromorphological features in relation to some mineralogical and chemical properties of volcanic ash soils in highland Papua New Guinea. Australian Journal of Soil Research 23: 339-354.
- Dalrymple, J.B. 1964. The application of soil micromorphology to the recognition and interpretation of fossil soils in volcanic ash deposits from the North Island, New Zealand, p. 339-349. In A. Jongerius (ed). Soil Micromorphology. Elsevier, Amsterdam.
- Dalrymple, J.B. 1967. A study of paleosols in volcanic ash-fall deposits from northern North Island, New Zealand, and the evaluation of soil micromorphology for establishing their stratigraphic correlation, p. 104-122. In R.B. Morrison and H.E. Wright (eds). Quaternary Soils.
- FAO. 1974. Soil Map of the World. Volume I, Legend. FAO. Rome.
- Farmer, V.C., W.J. McHardy, R. Robertson, A. Walker, and M.J. Wilson. 1985. Micromorphology and sub-microscopy of allophane and imogolite in a podzol horizon; evidence for translocation and origin. Journal of Soil Science 36: 87-95.

- Lembaga Penelitian Tanah.** 1974. Exploratory Soil Map of West Java at scale 1 : 250.000.
- Nanere, J.L., N.T. Livesey, E.A. Fitzpatrick, and J. Tinsley.** 1982. Some features affecting the classification of the Red Soils of Indonesia. Transactions 12th International Congress of Soil Science 6: 152.
- Pain, C.F.** 1971. Micromorphology of soils developed from volcanic ash and river alluvium in the Kokode Valley, Northern District, Papua. Journal of Soil Science 22: 275-280.
- Soil Survey Staff.** 1975. Soil Taxonomy. A basic system of soil classification for making and interpreting soil surveys. USDA Handbook No. 436.
- Subardja, and P. Buurman.** 1980. A toposequence of letosols on volcanic rocks in the Bogor-Jakarta area. In P. Buurman (ed): Red Soils in Indonesia, Agricultural Research Reports 889: 15-22, PUDOC, Wageningen.
- Suhardjo, H., and M. Soeprahardjo.** 1981. Jenis dan macam tanah di Indonesia untuk keperluan survei dan pemetaan tanah daerah transmigrasi. Pusat Penelitian Tanah Bogor, No. 28/1981.
- Van Der Gaast, S.J., K. Wada, S.I. Wada, and Y. Kakuto.** 1985. Small-angle X-ray powder diffraction, morphology, and structure of allophane and imogolite. Clays and Clay Minerals 33: 237-243.

4.2 Identification of clay coatings in an old Quaternary terrace of the Allier, Limagne, France

Soil Sci. Soc. Am. J. 53: 876-882.

T.C.J. Feijtel, A.G. Jongmans, and J.D.J. van Doesburg.

Identification of Clay Coatings in an Older Quaternary Terrace of the Allier, Limagne, France

T. C. Feijtel,* A. G. Jongmans, and J. D. J. van Doesburg

ABSTRACT

Micromorphologically three types of coatings were observed in B horizons of two planosol profiles (Albaqualis): (a) nonlaminated isotropic limp clay coatings, (b) nonlaminated anisotropic limp clay coatings, and (c) microlaminated anisotropic dusty clay coatings. Micromorphological observations suggested that coating types (a) and (b) were genetically similar, resulting from weathering and neoformation. Coating type (c) originated from clay illuviation. Elemental compositions of clay coatings were obtained with a scanning electron microscope-energy dispersive x-ray analyzer technique. Alumina contents decreased from 38% in isotropic coatings to about 28% in illuviation coatings. The Al content was inversely related to contents of K, Mg, Ca, and Fe. Factor analysis indicated that two factors accounted for 56.5 and 22.8% of the total elemental variance. The first factor associated with coating type revealed the antithetic behavior of Al vs. K, Mg, Ca, and Fe, and accounted for about 90% in the variability of Al. The second factor associated with the sample location explained >70% of the variability in Ti and Si. Chemical classification of investigated samples was based on elemental similarity. Cluster analysis revealed that coatings of the same type were more alike than coatings originating from the same profile. About 83% of grouped samples were classified correctly as isotropic and anisotropic weathering coatings, and anisotropic illuviation coatings. Clay minerals associated with individual coatings were identified with an x-ray step-scan method after sampling microquantities of these coatings with a microdrill. Anisotropic illuviation and weathering coatings consisted of illite and kaolinite. Anisotropic weathering coatings, however, were found to contain less illite than illuviation coatings. Isotropic coatings were x-ray amorphous, suggesting the presence of Al-Fe-Si gel.

MICROMORPHOLOGICAL STUDIES of soils developed on volcanic substrates have indicated that noncrystalline materials are important constituents (e.g., Eggleton, 1987; Buurman and Jongmans, 1987; Feijtel et al., 1988). The noncrystalline material generally resulted in undifferentiated b-fabrics, exhibiting isotropic characteristics (Bullock et al., 1985). Chartres et al. (1985) reported that the isotropic nature of the plasma in an andesitic tephra can be attributed to allophane associated with organic matter. Allophane is abundant in soils formed from weathered basic volcanic rocks and represents an early stage in the transition from primary minerals to clay minerals (Colman, 1982; Lowe, 1986; Chartres, 1987; Buurman and Jongmans, 1987). Eggleton (1987) demonstrated that clay minerals may also crystallize from noncrystalline precursors, such as Fe-Si-Al oxyhydroxides.

The chemical changes accompanying basalt weathering in temperate climates have received little attention (Colman, 1982; Chartres et al., 1985), especially with reference to the formation of weathering prod-

ucts. The goal of this study was to characterize the properties of some neoformed features in sediments of the Allier. Field observations in two planosols developed in gravelly quaternary sediments of the river Allier, Massif Central, France indicated an increasing alteration of volcanic and granitic fragments with decreasing depths in both profiles (Feijtel et al., 1988). Three types of coating could be identified micromorphologically. The B horizons showed evidence of neoformation of clay as firstly, nonlaminated isotropic, and secondly, anisotropic limped clay coatings. Thirdly, the presence of microlaminated anisotropic dusty clay coatings indicated the occurrence of clay illuviation (Feijtel et al., 1988). The hypothesis that the three coating types differed chemically and mineralogically was tested.

MATERIALS AND METHODS

Samples were taken from two Planosol profiles (Albaqualis) of one terrace of the Allier, Massif Central, France. Profiles are referred to as Croix-Mozat and Bulhon (Fig. 1). Feijtel et al. (1988) discussed the pedogenesis of Planosols in the Croix-Mozat and Mons profiles, located on two Allier terraces differing in altitude and age. In this study duplicate profiles from one terrace are used to test variability of investigated pedofeatures within and between profiles.

Particle-size analyses were performed after destruction of the organic matter with H_2O_2 and removal of any carbonates with 0.2 M HCl. Fractions >50 μm were collected by sieving after 4 h of shaking. Fractions <50 μm were determined with the pipette method after addition of $Na_3P_2O_7$ and Na_2CO_3 . Total chemical analyses were performed on clay fractions, collected with the pipette method, and fine earth fractions (<2 mm). Analyses of major and minor elements were made by x-ray fluorescence on $Li_2B_4O_7$ glass disks.

Soil pH (1:2.5 in water and 0.01 M $CaCl_2$) was determined by glass electrode; "free" Fe_2O_3 was extracted by Na-dithionite-EDTA at pH 4.5 (Begheijn, 1980); exchangeable bases and cation exchange capacity (CEC) by Li-EDTA (Begheijn, 1980).

Thin sections (8 by 15 cm) of Bt horizons were prepared following the method of Fitzpatrick (1970) and described following the terminology of Bullock et al. (1985). Quantitative micromorphological estimates by point counting were based on counting of 800 points, ignoring the fraction <15 μm and voids (van der Plas and Tobi, 1965). After microscopic examination of thin sections, textural pedofeatures were classified. In situ microchemical analysis on uncovered polished thin sections (5 by 3 cm) was performed with a Philips scanning electron microscope-energy dispersive x-ray analyzer (SEM-EDXRA) (Philips, Eindhoven, Netherlands). Multiple spot analyses on four isotropic and four anisotropic weathering coatings, and seven anisotropic illuviation coatings were made. In each coating the SiO_2 , Al_2O_3 , TiO_2 , Fe_2O_3 , MgO , CaO , K_2O , and Na_2O content was determined by EDXRA. Elemental composition was used as a possible indicator of discriminating differences between each type of coating.

Isolation of microquantities (<3 μg) of in situ coatings in uncovered thin sections was performed with a microscope-mounted drill (Verschuren, 1978). The instrument consists

Dep. of Soil Science and Geology, Agric. Univ. Wageningen, P.O. Box 37, 6700 AA Wageningen, The Netherlands. Contribution from the Dep. of Soil Science and Geology, Agric. Univ. Wageningen, Publication no. 1022. Received 1 July 1988. *Corresponding author.

Published in Soil Sci. Soc. Am. J. 53:876-882 (1989).

of an optical and a mechanical part that can both be attached to a polarization microscope. Microquantities of material were collected using a hardened stainless steel needle sharpened to 50 μm in the microdrill (Verschuren, 1978). Microdrilling was carried out in a small drop of distilled water, to limit the loss of material caused by rotation of the needle (Beaufort et al., 1983). After inverting the thin section with the droplet containing the suspended material, it was placed in contact with a clean glass slide. Due to adhesion the droplet was transferred to the glass slide (Beaufort et al., 1983). After ultrasonic dispersion of the extracted material, oriented specimen were obtained by drying at ambient conditions.

The x-ray diffraction patterns were obtained by a step-scan method (Meunier and Velde, 1982). The glass slide with sample was placed in the goniometer holder of a Philips PW1050-PW1710 diffractometer equipped with a graphite monochromator. Cobalt-K α radiation at 40 mA and 45 kV was used (0.5° divergence slit, 0.2 mm receiving slit, and 1° scatter slit). Step scanning was performed with steps of 0.05° 2 θ and counted for three times for 100 s. On well-dispersed standard clay samples, amounts of 0.04 μg kaolinite, 0.06 μg illite, and 0.5 μg montmorillonite were sufficient for mineralogical identification.

Statistical analyses were carried out with SPSS, Inc. (1986). The micromorphological coating type and the profile pit where the coating was encountered contribute to the variability in chemical composition of these coatings. Chemical variability of micromorphologically similar coatings was tested within profile location through the use of a nested design. Sampling locations were treated as covariates in the statistical analyses. In order to group elements, a factor analysis was used to reduce the number of variables and problems due to multicollinearity. This method produces a set of principal components, which maintains most of the information about the variation in the original data. A cluster analysis was carried out in order to group the investigated clay coatings on the basis of their chemical properties.

RESULTS AND DISCUSSION

Macromorphological, Mineralogical, and Chemical Soil Characteristics

A brief description of macromorphological properties and quantification of single and compound mineral grains of Bulhon and Croix-Mozat is given in Table 1. Numerous volcanic fragments in B horizons exhibited a clear patina of variable thickness and could be crushed by hand. Rubbing of the sandy material from Btg3 horizon of the Bulhon profile resulted in finer textures. The macromorphological characteristics provide evidence of weathering, predominantly of volcanic fragments in both profiles.

In both profiles kaolinite was the dominant clay mineral with lesser amounts of illite. Smectite contents were very low in the upper solum, and increased with increasing depth. X-ray diffraction patterns showed limited peak sharpness, suggesting a low crystallinity of smectite, especially in the eluviated highly weathered horizons. Chlorites and vermiculite, present in small amounts in the A and E horizons, were absent in underlying B horizons.

Both soils were medium to slightly acid. Base saturation was high reaching 100% at depth in the Bulhon profile and close to maximum throughout the Croix-Mozat profile. The latter was influenced by agricultural land use. Cation exchange capacity attained its maximum in Btg horizons (Table 2). The chemical composition of the fine earth and clay fractions are given in Table 3. The chemical composition of the fine earth fraction indicated a relative enrichment in SiO $_2$ in respect to Al $_2$ O $_3$, CaO, MgO, and Na $_2$ O in A and E horizons. Both profiles exhibited an increase in

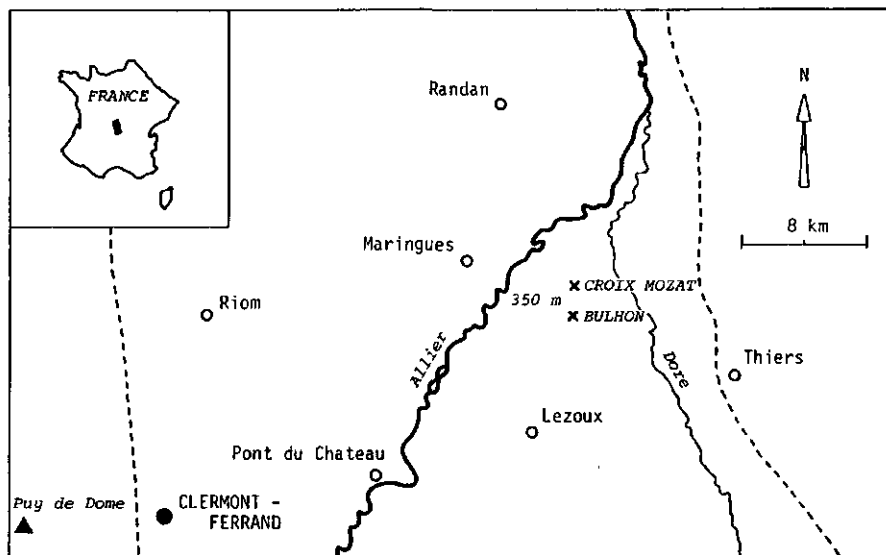


Fig. 1. Location of sampling sites in the Limagne Rift Valley. ---- represents limits of the Limagne Rift Valley, x shows sampling site.

Table 1. Major macromorphological properties of both profiles, and quantification of single and compound mineral grains.†

Horizon	Depth, cm	Color moist	Structure	Consistence moist	Quantification, vol%	
					Quartz	Volcanic fragments
Croix-Mozat						
Ap	0-28	10YR 4/2	0 m	mfi	61	4‡
Eg	28-40	10YR 5/2	0 m	ND	40	17
Btg1	40-60	5Y 5/1	2 vc pr	mefi	32	30
Btg2	60-80	5Y 5/1	1 vc pr	mefi	ND	ND
Btg3	82-84	5Y 5/1	0 m	mfi	ND	ND
Btg4	>84	10YR 3/3	0 m	ND	14	51
Bulhon						
Ahg	0-15	2.5Y 4/2	1 m sbk	mfr	72	2
Eg	15-30	2.5Y 5/2	0 m	mfr	ND	ND
Btg1	30-80	2.5Y 5/2	1 vc pr	mefi	66	2
Btg2	80-100	2.5Y 5/3	1 vc pr	mfi	35	24
Btg3	>100	10YR 3/3	0 m	mfr	32	27

† Abbreviations used as in Soil Survey Staff, 1951, p. 139. ND = not determined.

‡ Strongly Fe impregnated.

Table 2. Selected physical and chemical properties of Croix-Mozat and Bulhon.

Horizon	Depth cm	Clay	Silt	Sand	Gravel	pH _w	Organic C	Extr-Fe	CEC	% base saturation
		% of fine earth			% of total		%	%	mmol kg ⁻¹	
Croix-Mozat										
Ah	0-28	18.8	13.8	67.4	31.0	6.35	0.94	3.1	61	100
Eg	28-40	7.4	14.8	77.8	46.0	6.44	0.14	5.4	58	96
Btg1	40-60	30.9	10.5	58.6	9.5	6.48	0.16	3.6	163	100
Btg2	60-80	25.0	13.6	61.4	8.0	6.23	0.21	3.5	143	99
Btg3	80-84	26.2	7.0	66.9	14.0	6.04	0.18	2.5	144	99
Bt	84-110	16.8	9.7	73.5	7.5	5.99	0.09	3.0	92	100
Bulhon										
Ahg	0-15	10.1	19.6	70.4	10.5	6.36	1.72	0.9	29	40
Eg	15-30	11.2	17.9	70.9	10.5	5.69	0.37	2.0	28	50
Btg1	30-60	18.5	18.5	63.0	13.7	5.83	0.65	3.4	44	67
Btg1	60-80	21.8	10.3	67.9	17.5	5.73	0.14	3.3	107	84
Btg2	80-100	9.7	9.0	81.3	33.0	6.00	0.16	4.1	116	95
Btg2	>100	7.7	5.0	87.3	9.5	6.13	0.10	1.8	70	100

clay content up to about 30% clay in Croix-Mozat (Table 2). The bulk chemical composition of the clay fraction suggested a vertical differentiation due to clay migration and/or alteration. The K, Na, and Ti contents decreased significantly with depth (Table 3). The Si and Al content, however, varied little between horizons.

Micromorphological Characteristics

Micromorphological quantification of volcanic fragments and quartz indicated that volcanic fragments increased with depth. The quartz content showed the inverse relationship with depth (Table 1).

The nonaltered volcanic fragments consisted mainly of basalt containing opaque Fe minerals, distributed in a clustered pattern. Many volcanic fragments, however, lost their original internal fabric, subrounded shapes, and exhibited compressed structures with well expressed b-fabrics. The altered fragments became constituents of the fine material, but still contained opaque Fe mineral in clusters (Feijtel et al., 1988). The degree of alteration of the volcanic fragments decreases with increasing depth. Observed features provided evidence of weathering and a residual enrichment of the quartz content in A and E horizons of both profiles (Table 1).

In both profiles micromorphological features of

weathering and illuviation were observed. Three types of coatings were classified as follows (Fig. 2):

- a. Nonlaminated isotropic limpid clay coatings and infillings up to 500 μm, predominantly occurring in lower B-horizons.
- b. Nonlaminated anisotropic limpid clay coatings and infillings up to 500 μm, present in B horizons.
- c. Microlaminated, parallel, convolute anisotropic dusty clay coatings and infillings up to 800 μm in B horizons.

Observed coatings type (a) and (b) occurred often within one coating, as could be observed with crossed polarized light (Fig. 2). In Plain polarized light, however, the types (a) and (b) are indistinguishable. These observations revealed that type (a) and (b) were genetically identical. The nonlaminated limpid character, the simultaneous presence of coating type (a) and (b) within one coating, and the similar distribution pattern of type (a) and (b) coatings in both profiles suggested that they consist of neoformed clayey material. Isotropism points to amorphous material, while anisotropism points to crystallinity and orientation. The dominant presence of isotropic type (a) coatings in lower B horizons suggested that crystallization occurred after precipitation of material moving in solution or in suspension. Coating types (a) and (b) were originally present on surfaces of all types of mineral

Table 3. Total chemical composition of fine earth and clay fractions.

Horizon	Depth, cm	Total chemical composition (%) of fine earth fraction							
		SiO ₂	Al ₂ O ₃	TiO ₂	Fe ₂ O ₃	MgO	CaO	Na ₂ O	K ₂ O
Croix-Mozat									
Ah	0-28	75.7	9.8	0.58	3.57	0.35	0.31	1.42	3.12
Eg	28-40	70.2	12.3	0.90	6.53	0.44	0.32	1.60	3.24
Btg1	40-60	64.1	17.1	1.06	4.97	0.78	0.66	1.85	3.06
Btg2	60-80	64.0	17.5	0.97	4.62	0.70	0.81	2.58	3.26
Btg3	80-84	64.2	17.2	0.95	3.84	0.75	0.82	2.28	3.20
Bt	84-110	66.5	16.6	0.83	3.78	0.65	0.90	3.11	3.46
Bulhon									
Ahg	0-15	76.4	10.9	0.76	1.31	0.36	0.29	1.41	3.41
Eg	15-30	76.0	11.0	0.76	2.68	0.32	0.30	1.37	3.41
Btg1	30-60	71.8	12.7	0.95	3.86	0.42	0.28	1.38	3.24
Btg1	60-80	68.5	15.8	0.94	4.51	0.80	0.61	2.03	2.90
Btg2	80-100	68.0	14.9	1.11	4.73	0.88	0.91	1.99	2.90
Btg2	>100	74.4	13.4	0.60	2.58	0.50	0.61	2.02	3.27
Horizon	Depth, cm	Total chemical composition (%) of clay fraction							
		SiO ₂	Al ₂ O ₃	TiO ₂	Fe ₂ O ₃	MgO	CaO	Na ₂ O	K ₂ O
Croix-Mozat									
Ah	0-28	48.1	22.3	1.59	8.22	1.26	0.01	0.64	2.65
Eg	28-40	47.6	23.5	1.95	8.92	1.13	0.00	0.67	2.77
Btg1	40-60	46.1	23.9	1.39	9.62	1.16	0.00	0.23	1.49
Btg2	60-80	46.9	24.4	1.25	9.51	1.14	0.00	0.30	1.39
Btg3	80-84	47.4	24.5	1.40	8.44	1.14	0.00	0.27	1.46
Bt	84-110	46.6	24.3	1.13	9.52	1.21	0.00	0.26	1.38
Bulhon									
Ahg	0-15	50.5	24.8	2.16	4.89	1.22	0.00	0.52	2.55
Eg	15-30	49.9	24.9	2.13	5.77	1.13	0.00	0.50	2.48
Btg1	30-60	46.3	23.9	1.96	9.01	0.96	0.00	0.41	2.14
Btg1	60-80	46.4	23.5	1.38	9.08	1.24	0.00	0.16	1.42
Btg2	80-100	48.5	21.7	1.30	9.22	1.10	0.00	0.16	1.19
Btg2	>100	46.7	24.1	1.16	8.39	1.30	0.00	0.15	1.47

grains and voids. However, due to periglacial processes (Feijtel et al., 1988) many of these coatings were fragmented and redistributed throughout the whole matrix.

The internal fabric, optical behavior and textural composition of coatings type (c) were characteristic of clay illuvation processes and typically found in an argillic horizon (Soil Survey Staff, 1975). Neof ormation of clay as observed in coatings type (a) and (b) may be misleading in the identification of an argillic horizon. Many fragmented parts of all coatings were observed, especially in upper B horizons. Coating type (c) invariably covered coatings of type (a) and (b) if they occurred together within one void. Consequently, coating type (c) is considered younger than types (a) and (b).

Submicroscopical Coating Characterization

Energy dispersive electron microprobe analyses showed significant differences between all three types of clay coatings. The Al₂O₃ content in noncrystalline coatings averaging 37.6% was significantly higher than in both crystalline coatings (Table 4). The atomic Al/Si ratio decreased from 0.81 in isotropic coating type (a) to 0.68 and 0.59 for anisotropic coatings type (b) and (c), respectively. Upon crystallization of isotropic weathering coatings the K, Mg, Ti, and Fe content increased at the expense of Al (Fig. 2). Parfitt (1980) reported that noncrystalline soil constituents were characterized by a high surface area, making them particularly strong adsorbants of ions from solution. Upon

crystallization adsorbed K and Mg may be built into the structure of the clay mineral.

Factor analysis of elemental coating composition reveal that two factors accounted for about 80% of the chemical variability (Table 5). The first principal component, explaining 56.5% of the total variance, was dominated by positive loadings for MgO, K₂O, CaO, and Fe₂O₃, and a negative loading for Al₂O₃. Negative and positive loadings indicated a significant antithetic behavior of these elements. This factor apparently suggested a strong relationship with the coating type or coating crystallinity. The type of clay coating therefore explained 88, 79, 74, and 73% of the variability in the contents of Al, Mg, K, and Ca content, respectively. The second principal component, explaining 22.8% of the total variance, was composed mainly of Si and Ti. The factor apparently bears a relation to the chemical and textural composition of the profile. Sample location, therefore, explained 76% of the variability in Si and 64% of the variability in Ti (Table 5).

Varimax factor rotation supported this relationship as factor loadings of Ti shifted to 73% (Table 5). The variability in coating composition between both locations was due to the presence of variable amounts of weatherable volcanic fragments. Kaup and Carter (1987) reported that ilmenite, biotite, hornblende, and sphene may weather to produce Ti in argillans and noncrystalline materials. The Ti content of all coatings for Bulhon and Croix-Mozat were significantly different averaging 1.9 ± 1.5 and $1.0 \pm 0.7\%$, respec-

tively. The Ti contents of clay coatings suggested a redistribution of Ti from Ti-bearing minerals. Similarly, Ti contents of bulk clay analyses indicated higher amounts in Bulhon (Table 3). Within coating type (c) variation in chemical composition due to sample lo-

cation was also attributed to SiO_2 ($P > F = 0.03$) and TiO_2 ($p > F = 0.06$). However, within each group of neoformed weathering coatings type (a) and (b), significant differences in chemical composition due to sample location could only be detected in Al_2O_3 and

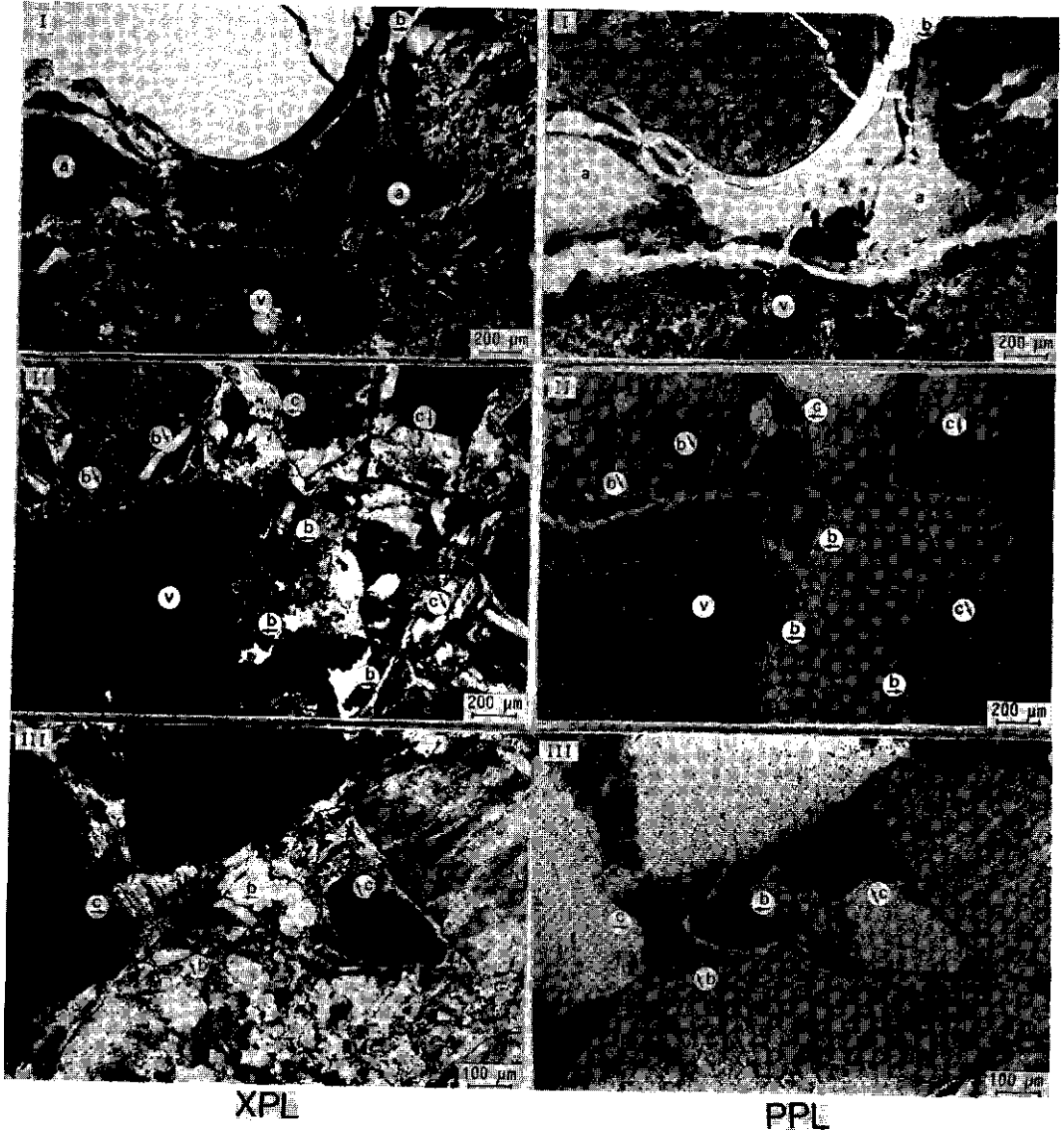


Fig. 2. Micromorphological view of coating types: I. Clay coating predominantly consisting of nonlaminated isotropic limpid clay coating type (a). Parts of the coating exhibited nonlaminated anisotropic limpid clay coating type (b). II. Nonlaminated anisotropic limpid clay coatings type (b) partly fragmented, covered by microlaminated anisotropic dusty clay coatings type (c). III. Fragmented nonlaminated anisotropic limpid clay coating type (b), covered by microlaminated anisotropic dusty clay coating type (c). v = volcanic fragment, XPL = crossed polarized light, and PPL = plain polarized light.

Fe₂O₃ content. In summary, significant variability in coating composition nested within profile locations were found for Al₂O₃ and Fe₂O₃.

Table 4. Mean elemental composition of clay coatings (mean ± standard deviation).

	Type a	Type b	Type c
Al ₂ O ₃	37.7 ± 1.7	31.4 ± 2.0	27.6 ± 2.0
SiO ₂	55.0 ± 0.9	54.2 ± 1.4	55.0 ± 2.3
Fe ₂ O ₃	6.8 ± 1.2	10.1 ± 1.7	11.6 ± 1.9
TiO ₂	0.3 ± 0.5	2.1 ± 1.1	1.6 ± 1.5
CaO	0.0 ± 0.1	0.6 ± 0.2	0.8 ± 0.4
MgO	0.0 ± 0.1	0.8 ± 0.5	1.5 ± 0.4
K ₂ O	0.1 ± 0.2	0.7 ± 0.3	1.5 ± 0.5

Table 5. Factor analysis of elemental composition of coatings (N = 53).

	Factor matrix		Varimax rotation	
	Factor 1	Factor 2	Factor 1	Factor 2
Al ₂ O ₃	-0.941	-0.079	-0.941	-0.070
SiO ₂	-0.018	0.879	0.120	-0.871
Fe ₂ O ₃	0.808	-0.188	0.769	0.313
TiO ₂	0.377	-0.805	0.246	0.854
CaO	0.856	-0.023	0.840	0.162
MgO	0.890	0.151	0.902	-0.009
K ₂ O	0.866	0.331	0.908	-0.191

	Eigenvalue	% of variance
Factor 1	3.956	56.2
Factor 2	1.597	22.8

Table 6. Cluster analysis of chemical compositions of investigated coatings.†

Cluster	Al ₂ O ₃	SiO ₂	Fe ₂ O ₃	TiO ₂	CaO	MgO	K ₂ O
Final cluster centers							
1	37.5	55.0	6.8	0.37	0.08	0.14	0.13
2	31.5	54.0	9.8	2.45	0.59	0.88	0.74
3	27.4	55.0	12.0	1.59	0.84	1.55	1.44
4	22.9	62.1	11.0	1.10	0.82	0.86	1.08

Cluster	No. of cases in cluster	Micromorphological group		
		Type a	Type b	Type c
Cluster membership				
1	13	12	1	0
2	17	0	13	4
3	22	0	3	19
4	1	0	0	1
	Total	12	17	24

† Percent of clustered cases correctly classified is 83%.

Cluster analysis was carried out to illustrate that coatings of the same type were more alike than coatings originating from the same profile. Clustering of investigated samples resulted in four distinct groups (Table 6). About 83% of grouped cases were classified correctly (Table 6). The discrimination between iso-

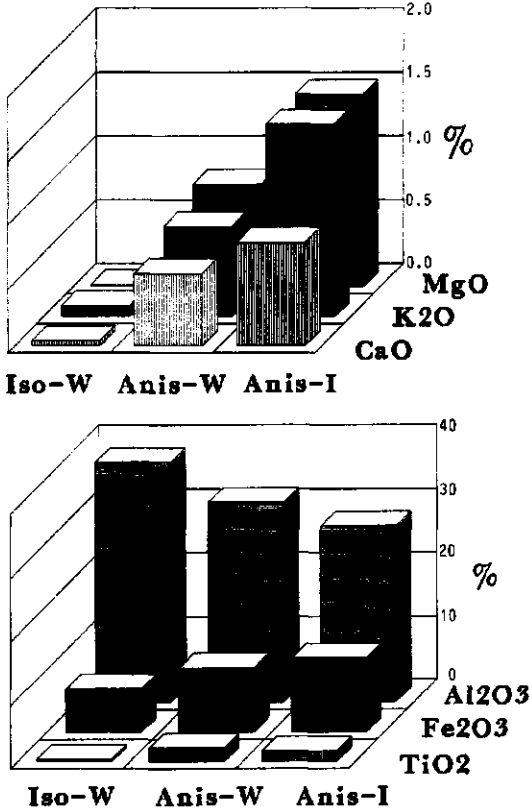


Fig. 3. Microchemical analyses of relative elemental coating composition (iso-w = isotropic weathering, anis-w = anisotropic weathering; and anis-i = anisotropic illuviation).

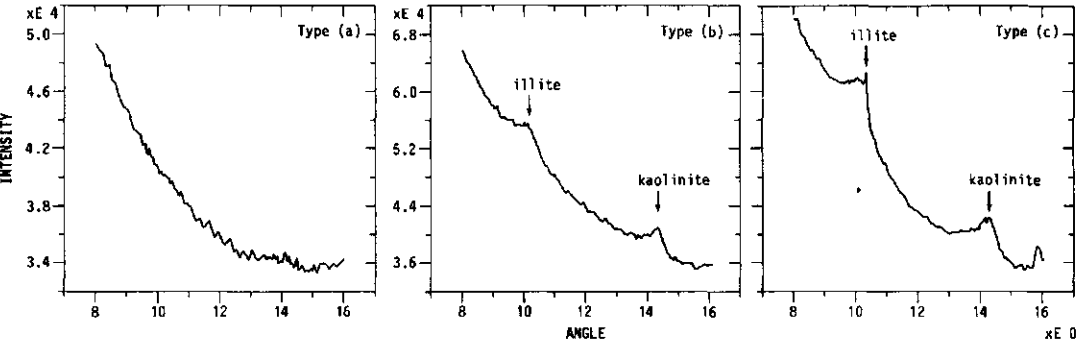


Fig. 4. X-ray diffraction patterns of coating type (a), (b), and (c).

tropic and anisotropic coatings was close to perfect (>92%). However, within the anisotropic coatings about 23 and 21% of weathering and illuviation coatings, respectively, were erroneously classified. The fourth cluster consisted of one illuviation coating, characterized by a typical Si/Al ratio of 2.3.

Analysis of x-ray diffraction patterns of in situ coatings indicated the presence of different clay minerals. Type (b) and (c) coatings consisted of illite and kaolinite (Fig. 3). However, triplicate measurements of coating types (b) and (c) suggested lesser amounts of illite in coatings type (b). This was corroborated by a increase in Si/Al ratio in illuviation coatings to 1.7, suggesting the predominance of 2:1 clays such as illite. X-ray diffraction patterns of coating type (a) revealed the absence of crystalline material (Fig. 4). Microchemical analyses indicated that type (a) coatings contained 37.7% Al₂O₃, 6.8% Fe₂O₃, and 55.0% SiO₂. The atomic Al/Si ratio of 0.81 lies within the range commonly reported for allophane (Henmi and Wada, 1976; Colman, 1982), and could therefore be categorized as "allophanelike" material or Al-Fe-Si gel. Allophane has been reported an intermediate in the formation of halloysite in tropical volcanic soils (e.g., Wada, 1977; Kirkman, 1980; Lowe, 1986). Similarly, Buurman and Jongmans (1987) reported in a West Java Oxisol the crystallization of isotropic allophanic coatings into halloysitic coatings. However, halloysite could not be detected in our profiles, nor could it be identified in type (b) coatings. Recrystallization of Al-Fe-Si coatings resulted in the formation of coating type (b), consisting predominantly of kaolinite.

CONCLUSIONS

Micromorphological observations indicated the occurrence of weathering and illuviation features in both profiles. The formation and presence of isotropic and anisotropic weathering coatings hinders the identification of an argillic horizon. Micromorphological and submicroscopical investigation may alleviate soil classification problems in soils with a volcanic component.

Classification of clay coatings in three distinct classes was corroborated by in situ mineralogical and microchemical analysis. Factor analysis of chemical coating composition revealed that two factors, coating type and sampling pit, accounted for 56.5 and 22.8% of the total variance, respectively. The antithetic behavior of Al vs. Mg, K, Ca, and Fe was apparent in the first factor or coating type. Clustering of investigated samples revealed the occurrence of three main groups. About 83% of grouped cases were classified correctly as isotropic, anisotropic weathering coatings, and anisotropic illuviation coatings. Variability due to profile pit location could be accounted for mainly by Ti, Al, and Fe. This corresponded to variations in the chemical bulk composition and variable degree of weathering and redistribution of volcanic fragments.

ACKNOWLEDGMENTS

The authors wish to thank N. van Breemen, R. Miedema, and E. Meijer for their assistance and helpful discussions. We are indebted to A. Clerckx and A. Boeckstein for their assistance with SEM-EDXRA measurements.

REFERENCES

- Beaufort, D., P. Dudoignon, D. Proust, J.C. Parneix, and A. Meunier. 1983. Microdrilling in thin section: A useful method for the identification of clay minerals in situ. *Clay Miner.* 18:223-226.
- Begheijn, L. Th. 1980. Methods of chemical analyses for soils and waters. Agric. Univ., Wageningen, The Netherlands.
- Bullock, P., N. Fedoroff, A. Jongerius, G. Stoops, and T. Tursina. 1985. Handbook for soil thin section description. *Wayne Res. Pub.*, Albrighton, England.
- Buurman, P., and A.G. Jongmans. 1987. Amorphous clay coatings in a lowland Oxisol and other andesitic soils of West Java, Indonesia. *Pemberitaan Penelitian Tanah dan Pupuk* 7:31-40.
- Chartres, C.F. 1987. The composition and formation of grainy void cutans in some soils with textural contrast in southeastern Australia. *Geoderma* 39:209-233.
- Chartres, C.F., A. Wood, and C.F. Pain. 1985. The development of micromorphological features in relation to some mineralogical and chemical properties of volcanic ash soils in highland Papua New Guinea. *Aust. J. Soil Res.* 23:339-354.
- Colman, S.M. 1982. Chemical weathering of basalts and andesites: Evidence from weathering rinds. *Geological Survey Professional Paper* 1246, U.S. Geological Survey, Alexandria, VA.
- Eggleton, R.A. 1987. Noncrystalline Fe-Si-Al oxyhydroxides. *Clays Clay Miner.* 35:29-37.
- Feijtel, T.C., A.G. Jongmans, N. van Breemen, and R. Miedema. 1988. Pedogenesis of two Planosols in Massif Central, France. *Geoderma* 43:249-269.
- Fitzpatrick, E.A. 1970. A technique for the preparations of large thin sections of soils and consolidated material. p. 3-13. *In* D.A. Osmond and P. Bullock (ed.) *Micromorphological techniques and application*. Techn. Monograph 2. Soil Survey of England and Wales. Rothamstead Exp. Stn., Harpenden.
- Henmi, T., and K. Wada. 1976. Morphology and composition of allophane. *Am. Mineral.* 61:379-390.
- Kaup, B.S., and B.J. Carter. 1987. Determining Ti source and distribution within a Paleustalf by micromorphology, submicroscopy and elemental analysis. *Geoderma* 40:141-156.
- Kirkman, J.H. 1980. Clay mineralogy of a sequence of andesitic tephra beds of western Taranaki, New Zealand. *Clay Miner.* 15:157-163.
- Lowe, D.J. 1986. Controls on the rates of weathering and clay mineral genesis in airfall tephra: A review and New Zealand case study. p. 265-330. *In* S.M. Colman and D.P. Dethier (ed.) *Rates of chemical weathering of rocks and minerals*. Academic Press, Orlando, FL.
- Meunier, A., and B. Velde. 1982. X-ray diffraction of oriented clays in small quantities (0.1 mg). *Clay Miner.* 17:259-262.
- Parfitt, R.L. 1980. Chemical properties of variably charged soils. p. 167-194. *In* B.K.G. Theng (ed.) *Soil with variable charge*. Soil Bureau D.S.I.R., Lower Hutt, New Zealand.
- SPSS, Inc. 1986. *Advanced statistics*. M.J. Norusis (ed.) SPSS, Inc., Chicago, IL.
- Soil Survey Staff. 1951. *Soil survey manual*. USDA Agric. Handb. 18. U.S. Gov. Print. Office, Washington, DC.
- Soil Survey Staff. 1975. *Soil taxonomy: A basic system of soil classification for making and interpreting soil surveys*. USDA-SCS Agric. Handb. 436. U.S. Gov. Print. Office, Washington, DC.
- van der Plas, L., and A.C. Tobi. 1965. A chart for judging the reliability of point-counting results. *Am. J. Sci.* 263:87-90.
- Verschuren, R.H. 1978. A microscope-mounted drill to isolate microgram quantities of mineral material from polished thin section. *Mineral. Mag.* 42:499-503.
- Wada, K. 1977. Allophane and imogolite. p. 603-658. *In* J.B. Dixon and S.B. Weed (ed.) *Minerals in soil environments*. SSSA, Madison, WI.

CHAPTER 5

EPILOGUE

EPILOGUE

The papers presented in this thesis reflect the results obtained in various research projects. As a result, a variety of issues within the topic of mineral transformation during weathering in volcanic soils was treated. Characterization of alteration of primary mineral and formation of secondary minerals in terms of morphology, chemistry, and mineralogy in relation to different (micro-)environmental conditions were the main topics. Thin sections were studied by micromorphology, and relevant features were characterized chemically and mineralogically by submicroscopical methods applied on samples isolated from thin sections. In this final chapter I will reported the main conclusions, and discuss the differences between clay-illuviation coatings and coatings resulted from secondary mineral formation. Finally implications for future research will be suggested.

Main conclusions

- * Weathering of primary- and formation of secondary minerals determines the nature and intensity of ongoing pedogenesis with age in soils developed on volcanic materials.
- * Conclusions about mineral transformation in soils drawn on the basis of mineralogical analysis in bulk samples can be misleading, because different micro environmental conditions at the pedon level exist. For this purpose, (un)disturbed micro-samples isolated from mineral transformation features in thin sections are better suited.
- * Data about the mineralogy of clay features in thin sections are essential for a correct interpretation of mineral transformation at the particle level.
- * Establishing of the mineralogy of clay features in thin sections with optical methods is ambiguous. Isolation of (un)disturbed micro-fragments of neoformed clay coatings by microdrilling in thin sections allows determination of the mineralogy, the morphology and the related distribution pattern of the individual clay constituents with TEM at the micron and nanometre scale.
- * Chemical and mineralogical analyses performed in situ on micromorphologically characterized volcanic fragments and surrounding clay coatings, offers the possibility to quantify chemical aspects of mineral transformation.
- * The occurrence of 2:1 Phyllosilicates in soils developed under strong leaching in perudic climates can explained by inheritance from hydrothermally altered parent material both in residual soils and in soils developed on sediments, derived from hydrothermally altered rock.
- * Morphologically similar isotropic Alumino-silicate coatings may differ chemically and mineralogically as a result of differences in environmental conditions at the micron scale.
- * Clayey coatings resulting from i) secondary mineral formation after weathering of primary minerals or ii) clay illuviation may co-exist in soils with appreciable amounts of easily weatherable minerals.

The latter two statements have repercussions for the identification of the argillic horizon in volcanic soils.

The identification of the Argillic horizon in volcanic soils

An argillic horizon is an illuvial horizon which contains significant accumulations of illuviated layer-lattice silicate clays (Soil Taxonomy, 1992). Some part of the horizon should have 1 percent or more oriented clay bodies in thin section. These clay bodies generally are

developed as coatings around voids, and in biological active soils as fragmented coatings. During this study the problem arises that neoformed clay features may be confused with illuviation clay phenomena. The handbook of soil thin section description, the current description system in micromorphology (Bullock et al. 1985), refer to neoformed clay pedofeatures. The authors state that such neoformed clay pedofeatures in general consist of small domains beyond the resolution of the optical microscope. In addition, they stated that neoformed clay coatings seem to be rather rare. They conclude that new techniques, using the optical microscope as a basis should facilitate detection of neoformed clay features (Bullock et al 1985), and they stress the importance of a proper description and interpretation of neoformed clay features.

Our study reveals that neoformed clay coatings are common features in volcanic soils both in tropical- and in the temperate humid regions.

There is a need to distinguish neoformed clay-coatings from clay-illuviation coatings, because the latter group is used as differentiating criterion to separate orders in the Soil Taxonomy. A number of morphological criteria will be considered to examine whether clay-illuviation coatings and neoformed coatings can be separated properly, resulting a correct interpretation of the involved soil forming processes in volcanic soils.

Potential criteria to characterize and differentiate clay-illuviation coatings and neoformed coatings are:

-Isotropy versus anisotropy:

All clay-illuviation coatings consist of crystalline material and are consequently anisotropic.

Neoformed clay-coatings may be isotropic and therefore amorphous. Our study reveals that they consist of short-range order materials like allophane and imogolite having different Al/Si molar ratios in dependence of external conditions. Their isotropic character exclude clay-illuviation as the cause of their presence. However some neoformed coatings are anisotropic and therefore crystalline. So crystalline coatings could result from clay illuviation or from neoformation. As a result, crystallinity is not a differentiating characteristic.

-Isotropy and anisotropy within one coating:

The occurrence of both anisotropic and isotropic parts within one clay coating, indistinguishable in plane polarised light, reveals a strong genetic relation between the parts. The presence of such coating types indicates the process of secondary clay formation rather than clay-illuviation and enable a correct classification.

-Texture and Limpidity:

In clay-illuviation coatings textures varies from limpid clay (fine clay, translucent, without microcontrasted particles) to dusty clay (coarse and fine clay, speckled, clay sized micro contrasted particles).

Textures of neoformed coatings always are made up of limpid clay (fine clay, translucent). Occurrence of inclusions is possible.

-Surface characteristics:

Clay-illuviation coatings dominantly have outer surfaces varying from smooth to wavy.

Neoformed coatings tends to have botryoidal (FitzPatrick, 1984) outer surfaces but occasionally smooth and wavy shapes are observed.

-Internal fabric:

Clay-illuviation coatings dominantly are microlaminated but non-laminated clay-illuviation coatings occur especially in lower B horizons.

Neoformed clay coatings are non-laminated. Micro-lamination is locally present but

is caused by thin layers of impurities.

-Orientation pattern:

The presence or absence of extinction lines reflect the degree of orientation of the clay domains. Clay domains in illuviation coatings are normally oriented parallel to the void surface, and the degree of orientation can range from weakly to strongly oriented.

The same is valid for anisotropic neoformed clay coatings, but there is a tendency that orientation in such coatings is generally weak and moderate rather than strong. Sometimes, neoformed clay domains have an orientation perpendicular to the void wall.

Considering the morphological comparison between neoformed coatings and clay illuviation coatings it appears that the best criteria to separate neoformed clay coatings from clay illuviation coatings are:

- i) The presence of anisotropic and isotropic parts within one coating and no differences between them with plane polarized light.
- ii) Botryoidal outer surfaces of the coatings
- iii) A perpendicular orientation of the clay domains to the void wall.
- iv) absence of any lamination
- v) a limpid character of the coating

However, in many cases it is not possible to distinguish clay-illuviation coatings and anisotropic neoformed clay coatings in volcanic soils on the base of morphological characteristics alone. Anisotropic, non-laminated, translucent (limpid) coatings with botryoidal outer surfaces may result from clay-neoformation rather than clay-illuviation, but a conclusive proof cannot be given. As a result, all soil horizons and the saprolite should be taken into account in terms of amount and distribution of coatings with depth, and presence of isotropic coatings or partly anisotropic coatings.

Studying the saprolite may give better insight in the morphology, chemistry, and mineralogy of the products of secondary mineral formation like coatings. Effects by soil forming processes other than weathering are generally neglectable in this part of the soil. Isotropic and anisotropic materials may occur in one coating, undistinguishable in plane polarized light, indicating a secondary formed genesis. As a result, the morphology and composition of the anisotropic part of the coating can be used to interpret anisotropic (fragmented) coatings present in overlying horizons.

In sediments with an appreciable amount of volcanic fragments isotropic, anisotropic coatings or combinations of both types around such fragments may occur. Such related distribution patterns point to mineral transformation rather than to clay-illuviation, because it is unlikely that clay illuviation coatings precipitate preferentially around volcanic fragments. So, the morphology of such coatings too can help to recognize coatings of similar genesis in overlying horizons.

If the saprolite or the deep subsoil of sediments containing volcanic fragment cannot be studied micromorphologically, interpretation of non-laminated, limpid, anisotropic, botryoidal clay coatings in terms of clay neoformation or clay-illuviation is highly uncertain. Consequently the identification of an argillic horizon in volcanic soils is haphazard and, at least in part, a number of argillic horizons could be Cambic horizons.

SAMENVATTING

Mineraal omzetting aan het aardoppervlak is een complex proces. In vulkanische materialen heeft het de neiging redelijk snel te verlopen. Veel verweringsstudies op vulkanisch materiaal zijn uitgevoerd op verschillende schalen van waarneming, waarbij overwegend gebruik werd gemaakt van "bulk" monsters. Echter, om een juist begrip te krijgen van de verwerking mechanismen van primaire mineralen en de vorming van secundaire mineralen is het nodig om ongestoord bodemmateriaal te verzamelen op een schaalniveau waar micromorfologie en submicroscopie zich bezig houden. Verweringsstudies uitgevoerd op de micrometer schaal met behulp van micromorfologische technieken tonen het heterogene karakter van mineraalverwerking aan alsmede het naast elkaar voorkomen van verschillende secundaire mineralen.

De voornaamste doelen van de artikelen in dit proefschrift waren het karakteriseren en het verklaren van verwerking van primaire mineralen en vorming van secundaire mineralen op het korrel niveau in vulkanische gronden in relatie tot (micro) omgevingsfactoren.

Slijpplaten van vulkanische gronden werden micromorfologisch bestudeerd, en relevante verschijnselen werden chemisch en mineralogisch gekarakteriseerd met behulp van submicroscopische methoden, die werden uitgevoerd op ongestoorde monstertjes geïsoleerd uit slijpplaten. Mineraalomzettingen werden zowel in de gematigde streken als in de humide tropen bestudeerd.

In een chronosequentie bestaande uit Kwartaire terrassen van de Allier in Frankrijk laten micromorfologische en submicroscopische analyses het volgende zien:

- Omzetting van basalt fragmenten leidt tot kleivorming, terwijl verwerking van granietdeeltjes bijdraagt tot de zandfractie.

- Een relatieve toename van Ti, Al, en Fe en een afname van K, Na, Ca, en Si gehalten vindt plaats in verweringsringen van basaltkorrels. Verschillen in verweringsintensiteit worden meer bepaald door de chemische samenstelling van de basalt dan door de verwerkingstijd.

- Een massabalans uitgevoerd aan een isovolumetrische verweerde basaltkorrel met een onverweerde kern demonstreert dat alle elementen, behalve Fe, werden uitgespoeld uit alle verweringsringen. Een nieuwvormende kleicoating omgeeft de gedeeltelijk verweerde korrel. Micromorfologie toont aan dat de coating uit de korrel gevormd is. Alleen Si, Al, en enig Ca werden teruggevonden in de kleicoating. Een deel van het Al was afkomstig van een andere bron dan de omsloten korrel.

- Isotrope en anisotrope coatings komen voor in een Paleosol gevormd in een ouder terras. Micromorfologische waarnemingen laten zien dat zulke coatings een genetische relatie hebben. De isotrope coatings bestaan uit allofaanachtig materiaal met kleine hoeveelheden 2:1 phyllosilicaten, terwijl het anisotrope type alleen uit 2:1 phyllosilicaten bevatten. Beide soorten werden gevormd onder beperkte uitspoelingsomstandigheden door een hercombinatie van trachitische verweringsproducten gedurende de coating vorming.

- Micromorfologische waarnemingen tonen drie typen kleicoatings aan, in twee Planosols gevormd, in twee oudere terrassen. Isotrope en anisotrope doorzichtige materialen komen plaatselijk voor binnen een coating hetgeen een genetische relatie suggereert. Deze coatings zijn het gevolg van secundaire mineraalvorming. Het derde type, zijn anisotrope kleicoatings die micro-onzuiverheden bevatten. zulke coatings zijn duidelijk het gevolg van klei-inspoeling. Cluster analyse toont aan dat coatings van hetzelfde type meer verwand zijn dan verschillende coatings in hetzelfde profiel. Ongeveer 83% van de gegroepeerde monsters werden correct benoemd als isotrope en anisotrope verwerings coatings of als anisotrope inspoelings coatings.

Een techniek om ongestoorde microdeeltjes van verschijnselen uit slijpplaten te isoleren wordt beschreven. Zulke microdeeltjes kunnen vervolgens met behulp van transmissie

elektronen microscopie geanalyseerd worden. Deze techniek maakt het mogelijk om op micron- en manometer schaal micromorfologische, mineralogische en chemische analyses uit te voeren in hetzelfde ongestoorde micromonster .

In de C horizont van een jonge Hapludand in Guadeloupe en in de C en R horizont van een oude Hapludand in Costa Rica, beiden ontwikkeld in andesitisch materiaal, bestaan isotrope coatings uit allofaanachtig materiaal. Isotrope coatings in de B horizonten van beide bodems bevatten allofaan en imogoliet. De Al/Si ratios van de coatings in de B horizont zijn hoger dan die van de coatings in de C en R horizont. Anisotrope coatings bestaan uit gibbsiet en komen alleen voor in de Bw horizont van de oudere Hapludand van Costa Rica. De gibbsiet coatings gaan geleidelijk over in isotrope coatings en beide typen zijn hetzelfde in gewoon doervallend licht, hetgeen een genetische relatie suggereert. De allofaan coatings zijn het resultaat van initiële verwerking van de moedermaterialen, terwijl de gibbsiet coatings het laatste stadium van secundaire mineraalvorming vertegenwoordigen. De verschillen in chemische en mineralogische samenstelling van de coatings worden toegeschreven aan verschillende uitspoelings omstandigheden zowel op macro- als op microschaal.

2:1 Phyllosilicaten in Hapludands, ontwikkeld in Holocene, andesitische strandwallen in Costa Rica, komen voor als klei-pseudomorfen gevormd uit primaire mineralen. Zij zijn geërfd van hydrothermaal veranderd moedermateriaal waarvan de strandwallen van afkomstig zijn. Ze zijn niet ontstaan ten gevolge van bodemvorming na de afzetting. Verwerking en biologische activiteit tasten de klei-pseudomorfen aan hetgeen leidt tot vorming van kleideeltjes die bestaan uit 2:1 phyllosilicaten. Deze worden vervolgens opgenomen in de allofaan grondmassa die het gevolg is van de huidige bodemvorming in de Hapludands.

Isoptope coatings in een Oxisol van West Java (Indonesië), gevormd in andesitisch moedermateriaal, zijn waarschijnlijk het resultaat van as depositie. De coatings rekristalliseren tot anisotrope coatings hetgeen op nieuwvorming duidt. Beide coating typen lijken regelmatig voor te komen in drie andesitische catena's in Indonesië. De hoeveelheid coatings alsmede de kristalliniteit lijken groter te worden naarmate het droge seizoen meer uitgesproken wordt. De anisotrope coatings kunnen gemakkelijk worden verward met inspoelings coatings.

NAWOORD

Toen ik in 1968 bij de vakgroep Bodemkunde en Geologie werd aangesteld, had de Landbouwhogeschool nog ruimte in termen van personeel en materieel. In mijn beginnende functie was het werk in de zomerperiode vastgesteld, 's winters moest ik het zelf maar invullen. Boet Slager heeft mij behoed voor structurele winterslapen, omdat hij mij gedurende deze perioden een plaats gaf in de sectie morfologie. Door zijn begeleiding in de (micro)morfologie en aanmoediging tot het aanpakken van steeds nieuwe activiteiten binnen het vakgebied heeft hij de basis gelegd voor mijn verdere ontwikkeling. Boet, ik ben je daarvoor zeer erkentelijk.

Tom Pape heeft mij in deze eerste fase veel geleerd over de micromorfologie, samen deelden we meer dan 10 jaar een kamer. Deze periode heeft ervoor gezorgd dat we tot in het heden meer dan alleen maar over het vakgebied met elkaar van gedachten wisselen. Ik waardeer dat zeer.

Leen Pons ben ik dankbaar voor de grote mate van vrijheid die hij in de vakgroep creëerde en daardoor alle ruimte gaf aan eigen initiatief. Hij heeft me aangemoedigd om college te gaan geven in een van zijn OWELS. Dit alles heeft mijn ontwikkeling in het vakgebied sterk beïnvloed.

Rienk Miedema ben ik zeer erkentelijk omdat ook hij mij een grote mate van vrijheid in mijn werk heeft gegund en me altijd heeft geadviseerd en gestimuleerd. Rienk, ik heb je veel meer als een collega mogen ervaren dan als een directe chef.

Tom Feijtel heeft een belangrijke impuls aan mijn loopbaan gegeven. Mijn onderzoeksactiviteiten en de zijne waren uitstekend te koppelen. Tom, je hebt mijn schrijfactiviteiten gestimuleerd en sterk verbeterd. Zonder jouw inbreng in de beginfase was dit proefschrift er nooit gekomen, en ik kijk met zeer veel plezier terug op onze gezamenlijke onderzoeks- en familie activiteiten in de Limagne in Frankrijk. Ik ben je er zeer erkentelijk voor.

Ed Veldkamp wil ik bedanken voor zijn wetenschappelijke inbreng in dit proefschrift. Ed, ik heb veel respect voor je wetenschappelijke kwaliteiten en je geestdrift die je al demonstreerde voordat je afgestudeerd was. Hoofdstuk 2.2 van dit proefschrift is in hoofdzaak van jouw hand en je schreef het als afsluiting van een doctoraal leeronderzoek.

Fok van Oort bracht me in aanraking met een nieuwe techniek: de transmissie elektronen microscopie. Fok, door jou enthousiasme en inzet hebben we deze techniek kunnen inzetten op ongestoorde ultradunne doorsneden van verschijnselen gemonsterd uit slijpplaten. Samen hebben we menige bezielende bodemkundige discussie gevoerd, plannen gemaakt en uitgevoerd tijdens jouw bezoeken in Wageningen en de mijne in Frankrijk en Guadeloupe. Jouw samenwerking en aanmoediging heeft in sterke mate bijgedragen tot het slagen van dit proefschrift.

Andres Nieuwenhuysse wil ik bedanken voor zijn inzet en begeleiding tijdens mijn bezoeken aan Costa Rica. Andres, je hebt mijn veldkennis van de tropen mede ontwikkeld. Zowel uit jouw aankomend proefschrift als uit het mijne blijkt dat we een vruchtbaar samenwerkingsverband hebben gehad.

Paul Verburg, jou wil ik bedanken voor de steun die je hebt gegeven door middel van de vele kritische discussies die we over verschillende manuscripten hadden en voor de SEM-EDXRA berekeningen die je voor mij hebt uitgevoerd. Uit aspecten van jouw doctoraal leeronderzoek is hoofdstuk 3.2 voortgekomen, terwijl in een artikel in het proefschrift van Andres Nieuwenhuysse je gehele leeronderzoekresultaat is weergegeven. Hieruit blijkt het hoge niveau van je leeronderzoek.

Tom Veldkamp wil ik bedanken voor zijn aandeel in hoofdstuk 2.1 en voor zijn kritische discussies over mijn onderzoek. Samen met zijn broer Ed is een veldcampagne in Frankrijk

gevoerd waar hoofdstuk 3.3 uit voort gekomen is.

Je tiens à remercier l'équipe de microscopie de la station de Science du Sol de l'INRA de Versailles, en particulier Anne Marie Jaunet, ainsi que mesdames R. Dupont et M. Lemain pour la qualité du travail réalisé en Microscopie Electronique à Transmission.

Jan van Doesburg heeft de Step Scan X-ray diffractie analyse voor mij toegankelijk gemaakt, vele analyses uitgevoerd, en me geleerd de resultaten ervan op kritische wijze te hanteren. Jan, jouw bijdrage in de ontwikkeling van de analyse techniek m.b.t. mineralogische karakterisering van micro hoeveelheden materiaal heeft sterk bijgedragen aan de synthese in diverse artikelen, hetgeen blijkt uit een co-auteurschap. Je was altijd bereid monsters te analyseren, waarbij je zelfs je vrije tijd gebruikte om een en ander efficiënt te kunnen afhandelen. Ik ben je hier zeer erkentelijk voor.

Arie van Dijk heeft alle slijpplaten gemaakt die in dit onderzoek zijn gebruikt. Dit was geen gemakkelijke taak, omdat veel monsters zeer zwaar van textuur waren en daarom lastig te impregneren en te slijpen. Verder heeft hij vele kleine niet afgedekte slijpplaatjes gemaakt die ik gebruikte voor submicroscopisch werk, en dit ging er dan altijd bij Arie "even tussendoor". Arie, bedankt hiervoor.

Salle Kroonenberg is de eerste die gedurende het onderzoek in de Limagne tegen me zei: "je moest maar eens gaan promoveren", waarbij hij doelde op de terrassensequentie van de Allier. Het is niet helemaal zo gelopen, maar in dit proefschrift is toch een deel van de resultaten van de geologisch-bodemkundige samenwerking in de Limagne neergelegd. In het nieuwe VF Tropen hoop ik weer met je samen te werken.

Leendert van der Plas jij hebt mij de eerste beginselen van optische mineralogie bijgebracht en ik heb het vermoeden dat je af en toe moet hebben gemerkt dat ik de ellips van doorsnede niet door had. Bedankt voor je geduld en begrip.

Peter Buurman heeft vanaf mijn debuut in de vakgroep tot in het heden (met een korte onderbreking van 4 jaar Indonesië) met mij te maken gehad als de (micro)morfoloog die meedeed in zijn vele onderzoeken. Peter, door je grote werkdrijf en je wetenschappelijke diepgang heb ik erg veel van je geleerd, soms met enige moeite mijnerzijds. De verschillende gezamenlijke publicaties getuigen van een langdurige vruchtbare samenwerking die voor mij sterk vormend en stimulerend is. In het nieuwe VF Tropen hoop ik op een vruchtbare samenwerking. Ik wil je speciaal bedanken voor de snelheid en de grondigheid waarmee je verschillende manuscripten van mij hebt gereviewd. Het heeft sterk bijgedragen aan de kwaliteit van dit proefschrift en je co-promotorschap meer dan rechtvaardigt.

Nico van Breemen, jij bent mijn uiteindelijke promotor geworden. Tijdens het onderzoek in Frankrijk en in de humide tropen heb ik je leren kennen als een stimulerende, kritische en creative promotor die de mogelijkheden van de (micro) morfologie en submicroscopie in verweringsstudies in bodems in hun natuurlijke liging erkende en een plaats gaf in je leerstoel. Dat lijkt vanzelf sprekend maar dat is het m.i. niet, gezien de onderzoeksprojecten waarmee jezelf bezig was en nu ontwikkelt. Zonder dat je het waarschijnlijk weet heb je me geleerd hoe je een onderzoeksonderwerp aanpakt, hoe je kritisch moet omgaan met gegevens en hoe je uiteindelijk de resultaten neerlegt in een manuscript. Voor een micromorfoloog is de bekoring te vervallen in omvangrijke beschrijvingen in niet te volgen jargon sterk. Daar heb je een grote hekel aan, hetgeen ik dan ook diverse malen in mijn manuscripten heb gemerkt. Je wees me er op dat micromorfologische data in een bodemkundige studie gecombineerd dienen te worden met andere bodemkundige data om tot een gewogen synthese te komen. Voorts heb ik goede herinneringen aan onze reizen naar Costa Rica waardoor we de gelegenheid hadden ook eens over andere onderwerpen dan bodemkunde van gedachten te wisselen.

Berry Geerlings, Jan Bakker, Joop van Brakel en Wim van het Hof van de fotolocatie

Binnenhaven, jullie hebben veel werk voor dit proefschrift gedaan. Het was niet altijd even makkelijk om de voor jullie onbekende afbeeldingen op de juiste manier af te drukken. Jullie bereidwilligheid om een afdruk van een microfoto nog eens proberen te verbeteren, en om af en toe een haastklus uit te voeren demonstreert dat jullie fotolocatie een goede mentaliteit heeft; bedankt voor alle inspanningen.

Thea van Hummel wil ik bedanken voor het bijstellen van de lay-out en het corrigeren van teksten.

Elly, door me de tijd en de ruimte te geven die ik nodig had om me bodemkundig te ontwikkelen ben je een belangrijke factor in de tot standkoming van dit proefschrift, bedankt.

CURRICULUM VITAE

Toine Jongmans werd op 16 april 1945 in De Bilt geboren. In juni 1965 studeerde hij af aan de Hogere Landbouwschool te Ede (thans gevestigd in Dronten). In maart 1968 trad hij in dienst van de Landbouwhogeschool bij de vakgroep Bodemkunde en Geologie als technisch assistent, belast met het medebegeleiden van bodemkundige veldpractica en excursies. In 1970 volgt een vaste aanstelling en wordt hij voor een deel van zijn taak toegevoegd aan de sectie Bodemmorfologie en belast met het beschrijven van bodemprofielen en slijpplaten t.b.v. onderzoeksprojecten. In 1986 wordt hij op basis van aanbevelingen van een externe beoordelingscommissie opgenomen in het wetenschappelijke rangenstelsel als toegevoegd docent. In 1990 wordt hij bevorderd tot universitair docent op grond van het zelfstandig geven van onderwijs en het zelfstandig uitvoeren van onderzoek resulterend in publicaties in internationale bodemkundige tijdschriften. Vanaf 1986 werkte hij als (micro)morfoloog mee in verschillende VF-projecten van de vakgroep in Frankrijk en Costa Rica. Vanaf 1994 werkt hij mee in het VF-project Tropen.